Advanced Analytical Model for the Prognostic of Industrial Systems Subject to Fatigue

Abdo Abou Jaoudé

Université Libanaise

Université Libanaise
École Doctorale
Sciences et Technologie

Alx*Marsellle université

LSIS

CO-ADVISED THESIS

Between the

LEBANESE UNIVERSITY

And

AIX-MARSEILLE UNIVERSITY

École Doctorale en Mathématiques et Informatique de Marseille - ED 184

To obtain the Ph.D. diploma in

Automatic Control

Advanced Analytical Model for the Prognostic of Industrial Systems Subject to Fatigue

Presented and defended by:

Abdo ABOU JAOUDÉ

The Jury is composed of:

Pr. Fouad Kaddah	Université Saint Joseph, Liban	Rapporteur
Pr. Didier Theilliol	Université de Lorraine, France	Rapporteur
Pr. Ahmed El Hajjaji	Université de Picardie Jules Verne, France	Examinateur
Dr. Clovis Francis	Université Libanaise, Liban	Examinateur
Dr. Seifedine Kadry	Université Libanaise, Liban	Directeur de thèse
Pr. Hassan Noura	UAE University, UAE	Directeur de thèse
Pr. Mustapha Ouladsine	Aix-Marseille Université, France	Directeur de thèse
Dr. Khaled El-Tawil	Université Libanaise, Liban	Invité

Thesis prepared at

Laboratoire des Sciences de l'Information et des Systèmes (LSIS - UMR CNRS 7296) - France
and the École Doctorale Sciences et Technologie (EDST) - Liban

"The Ancient of Days", William Blake, 1794

William Blake

DES PENSÉES INSPIRANTES

"Ce qu'il y a d'incompréhensible, c'est que l'univers soit compréhensible."

Albert Einstein

"Le hasard est le pseudonyme de Dieu quand Il ne veut pas signer."

Anatole France

"Si j'ai appris une chose au cours de ma longue vie, c'est que toute notre science, confrontée à la réalité, apparaît primitive et enfantine – et pourtant, c'est ce que nous possédons de plus précieux."

Albert Einstein

"Sa sacrée majesté le Hasard décide de tout."

Voltaire

"Toute pensée émet un coup de dés."

Stéphane Mallarmé

"Le mathématicien, emporté par son courant de symboles traitant de vérités purement formelles, peut cependant obtenir des résultats d'une importance infinie pour notre description de l'univers physique."

Karl Pearson

"Ainsi, joignant la rigueur des démonstrations de la science à l'incertitude du sort, et conciliant ces deux choses en apparence contradictoires, elle peut, tirant son nom des deux, s'arroger à bon droit ce titre stupéfiant: la géométrie du hasard. "

Blaise Pascal

"Dieu est subtil, mais il n'est pas malveillant."

Albert Einstein

"Une intelligence qui, à un instant donné, connaîtrait toutes les forces dont la nature est animée et la situation respective des êtres qui la compose embrasserait dans la même formule les mouvements des plus grands corps de l'univers et ceux du plus léger atome ; rien ne serait incertain pour elle, et l'avenir, comme le passé, serait présent à ses yeux."

Marquis Pierre-Simon de Laplace

"Le plus beau sentiment du monde, c'est le sens du mystère. Celui qui n'a jamais connu cette émotion, ses yeux sont fermés."

Albert Einstein

TABLE OF CONTENTS

General Introduction.....1

I Introduction to Systems Prognostic.....5

I.1 Introduction..... 6

I.1.1 Maintenance Evolution..... 6

I.1.2 Maintenance Optimization..... 8

I.2 Intelligent Maintenance..... 9

I.3 Degradation Prognostic..... 11

I.3.1 Degradation versus Prognostic.....11

I.3.2 Equipment Degradation Trajectory.....12

I.3.3 Definition and Methodologies.....15

I.4 Prognostic Definition.....17

I.5 The Role of Prognostic in Lifetime Process.....18

I.6 State-of-the-Art of the Prognostic Approaches..... 19

I.6.1 Prognostic Based on Models..... 21

I.6.1.1 Advantages and Drawbacks of the First Approach.....25

I.6.2 Prognostic Guided by Data..... 26

I.6.2.1 Prognostic by Trend Analysis..... 27

I.6.2.2 Prognostic by Learning..... 28

I.6.2.3 Prognostic by State Estimation.....30

I.6.2.4 Advantages and Drawbacks of the Second Approach.....31

I.6.3 Prognostic Based on Experience..... 32

I.6.3.1 Stochastic Approach..... 33

I.6.3.2 Reliability Approach..... 34

I.6.3.3 Advantages and Drawbacks of the Third Approach..... 37

I.6.4 Methodology Based on Abaci of Degradation.....38

I.7 Summary..... 40

I.8 Conclusion..... 43

References..... 44

II Analytic Linear Prognostic Model of Dynamic Systems..... 53

II.1 Introduction..... 54

II.2 Proposed Prognostic Model..... 55
II.2.1 Damage Evolution Law..... 56
II.2.2 Paris-Erdogan's Law..... 57
II.2.3 Palmgren-Miner's Rule..... 59
II.2.4 WÖhler's Curve..... 59
II.2.5 Stress Intensity Factor..... 60
II.2.6 Additivity Rule in Palmgren-Miner's Rule..... 61
II.2.7 Maintenance and Diagnostic/Prognostic..... 63
II.2.7.1 Flowchart of Various Components of Diagnostic/Prognostic/Maintenance Process..... 64
II.2.7.2 Cycle of Prognostic-Diagnostic-Maintenance..... 65
II.2.8 Accumulation of Fatigue Damage..... 66
II.2.9 Flowchart of the Prognostic Model..... 69
II.2.10 Environment Effects in the Proposed Prognostic Model..... 70
II.3 Application of the Prognostic Method to Industrial Systems..... 71
II.3.1 Vehicle Suspension Fatigue Life..... 71
II.3.1.1 Types of Mechanical Effects, Their Mechanisms, and Possible Consequences..... 76
II.3.1.2 Automatic Diagnostic of a Bad Suspension Bushing..... 76
II.3.1.3 Prognostic Study for Vehicle Suspension Systems..... 77
II.3.1.4 System Identification..... 78
II.3.1.5 Fatigue Damage Modeling of a Suspension..... 79
II.3.1.6 Simulation of the Degradation Model..... 81
II.3.1.7 Simulation of Three Road Profiles..... 82
II.3.1.8 Simulation Results..... 83
II.3.1.9 Analysis of the Simulation Results..... 86
II.3.1.10 Conversion of RUL into Years..... 87
II.3.2 Prognostic Study for Pipelines Systems..... 88
II.3.2.1 Introduction..... 88
II.3.2.2 Pipes Stress Modeling..... 89
II.3.2.3 State of Stresses in the Tube Body..... 90
II.3.2.4 Stress Intensity Factor..... 91
II.3.2.5 Degradation Model Expression of Pipes..... 91
II.3.2.6 Simulations of Three Levels of Internal Pressure..... 92
II.3.2.7 Unburied Pipe Case..... 93

II.3.2.8 Buried Pipe Case....95
II.3.2.9 Offshore Pipe Case....98
II.4 Conclusion.... 101
References....102

III Analytic Nonlinear Prognostic Model of Dynamic Systems....105

III.1 Introduction....106
III.2 State-of-the-Art: Nonlinear Damage Accumulation....107
III.2.1 Damage Theories Based on Endurance Limit Reduction....110
III.3 Nonlinear-Damage-Based Prognostic....111
III.3.1 Disadvantages of Linear Damage Accumulation.... 113
III.3.2 Double Linear Damage Rule (DLDR)....113
III.3.3 Damage Curve Approach (DCA)....114
III.3.4 Double Damage Curve Approach (DDCA)....115
III.4 Nonlinear Cumulative Damage Model.... 116
III.4.1 Solution of the Differential Equation of Degradation....117
III.4.2 Relation between D and N at a Specific Cycle N_1....119
III.4.3 Recursive Relation of Nonlinear Damage D....120
III.5 Application to a Suspension System....121
III.5.1 Results of the Simulation....121
III.5.2 Conversion of RUL into Years.... 124
III.5.3 Comparison with the Linear Case....125
III.5.4 Advantages of the Proposed Model.... 126
III.6 Application to a Pipeline System....127
III.6.1 Unburied Pipe Case....128
III.6.1.1 Comparison with the Linear Case....130
III.6.2 Buried Pipe Case....131
III.6.2.1 Comparison with the Linear Case....134
III.6.3 Offshore Pipe Case.... 134
III.6.3.1 Comparison with the Linear Case....137
III.6.4 Validation of the Pipelines Lifetimes.... 138
III.7 Conclusion.... 139
References....140

IV Stochastic Linear and Nonlinear Analytic Prognostic Model..... 143

IV.1 Introduction..... 144

IV.2 State-of-the-Art: Stochastic Fatigue Modeling..... 144

IV.2.1 Definition of the J-Integral..... 148

IV.3 Stochastic Linear Damage Accumulation..... 150

IV.4 Stochastic Modeling..... 151

IV.5 Stochastic RUL..... 152

IV.6 Reliability Evaluation of Damage State..... 153

IV.7 Stochastic Basic Parameters..... 155

IV.7.1 Initial Crack Width a_0..... 155

IV.7.2 PDF of Crack Length a_N at Loading Cycle N..... 156

IV.7.3 PDF of the Initial Damage D_0..... 159

IV.8 Equation of the Stochastic-Based Prognostic..... 160

IV.8.1 Development of $d\widetilde{D}_N$ 160

IV.8.2 Development of $d\widetilde{a}_N$ 161

IV.9 Flowchart of the Stochastic-Based Linear Prognostic..... 162

IV.10 Application to the Suspension System..... 163

IV.10.1 Linear Stochastic Case..... 164

IV.10.1.1 One Random Variable..... 164

IV.10.1.1.1 Conversion of Lifetimes into Years..... 165

IV.10.1.2 Two Random Variables..... 166

IV.10.1.2.1 Conversion of Lifetimes into Years..... 168

IV.10.1.2.2 Comparison: Deterministic - Stochastic Results (for Linear Damage Law)..... 168

IV.10.1.2.3 RUL Evaluation of a Suspension in Stochastic Case..... 169

IV.10.1.3 Validation of the Suspension Life under Linear Damage Rule..... 170

IV.10.2 Nonlinear Stochastic Case..... 170

IV.10.2.1 Stochastic Nonlinear Cumulative Damage..... 170

IV.10.2.2 Flowchart of the Stochastic-Based Nonlinear Prognostic..172

IV.10.2.3 One Random Variable..... 173

IV.10.2.3.1 Conversion of Lifetimes into Years..... 173

IV.10.2.4 Two Random Variables..... 174

IV.10.2.4.1 Conversion of Lifetimes into Years.....176
IV.10.2.4.2 Comparison: Deterministic - Stochastic Results (Nonlinear Damage Law)..... 176
IV.10.2.5 Validation of the Suspension Life under Nonlinear Damage Rule.....178
IV.11 Application to the Pipeline Systems to Three Cases.....178
IV.11.1 Equation of the Stochastic-Based Prognostic..... 178
IV.11.2 Generation of Internal Pressure P_i.....179
IV.11.2.1 Monte-Carlo Simulation Principle.....180
IV.11.2.2 Model A: Uniform Generation of Time *t*.....180
IV.11.2.3 Model B: One Initial Triangular Period T_P.....181
IV.11.2.4 Model C: Multi-Triangular Period.....182
IV.11.3 Linear Case of Damage.....183
IV.11.3.1 One Random Variable (Pressure)..... 183
IV.11.3.1.1 Model A for Pressure Generation..... 183
IV.11.3.1.2 Model B for Pressure Generation..... 185
IV.11.3.1.3 Model C for Pressure Generation..... 187
IV.11.3.2 Two Random Variables: Pressure (One Triangular Period)-a_0 (Lognormal Law)..... 188
IV.11.4 Nonlinear Case.....192
IV.11.4.1 One Random Variable (Pressure)..... 192
IV.11.4.2 Two Random Variables (Pressure and Initial Crack Length)..... 194
IV.11.4.2.1 Comparison: Deterministic - Stochastic Results (Nonlinear Damage Law)..... 198
IV.11.5 Validation of the Pipelines Lifetimes in Stochastic Conditions..... 199
IV.12 Conclusion..... 200
References.....201

Conclusion and Future Works..... 205

List of Publications.....209

Thesis Abstracts.....211

Résumé de la Thèse..... 213

GENERAL INTRODUCTION

Due to technological advances and to increasing competitiveness of countries of low production costs, the industrial sectors of developed countries have to face constantly new challenges which are increasingly difficult. These challenges have as principal objective the maximization of competitiveness by the reduction of production costs, the augmentation of the installations profitability, and the creation of innovative products by guaranteeing staff and equipments security, and by respecting the regulations in terms of environmental requirements. The development of solutions capable of improving the production systems performances is then necessary in order to maintain the production sites survival at the heart of the developed countries [1]. Industry is one of the engines of the economic development of a country.

The performance was always a major preoccupation of companies. Nowadays, its evaluation is not only a function of productivity but also of flexibility, costs, delays, quality, safety, social performances, environmental performances, etc. We have shifted then from a one-criterion-evaluation to a multi-criteria-evaluation that can extend the products complete life cycle. We speak then of global performances and long-lasting development. Maintenance is thus a strategic point in the competitiveness progress and improvement. Hence, maintenance knows nowadays a spectacular upswing. In fact, maintenance provides the possibility of exploiting enterprise resources in order to improve their performances by optimizing the utilization of human and material means. Since its beginning, maintenance has not ceased to progress and improve due to the emergence of Information and Communication Technologies (ICT) as well as due to the requirement and exigency imposed by the worldwide economic context. Maintenance has become a true discipline with its own methodologies and concepts.

To make the classical strategies of maintenance more efficient and to take into account the evolving product state and environment, prognostic models need to be developed as a complement of existent maintenance strategies. When the maintenance strategy includes a prognostic function of the equipment remaining useful lifetime, we speak of Prognostics and Health Management (PHM), a domain from which has emerged the "PHM society".

The prognostic is a quite new area of interest, it is the ability to “predict and prevent” possible fault or system degradation before failures occur. Actually, If it is possible to predict the condition of machines and systems, maintenance actions can be taken ahead of time. As a result, minimum downtime can be achieved. Prognosis has been defined as “prediction of when a failure may occur” i.e. a means to calculate the Remaining Useful Lifetime (RUL) of an asset. In order to make a good and reliable prognosis it must have a good and reliable diagnosis.

As a recent discipline, prognostic is a key sub-process for the proactive maintenance [2] for Maintaining systems in Operational Condition (MOC). The integration of a prognostic function in a proactive maintenance process allows in advance, guaranteeing to respond to the different tasks assigned to the system, and to prevent a functioning breakdown as well as expensive maintenance interventions. Let us take for example a ship making journeys for several weeks; it is more appropriate to change an equipment or to embark good replacement equipments before starting the journey than to make a maintenance intervention on the other side of the planet [3].

The systems major part (planes, ships, vehicles, petrochemical systems, etc.) presents a big complexity in terms of their hybrid character. The continuous aspect of the mechanical parts (degraded failure: fatigue for instance) is largely related to the discrete aspect of the electric and electronic parts (binary failure: On/Off). They are systems that contain a large number of variables having complex relationships; hence, they are called: complex systems. Whereas there exists nowadays for the domain of diagnostic instruments that integrate the notion of systems due to experience and methods acquired in the last decades.

Few tools or very specific tools are available in the prognostic domain. Most of the publications on this topic present prognostic in the framework of an elementary system. The objective of diagnostic is to detect and to explain the occurrence of a system failure or breakdown whereas the objective of prognostic is to predict the future state of degradation of a system extrapolated from its current state. In the case of diagnostic we walk backward in time, whereas in the case of prognostic we walk forward in time, or in other words, we anticipate time.

Moreover, predicting the remaining useful lifetime of industrial systems becomes an important aim for industrialists to overcome the occurrence of sudden failures that can lead to very expensive consequences. Then, the recent prognostic approaches try to compensate for the inconveniences emanating from classical maintenance strategies because they neglect the evolving product state and environment. The earlier recent developments in system design technology like in aerospace, defense, petro-chemical and automotive industry have the goal to ensure their high availability.

In the Automatic meaning of the term, prognostic is generally associated with the notion of degradation which represents the accumulation of the system wear out. A prognostic consists of predicting the future evolution of degradation by taking into consideration the factors that modify the degradation dynamics. These factors can be subdivided into two categories: the factors linked to the solicitation of the system (road excitation in mm, gas pressure in MPa, etc.) and those linked to the environment in which the system evolves (humidity, temperature, soil pressure, etc.). Usually, the influence of these two components on degradation is not very well known or even totally ignored.

Various methods have been applied to the prognostic of degraded components. Generally, they are classified in three fundamental families:

- The approaches based on models (**Model-based prognostics**)
- The approaches guided by data (**Evolutionary or trending models**)
- The approaches based on probabilistic techniques (**Experience-based prognostics**)

The model-based prognostic approach is very precise because it has mainly two advantages: the capacity of including the systems physical information and the capacity of re-adaptation to any new information. The data-driven approach requires a large and reliable data sample in order to be accurate. The experience-based approach is well adapted to complex systems but requires an excellent historic data, large feedback and expert knowledge. The new prognostic procedure proposed in this work belongs to the first approach.

This thesis is dedicated to the prognostic evaluation of dynamic systems. The work presented here aims at developing an advanced tool to treat the prognostic evaluation in linear

and nonlinear deterministic context in a first part as well as in the stochastic context in a second part. Our purpose is to prepare a general prognostic tool that can be capable of well predicting the RUL of a system based on an analytical damage accumulation law in either a deterministic or a stochastic context.

Chapter I is devoted to a general prognostic state-of-the-art that encompasses the prognostic approaches existing in specialized literature. Chapter II defines the adopted damage criterion and damage accumulation then develops a recursive model expressed in terms of a degradation index based on a linear aspect of damage accumulation. In order to illustrate the presented methodology, the simulation of an automotive suspension system is considered. Then, a simulation of petrochemical pipelines is illustrated in three modes: unburied, buried, and offshore. Chapter III introduces a nonlinear model for damage accumulation followed by the same applications. Finally, Chapter IV expands the proposed deterministic paradigm to a stochastic domain. The two applications to suspensions and pipelines are considered in this final chapter.

References

[1] K.M. GOH, B. TJAHJONO, T.S. BAINES, and S. SUBRAHMANIAN, "A Review of Research in Manufacturing Prognostics", In 2006 IEEE International Conference on Industrial Informatics, pp. 412-422, New York, USA, August 2006.

[2] A. MULLER: *Contribution à la maintenance prévisionnelle des systèmes de production par la formalisation d'un processus de pronostic.* Thèse de doctorat, Université Henri Poincaré - Nancy I, France, Juin 2005.

[3] F. PEYSSON, *Contribution au pronostic des systèmes complexes*, thèse de doctorat, Université d'Aix-Marseille, France, Décembre 2009.

CHAPTER I

INTRODUCTION TO SYSTEMS PROGNOSTIC

I.1 - Introduction

In the current chapter we present the evolution of maintenance in order to introduce the concept of intelligent maintenance and the role of *Prognostics and Health Management* during the system life cycle. It develops also the state of the art of prognostic approaches: model-based prognostic, data-based prognostic, and experience-based prognostic. This state of the art paves the way for the present work and contribution to this field.

Whether in the domain of mechanics or in civil engineering or in electronics, the desire and the need to make a diagnostic as precise as it can be and to acquire real capacities of prognostic, exist since the first human exploitation of expensive and complex machines. This motivation led to a great number of scientific and industrial works in the purpose to develop and implement different levels of diagnostic and prognostic and hence to optimize maintenance strategies [1]. Maintenance activities have always existed. At the beginning, they consisted of an intervention after a system failure. But rapidly, the unpredicted and sometimes very long shutdowns, due to maintenance interventions, were found to be very expensive. Therefore more advanced maintenance strategies have evolved and were afterward developed.

I.1.1 - Maintenance Evolution

The different maintenance concepts can be classified into three big categories which are: *corrective maintenance*, *preventive maintenance*, and *predictive maintenance*. The corrective maintenance is the maintenance that intervenes after the occurrence of failure in the system, whereas the preventive maintenance is realized when the system is currently functioning [2]. It is important to note that corrective operations intervene only when a failure occurs, whereas preventive maintenance can be programmed in function of different parameters.

Predictive Maintenance (PdM) techniques help determine the condition of in-service equipment in order to predict when maintenance should be performed. This approach offers cost savings over routine or time-based preventive maintenance, because tasks are performed only when warranted. The main value of Predicted Maintenance is to allow convenient scheduling of corrective maintenance, and to prevent unexpected equipment failures. The key is "the right information in the right time". By knowing which equipment needs maintenance, maintenance work can be better planned (spare parts, people etc.) and what would have been "unplanned stops" are transformed to shorter and fewer "planned stops", thus increasing plant

availability. Other advantages include increased equipment lifetime, increased plant safety, fewer accidents with negative impact on environment, and optimized spare parts handling.

The concept of corrective maintenance has the goal of resetting the system to its normal functioning state after the occurrence of its failure.

During the seventies, the concept of preventive maintenance has appeared, and it has the goal of reducing the probability of failure as well as to optimize the costs related to the system usage. One of the first used strategies was the *systematic maintenance* that consists of executing regular interventions at equal time intervals, following an a priori and well determined schedule. The optimization of such strategy consists of evaluating the operations periods albeit in preventing the system failure by following very frequent operations. The system availability is thus increased but financially this strategy remains not very rewarding and many studies have shown that the usage time is not the only factor leading to failure occurrence. The periodicity of interventions can be calculated in function of time or of the number of usage units (number of functioning cycles, number of kilometers, number of manufactured products, etc...).

Since the eighties, due to the evolution of information resources, new maintenance strategies were born. Their principle consists of using real-time information in order to monitor continuously certain significant parameters of degradation or of system performance. We speak then of *conditional maintenance*. The interventions planning rely then on the existence and determination of the critical thresholds of these significant parameters; hence, we speak of decision thresholds. Thus, the predictive maintenance appears. It is subordinated to the analysis of the surveyed evolution of the significant parameters of degradation. The estimation of the output of this parameters monitoring, allows to delay or to speed up maintenance interventions.

The conditional and predictive maintenances assume that the intervention will occur before the occurrence of the failure of the monitored system evolution. This is why, during the nineties, new methodologies, called *proactive maintenance*, were invented in order to monitor continuously not the system evolution but the evolution of primary causes of failure occurrences of the monitored system.

It is important to note that during the period of the evolution of maintenance strategies, we observe also a change in maintenance management. In fact, distant maintenance has rapidly evolved and advanced local maintenance due to communication networks. Following the Internet big bang, the concept of distant maintenance has transformed to e-maintenance [3]: it is a concept that uses web services for a better cooperation among the different components of maintenance, for a better sharing of knowledge, and a follow up in real time of the system from anywhere around the world. The emergence of these concepts and the economic context allowed the enterprises to externalize this service by using specialized agents.

I.1.2 - Maintenance Optimization

The maintenance optimization consists of finding a middle point between preventive maintenance and corrective maintenance, all this by respecting fixed objectives. The maintenance interventions dates are then determined in a way to optimize a criterion reliant on maintenance cost, on equipments availability, as well as on security, or more on a compromise among the three of them.

Moreover, if we have many ways of monitoring many financial resources, and if we replace very frequently the system equipments, then we will observe few failures. On the contrary, if we dispose few financial means, and we don't do the equipment maintenance, then we will observe a great number of failures. It seems evident that the failure costs are inversely proportional to the maintenance costs. In fact, the money saved due to less maintenance will be spent on the interventions for the system recovery in order to return to its normal state. The absence of system maintenance leads equally to system failures in chain. The sum of the costs of maintenance and failures represents the total cost to maintain the system functioning. An optimal maintenance is a maintenance that minimizes at the same time the costs related to systematic maintenance and the costs related to system recovery after a failure. This optimal maintenance can be attained by using a helping automated system to maintenance in order to identify the equipments that have to be maintained and sustained.

This first analysis shows that there exists an increasing interest in intelligent maintenance in which surveillance occupies a fundamental place [4]. In the scientific community, principally in the Automatic and Artificial Intelligence communities, surveillance led and is still leading to a big number of research and works. These works have equally evolved with time, starting from a simple detection of a bad functioning, passing by failures

diagnostic and degradation diagnostic, and is oriented nowadays to prognostic and the prediction of degradation and failures. The following section presents the intelligent maintenance as well as the principal concepts and the notion of degradation for prognostic is then introduced, followed afterward by the state of the art of the known approaches to prognostic. At the end of this chapter, a summary of the different approaches is presented.

I.2 - Intelligent Maintenance

As we have already discussed in the previous paragraph, the maintenance function cannot be reduced to the sole activity of maintenance of a set of machines. It has also the task to intervene during the whole system exploitation cycle: the choice and the conception of the material, the determination of the maintenance plans, the organization and the logistic of the maintenance activities, the follow up and the analysis of the system evolution, the prediction of the system future evolution, etc. The intelligent maintenance differs from the traditional policies of maintenance which are based on a static threshold of alarm. The power of intelligent maintenance lies in the analysis and the follow up of the health of the equipments coming from a set of data inferred from the ERP (Enterprise Resource Planning), the MPAC (Management of Production Assisted by Computers), the MMAC (Management of Maintenance Assisted by Computers), or even from surveillance systems which are based on the measurements of physical variables provided by sensors. This dynamic follow up of the performances and of the system state of degradation requires the acquisition, the centralized management, the validation, and finally the analysis of the huge set of data of very different nature.

Appearing at the beginning of the third millennium, the term *Prognostic and Health Management* (PHM) was defined as an approach that uses measurements, models and algorithms to detect failures, to evaluate the health and to predict the system degradation evolution [5]. The PHM is a sustaining approach during the whole system life cycle, and whose objective is to reduce, even also to eliminate the inspections of the system and the maintenance at regular intervals, by using monitoring and prediction instruments dedicated and related to the logistic chain of the system, leading hence to an unprecedented reactivity. Inheriting the principles of Condition Based Maintenance (CBM), the concept of PHM expands its capacities and proposes a robust framework for the optimization of maintenance and of the logistic in order to increase the operational availability of the system.

A modern tool of PHM can include a great number of functions [6] such as:

- The detection and the isolation of failures
- Advanced algorithms of diagnostic and prognostic
- Algorithms of failures and degradation tolerance
- Estimation of the remaining useful lifetime of an equipment
- The follow up of the health and/or of the degradation of an equipment
- The filtering: the alarms and information management by yielding the right information to the right person at the right time
- Helping algorithms to the decision making for the system management
- Etc.

The major part of these functions is the evolutions of the functions put in order in monitoring and diagnostic systems [7]. Based on the concepts of the management of equipments health, the tool of PHM uses these functions in a complementary way in order that they have a better impact on maintenance activity, rather than by using them each one alone. Even if each of these functions is developed and improved at the same time as the tool of PHM, the prognostic represents a new function which seems to be very difficult and even to be risky from a technological point of view [8]. In literature, the PHM approach of maintenance is usually represented by the cycle PHM [8,9].

One of the main differences is the positioning of the diagnostic relatively to prognostic. The implementation of the PHM approach is done in two phases:

- A first phase that has the objective of studying which factors act on the system health and how they influence it. This study allows determining which health indicators pertain for the considered system and to establish the adequate diagnostic and prognostic algorithms.

- A second phase that consists in the integration and the implementation of the tools determined in the first phase. The first step is a step of signal processing in order to extract the system health indicators. These indicators are used by the step of monitoring to estimate the system current health state. The current health state serves then as a starting point for the diagnostic and prognostic algorithms whose corresponding goals are the isolation of failures and the prediction of the system health evolution. The outputs of these algorithms are used to adjust the plan of maintenance and/or to modify the system control parameters. We speak then of tolerance to failures or to degradation.

The *Prognostic* is currently one of the most difficult aspects in the PHM cycle as well as the aspect having the biggest potential in terms of reducing the costs of functioning and of logistic during the whole lifetime cycle of a complex system, even in terms of improving its availability and security [10]. With the advent of the prognostic techniques, we observe equally a change in the behavior of the industrialists who do not buy anymore nowadays a maintenance service but who buy an availability machine.

I.3 - Degradation Prognostic

I.3.1 - Degradation versus Prognostic

Diagnostic and prognostic are two words of Greek origins. In the etymological sense, diagnostic is the acquisition of knowledge from observable signs, whereas prognostic is precognition or knowing in advance. In the automatic sense, the meaning of the two words is more precise and technical. Diagnostic consists in the regression in time in order to explain why the system is in a given state at instant t. Prognostic consists of anticipating in time in order to predict the system future state at the instant $t + \Delta t$. Diagnostic and prognostic are two parallel processes that can be used complementarily or separately [1].

Diagnostic and prognostic remain intrinsically linked by the chain "causes-consequences", as well as by the concepts that they manipulate to learn: defects, failures and degradations. These last concepts have in literature different definitions for different authors. We will use the following definitions [10]:

- A *fault* is the deviation in behavior between an observed characteristic and a theoretical characteristic.
- A *failure* is the inability of an equipment to accomplish its function.
- A *degradation* is the wear out of the equipment, and the decrease of its performances.

Fault and failure are concepts that we qualify as discrete since they represent a state of the equipment, whereas degradation is a continuous concept that evolves during the equipment lifetime.

I.3.2 - Equipment Degradation Trajectory

The Assurance In Functioning (AIF) is nowadays a discipline largely used in order to predict equipment failures. The component of this discipline dedicated to prediction is the reliability that characterizes the probability that an apparatus accomplishes a required function in given conditions, and during a given time [11]. The graphs of oriented states are a tool used by reliability experts in order to represent the evolution of equipments states. The nodes of the graph constitute the equipment states and the arcs represent the transition among states (figure 1.1).

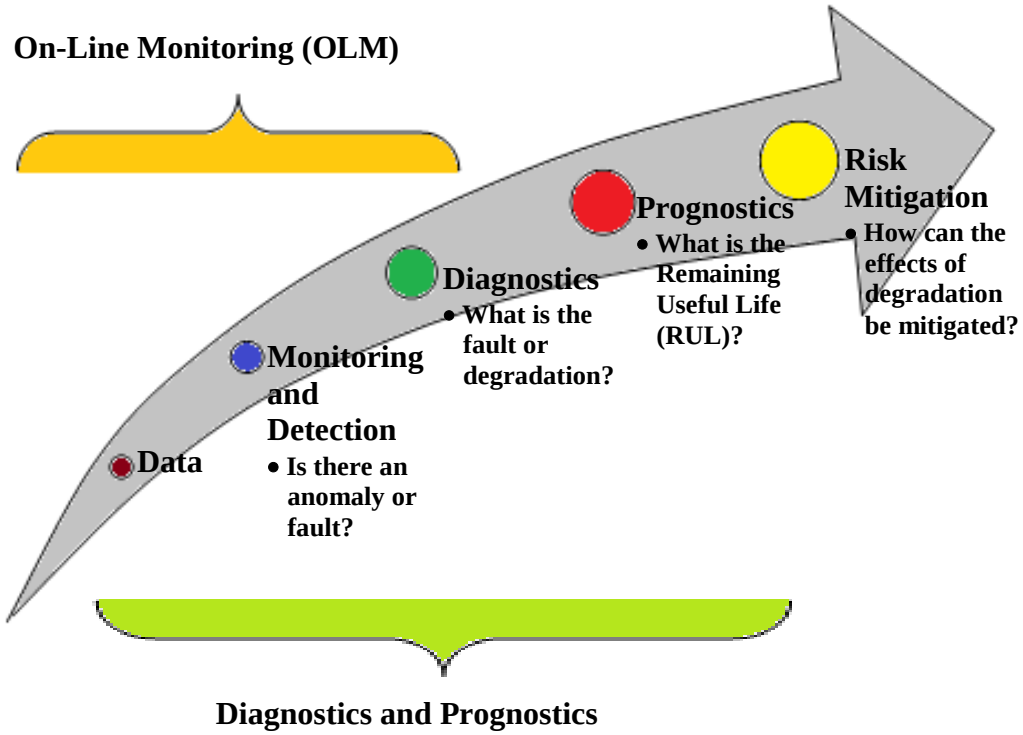

Figure 1.1 - Diagnostic-Prognostic Chain of "Causes-Consequences".

The state "New" represents the equipment newly coming from the factory. It is a phase whose objective is to eliminate the initial faults. Following this phase, the equipment is put in service and is integrated in a set in order to function in its nominal state. When the equipment reaches the end of its life, it passes to the state of fault. In the fault state, the equipment is still functioning but in a non-nominal way and with reduced performances, till it passes to the state of failure where it is no more functioning. When the equipment is in the state of fault or the state of failure, an operation of maintenance allows restoring the equipment nominal state (figure 1.2).

The reliability community has a discrete vision of the equipment life to the contrary of the automatic community of PHM that characterizes the life of an equipment by a continuous variable. The members of the automatic community consider that degradation is a process that evolves during the whole equipment lifetime till it attains a critical threshold of fault that leads to the state of failure. This variable is generally an indicator of health or of degradation of the equipment and that is normalized between 0 and 1 where degradation is the complement of the 1 of health.

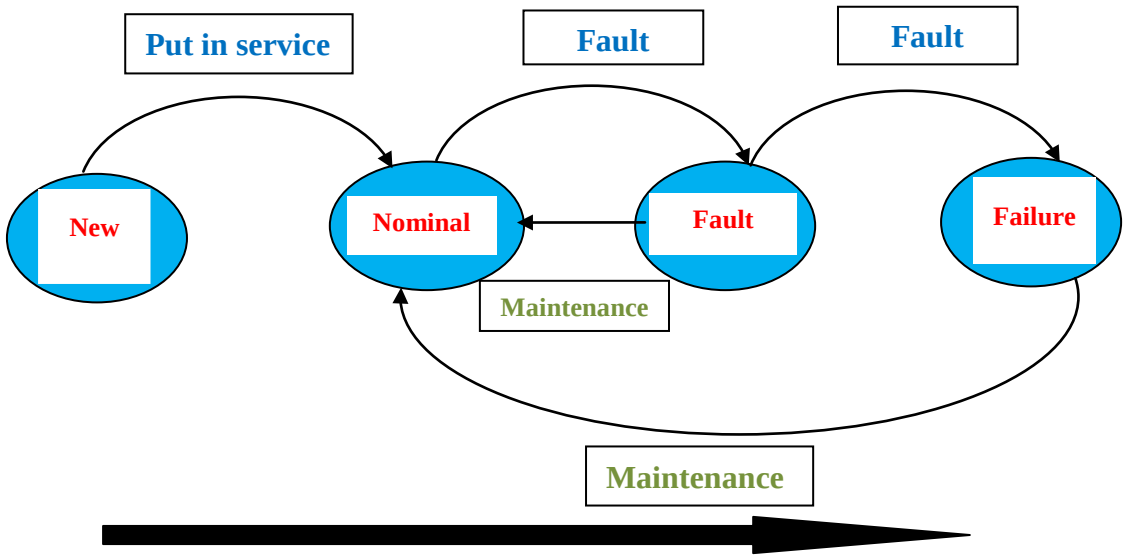

Figure 1.2 - Oriented Graph of the Equipment Life States

A degradation trajectory is defined in a state space as the way followed by the degradation state, in function of the modes of equipment degradation. Most of the equipments have many modes of degradation, where each mode has a unique trajectory [5]. The objective of PHM tools is to follow and to update the real degradation trajectory of given equipment and to predict the evolution of this trajectory in function of the future usage of the equipment [12] (figure 1.3).

In damage theory, there exist two types of degradation: isotropic and non-isotropic. The models of isotropic degradation are the simplest models of damage theory, where the nonlinear degradation behavior is represented by one internal variable [13]. This variable can be considered as a degradation indicator. In the case of non-isotropic degradation models, the nonlinear degradation behavior is represented by a tensor [14]. In the PHM approaches, we consider usually the isotropic models, because they are generally sufficient in order to achieve

a good prediction and measurement of the remaining useful lifetime of an equipment [15]. Each scientific discipline has its own proper models, but whatever the concerned phenomenon, the degradation trajectory emanating from these models, adopts either a linear, concave, or convex form (figure 1.4).

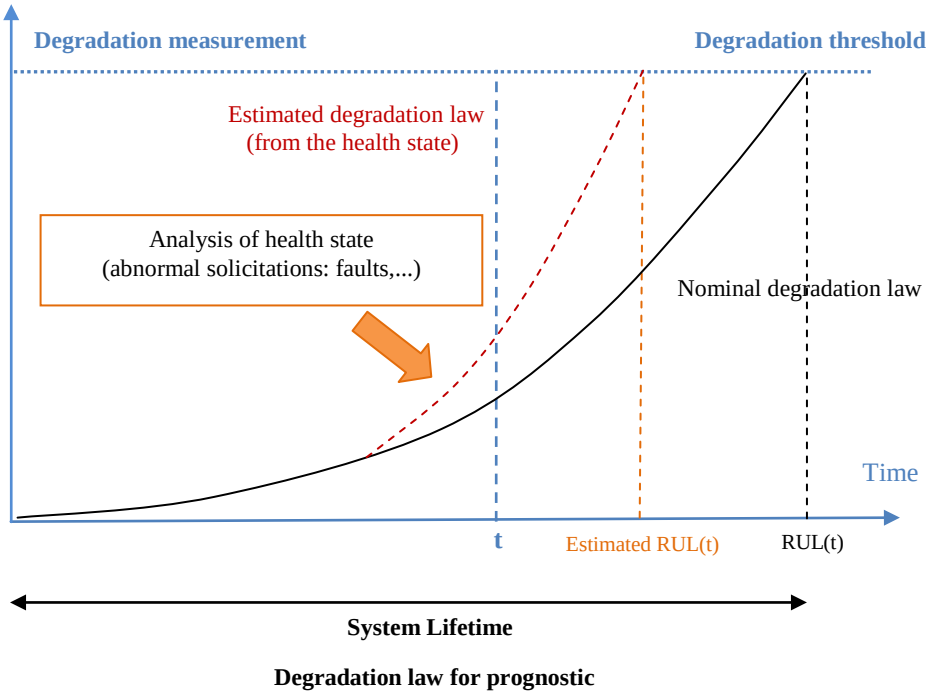

Figure 1.3 - Estimated and Nominal Degradation Trajectory of an Equipment.

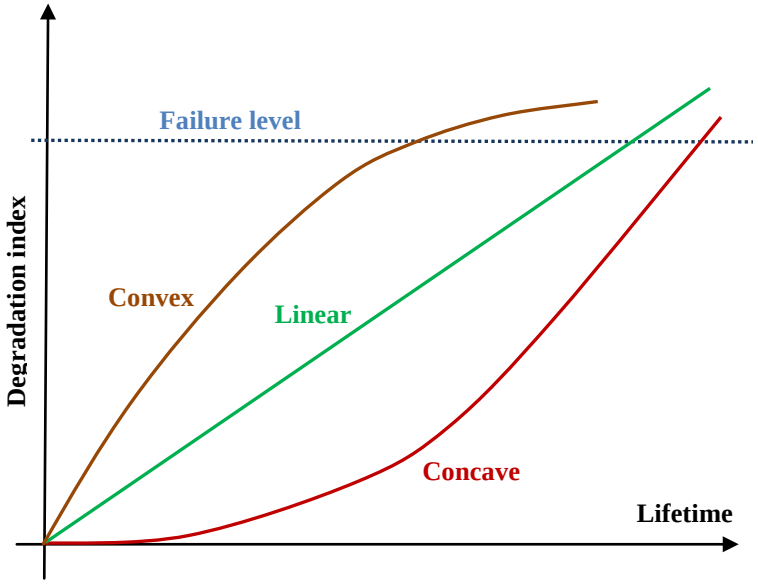

Figure 1.4 - Different Trends for Degradation Trajectory.

I.3.3 - Definition and Methodologies

In literature, from one author to another, the definition of prognostic changes [16-21], but they all agree on one point: prognostic is a process encompassing a capacity of prediction. The main difference among the proposed definitions is the horizon on which this prediction is performed. For some authors, prognostic is the capacity to detect and isolate the newborn defects or even the elements leading to defects. For others, prognostic is the capacity to estimate the remaining useful lifetime (RUL) of an equipment in function of its functioning history and its future usage. The remaining lifetime is typically defined in terms of time, of charge cycle, or of mission [5]. In the first case, the horizon of prediction is the short term since the defect already exists, whereas in the second case, the horizon is the long term. The expression "predictive diagnostic" is more explicit in the first case [7].

Whatever the methodology used for prognostic or predictive diagnostic, the notion of degradation is an intrinsic element since it characterizes the equipment usage. The predictive diagnostic can be considered as being the diagnostic of a degradation state, where the degradation state is a sub-state of the equipment nominal state. A notion equally linked to prognostic is the notion of uncertainty since it is very difficult to predict the future in a sure and certain way [22].

The analysis of different methodologies of prognostic in literature allows us to put in evidence two principles of prognostic approaches. The difference between the two principles is situated at the level of usage of the degradation variables in a direct or indirect way.

In the first principle of approach, where these variables are used, the process of prognostic is based on the concept of degradation trajectory. It consists of estimating the evolution of the trajectory from the available given data and to make this trajectory evolve in the future by using or not the future utilization conditions of the equipment. In the second principle of approach, we do not seek to know the level of the equipment degradation. It consists of estimating, then to extrapolate an indicator, such as for example the RUL, from the observations of the equipment output variables.

The behavior of the equipment is represented by an input variable vector $\underline{U}$, an output variable vector $\underline{Y}$, and three functions that express:

- The evolution of the internal variables that characterizes the equipment dynamics, its behavior in function of the input variables, in function of its environment, and in function of its degradation state.

- The evolution of the degradation variables. It is this evolution that defines the degradation trajectory of the equipment. It is conditioned by the usage of the equipment and characterized by its environment and its input variables as well as by the internal variables.

- The output function that defines the output variables from the internal variables. The output variables are directly observable on the contrary to the internal variables.

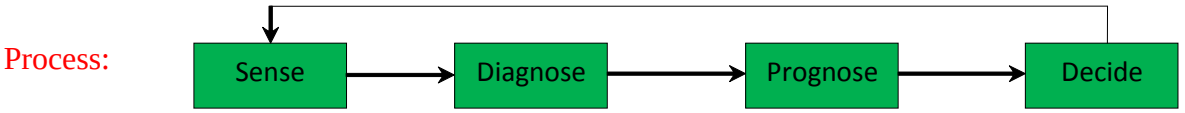

Determine:	Vibration Temperature Pressure Fuel flow Speed Material damage	Trends Deviations Fault location Fault classification Damage mechanism - wear (high probability) - cracking (low probability)	Limits for reliable performance. Probability of failure Remaining useful life	Short-term readiness (days) - mission plan Long-term readiness (yrs.) - maintain/inspect - retire/replace
Tools:	Accelerometers Thermocouples Pres. transducers On-line-NDE (Non Destructive Evaluation) Human senses	Pattern recognition Neural nets Physics models	Expert systems - experience - rules/AI Life prediction -physics/materials models Fuzzy logic Probabilistic mechanics	Risk analysis Decision analysis Optimization Financial analysis

Table 1.1 - Key Elements in the Prognosis Process.

As indicated in table 1.1 [23], the fundamental goal of all of these approaches is to facilitate decisions based on better information — whether for mission planning in the field (over the short term), or sustainment at the depot (over the longer term). In fact, the optimum prognosis system is likely to be some combination of traditional data-driven methods and probabilistic mechanics methods. Thus, in many respects the above tools can be viewed as being complementary.

I.4 - Prognostic Definition

The term prognostic founds its origin in the Greek word “progignôskein” which means “to know in advance”. Industrial Prognostic is called the prediction of a system’s lifetime and corresponds to the last level of the classification of damage detection methods introduced by [1]. Prognostic can also be defined as a probability measure: a way to quantify the chance that a machine operates without a fault or failure up to some future time. This "probabilistic prognostic value" is all the more an interesting indication as the fault or failure can have catastrophic consequences (e.g. nuclear power plant) and maintenance manager need to know if inspection intervals are appropriate. However, a small number of papers address this connotation for prognostic [24,25].

Finally, although there are some divergences in literature, prognostic can be defined as: "prognostic is the estimation of time to failure and risk for one or more existing and future failure modes" [26]. In this connotation, prognostic is also called the "prediction of a system's lifetime" as it is a process whose objective is to predict the remaining useful life (RUL) before a failure occurs given the current machine condition and past operation profile [27]. The main steps defined in this standard are summarized in figure 1.5.

Figure 1.5 - Summary of the ISO 13381-1: 2004 Standard Main Steps

The first step consists of monitoring the system by a set of sensors or inspections achieved by operators. The monitored data are then pre-processed in order to be used by the Diagnostic module. The output of this module identifies the actual operating mode. This state is then projected in the future, by using adequate tools, in order to predict the system’s future state. The intersection point between the value of each projected parameter or feature and its corresponding alarm threshold leads to what is known as RUL (Remaining Useful Life) of the system (figure 1.6). Finally, appropriate maintenance actions can be taken depending on the estimated RUL. These actions may aim at eliminating the origin of a failure which can lead the system to evolve to any critical failure mode, delaying the instant of a failure by some maintenance actions or simply stopping the system if this is judged necessary.

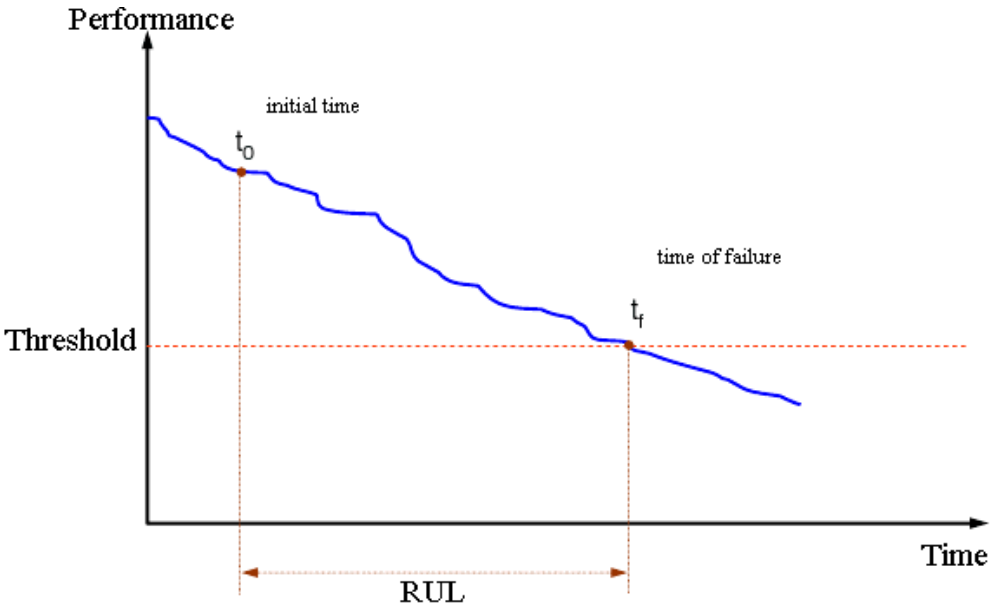

Figure 1.6 - RUL Interval Definition.

I.5 - The Role of Prognostic in Lifetime Process

Each system or component of a system passes by three periods during its functioning life. The last phase during each system life represents the degradation period leading to failure by progressive deterioration. It is important to predict, at each instant, the remaining lifetime in order to prevent expensive defects and to avoid catastrophic failures.

Prognostic is a process encompassing a capacity of prediction. It is the ability to estimate the remaining useful lifetime (RUL) of equipment in terms of its functioning history and its future usage. Predicting the RUL of industrial systems becomes currently an important aim for industrialists knowing that the failure, whose consequences are generally very expensive, can occur suddenly.

The classical strategies of maintenance [8] based on a static threshold of alarm are no more efficient and practical because they do not take into consideration the instantaneous product functioning state. Adopting preventive systematic maintenance by frequent replacement to increase the system availability is an expensive strategy [28,29]. The introduction of a prognostic approach as an "intelligent" maintenance consists of the analysis, the health follow up and monitoring, based on physical measurements using sensors.

The RUL of a system in service can be expressed in hours of functionning, in Kilometers run or in cycles. If we can effectively predict the condition of machines and systems, maintenance actions can be taken ahead of time. Good and reliable prognosis needs good and reliable diagnosis.

The science and technology of prognosis and structural health management offer the potential for significant enhancements in the safety, reliability and availability of high-value resources [30,31]. This concept is based on a closed-loop process whose successful implementation depends on the integration of several multi-disciplinary elements including [23]:

1) Onboard sensing of operational parameters and material damage states;

2) Diagnosing trends, fault conditions, and underlying damage;

3) Predicting remaining useful life in terms of probability of failure and limits on reliable performance,

4) And deciding upon appropriate courses of action: whenever or not the resource is capable of performing a given mission, or alternatively, is in need of inspection, maintenance, or replacement.

I.6 - State-of-the-Art of the Prognostic Approaches

Various approaches to prognostics have been developed that range in fidelity from simple historical failure rate models to high-fidelity physics-based models [32]. The required information (depending on the type of prognostics approach) include: engineering model and data, failure history, past operating conditions, current conditions, identified fault patterns, transitional failure trajectories, maintenance history, system degradation and failure modes.

Putting at work a prognostic process consists of executing a set of treatment from input information. The different approaches of prognostic are grouped in function of their applicability as well as their economic yield. They are three families [20,32]:

- The approaches based on models (**Model-based prognostics**)
- The approaches guided by data (**Evolutionary or trending models**)
- The approaches based on experience (**Experience-based prognostics**)

The pyramid reproduced in the figure 1.7 highlights the hierarchy of these different families. According to [33], making the choice of an approach family is done by answering two questions:

- Is it possible to construct a physical model for the degradation mechanisms?
- Is the instrumentation of the equipment sufficient in order to evaluate a degradation evolution indicator?

If the answer to the first question is positive, the implementation of an approach based on physical models is considered. Moreover, if the answer to the second question is positive, an approach guided by data is possible. In the case where the answer to the two questions is negative then an approach based on expert knowledge and feedback is the best solution. A study realized on more than 100 publications in the field of prognostic [34] shows that in the industrial sector, the approaches guided by data and based on experience are the most implemented ones.

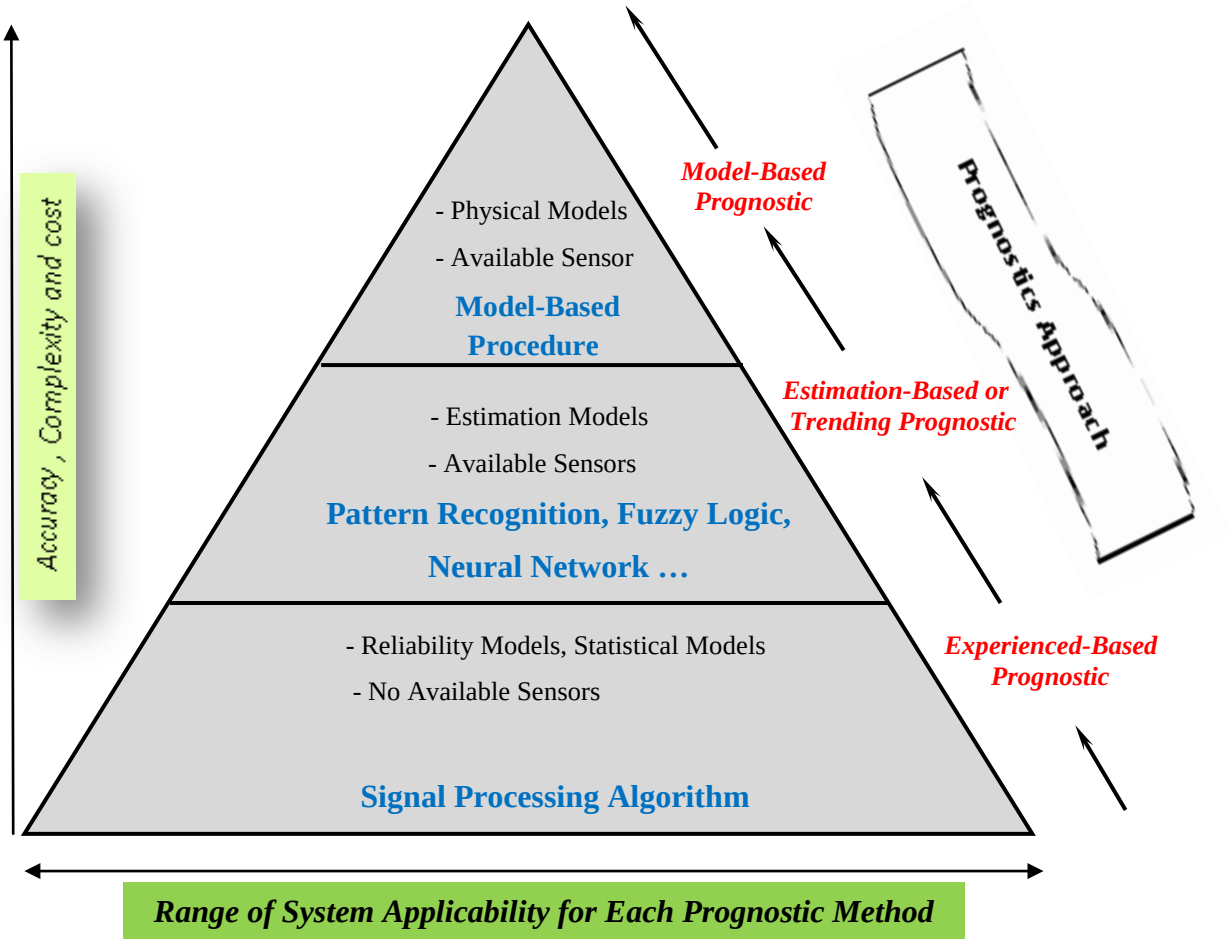

Figure 1.7 - Prognostic Technical Approaches.

I.6.1 - Prognostic Based on Models

This approach is also called model-driven or physical model. As its name indicates, this approach family uses models that can be of two different types [35,10]:

- Model based on the equipments physics
- Mathematical models constructed by experimentation

This "Physical model" is based on mathematical description of degradation process and on its level evolution using NDI monitoring (Non-Destructive Inspection). It is described to be more flexible and precise than the two other approaches.

The degradation is then considered as a continuous variable whose evolution is characterized by a deterministic or a stochastic law. The concept of these methodologies is to make the constructed model evolve till a wanted future instant, from an initial degradation state and the future usage of the equipment [36]. The equipment is considered as faulty when the degradation variable reaches a predefined threshold in the case of an isotropic model, or a predefined surface in the case of non-isotropic model. These models can be: nonlinear equations [37], models defined by expert analysis [38], or even by physical models of chemical corrosion [39], of mechanical fatigue [40], etc.

For some equipments and critical structures, it is necessary to estimate the initiation and the crack propagation. The models based on crack propagation are interested in the problems dealing with material properties, and they have evidently an important interest in prognostic, but they are usually adapted for a real-time treatment due to their big computational complexity [8]. A technique, among others, capable of predicting the slope of increase and the directions of the crack, is the simulation by decomposition in finite elements.

The decomposition in finite elements is used to study the behavior of an equipment in different disciplines such as thermodynamics, fluids mechanics, structures mechanics etc...The method of finite elements is based on the idea that a complex system can be subdivided into small parts called elements. Each element is completely defined by its geometry and its physical properties. The study of each element is then simpler than the study of the complete structure that they compose. Each element can be considered as a continuous part of the structure. The decomposition in finite elements converts a continuous structure into a system of algebraic equations or into ordinary differential equations. The solution of a

problem using the theory of finite elements invokes methods of research of simultaneous solutions to the reaction of each element to charges, to constraints, and to the interaction among the adjacent elements. An example of the application of this theory is the prognostic for a system of transmission of a helicopter; it is presented in [41].

The model-based methods assume that an accurate mathematical model can be constructed from first principles. This approach to prognostic requires specific failure mechanism knowledge and theory relevant to the monitored machine. The existing papers propose different model based solution for the industrial problems. Bartelmus and Zimroz [42] estimated through a demodulation process, the vibration signal for a planetary gearbox in good and bad conditions. Kacprzynski *et al.* [43] proposed fusing the physics of failure modeling with relevant diagnostic information for helicopter gear prognostic.

Chelidze and Cusumano [44] proposed a general method for tracking the evolution of a hidden damage process given a situation where a slowly evolving damage process is related to a fast, directly observable dynamic system. Luo *et al.* [45] introduced an integrated prognostic process based on data from model-based simulations under nominal and degraded conditions. Oppenheimer and Loparo [46] applied a physical model for predicting the machine condition in combination with a fault strengths-to-life model, based on a crack growth law, to estimate the RUL. Adams [37] proposed to model damage accumulation in a structural dynamic system as first/second order nonlinear differential equations. Chelidze [47] modeled degradation as a "slow-time" process, which is coupled with a "fast-lime", observable subsystem. The model was used to track battery degradation (voltage) of a vibrating beam system.

Li *et al.* [48] and [49] introduced two defect propagation models via failure mechanism modeling for RUL estimation of bearings. Ray and Tangirala [50] used a nonlinear stochastic model of fatigue crack dynamics for real-time computation of the time-dependent damage rate and accumulation in mechanical structures. A different way of applying model-based approaches to prognostic is to derive the explicit relationship between the condition variables and the lifetimes (current lifetime and failure lifetime) via failure mechanism modeling. Two examples of research along this line are [51] for machines considered as energy processors subject to vibration monitoring and [52] for bearings with vibration monitoring. In [53] and [54] the problem of forecasting machine failure is illustrated for a high power fan bearing and a railroad diesel engine. Engel *et al.* [18] discussed some

practical issues regarding accuracy, precision and confidence of the RUL estimates. Lesieutre *et al.* [55] developed a hierarchical modeling approach for system simulation to assess the RUL.

A first example is given by Chelidze who models the loss of tension (degradation) of a battery providing energy to an electromagnetic oscillator, by coupling two models [56,57]:

$$\begin{cases} \dot{x} = f\left(x, \mu(\phi), t\right) \\ \dot{\phi} = \varepsilon\, g\left(\phi, x, t\right) \end{cases} \tag{1}$$

where x is an observable variable of the system state, ϕ is an internal scalar variable related to the degradation, ε represents the difference in time scale, $0 < \varepsilon << 1$. $\mu(\phi)$ represents the variation of the battery characteristics in function of the degradation. Moreover, a Kalman filter is used to determine the current value $\tilde{\phi}(t)$ in function of the observed measures. The estimation of the Time To Failure (TTF) denoted by T_{TTF} is then given by the solution of the equation [58]:

$$\dot{\phi} = \bar{g}(\phi) \tag{2}$$

where $\bar{g}$ is obtained by applying the concept of means to g. The model of degradation used for prognostic is then related to the original slow subsystem (1) by taking the mean on a long period of the field of vectors of g, hence the time to failure will be:

$$T_{TTF} = \int_{\tilde{\phi}(t)}^{\phi_{\text{limit}}} \frac{d\phi}{\bar{g}(\phi)} \tag{3}$$

with ϕ_{limit} is the critical value of degradation for which the battery is considered as unusable.

A second example is the proposition of the generic methodology in the case of models with an application to a quarter of a vehicle suspension [59]. This used model is very close to the previous one:

$$\begin{cases} \dot{x} = f\left(x, \lambda(\theta), u, t\right) \\ \dot{\theta} = \varepsilon\, g(x, \theta, t) \\ y = Cx + Du + v \end{cases} \tag{4}$$

where x is the system state vector, θ is the degradation state vector, λ is the system parameter vector in function of the degradation state, u is the system input vector, ε is the time scale, y is the system output vector, and v is the measure noise.

The generic methodology proposed for model based prognostic is reproduced in figure 1.8 below:

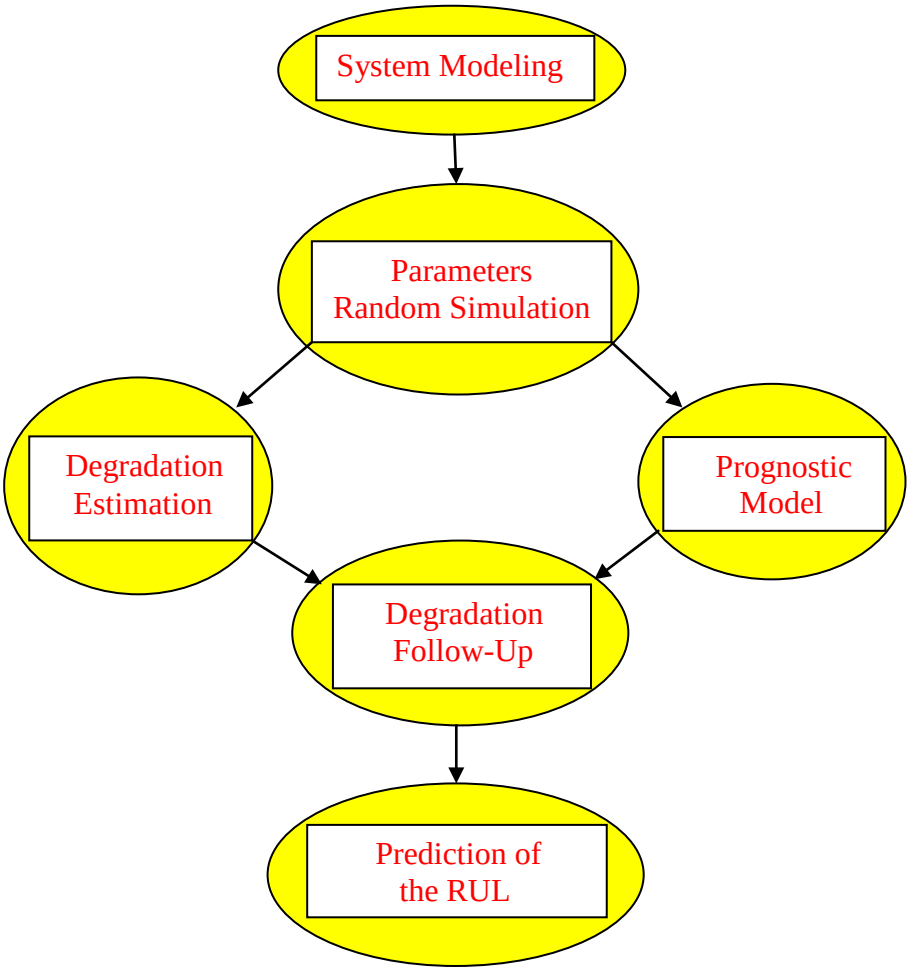

Figure 1.8 - Generic Methodology for the Model-Based Prognostic According to [60]

The first step consists of establishing a model using coupled differential equations (4). The second step is the simulation of the model obtained under different operating conditions. The input vector u is an uncertain element corresponding to inputted loading or excitation. It is then necessary to identify the different operating modes (the different classes of the input

vector) whose parameters are defined by the laws of probability. A Monte Carlo simulation is then executed for each operating mode. The result is a set of degradation trajectories.

During the simulation, in order to decouple the slow-time mode from the fast-time mode, the principle of the mean is used. That means that the state of degradation is computed at a fixed period before injecting it in the fast-time mode. The different trajectories obtained for the different functioning modes define the prognostic model. The degradation estimation step consists of defining a method of degradation observation or an image of degradation from the system measure vector *y*. The follow up step of degradation allows on one hand to determine the current value of the degradation state and on the other hand to construct a prediction model of the operating modes by using a tool such as Markov models. To finish, the prognostic is realized by projecting the degradation trajectory following the prediction model of the functioning mode established in the previous step, until the state of degradation reaches the limit threshold ϕ_{limit} .

The estimation of the degradation state is a key point in the success of the methodology but it remains very difficult due to the fact of the very weak degradation dynamics and due to the measurements noises. A method based on the use of observers of convergence in finite time in order to estimate the state of degradation of a model similar to (4), is presented in [61].

I.6.1.1 - *Advantages and Drawbacks of the First Approach*

The main advantage of model based approaches is their ability to incorporate physical understanding of the monitored system [58]. In addition, in many situations, the changes in feature vector are closely related to model parameters and a functional mapping between the drifting parameters and the selected prognostic features can be established [58]. Moreover, if the understanding of the system degradation improves, the model can be adapted to increase its accuracy and to address subtle performance problems. Consequently, they can significantly outperform data-driven approaches (next section). But, this closed relation with a mathematical model may also be a strong weakness: it can be difficult, even impossible to catch the system's behavior. Further, some authors think that the monitoring and prognostic tools must evolve as the system does.

I.6.2 - Prognostic Guided by Data

This approach is also called Data-driven or evolutionary or trending or estimation-based approach or artificial intelligence.

In certain cases, it happens that we dispose of a database containing the history of scenario degradation/failure represented by a set of time series. These bases are given without the use of a physical model of equipment behavior. The evolution of the degradation indicator is then realized with the help of a statistical method. Depending on the method used, three classes of approaches can be distinguished [32,62]:

- The prognostic by trend analysis
- The prognostic by learning
- The prognostic by state estimation

The indicator or the indicators of degradation are primordial elements of prognostic driven by data. They are determined by a statistical calculation that quantifies the state of the equipment wear out. The multi-variables statistical techniques are powerful tools capable of compressing data and reducing their dimensions in a way that the essential information is maintained. They can also manipulate the noise and the correlation in order to extract information efficiently. The principle function of this type of techniques is, using a mathematical procedure, to transform a certain number of correlated variables into a smaller set of non-correlated variables [63].

The data-based approaches require that the information extracted from sensors be sufficient in quality and quantity in order to evaluate the current state or the image of the current state of the system degradation.

The concept of this approach consists of collecting information and data from the system and projecting them in order to predict the future evolution of some parameters, descriptors or features, and thus, predict the possible probable faults. Without being exhaustive, mathematical tools used in this approach are mainly those used by the artificial intelligence community, namely: temporal prediction series, trend analysis techniques, neuronal networks, neuro-fuzzy systems, hidden Markov models and dynamic Bayesian networks [4,7,62].

The advantage of this approach is that, for a well monitored system, it is possible to predict the future evolution of degradation without any need of prior mathematical model of the degradation. However, the results obtained by this approach suffer from precision, and are sometimes considered as local ones (for the case of neural networks and neuro-fuzzy methods). In addition, the monitoring system must be well designed to insure acceptable prognostic results.

The Data-driven approaches use real data gathered on-line with sensors or by operator measures to approximate and track features revealing the degradation of components and to forecast the global behavior of a system. Indeed, in many applications, measured input/output data is the major source for a deeper understanding of the system degradation. Data-driven approaches can be divided into two categories: artificial intelligence (AI) techniques (neural networks, fuzzy systems, decision trees, etc.), and statistical techniques (multivariate statistical methods, linear and quadratic discriminators, partial least squares, etc.) [4,7,62].

I.6.2.1 - Prognostic by Trend Analysis

This type of approach is based on the derivation of the indicator of the degradation state from its normal functioning state. The tools used in order to put in work these approaches are the tools of prediction of time series and the models of multi-variables classification. The choice of a tool depends on the number of degradation indicators as well as on the number of modes of functioning identified.

The tool may be very simple like for example a linear regression. In this case, the *n* last points computed from the degradation indicator are used to estimate the coefficients of the affine function characterizing the indicator trend. Prognostic is then accomplished by the determination of the point of intersection of this function with the critical threshold of failure. The result of prognostic is then in this case, the time before equipment failure [44]. Based on the same principle, a predictive model of type ARMA (Auto Regressive with Mobile Average) can be used [64]. The parameters of this model are then updated in real time with the help of a least squares algorithm. The authors in [65] use a prediction method for the degradation state of a compressor. The tool used for this type of prognostic could be the Principle Components Analysis technique (PCA) or the linear and quadratic discrimination [66]. These tools can be also applied on temporal indicators or on frequency indicators [67].

Generally, this type of prognostic gives better results at the system level rather than at the equipment level since the system performances degradation is usually the result of the interaction of the different constituent equipments with degraded functioning [44]. The trend analysis and the indicator prevision can be also realized in function of the variables influencing the degradation [68].

I.6.2.2 - Prognostic by Learning

This type of prognostic uses principally techniques issued from machine learning and artificial intelligence. Currently, the principle techniques used are Artificial Neural Networks (ANN) [69]. An ANN is a tool, generally used for nonlinear models, that allows establishing a functional relation between an inputs vector and a desired outputs vector. The parameters of these models are adjusted in order to have optimal performances. Different techniques can be used to adjust these parameters such as the optimization technique.

The network is, firstly, trained by using data representing the evolution of degradation during the whole equipment lifetime, until a failure occurs. Afterward, the network is used to detect or predict an evolution of the degradation indicator using other data, always remaining in the same modes of functioning during the period of learning. The inputs of the network are generally the discrete values of the indicators from instant t_{k-n} till t_k and the outputs are:

- Either the current state of the equipment. In this case the network realizes a classification in order to know the input situation based on the learned situations.
- Or either the values of the degradation indicators at instant t_{k+T}. The network realizes then an extrapolation from the input situation.

In the domain of ANN, the Dynamic Wavelet Neural Networks (DWNN) are used. Their structure is of the form:

$$y_{k+1} = \mathrm{WNN}\left(y_k, \ldots, y_{k-m}, u_k, \ldots, u_{k-n}\right) \tag{5}$$

with u_k is the input vector and y_k is the output vector, *m* and *n* as being the number of inputs and outputs history vectors and which are kept in memory.

WNN is a neural network with static wavelets. It is then a recursive model that links in a dynamic way actual, old, and future data. This type of networks can be trained in function of time, by using algorithms which can be advanced ones such as the genetic algorithms [70], [71]. One of the principal advantages of this kind of networks is that the input vector can be made out of signals of different kinds and even of a mixture of temporal and frequency signals. This network was used for prognostic from the vibrations signals of a rotating machine [72] and also for the prediction of a crack evolution in a compressor.

Other forms of ANN can be also used [73,74] such as the recurrent networks of radial functions. An application for the prognostic of a gas oven is presented in [75]. A case study on the prognostic of the failure of the opening door system in an airport bus is described in [76].

Since few years, other techniques such as the Relevance Vector Machine (RVM) algorithm have been used [77]. It allows the construction of a probabilistic model of a Bayesian form representing the generalized linear model in a form of function identical to the algorithm of Support Vectors Machine (SVM). The algorithm RVM considers a set of *n* given data $\{\underline{x}_i, y_i\}$ with $i \in [1,n]$ and with $\underline{x}$ a vector of dimension *q* associated with y_i.

The algorithm was initially defined in order to determine the probability $p(y \mid \underline{x}) \sim N(f(\underline{x}), \sigma^2)$ where σ^2 is the variance of the noise added to the data. The principle of the algorithm is to guess the underlying probability distribution that generates the data:

$$p(y \mid \omega, \sigma^2) = \frac{1}{\sigma\sqrt{2\pi}} \exp\left(\frac{-1}{2\sigma^2} \| y - \phi_\omega \|^2 \right) \tag{6}$$

where ϕ is a matrix containing the nucleus. The prediction function obtained then is of the form:

$$f(\underline{x}) = \sum_{i=1}^{n} \omega_i \phi(\underline{x}, \underline{x}_i) + \omega_0 \tag{7}$$

with ω_i as the weights associated with each support [78]. The key concept of the algorithm RVM for prognostic is its probabilistic interpretation of the output *y*.

Other techniques like fuzzy logic can be equally used to complement the tools of machine learning for the prognostic of learning [79]. Fuzzy logic, particularly, allows the use of linguistic variables in the dynamic model in order to treat uncertainty that lies at the heart of the performance of a prognostic algorithm [80].

Within the field of maintenance problems, Artificial Neural Networks (ANNs) and neuro-fuzzy systems (NF) have successfully been used to support the detection, diagnostic and prediction processes, and research works emphasize the interest of using it [71,81,82,83,84]: ANNs and NFs are a general and flexible modeling tool, especially for prediction problems.

I.6.2.3 - Prognostic by State Estimation

The approach by state estimation is usually used when a monitoring system by images and pattern recognition is already put at work on the equipment [85]. The form is, in this case, considered like an image of the equipment degradation. The goal of prognostic is then to predict the form evolution. Prognostic by state estimation assumes that the degradation evolution can be expressed by the following stochastic form of discrete time [8]:

$$\begin{cases} x_k = f_k(x_{k-1}, \omega_{k-1}) \Leftrightarrow p(x_k \mid x_{k-1}) \\ z_k = g_k(x_k, \nu_k) \Leftrightarrow p(z_k \mid x_k) \end{cases} \quad (8)$$

where x_k is a vector containing the degradation state, and ω_k and ν_k are the parameters of the environment that influence the evolution of the degradation, they are non-Gaussian noises, f_k and g_k are functions, and z_k is a vector of degradation state.

Like in the other prognostic approaches, the first step consists first of all in estimating the current vector x_k, and then prognostic is done. Two cases are possible depending on the form of functions f_k and g_k.

In the case where f_k and g_k are such that:

$$\begin{cases} f_k(x_{k-1}, \omega_{k-1}) = A_{k-1}x_{k-1} + \omega_{k-1} \\ g_k(x_k, \nu_k) = x_k \end{cases} \quad (9)$$

where A_{k-1} is a matrix containing the model transition parameters, it is possible to predict the evolution of the sequence $\{\hat{x}_{k+i}\}$, $i \in [1,n]$, from the sequence of observations $\{\hat{x}_j\}$, $j \in [0,k]$. This technique was applied on engines of continuous currents [86] and on gear systems when combined to fuzzy logic [87].

If now f_k and g_k are nonlinear functions, it is possible to use a method based on particular filtering [80] that seeks to remove noise, to reduce data size by compression, and to smooth the resulting time series in order to identify their general patterns (velocity, acceleration, etc.), and this by using typical signal-processing algorithms (median filter and rectangular filter). The estimation of the current state is then given by the knowledge of process model and by the estimation of the previous state:

$$p\left(x_k \mid z_{1,\ldots,k-1}\right) = \int p\left(x_k \mid x_{k-1}\right) p\left(x_{k-1} \mid z_{1,\ldots,k-1}\right) dx_{k-1} \tag{10}$$

The prediction of the degradation evolution from the estimation of the current state on a horizon *q* is given then by:

$$p\left(x_{k+q} \mid z_{1,\ldots,k}\right) = \int p\left(x_k \mid z_{1,\ldots k}\right) \prod_{j=k+1}^{k+q} p\left(x_j \mid z_{j-1}\right) dx_{k,\ldots,k+p-1} \tag{11}$$

An example of fault anticipation with the help of particular filtering is a system composed of three curves and presented in [88]. Using the same principle, an application of time prediction before failure of a system having a crack, is achieved in [89].

I.6.2.4 - *Advantages and Drawbacks of the Second Approach*

The strength of data-driven techniques is their ability to transform high-dimensional noisy data into lower dimensional information for diagnostic/prognostic decisions. AI techniques have been increasingly applied to machine prognostic and have shown improved performances over conventional approaches.

In practice however, it isn't easy to apply AI techniques due to the lack of efficient procedures to obtain training data and specific knowledge. So far, most of the applications in

the literature just use experimental data for model training. Thus, data-driven approaches are highly-dependent on the quantity and quality of system operational data.

I.6.3 - Prognostic Based on Experience

This approach is called experience based or probability based or statistical based prognostic approach.

It is necessary where we cannot use the two previous approaches. It is based on a reliability function or on a Bayesian process where the parameters are taken from feedback experience or expert opinion. Its disadvantages are the incapacity to treat complex systems of many components and its exclusive binary principle (success/failure) rather than continuous states of degradation.

When obtaining a physical model of an equipment is difficult and it is impossible to estimate degradation from the sensors installed on the equipment, prognostic based on experience can be the only alternative [32]. This form of prognostic is the less complex but requires an excellent feedback from experts in form of historical data, of knowledge base or of expert data. This expertise allows a stochastic or probabilistic modeling of degradation. It is the form the best adapted to complex systems that are very difficult to model physically and whose degradation indicators are sensitive to usage conditions [33].

This prognostic approach consists of using probabilistic or stochastic models of the degradation phenomenon, or of the life cycle of the components, by taking into account the data and knowledge accumulated by experience during the whole exploitation period of the industrial system.

The probabilistic model can be a simple probability function or a modeling in the form of stochastic process. In this framework, the most used probability functions are: Weibull law, exponential law when the failure rate is supposed to be constant, and normal, log-normal and Poisson laws. The parameters of each law are estimated from the data gathered during the whole exploitation period of time (experience feedback, maintenance data, etc.). Stochastic process models can be Markovian or semi-Markovian.

The experience-based models [62] are based on measurements taken from health monitoring of machine like for example those based on expert judgment, stochastic model,

Markovian process, Bayesian approach, Reliability analysis, Optimization of preventive maintenance, etc.). Their prognostic methodology proves to be simple but inflexible toward changes in system behavior and environment.

I.6.3.1 - Stochastic Approach

This type of approach is characterized by modeling the equipment life by a stochastic degradation process. The major part of the works in this field represents the degradation process by Markovian or semi-Markovian models [90,91]. The equipment passes then through different states of degradation. Prognostic consists of determining either the remaining useful lifetime, or the probable future state or states of the equipment in function of its current state if the process used is Markovian or in function of its state and of time spent in this state if the process is semi-Markovian.

Figure 1.9 illustrates a semi-Markovian process. The set $\{d_j\},\ j \in [1,n]$, represents the different degradation states: d_1 no degradation, ... , d_n maximal degradation. The $p_{i,j}$ represent the transitions probabilities from state d_i to state d_j. The remaining useful lifetime of the equipment T_v is given by:

$$T_v = \sum_{j=1}^{n} D(d_j) \tag{12}$$

with $D(d_j)$ is the duration associated with the state d_j. The prognostic algorithm used is the following [92]:

- Obtain the transition probabilities matrix from a learning procedure.
- Determine the probability densities of the duration of each state d_j.
- Identify the current state d_k of the equipment.
- Calculate the current remaining useful lifetime RUL_k from the remaining useful lifetime RUL_{k+1} at next instant in terms of the transition probability between the two instants and the self-state probability.

$$RUL_k = p_{k,k}\left(D(d_k) + RUL_{k+1}\right) + p_{k,k+1} RUL_{k+1} \tag{13}$$

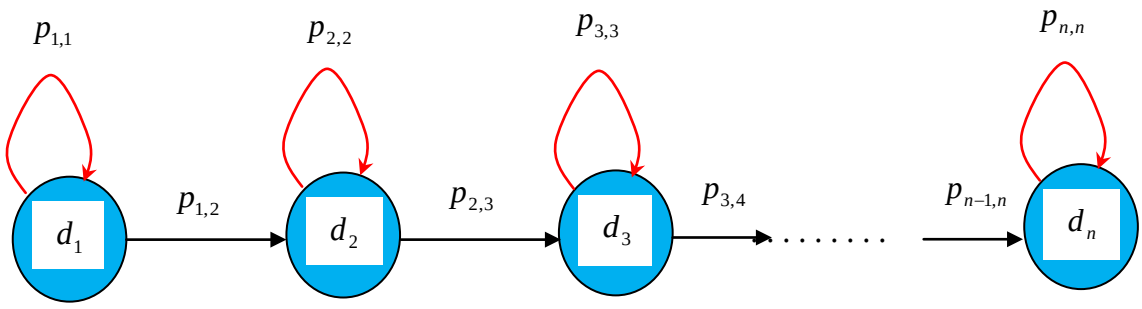

Figure 1.9 - Prognostic Based on a Hidden Semi-Markovian Process.

The use of the semi-Markovian model is preferable compared to the Markovian model since, the latter, assumes that the characteristics of the degradation process cannot be modified gradually with time. Moreover, the previous models are insufficient in order to model the degradation process that takes into consideration factors of influence linked to the environment or the equipment use. To do so, it is necessary to use models of state change that take into consideration the influence of these factors. The state of these factors modifies the value of the evolution parameters of the degradation process model [33].

I.6.3.2 - Reliability Approach

This approach is based on a probabilistic modeling of the failure instant, of the equipment reliability. The reliability of an equipment group at an instant t is the probability of operating without failure during the period $[0,t]$. Although it is represented by a temporal form, this definition remains valid with other units such as the kilometer or even the number of cycles of operation. The reliability function $R(t)$ of an equipment is determined from a large population of the same equipment. It is computed by:

$$R(t) = \frac{\text{Number of elements in life at the instant } t}{\text{Total number of elements}}, \quad \forall t \geq 0 \tag{14}$$

The function $R(t)$ allows, then, to define $f(t)$, the probability density of the variable T which represents the failure instant. The function $f(t)dt$ characterizes thus the probability that the failure instant T is between t and $t + dt$.

$$f(t) = -\frac{dR(t)}{dt}, \quad \forall t \geq 0 \tag{15}$$

There exists many standard distribution functions that allow to model $f(t)$. The mostly used is the Weibull distribution:

$$\text{Weibull}(t,\beta,\eta,\gamma)=\frac{\beta}{\eta}\left(\frac{t-\gamma}{\eta}\right)^{\beta-1}\times\exp\left[-\left(\frac{t-\gamma^{\beta}}{\eta}\right)\right] \tag{16}$$

Where:

β is the form or shape parameter,

η the scale parameter,

and γ the shifting parameter function of time or location.

We note that the curves of the Weibull distribution change in shape considerably for different values of the parameters, particularly the parameter β. If β=1, The Weibull distribution reduces to the exponential distribution. For values of $\beta>1$ the curves become somewhat bell-shaped and resemble the Normal curves but display some skewness.

Other distributions are equally used such as: the Poisson law or the Binomial law, the normal law, the exponential law, the gamma law, etc...

In the reliability approaches, prognostic is achieved with the help of the rate of failure $\lambda(t)$ that defines the conditional probability of the occurrence of a failure at instant *t* given that the device survived until instant *t*-1. In the case of a Weibull distribution, $\lambda(t)$ is as follows:

$$\lambda(t)=\frac{f(t)}{R(t)}=\frac{\beta}{\eta}\left(\frac{t-\gamma}{\eta}\right)^{\beta-1},\quad \forall t\geq 0 \tag{17}$$

Experimental observation shows that $\lambda(t)$ has the form of a curve said *bathtub curve* reproduced in figure 1.10. The evolution of $\lambda(t)$ is generally decomposed into three periods:

- Youth symbolizes the precocious failures, in the case of a Weibull law: $\beta<1$,
- Exploitation where the failure rate is almost constant, $\beta\approx 1$,
- End of life, wear-out, where we observe the occurrence of failures, $\beta>1$.

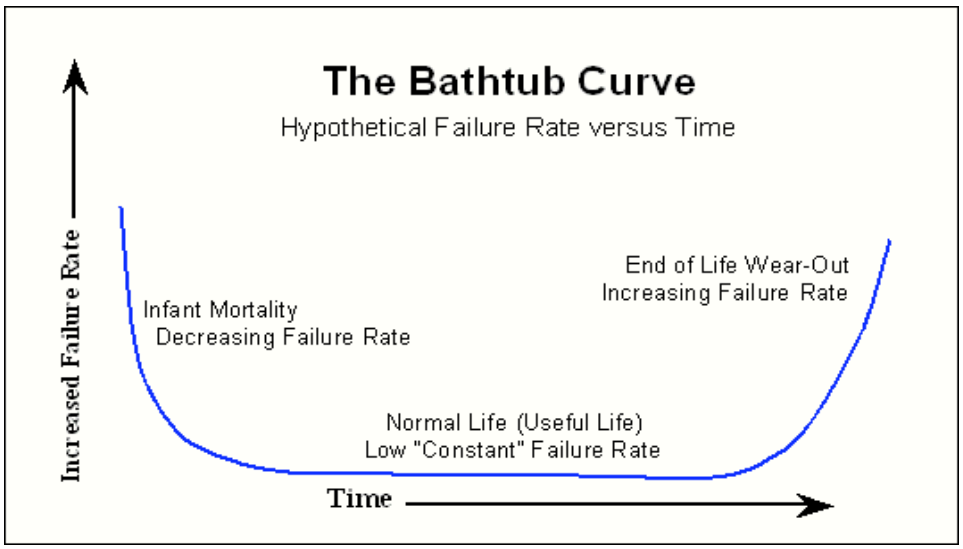

Figure 1.10 - The Bathtub Curve of Failure Rate versus Time.

In real usage conditions, reliability and degradation of an equipment are influenced by two sets of parameters [93]:

- The environment (temperature, humidity, etc),
- The mode of functioning (work load, state, etc).

In modeling point of view, the introduction of a vector $z(t)$ permits to take into consideration these two sets of parameters in the expression of $R(t)$ or $\lambda(t)$. In the first case, the deterioration process $R(t)$ is accelerated. We speak hence of an Accelerated Life Model (ALM) [94]:

$$R(t) = R_0(t)^{\Psi(z(t))}, \quad \forall t \geq 0 \tag{18}$$

In the second case, the rate of failure $\lambda(t)$ increases in function of usage conditions. We speak thus of Proportional Hazard Model (PHM) [95]:

$$\lambda(t) = \Psi\big(z(t)\big)\,\lambda_0(t), \quad \forall t \geq 0 \tag{19}$$

$\Psi\big(z(t)\big)$ is a function of the vector $z(t)$. It represents the physical behavior that governs the degradation in terms of the environment and the mode of functioning of the equipment. $R_0(t)$

and $\lambda_0(t)$ are respectively the reliability and the rate of failure in the nominal usage conditions.

In the domain of the prediction of the reliability of electronic systems, a consortium of eight industrials of defense aeronautics, has developed a new methodology called FIDES (Fonds D'investissement pour le Développement Économique et Social) [96]. This methodology is based on taking into consideration three components: Technology, Process, and Usage. The usage considers the equipment employment constraints through the profile of the mission, by subdividing the mission into phases into which the constraints are constant. The objective of the FIDES models is to allow a realistic evaluation of the electronic equipments reliability including for the equipments that encounter severe environments. The general model is of the form [97]:

$$\lambda_{\text{equipment}} = \sum_{\text{Physical Contributions}} \prod_{\text{Process Contributions}} \tag{20}$$

where the term *Physical Contributions* is an additive term that represents the physical and technological contribution to reliability such as: the type of materials used in the equipment construction. The term *Process Contributions* is a multiplicative term that represents the impact of the development process, of production and exploitation on reliability. This methodology gave birth to a guiding manual containing, for each electronic equipment, tables of the different factors that contribute to reliability.

I.6.3.3 - *Advantages and Drawbacks of the Third Approach*

The advantage of the methods of this approach is that it is not necessary to have complex mathematical models to do prognostic. Moreover, this approach is easy to apply on systems for which significant data are stored in a same standard that facilitates their use. For example, a company which has built during a long period of time a production and maintenance database with some minor rules and standards for data storing, can easily get the estimation of the parameters of the probability laws.

However, the main drawback of this approach dwells in the amount of data needed to estimate the parameters of the used laws. Indeed, huge and significant amount of exploitation data are needed in order to determine parameters that model faithfully the degradation phenomenon or the life cycle of the concerned system. Consequently, this approach cannot be

applied in the case of new systems for which data from experience feedback do not exist. The other kind of problem is that in most cases, it is necessary to filter and pre-process the data to extract the useful ones, because the stored data are not always directly exploitable (for example, in the same company, two maintenance operators may enter in two different information or appreciations for the same resolved problem).

I.6.4 - Methodology Based on Abaci of Degradation

Several prognostic studies are proposed and are based on abaci of degradation under a class of increasing functions without any analytic form like in the work of Peysson *et al.* [98]. Their approach belongs to the Data-driven family of prognostic approaches.

The prognosis work of Peysson *et al.* on a vehicle suspension system was based on the abacus of degradation under a class function $\mathcal{F}$. We know that these functions are increasing. Figure 1.11 shows three modes of degradation relative to the three states of the road (very good condition in red, fair condition in blue, and severe condition in green).

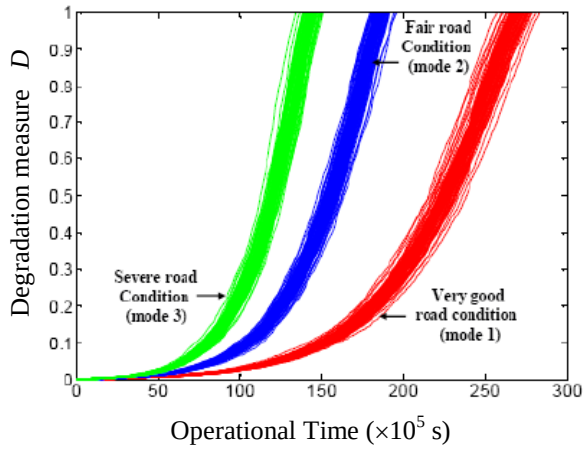

Figure 1.11 - The Three Modes of Degradation.

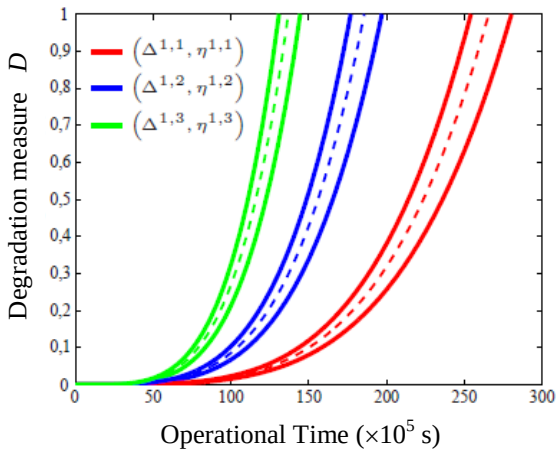

Figure 1.12 - The Modelisation of the Abaci of Degradation.

The degradation set $\mathcal{D}_r$ is given by: $D_{r^1} = \left\{\Delta^{1,1}(\tau), \Delta^{1,2}(\tau), \Delta^{1,3}(\tau)\right\}$ (figure 1.12) . To obtain this set, the values of the following parameters must be calculated by:

$$\begin{cases} \beta^{i,k} = \dfrac{Ln\, y_a - Ln\, y_b}{Ln\, x_a - Ln\, x_b} \\ \alpha^{i,k} = \exp\left(Ln\, y_b - \beta^{i,k} \times Ln\, x_b\right) \\ \eta^{i,k} = 1 - \dfrac{e_a}{2y_a} - \dfrac{e_b}{2y_b} \end{cases} \tag{21}$$

Where,

x : the operating time

y : the degradation state, with: $y_a < y_b$

e : the deviation from extreme points : $y + e$; $y - e$

The results of the three modelisations for abaci of degradation are indicated in [98].

The values of the triplets (x_a, y_a, e_a) and (x_b, y_b, e_b) for the three modes are called the abaci coefficients and are indicated in [98]. For the unique utilization profile $u^{1,1}$, the environmental variable (state of the road) is made discrete into three context conditions $\{c_1, c_2, c_3\}$, shown in [98].

To analyze the trajectory of degradation of the resources, we take here the suspension as the only resource $\mathcal{R}$, we consider a society of brake delivery equipped with two identical vehicles: *veh*1 and *veh*2. They make a weekly mission of the same duration (35 h) and of the same distance but with different road quality. They complete the same mission $\mathcal{M}$ but they are subject to different environmental constraints (road state). The environmental sequences encountered by the two vehicles are respectively C_1 and C_2. The duration is expressed in hours by:

$$\begin{cases} C_1 = ((c_3,1),(c_1,12),(c_2,6),(c_1,14),(c_3,3)) \\ C_2 = ((c_3,1),(c_1,17),(c_2,6),(c_1,3),(c_3,9)) \end{cases} \quad (22)$$

The analysis of degradation trajectory relative to the suspension resource of the two vehicles allows to better plan the maintenance of each vehicle in order to prevent failure and to increase the profitability. To estimate the time before suspensions failure, then the algorithm is executed while $D < 1$ (no failure case). The authors deduce in [98] the abaci curves and the degradation trajectories.

According to the methodology of Peysson *et al.*, the curve of each trajectory is given in terms of its use profile in function of the environmental context. The model can be simply modified to add some dynamics of degradation. The realized prevision allows us to determine the success of the mission.

This proposed approach can be treated by three different ways:

- Firstly, before the mission, the analysis of the trajectory identifies the defective resources and it gives also the approximate availability time.
- Secondly, after the mission, the necessary variables for the operating model are registered and stored during the mission in order to be treated, to analyze subsequently the degradation trajectories, and to know the mission impact on the system degradation.
- Thirdly, during the mission, this way is the intersection between the two previous utilizations. The use during the mission allows readjusting the prevision in real time. The follow up of the degradation trajectories in real time and the correction of previsions can also be used as tools that help in decision making to minimize the resources of degradation.

This methodology can also be used as a tool to understand the behavior of complex systems, in order to avoid strong degradations.

Peysson *et al.* have concluded with an example of application using the GPS data. If we assume that the cartography GPS includes data on the state of the roads, then the GPS disposes meteorological previsions and is connected to the vehicle sensor.

As the methodology of Peysson *et al.* is essentially based on expert systems, it is relying on the statistics of large measured data (as examples we can cite the works based on degradation behavior described by abaci and using expert description of system: Process-Mission-Environment [12], the works based on artificial intelligence, machine learning [99], neural network [62], fuzzy logic [100], etc.).

Their methodology based on abaci of degradation belongs to the Data-driven family of prognostic approaches. It is useful in many real cases (like the ship example where many internal and external parameters influence its mission). It is adequate when a huge number of data is necessary to be included into the prognostic process.

I.7 - Summary

We have presented in the previous sections a state of the art of the different approaches invented and applied for a prognostic function. Table 1.2 presents a comparative summary for a need of prognostic in the case of three families of approaches. We note that the

major part of the presented approaches apply for an elementary component of prognostic and remain difficult to use for a complex system.

In the approaches based on physical or mathematical models, the knowledge of the equations of the dynamic behavior of degradation makes their use very flexible. In case when the system properties or of degradation change, then the model parameters can be readjusted. But the development of such a model is very expensive because it is necessary to have a high level of qualification in order to master the mechanisms of equipment degradation. This type of model also presents computational difficulties during its simulation.

Prognostic accuracy →	Experience-Based	Evolutionary	Physics-Based
Engineering model	Not required	Beneficial	Required
Failure history	Required	Not required	Beneficial
Past operating conditions	Beneficial	Not required	Required
Current conditions	Beneficial	Required	Required
Identified fault pattern	Not required	Required	Required
Maintenance history	Beneficial	Not required	Beneficial
In general	No sensors/no model	Sensors/no model	Sensors and model

Table 1.2 - Summary of the Three Prognostic Approaches [62]

The approaches guided by data assume a reliable estimation of the state or the image of the current state of degradation in order to predict the future evolution of the system. The methods of trend analysis lack reactivity when facing a change in usage conditions. The efficiency of the learning methods is strongly linked to the sampling of data that serves to compute the model parameters. If an unlearned situation occurs, prognostic can be random. These methods based on state estimation require a model of the degradation indicator behavior and they are sensitive to the operating mode.

Experience based prognostic, either the stochastic approach or the reliability approach, requires little expert knowledge of the degradation mechanisms. It remains easy to implement but it is not reactive when facing a change in the system operating mode. In fact, the models usually created and devised are considered as average models of many equipments. Although

many solutions were found in order to answer to the problem of reactivity, these models remain usually difficult to implement. In addition, the constructed models have only two states, a state of nominal operation and a state of failure and do not comprise a state of degraded operation. Many works were realized to increase the number of states and this by using Monte Carlo simulations, but computation time remains very long [101].

Facing this fact, [33] introduces a prognostic process based on the coupling of a probabilistic representation of the system state with an event representation of the surveillance of its components degradation. The process allows to predict the performance of the system at instant $t + \Delta t$, from the observation of the system current state at time instant *t*. The conception of the prognostic model takes place in four steps:

- Knowledge formalization: this step consists of a functional analysis and a dysfunctional analysis (AMDEC and HAZOP) in order to determine two models. The operating model formalizes the operation of the system by using causal and qualitative relations, and relations among the different components. The dynamic model is based on the formalization of the set of the components degradation processes of the system by using Markovian processes.

- Construction of the probabilistic behavioral model: this step consists of the integration of the operating model and of the dynamic model in a set of unique formalism: the Bayesian Dynamic Networks (BDN). This step is realized from the generic mechanism of construction.

- Construction of the eventual model: This model formalizes the knowledge of the system current state, of its components, as well as its different actions of predicted maintenance.

- Construction of the prognostic model: the model is constructed by coupling the two previous models. That means the integration of the eventual model in the probabilistic model, thus the result appears as a BDN.

The realization of prognostic on a period of time, begins by updating the eventual model in function of the data issued from system monitoring. The integration of the eventual model in the prognostic model allows to initialize and to define a simulation scenario on that period of time. The simulation is then based on the temporal inference mechanism and on the

scenario defined by the maintenance operations. This methodology was applied on an experimental pressing system [97].

The advantage of this methodology is that it is applicable to a complex system and not only to one of its components, and prognostic is done in function of the maintenance actions. Hence, the prognostic model constructed does not take into consideration the modes of functioning to which the system is submitted.

I.8 - Conclusion

In this chapter a complete review of the prognostic approaches has been presented. The advantages and disadvantages of each of the three prognostic families have been also detailed. They show the great importance of these studies for the industrial systems.

The methodology based on abaci of degradation was discussed and showed, as a consequence of this bibliographic study.

For example, the main problem of the experience-based approach is that it cannot be applied in the case of new systems for which data from experience feedback do not exist. Also, the approaches guided by data lack reactivity when facing a change in usage conditions. When the approaches miss analytic forms like those based on abaci of degradation, they prove some inflexibility during application to various system behaviors.

At the expense of cost, precision and accuracy are sought, thus the choice of a novel physical-based prognostic approach, based on a mathematical model of degradation, becomes an important goal in prognostic. Therefore, precise, useful, and elegant mathematical laws come to our help in the following chapters in order to achieve the goal of this thesis. Our proposed model is based on famous analytic laws of degradation like Paris-Erdogan's law which is a law of degradation by fatigue, and Palmgren-Miner's law which is a cumulative law of damage. Despite this fact, a long and complex analytical development will be made in the following chapters to achieve a novel degradation model as a tool for prognostic analysis.

Whenever such analytic damage laws are available, the proposed approach permits to determine the Remaining Useful Lifetime (RUL) of the system.

References

[1] A.K.S. JARDINE. D.L., and D. BANJEVIC: A review on machinery diagnostics and prognostics implementing condition-based maintenance. *Mechanical Systems and Signal Processing*, 20 (7): 1483-1510, 2006.

[2] E. DELOUX: *Politiques de maintenance conditionnelle pour un système à dégradation continue soumis à un environnement stressant.* Thèse de doctorat, École Nationale Supérieure des Techniques Industrielles et des Mines de Nantes, France, Octobre 2008.

[3] A. MULLER, A.C. MARQUEZ, and B. IUNG: On the concept of e-maintenance: Review and current research. *Reliability, Engineering, and System Safety*, 2007.

[4] D. RACOCEANU: Mémoire d'habilitation à diriger des recherches, Contribution à la surveillance des Systèmes de Production en utilisant les Techniques de l'Intelligence Artificielle. Université de Franche-Comté de Besançon, France, Janvier 2006.

[5] P.W. KALGREN, C.S. BYINGTON, M.J. ROEMER, and M.J. WATSON: Defining PHM, A Lexical Evolution of Maintenance and Logistics. 2006 *IEEE AUTOTESTCON*, pages 353-358, 2006.

[6] A. HESS, G. CALVELLO, and P. FRITH: Challenges, Issues, and Lessons Learned Chasing the Big P: Real Predictive Prognostics Part 1. *In IEEE Aerospace Conference*, Big Sky, Montana, USA, 2005.

[7] M.R. ZEMOURI: *Contribution à la surveillance des systèmes de production à l'aide de réseaux de neurones dynamiques: Application à l'e-maintenance.* Thèse de doctorat, Université Franche-Comté, France, Novembre 2003.

[8] G.J. VACHTSEVANOS, L.L. FRANK., M. ROEMER, A. HESS, and W. BIQING: *Intelligent Fault Diagnosis and Prognosis for Engineering Systems.* Hoboken, NJ: John Wiley & Sons, 2006.

[9] J.W. SHEPPARD, M.A. KAUFMAN, and T.J. WILMERING: IEEE Standards for Prognostics and Health Management. *2008 IEEE AUTOTESTCON*, pages 97-103, 2008.

[10] A. MARTHUR, K.F. CAVANAUGH, K.R. PATTIPATI, P.K. WILLETT, and T.R. GALIE: Reasoning and modeling systems in diagnosis and prognosis. *In Proceedings of the 2001 SPIE*, volume 4389, pages 194-203, 2001.

[11] P. CHAPOUILLE: Fiabilité, Maintenabilité, Techniques de l'ingénieur. L'Entreprise industrielle, 3(T 4300): 4300-4300, 1980.

[12] F. PEYSSON, M. OULADSINE, R. OUTBIB, J-B. LEGER, O. MYX, and C. ALLEMAND, "A generic prognostic methodology using damage trajectory models", IEEE transactions on reliability, vol. 58 (no. 2), June 2009.

[13] H.O. KOKSAL and C. KARAKOC: An isotropic damage model for concrete. *Materials and Structures, Springer*, 32 (8): 611-617, 1999.

[14] G.Z. VOYIADJIS, Z.N. TAQIEDDIN, and P.I. KATTAN: Anisotropic damage-plasticity model for concrete. *International Journal of Plasticity*, 24 (10): 1946-1965, 2008.

[15] G.Z. VOYIADJIS and P.I. KATTAN: *Damage Mechanics,* Taylor & Francis, 2005.

[16] T. BROTHERTON, G. JAHS, J. JACOBS, and D. WROBLEWSI: Prognosis of faults in gas turbine engines, *In IEEE Aerospace Conference,* volume 6, pages 163-171, 2000.

[17] C.S. BYINGTON, P.W. KALGREN, R. JOHNS, and R.J. BEERS: Prognosis enhancements to diagnostic system for improved condition based maintenance. *In IEEE Systems Readiness Technology Conference, AUTOTESTCON,* pages 320-329, California, USA, September 2003.

[18] S.J. ENGEL, B.J. GILMARTIN, K. BONGORT, and A. HESS: Prognostics, the real issues involved with predicting life remaining. *In 2000 IEEE Aerospace Conference Proceedings,* volume 6, 2000.

[19] S. KATIPAMULA and M.R. BRAMBLEY: Methods for fault detection, diagnostics, and prognostics for building systems - A review, part I. *HVAC&R Research,* 11 (1): 3-25, 2005.

[20] M. LEBOLD and M. THURSTON: Open standards for condition-based maintenance and prognostic systems. *In 5th Annual Maintenance and Reliability Conference, MARCON,* GATLINBURG, USA, 2001.

[21] J. LEE, H. QIU, J. NI, and D. DRAGAN: Infotronics technologies and predictive tools for next-generation maintenance systems. *In 11th IFAC Symposium on Information Control Problems in Manufacturing,* Salvador, Brazil, April 2004.

[22] G. PROVAN: Open systems architecture for prognostic inference during condition-based monitoring. *Aerospace Conference, 2003. Proceedings. 2003 IEEE,* 7, 2003.

[23] S.J. HUDAK, Jr., M.P. ENRIGHT, R.C. MCCLUNG, H.R. MILLWATER, A. SARLASHKAR, and M.J. ROEMER, "Potential Benefits of Adding Probabilistic Damage Accumulation to Prognosis of Turbine Engine Reliability," SwRI Final Report to AFRL/DARPA, Contract No. F33615-97-D-5271, June 30, 2002.

[24] C.R. FARRAR, F. HEMEZ, G. PARK, A.N. ROBERTSON, H. SOHN, and T.O. WILLIAMS, "A Coupled Approach to Developing Damage Prognosis Solutions", in: Damage Assessment of Structures - The 5th Intern. Conf. on Damage Assessment of Structures (DAMAS 2003), 2003.

[25] A. RYTTER, "Vibration Based Inspection of Civil Engineering Structures", PhD Thesis, Aalborg University, Denmark 1993.

[26] D. LIN and V. MAKIS, "Recursive filters for a partially observable system subject to random failure", Advances in Applied Probability, Vol. 35, pp.207-227., 2003.

[27] ISO, 13381-1, *Condition monitoring and diagnostics of machines - prognostics* - Part1: General guidelines. Int. Standard, ISO, 2004.

[28] C.R. FARRAR, N. A.J. LIEVEN, and M.T. BEMENT, *Damage Prognosis for Aerospace, Civil and Mechanical Systems,* John Wiley & Sons, Inc., ch. 1 and 2, 2005.

[29] J. LEE., Smart products and service systems for e-business transformation, 3e Conférence Francophone de Modélisation et Simulation « Conception, Analyse et Gestion des Systèmes Industriels » MOSIM'01 – du 25 au 27 avril - Troyes (France), 2004.

[30] J.M. LARSEN and L. CHRISTODOULOU, "Integrated Damage State Awareness and Mechanism-Based Prediction," Journal of Metals, TMS, p.14, March 2004.

[31] L. CHRISTODOULOU and J.M. LARSEN, "Using Materials Prognosis to Maximize the Utilization Potential of Complex Mechanical Systems," Journal of Metals, TMS, pp. 15-19, March 2004.

[32] C.S. BYINGTON, M.J. ROEMER, and T.R. GALIE: Prognosis enhancements to diagnostic system for improved condition based maintenance. *In IEEE Aerospace Conference,* volume 6, pages 2815-2824, 2002.

[33] A. MULLER: *Contribution à la maintenance prévisionnelle des systèmes de production par la formalisation d'un processus de pronostic.* Thèse de doctorat, Université Henri Poincaré - Nancy I, France, Juin 2005.

[34] K.M. GOH, B. TJAHJONO, T.S. BAINES, and S. SUBRAHMANIAN: A Review of Research in Manufacturing Prognostics. *In 2006 IEEE International Conference on Industrial Informatics,* pages 412-422, New York, USA, August 2006.

[35] K. GOEBEL, N. EKLUND, and P. BONANNI: Fusing competing prediction algorithms for prognostics. *In IEEE Aerospace Conference,* Big Sky, Montana, USA, 2005.

[36] G.J. KACPRZYNSKI, M.J. ROEMER, G. MODGIL, A. PALLDINO, and K. MAYNARD: Enhancement of physics-of-failure prognostic models with system level features. *Aerospace Conference Proceedings,* 2002. IEEE, 6, 2002.

[37] D.E. ADAMS: Nonlinear damage models for diagnosis and prognosis in structural dynamic systems. *In SPIE conference,* volume 4733, pages 180-191, 2002.

[38] W.Q. MEEKER and L.A. ESCOBAR: *Statistical methods for reliability date.* Wiley New York, 1998.

[39] P.L. HALL and J.E. STRUTT: Probabilistic physics-of-failure models for component reliability using Monte Carlo simulation and Weibull analysis: a parametric study. *Reliability Engineering and System Safety,* 80: 233-242, June 2003.

[40] J. LEE: Measurement of machine performance degradation using a neural network model. *Computers in Industry,* 30(3): 193-209, 1996.

[41] R. PATRICK-ALDACO: *A Model Based Framework for Fault Diagnosis and Prognosis of Dynamical Systems with an Application to Helicopter Transmissions.* Thèse de doctorat, Georgia Institute of Technology, USA, 2007.

[42] W. BARTELMUS and R. ZIMROZ, "Vibration condition monitoring of planetary gearbox under varying external load", Mechanical Systems and Signal Processing, Vol. 23, pp. 246- 257, 2009.

[43] G.J. KACPRZYNSKI, A. SARLASHKAR, and M.J. ROEMER, "Predicting remaining life by fusing the physics of failure modeling with diagnostics", Journal of Metal, Vol. 56, pp. 29-35, 2004.

[44] D. CHELIDZE, J. P. CUSUMANO: A dynamical systems approach to failure prognosis. *ASME, Journal of Vibration and Acoustics,* 126: 1-8, January 2004.

[45] J. LUO, A. BIXBY, K. PATTIPATI, L. QIAO, M. KAWAMOTO, and S. CHIGUSA, "An interacting multiple model approach to model-based prognostics", Syst. Secur. and Assurance, Vol. 1, pp. 189-194, 2003.

[46] C.H. OPPENHEIMER and K.A. LOPARO, "Physically based diagnosis and prognosis of cracked rotor shafts", in: Comp. & Syst. Diagnostics, Prognostics, and Health Manag. II, Vol. 4733, pp. 122-132, 2002.

[47] D. CHELIDZE, "Multimode damage tracking and failure prognosis in electromechanical system", in SPIE Conference Proceedings, Vol. 4733, pp. 1-12, 2002.

[48] Y. LI, S. BILLINGTON, C. ZHANG, T. KURFESS, S. DANYLUK, and S. LIANG, "Adaptive prognostics for rolling element bearing condition", Mech. Systems and Signal Processing, Vol. 13, pp. 103-113, 1999.

[49] Y. LI, T. R. KURFESS, and S. Y. LIANG, "Stochastic prognostics for rolling element bearings", Mechanical Systems and Signal Processing, Vol. 14, pp. 747-762, 2000.

[50] A. RAY and S. TANGIRALA, "Stochastic modeling of fatigue crack dynamics for on-line failure prognostics", IEEE Transactions on Control Systems Technology, Vol.4, pp. 443-451, 1996.

[51] C. CEMPEL, H.G. NATKE, and M. TABASZEWSKI, "A passive diagnostic experiment with ergodic properties", Mechanical Systems and Signal Processing, Vol. 11, pp. 107-117, 1997.

[52] J. QIU, C. ZHANG, B.B. SETH, and S.Y. LIANG, "Damage mechanics approach for bearing lifetime prognostics", Mechanical Systems and Signal Processing, Vol. 16, pp. 817-829, 2002.

[53] C. CEMPEL, "Simple condition forecasting techniques in vibroacustical diagnostics", Mechanical Systems and Signal Processing, Vol. 1(1), pp. 75-82, 1987.

[54] C. CEMPEL, Vibroacustic condition monitoring, Ed. Horwood, New York, 1991.

[55] G.A. LESIEUTRE, L. FANG, and U. LEE, "Hierarchical failure simulation for machinery prognostics", in: Critical Link: Diagnosis to Prognosis, Haymarket, pp. 103-110, 1997.

[56] D. CHELIDZE, J.P. CUSUMANO, and A. CHATTERJEE: A dynamical systems approach to damage evolution tracking, Part 1: Description and experimental application. *ASME, Journal of Vibration and Acoustics,* 124: 250-257, April 2002.

[57] D. CHELIDZE, J.P. CUSUMANO, and A. CHATTERJEE: A dynamical systems approach to damage evolution tracking, Part 2: Model-based validation and physical interpretation. *ASME, Journal of Vibration and Acoustics,* 124:258-264, April 2002.

[58] J. LUO, M. NAMBURU, K. PATTIPATI, L. QIAO, M. KAWAMOTO, and S. CHIGUSA: Model-based prognostic techniques. *In IEEE Systems Readiness Technology Conference, AUTOTESTCON,* volume 6, California, USA, September 2003.

[59] J. LUO, A. BIXBY, K. PATTIPATI, L. QIAO, M. KAWAMOTO, and S. CHIGUSA: An interacting multiple model approach to model-based prognostics. *In IEEE International Conference on Systems, Man and Cybernetics,* volume 1, pages 189-194, California, USA, October 2003.

[60] D. GUCIK-DERIGNY, R. OUTBIB, and M. OULADSINE: Estimation of Damage Behavior for Model-Based Prognostic. *In 7th IFAC Symposium on Fault Detection, Supervision and Safety of Technical Processes, SAFEPROCESS'09,* Barcelona, Spain, 2009.

[61] M.J. ROEMER, C.S. BYINGTON, G.J. KACPRZYNSKI, and G. VATSEVANOS: An overview of selected technologies with reference to integrated phm architecture. *In First International Forum on Integrated System Health Engineering and Management in Aerospace,* Napa Valley, California, USA, October 2005.

[62] O.E. VASILE: *Contribution au pronostic de défaillance par réseau neuro-flou: maitrise de l'erreur de prédiction.* Thèse de doctorat, UFR de Sciences et Techniques de l'Université de Franche-Comté, 2008.

[63] F.L. GREITZER and R.A. PAWLOWSKI: Embedded prognostics health monitoring. *In International Instrumentation Symposium,* May 2002.

[64] J. YAN, J. LEE, and M. KOC: Predictive algorithm for machine degradation detection using logistic regression. *In 5th International Conference on Managing Innovations in Manufacturing, MIM,* pages 172-178, Milwaukee, Wisconsin, USA, September 2002.

[65] G.J. KACPRZYNSKI, T.R. GALIE, M.J. ROEMER, M. GUMINA, and D.E. CAGUIAT: A Prognostic Modeling Approach for Predicting Recurring Maintenance for Shipboard Propulsion Systems, *In ASME Turbo Expo,* New Orleans, LA USA, June 2001.

[66] M. AZAM, F. TU, and K.R. PATTIPATI: Condition-based predictive maintenance of industrial power systems. *In Proceedings of SPIE,* volume 4733, page 133, 2002.

[67] W.G. ZANARDELLI and E.G. STRANGAS: Failure prognosis for permanent magnet AC machines based on time-frequency analysis. *In International Conference on Electrical Machines,* Cracovie, Pologne, September 2005.

[68] D. JARELL, D. SISK, and L. BOND: Prognostics and condition based maintenance, a scientific crystal ball. *In international Congress on Advanced Nuclear Power Plants, ICAPP, June 2002.*

[69] M.A. SCHWABACHER: A survey of data-driven prognostics. *In AIAA Infotech@Aerospace Conference,* Arlington, Virginia, September 2005.

[70] Z. LEI, L. XINGSHAN, Y. JINSONG, and Z.B. GAO: A Genetic Training Algorithm of Wavelet Neural Networks for Fault Prognostics in Condition Based Maintenance. *In The Eighth International Conference on Electronic Measurement and Instruments - ICEMI,* pages 584-589, 2007.

[71] G. VACHTSEVANOS and P. WANG: Fault prognosis using dynamic wavelet neural networks. *In IEEE Systems Readiness Technology Conference AUTOTESTCON Proceedings, 2001,* pages 857-870, 2001.

[72] X. WANG, G. YU, M. KOC, and J. LEE: Wavelet Neural Network for Machining Performance Assessment and Its Implications to Machinery Prognostics. *Proceedings of the 5th International Conference on Managing Innovations in Manufacturing (MIM),* 2002.

[73] C. S. BYINGTON, M.J. WATSON, and D. EDWARDS: Data-driven neural network methodology to remaining life predictions for aircraft actuator components. *In Proceedings of the IEEE Aerospace Conference,* 2004.

[74] N. GEBRAEEL, M. LAWLEY, R. LIU, and V. PARMESHWARAN: Residual life predictions from vibration-based degradation signals: a neural network approach. *IEEE Transactions on Industrial Electronics,* 51 (3): 694-700, 2004.

[75] R. ZEMOURI, D. RACOCEANU, and N. ZERHOUNI: Réseaux de neurones récurrents à fonctions de bases radiales: RRFR, application au pronostic. *Revue d'intelligence artificielle, RSTI série RIA,* 16:307-338, 2002.

[76] A.E. SMITH, D.W. COIT, and Y.C. LIANG: A neural network approach to condition based maintenance: Case study of airport ground transportation vehicles. Rapport technique, Department of Industrial and Systems Engineering, Auburn University, 2002.

[77] K. GOEBEL, B. SAHA, and A. SAXENA: A comparison of Three Data-Driven Techniques for Prognostics, *In 62nd Meeting of the Society for Machinery Failure Prevention Technology (MFPT),* pages 119-131, Virginia Beach, VA, 2008.

[78] F. SUARD and D. MERCIER: Application des noyaux multiples de type kernel basis à la méthode relevance vector machine pour la sélection de modèles. *In gretsi09, Dijon, France,* 2009.

[79] M. SCHWABACHER and K. GOEBEL: A survey of Artificial Intelligence for Prognostics. *In AAAI Fall Symposium,* Arlington, V. A., 2007.

[80] P.P. BONISSONE and K. GOEBEL: When will it break? a hybrid soft computing model to predict time-to-break margins in paper machines. *In SPIE 47th Annual Meeting, International Symposium on Optical Science and Technology,* volume 4787, pages 53-64, 2002.

[81] Y.L. DONG, Y.J. GU, K. YANG, and W.K. ZHANG, "A combining condition prediction model and its application in power plant", in: Proceedings of 2004 International Conference on Machine Learning and Cybernetics, Vol. 6, pp. 3474-3478, 2004.

[82] N. FREITAS, I.M. MACLEAOD, and J.S. MALTZ, "Neural networks for pneumatic actuator fault detection", Transactions of the SAIEE, Vol. 90, pp. 28-34, 1999.

[83] R.C.M. YAM, P.W. TSE, L. LI, and P. TU, "Intelligent predictive decision support system for condition-based maintenance", Inter. Jour. of Adv. Manufacturing Technology, Vol. 17 pp. 383-391, 2001.

[84] S. ZHANG and R. GANESAN, "Multivariable trend analysis using neural networks for intelligent diagnostics of rotating machinery", Transactions of the ASME. Journal of Engineering for Gas Turbines and Power, Vol. 119, pp. 378-384, 1997.

[85] T. DENOEUX, M. MASSON, and B. DUBUISSON: Advanced pattern recognition techniques for system monitoring and diagnosis: A survey. *Journal européen des systèmes automatisés*, 31 (9-10): 1509-1539, 1997.

[86] S.K. YANG: An experiment of state estimation for predictive maintenance using Kalman filter on a DC motor. *Reliability Engineering and System Safety*, 75:103-111, 2002.

[87] D.C. SWANSON: A general prognostic tracking algorithm for predictive maintenance. *Aerospace Conference, 2001, IEEE Proceedings*, 6, 2001.

[88] Z. CHEN and D.H. ZHOU: Particle Filtering Based Fault Prediction Of Nonlinear Systems. *In IFAC Symposium Proceedings of Safe Process*, Washington, D.C. (USA), June 2003.

[89] M. ORCHARD, B. WU, and G. VATCHTSEVANOS: A Particle Filtering Framework for Failure Prognosis. *In WTC2005 World Tribology Congress III*, Washington, D.C., USA, 2005.

[90] A. GRALL, C. BERENGUER, and L. DIEULLE: A condition-based maintenance policy for stochastically deteriorating systems. *Reliability Engineering and System Safety*, 76 (2): 167-180, 2002.

[91] V.A. KOPNOV: Optimal degradation processes control by two-level policies. *Reliability Engineering and System Safety*, 66(1): 1-11, 1999.

[92] M. DONG and D. HE: Hidden semi-Markov model-based methodology for multi-sensor equipment health diagnosis and prognosis. European Journal of Operational Research, 178 (3): 858-878, 2007.

[93] S. MARTORELL, A. SANCHEZ, and V. SERRADELL: Age-dependent reliability model considering effects of maintenance and working conditions. *Reliability Engineering and System Safety*, 64: 19-31, April 1999.

[94] D.W. COIT and J.R. ENGLISH: System reliability modeling considering the dependence of component environmental influences. *Reliability and Maintainability Symposium*, 1999 *Proceedings Annual*, pages 214-218, 1999.

[95] M.S. FINKELSTEIN: Wearing-out of components in a variable environment. *Reliability Engineering and System Safety*, 66 (3): 235-242, 1999.

[96] P. CHARPENEL, R. DIGOUT, M. GIRAUDEAU, M. GLADE, J.P. GUERVENO, N. GUILLET, A. LAURIAC, S. MALE, D. MANTEIGAS, R. MEISTEIN, E. MOREAU, D. PERIE, F. RELMY-MADINSKA, AND P. RETAILLEAU: FIDES, la nouvelle méthodologie pour la prévision de fiabilité des systèmes électronique. In $\lambda\mu$ 14, October 2004.

[97] A. GLADE: *Modélisation des couts de cycle de vie: prévision des couts de maintenance et de la fiabilité, Application à l'aéronautique.* Thèse de doctorat, Ecole Centrale de Lyon, France, Janvier 2005.

[98] F. PEYSSON, *Contribution au pronostic des systèmes complexes*, thèse de doctorat, Université d'Aix-Marseille, France, Décembre 2009.

[99] PROTEUS WP2 Team, *On the use of Artificial Intelligence for Prognosis and Diagnosis in the PROTEUS E-maintenance platform*, ITEA European Project, 2005.

[100] M.E. CONCHA, *Fault Diagnostic and Failure Prognostic in Nonlinear Dynamic System*, IEEE Trans. on Control System Technology, 2007.

[101] J. BARATE, C.G. SOARES, M. MARSEGUERRA, AND E. ZIO: Simulation modeling of repairable multi-component deteriorating systems for 'on condition' maintenance optimization. *Reliability engineering and system safety*, 76(3): 255-264, 2002.

CHAPTER II

ANALYTIC LINEAR PROGNOSTIC MODEL OF DYNAMIC SYSTEMS

II.1 - Introduction

Predicting the remaining useful lifetime of industrial systems becomes currently an important aim for industrialists knowing that the failure which can occur suddenly is generally very expensive at the level of reparation, of production interruption, and is bad for reputation. The classical strategies of maintenance [1] are no more efficient and practical because they do not take into consideration the instantaneous evolving product state, so it is important to understand the product in real time in order to prevent a failure during operation. In fact, we introduce a prognostic approach that seeks to provide an intelligent maintenance.

In specialized literature, several studies on prognostic procedure are presented, among them we mention, the model-based, statistic-based, and data-based models. The works based on abaci of degradation as in the work of Peysson *et al.* [2,3] are useful at this level. As the latter is related to the three influent components: process, mission, environment, it is a non-analytic based model founded on expert knowledge and on a large database.

A proposed analytic prognostic methodology based on some laws of damage in fracture mechanics is developed here. The damages are generally: crack propagation, corrosions, chloride attack, creep, excessive deformation and deflection, and damage accumulation. Whenever their analytic laws are available, the advantage of a prognostic approach based on a known damage law for a mechanical system is that it is adaptable to new situations and useful in determining the Remaining Useful Lifetime (RUL) of the system.

The procedure proposed in this work belongs to the model based prognosis approach related to the physical model. It is focused on developing and implementing effective diagnostic and prognostic technologies with the ability to detect faults in the early stages of degradation. Early detection and analysis may lead to better prediction and end of life estimations by tracking and modeling the degradation process. The idea is to use these estimations to make accurate and precise prediction of the time to failure of components. Early detection also helps avoid catastrophic failures.

Any prognostic methodology must lie on a type of damage. In mechanical systems, the damage can take many shapes. In this thesis, the case of fatigue degradation has been

chosen due to the fact that it can be mathematically formulated by available analytic laws such as Paris-Erdogan's and Palmgren-Miner's laws.

This approach shows to be important in ensuring high availability of industrial systems, like in aerospace, defense, petro-chemistry and automobiles. Among these systems, the petrochemical industries can be cited as an example of prognostic importance for the reason of favorable economic and availability consequences on their exploitation cost [4].

Among petrochemical systems, pipelines serve to transport oil and natural gas between petrochemical plants. Their life prognostic is vital in this industry since their availability is crucial here. The main cause of failure for these systems is the fatigue due to internal pressure-depression variation along operating time. In pipelines study, the results of model simulations are done for three cases of pipes: unburied, buried, and offshore (under sea water).

In automobile industry, like for example the suspension component, also this approach shows its importance for the same earlier reasons as it is explained later in this chapter. In vehicle suspension study the results of model simulations are done for three cases of road profile excitations.

This chapter is organized as follows: first the mechanical model of fatigue is presented in the linear cumulative damage case then the prognostic model of fatigue failure is developed and finally a case study of pipelines system and vehicle suspensions is illustrated.

II.2 - Proposed Prognostic Model

The purpose of this thesis is to construct a process of prognostic capable of predicting the degradation trajectories of a complex system for a given mission under a given environment and starting from an initial known damage. The complex system is decomposable into sub-systems where each one can comprise a damage function.

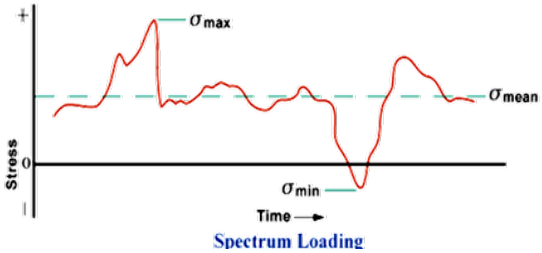

Figure 2.1 - Load fluctuation.

The fatigue failure is one of the famous damage phenomena in mechanical systems like

in aircraft where the wings are subject to the fluctuation of air pressure between a maximal value (σ_{max}) and a minimal value (σ_{min}) (figure 2.1) [5]. This type of loadings leads to crack propagation that can accelerate rapidly. Usually, micro-cracks exist originally in the materials due to fabrication process where stresses remain after manufacture. These micro-cracks are detected and measured and denoted by a_0.

The advantage of the choice of fatigue damage for the developed prognostic methodology is that it is a failure mechanism very well studied in literature and described under many known analytic laws. This mechanism has relatively the simplest formulation in comparison to the other damage phenomena. The fatigue characterizes the main failure cause of industrial equipments.

II.2.1 - Damage Evolution Law

The fatigue of materials under cyclic loading creates micro-cracks. Starting from an initial length a_0 corresponding to an initial cycle number N_0, the macro-cracks become detectable and unstable. These macro-cracks will grow under loading cycles N to a critical length a_C reached at N_C cycles and creating thus fractures that lead to failure. This evolution is represented in figure 2.2 in terms of normalized number of cycles N/N_C for simplicity of reading.

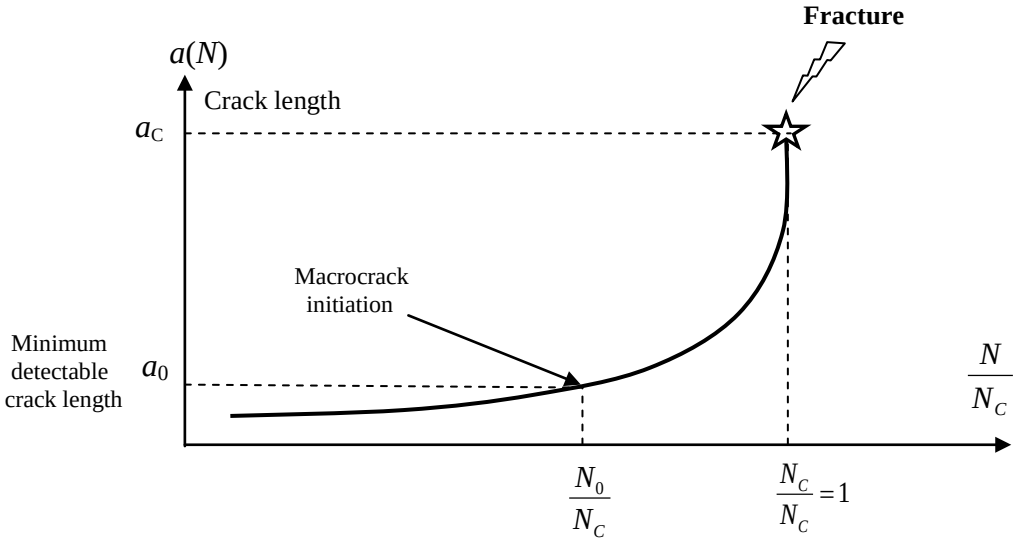

Figure 2.2 - Pre-Crack fatigue damage.

It can be assumed that $a_C = e/8$, where e and ℓ are respectively the device dimension in the crack direction and the perpendicular dimension to the crack direction (figure 2.3).

Δa_N is the crack length increment due to a loading cycle dN. t_N is the instant corresponding to cycle N and to crack length a_N.

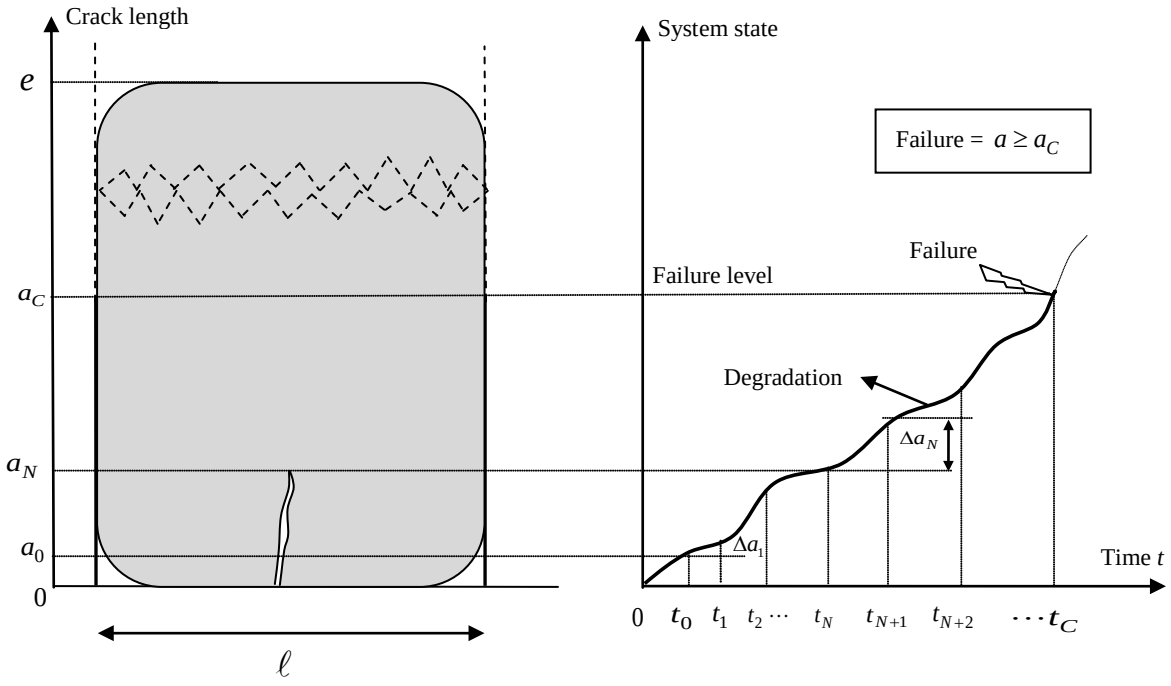

Figure 2.3 - Crack length evolution.

II.2.2 - Paris-Erdogan's Law

The Paris-Erdogan's law [6] permits to determine the propagation rate of crack length a after its detection. The law of damage growth is given by equation (1):

$$\frac{da}{dN} = C \cdot (\Delta K)^m \tag{1}$$

Where,

C and m are the material and environment parameters. ($0 < C << 1$); ($2 \leq m \leq 4$);

a is the crack length, N is the number of cycles (where the RUL is derived directly), and ΔK is the stress intensity factor.

It can be distinguished (figure 2.4):

- The long cracks that obey to Paris-Erdogan's law
- The short cracks that serve to decrease the speed of propagation
- The short physical cracks that serve to increase the speed of propagation.

The law can be written also as:

$$\log\left(\frac{da}{dN}\right) = \log C + m\log(\Delta K) \tag{2}$$

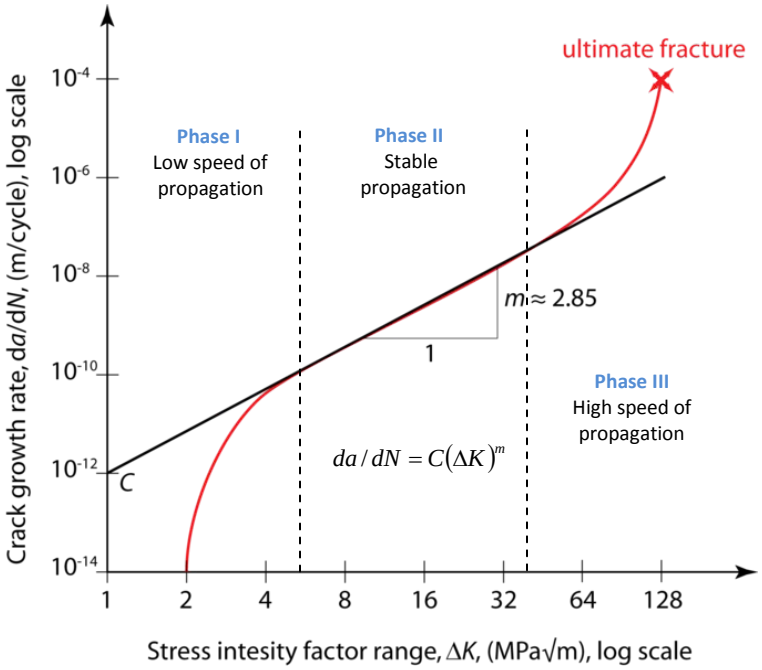

Figure 2.4 - The three phases of crack growth, Paris-Erdogan's law.

From the general form of Paris-Erdogan's law, McEvily A.J. and Ritchie R.O. [7] have proven the following form (equation 3):

$$\frac{da}{dN} = C \cdot \left(\Delta K_{eff}\right)^m \cdot \left(K_{max}\right)^m \tag{3}$$

Where $\Delta K_{eff} = K_{max} - K_{op}$,

K_{max} : maximum stress intensity factor,

K_{op} : stress intensity factor required to open the fatigue crack.

So the decoupled form where two different functions of crack length *a* and of load *P* can be deduced:

$$\frac{da}{dN} = C \cdot \phi_1(a) \cdot \phi_2(P) \tag{4}$$

Where,

The function: $\phi_1(a) = \left(Y(a) \cdot \sqrt{\pi a}\right)^m$

and the load function $\phi_2(P) = (P)^m$; $P = K_{max}$;

with $Y(a)$: the geometric factor function of the body dimensions,
and P : the load parameter.

The Palmgren-Miner's rule can be used now to count the damages [8].

II.2.3 - Palmgren-Miner's Rule

The Palmgren-Miner's rule [8] serves to compute the cumulative damage d_i of different stresses levels σ_i (i=1, i=2, ... , i=k) applied for n_i cycles. Knowing that N_i is the total cycle's number of stress σ_i to be applied, and that lead to failure. The linear cumulative damage relative to applied stresses (i=1 to k) is given by (5) (figure 2.5):

$$D_k = \sum_{i=1}^{k} d_i = \sum_{i=1}^{k} \frac{n_i}{N_i} \tag{5}$$

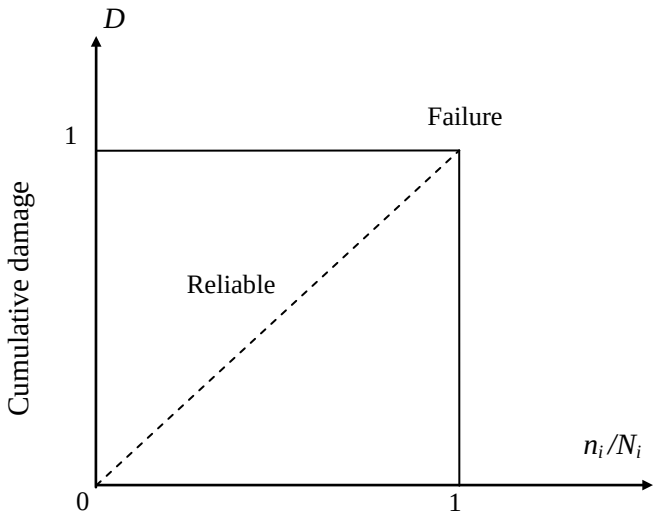

Figure 2.5 - Palmgren-Miner's linear rule of damage.

II.2.4 - Wöhler's Curve

In material fatigue, it is important to know the critical level of applied stresses. When repeated stresses $\sigma(t)$ are applied along the time under cyclic model, they are limited between two extreme values σ_{max} and σ_{min}. Wöhler's curve governs the relation between the applied stress levels σ and the critical number of cycles N_C during the fatigue process of the material (figures 2.6 & 2.7). For example, if the equipment is loaded by a stress level σ_1 then the critical cycle number is N_{C1}. Each stress level has its own critical cycle number.

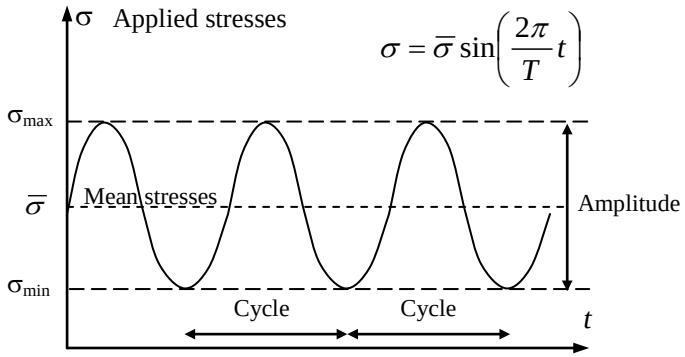

Figure 2.6 - Cyclic applied stresses.

The stress range: $\Delta\sigma = \sigma_{max} - \sigma_{min}$

The stress amplitude: $\Delta\sigma/2$

The stress mean: $\overline{\sigma} = \frac{\sigma_{max} + \sigma_{min}}{2}$

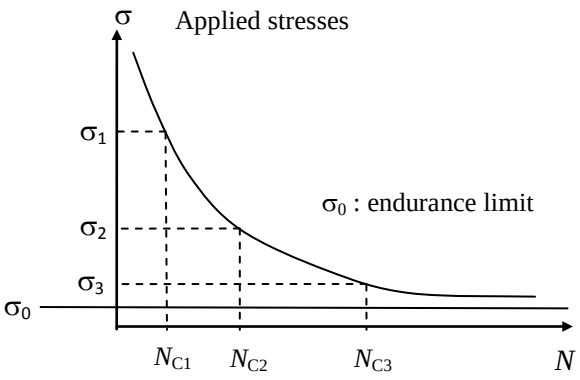

Figure 2.7 - Wöhler's curve of fatigue.

II.2.5 - Stress Intensity Factor

The stress intensity factor is an important term in Paris' law expression; it represents the effect of stress concentration in the presence of a flat crack. When a flat crack occurs in the system body, the internal stresses in this section change from a uniform to a non-uniform distribution around the crack (figure 2.8). This change is expressed by a factor K_I called the stress intensity factor [9,10] given, for mode-I crack opening (mode I: the crack opening is in the same direction of applied stresses), by (6):

$$(K_I)^m = \left(Y(a)\cdot\sqrt{\pi a}\right)^m \cdot (\sigma_{max})^m = \phi_1(a)\cdot\phi_2(P) \qquad (6)$$

.

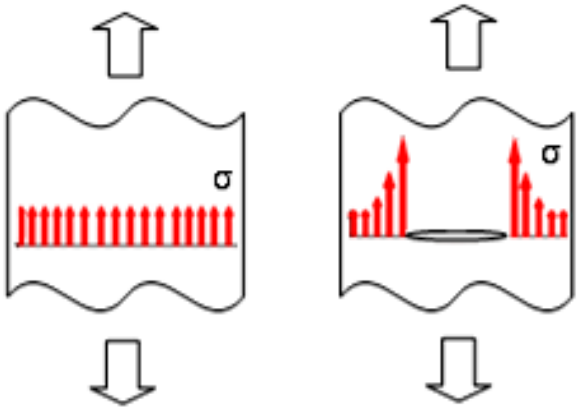

Figure 2.8 - Non-uniform stress distribution near crack.

II.2.6 - Additivity Rule in Palmgren-Miner's Rule.

The case where damage is caused by fatigue is an important application of the additivity rule [11,12]. In this case the measurement of damage is the length of the fatigue crack. The additivity rule in Palmgren-Miner's rule [8] has been proposed as an empirical rule in case of damage due to fatigue controlled by crack propagation. The rule states that in a fatigue test at a constant stress amplitude $\Delta\sigma_i$, damage could be considered to accumulate linearly with the number of cycles. Accordingly, if at a stress amplitude $\Delta\sigma_1$ the component has N_1 cycles of life, which correspond to amount of damage a_C, after Δn_1 cycles at a stress amplitude $\Delta\sigma_1$, the amount of damage will be $(\Delta n_1/ N_1)\, a_C$. After Δn_2 stress cycles spent at a stress amplitude $\Delta\sigma_2$, characterized by a total life of N_2 cycles, the amount of damage will be $(\Delta n_2/ N_2)\, a_C$, etc.

Failure occurs when, at a certain amplitude $\Delta\sigma_M$, the sum of partial amounts of damage attains the amount a_C , i.e. when

$$\frac{\Delta n_1}{N_1} a_C + \frac{\Delta n_2}{N_2} a_C + \cdots + \frac{\Delta n_M}{N_M} a_C = a_C \tag{7}$$

is fulfilled.

As a result, the analytical expression of the Palmgren-Miner's rule becomes:

$$\sum_{i=1}^{M} \frac{\Delta n_i}{N_i} = 1 \tag{8}$$

Where N_i is the number of cycles needed to reach the specified amount of damage a_C at constant stress amplitude $\Delta\sigma_i$.

The Palmgren-Miner's rule is central to reliability calculations yet no comments are made whether it is compatible with the damage development laws characterizing the different stages of fatigue crack growth. The necessary and sufficient condition for validity of the empirical Palmgren-Miner's rule is the possibility of factorizing the rate of damage as a function of the amount of accumulated damage a and the stress or strain amplitude Δp:

$$\frac{da(N)}{dN} = F(a) \cdot G(\Delta p) \tag{9}$$

The theoretical derivation of the Palmgren-Miner's rule can be found in Todinov [11].

A widely used fatigue crack growth model is the Paris-Erdogan's power law given by:

$$\frac{da(N)}{dN} = C \cdot (\Delta K)^m \tag{1}$$

Where,

$\Delta K = Y(a) \cdot \Delta\sigma \cdot \sqrt{\pi a}$: is the stress intensity factor range; C and m are material constants and $Y(a)$ is a parameter which can be presented as a function of the amount of damage a.

Clearly, the Paris-Erdogan's fatigue crack growth law can be factorized as in the previous stated equation and therefore it is compatible with the Palmgren-Miner's rule. In the cases where this factorization is impossible, the Palmgren-Miner's rule does not hold. Such as, for example, the fatigue crack growth law given by (10):

$$\frac{da(N)}{dN} = B \cdot \Delta\gamma \cdot a^{\beta} - D \tag{10}$$

discussed by Miller [11], who characterises physically small cracks.

In the equation above:
B and β are material constants,
$\Delta\gamma$ is the applied shear strain range,
a is the crack length at cycle N,
D is a threshold value.

Thus, following what has been said, the proposed model can use the additivity characteristic of Paris' law.

II.2.7 - Maintenance and Diagnostic/Prognostic

It is proved that the schedule-based inspection/maintenance NDI (Non Destructive Inspection) is less beneficial than the on-demand (or continuous) inspection with permanently installed sensors/condition based maintenance SHM (Structural Health Monitoring) for many reasons like the increased availability, quick assessment of potential/actual damage events, increasing safety, and performance of advanced materials.

But the major technical challenges for SHM reside in the sensors. The monitoring should be directed to the detection of the cracks and corrosion, the multiple damage modes, the pre-crack fatigue damage, and the account for residual stresses.

We can say that the NDI leads to prognostics based on the followings:

- NDI performed at the time of fabrication and as in-service inspections
- Condition based maintenance-active component monitoring
- Move from diagnosis to prediction of remaining life and structural health monitoring/management.
- Prognostics (for machinery) is the prediction of a remaining safe or service life, based on an analysis of the system or material condition, stressors and degradation phenomena.

For example, bearing crack faults may be prognosed by examining and predicting their vibration signals.

The relation between maintenance and prognostic is summarized by figure 2.9.

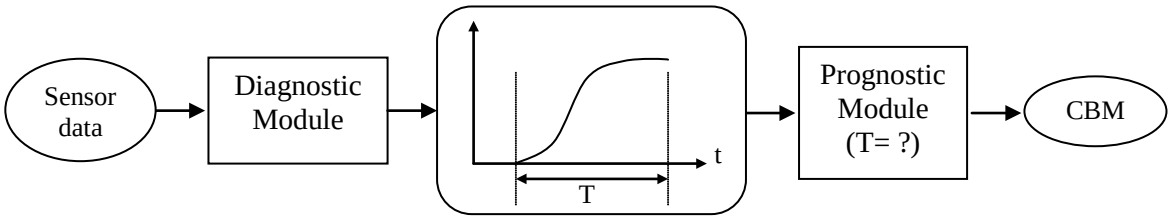

Figure 2.9 - Diagnostic-Prognostic-Maintenance

CBM: Condition-Based Maintenance

II.2.7.1 - Flowchart of Various Components of Diagnostic/Prognostic/Maintenance Process

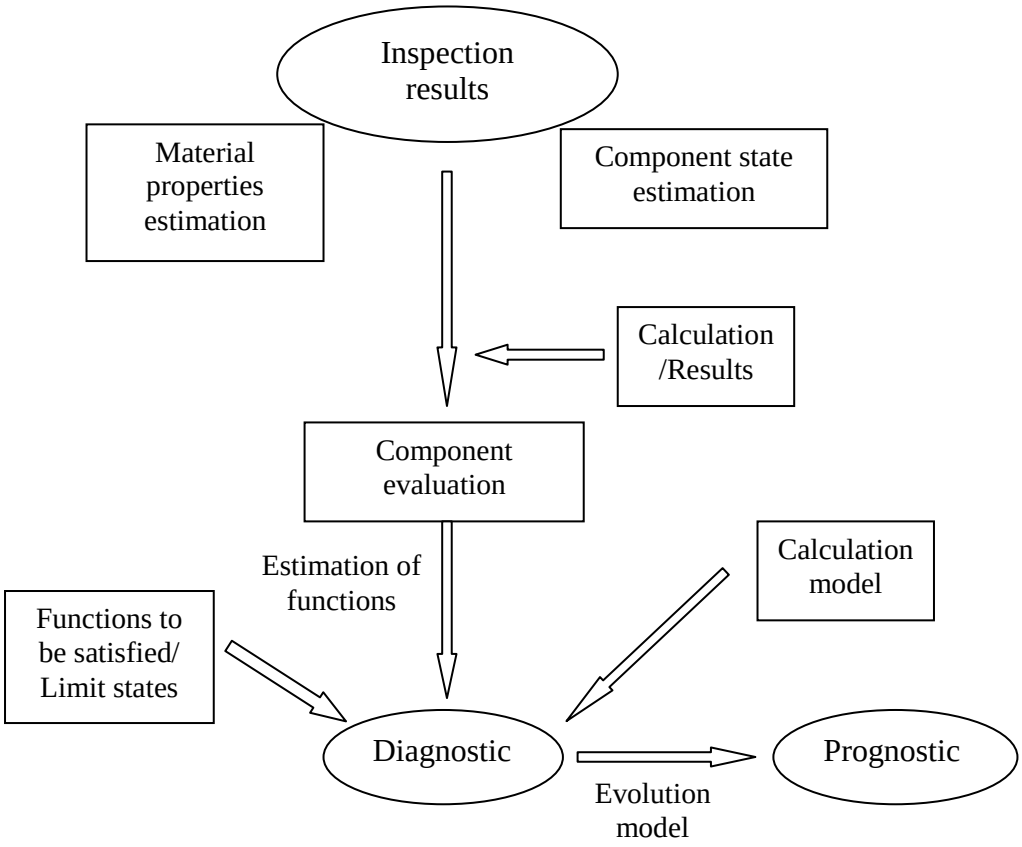

II.2.7.2 - Cycle of Prognostic-Diagnostic-Maintenance

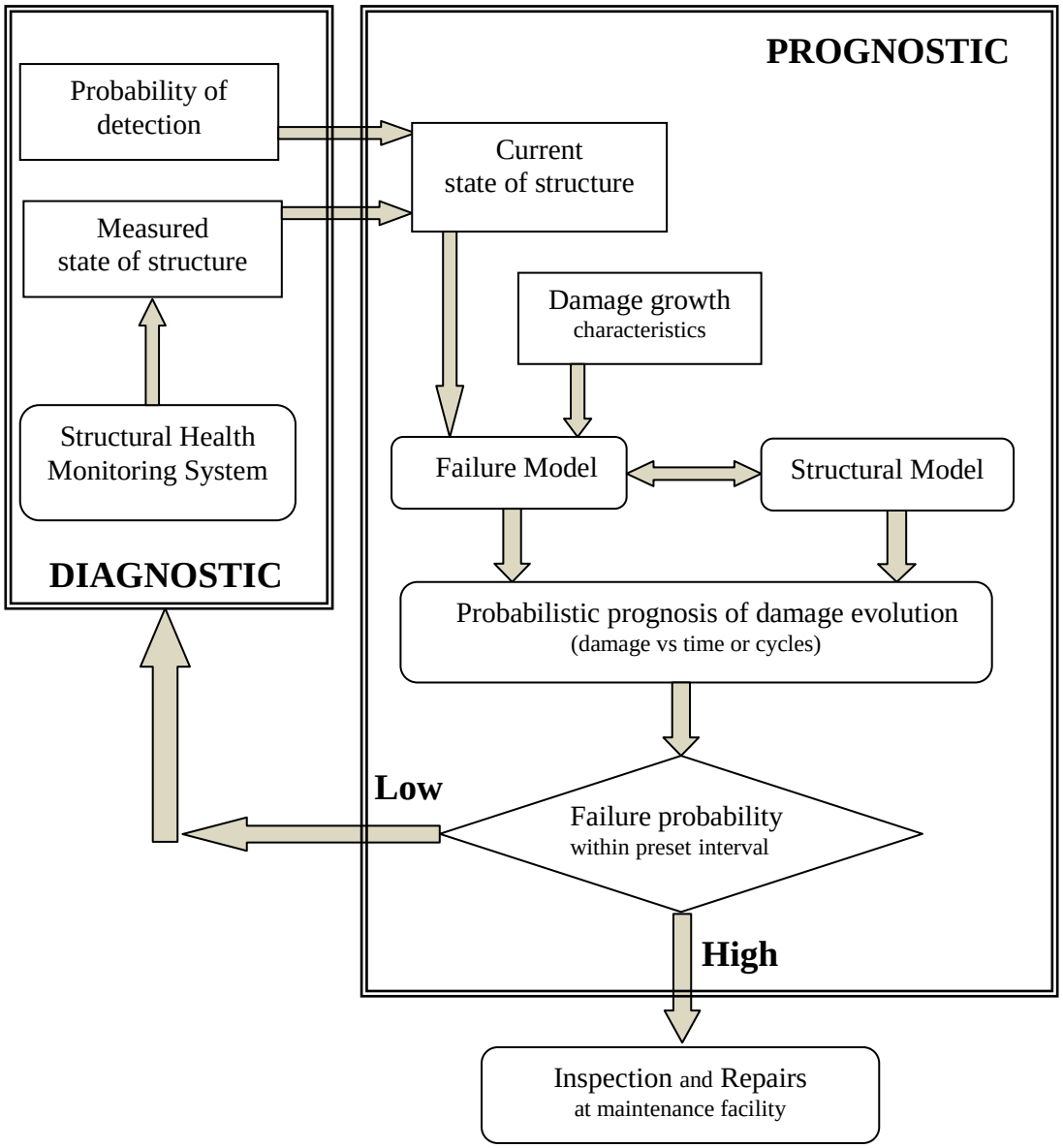

II.2.8 - Accumulation of Fatigue Damage

In fatigue damage, to study the prognosis of a degraded component, our idea is to predict and estimate the end of life of an equipment component subject to fatigue by tracking and modeling the corresponding degradation function. To facilitate the analysis, it is convenient to adopt a normalized damage measurement $D \in [0,1]$ by using the advantage of the cumulative damage law of Palmgren-Miner (figure 2.5). In fact, this law helps estimate the lifetime of components subject to load cycles, it considers that the damage fraction d_i at stress level σ_i is the ratio of n_i over the total cycle number N_i producing the failure.

For a body of equipment of thickness *e*, take the initial crack length as a_0 ($a_0 \le a \le a_C$). Knowing that $1.01 \le e/a \le 10$ and $e/a_C = 8$, from (1) a recurrent form of crack length growth *a* can be deduced as [4]:

$$da = a_N - a_{N-1} = C \cdot \phi_1(a_{N-1} - a_0) \cdot \phi_2(P_j) \;; \quad P_j : \text{is a realization of } P$$

$$\Rightarrow \quad a_N = a_{N-1} + C \cdot \phi_1(a_{N-1}) \cdot \phi_2(P_j); \quad \text{where } (a_0 \approx 0)$$

For the other sequences:

$$\begin{aligned} a_1 &= a_0 + C\phi_1(a_0)\phi_2(P_j) \\ a_2 &= a_1 + C\phi_1(a_1)\phi_2(P_j) \\ &\vdots \quad \vdots \\ a_N &= a_{N-1} + C\phi_1(a_{N-1})\phi_2(P_j) \end{aligned}$$

$$\Rightarrow da = a_N - a_{N-1} = C \cdot (K_I)^m \times dN$$

For each cycle we have: $dN = 1$, therefore: $a_N = a_{N-1} + C \cdot (K_I)^m$

As $D_k = \sum_{i=1}^{k} d_i = \sum_{i=1}^{k} \frac{n_i}{N_i}$ (Miner's law with i in Miner's law = N in our model)

Based on the additivity characteristic of Paris' law, the addition of damages gives the total crack growth at failure point $(a_C - a_0)$ realized at the total number of cycle N_C:

$$a_C - a_0 = \sum_{N=1}^{N_C} da_N = \text{Total damage}$$

At each n_i the crack grows of length $da_i = da_N$, therefore the Miner's damage fraction, for any stress level (figure 2.10), is given in terms of crack length by (11):

$$d_i = \frac{n_i}{N_i} = \frac{da_N}{(a_C - a_0)} \tag{11}$$

Where,

n_i is the damage increment due to stress number i

N_i is the total damage for stress number i

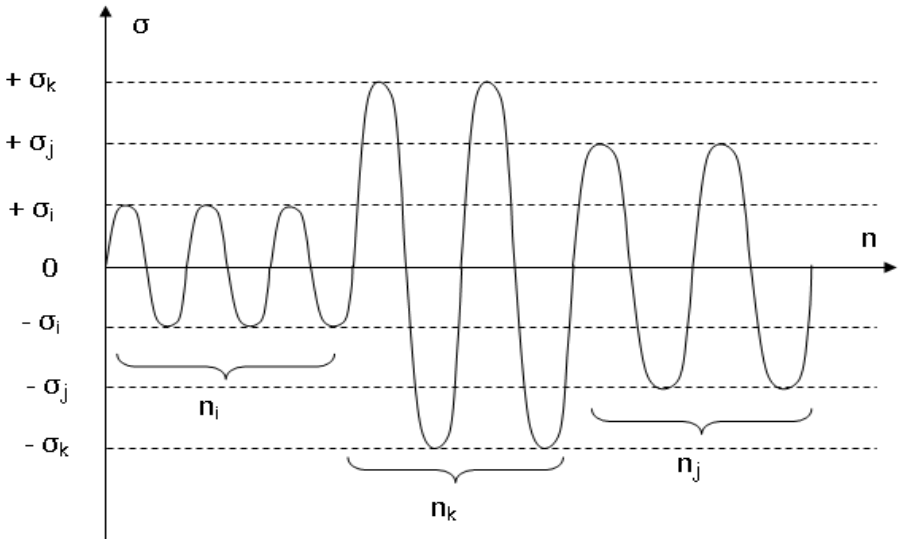

Figure 2.10 - Cumulative stress levels.

Then, the cumulated total damage at cycle N is given by (12):

$$D_N = \sum_{i=1}^{N} d_i = \sum_{i=1}^{N} \frac{da_i}{a_C - a_0} = \frac{\sum_{i=1}^{N} da_i}{a_C - a_0} = \frac{a_N}{a_C - a_0} \tag{12}$$

It can be easily proved that:

$$D_C = \sum_{i=1}^{N_C} d_i = \frac{a_C - a_0}{a_C - a_0} = 1$$

$$\text{As}: a_0 \le a \le a_C \text{ then}: \quad D_0 \le D \le D_C = 1$$

$$D_0 = \frac{a_0}{a_C - a_0} \Rightarrow a_0 = \frac{D_0 a_C}{1 + D_0}$$

The other sequences are $(0 \le N \le N_C)$:

$$D_0 = \frac{a_0}{a_C - a_0}; \quad D_1 = \frac{a_1}{a_C - a_0}; \quad D_2 = \frac{a_2}{a_C - a_0}; \quad \cdots\cdots \; ; \quad D_N = \frac{a_N}{a_C - a_0}$$

A recurrent form of degradation can be deduced as follows:

$$
\begin{aligned}
D_N &= \frac{a_N}{a_C - a_0} \\
&= \frac{a_{N-1} + C \cdot (K_I)^m}{a_C - a_0} \\
&= \frac{a_{N-1}}{a_C - a_0} + \frac{C \cdot (K_I)^m}{a_C - a_0} \\
&= \frac{a_{N-1}}{a_C - a_0} + \frac{C \cdot \left(Y(a_{N-1}) \cdot \sqrt{\pi \cdot a_{N-1}} \cdot \sigma_j\right)^m}{a_C - a_0} \\
&= \frac{a_{N-1}}{a_C - a_0} + \frac{C \cdot Y(a_{N-1})^m \cdot \left(\sqrt{\pi \cdot a_{N-1}}\right)^m \cdot {\sigma_j}^m}{a_C - a_0} \\
&= \frac{a_{N-1}}{a_C - a_0} + \frac{C}{a_C - a_0} \cdot Y(a_{N-1})^m \cdot \left(\sqrt{\pi \cdot a_{N-1}}\right)^m \cdot {\sigma_j}^m \\
&= D_{N-1} + \eta \cdot \phi_1(D_{N-1}) \cdot \phi_2\left(P_j\right)
\end{aligned}
\tag{13}
$$

Where,

$D_{N-1} = \frac{a_{N-1}}{a_C - a_0}$;

$\eta = \frac{C}{a_C - a_0}$;

$\phi_1(D_{N-1}) = Y(a_{N-1})^m \cdot \left(\sqrt{\pi \cdot a_{N-1}}\right)^m$;

$\phi_2(P_j) = \sigma_j^m$.

Hence, the new prognostic analytic model is presented by the general function given by (14):

$$
D_N = D(N) = P_{rog}(a_N) = \frac{a_{N-1}}{a_C - a_0} + \frac{C}{a_C - a_0} \cdot Y(a_{N-1})^m \cdot \left(\sqrt{\pi \cdot a_{N-1}}\right)^m \cdot {\sigma_j}^m \tag{14}
$$

And therefore, the degradation trajectories $D(N)$ along the total number of loading cycles N can be drawn [13].

II.2.9 - Flowchart of the Prognostic Model

The following flowchart summarizes all the procedures of the proposed model [14]:

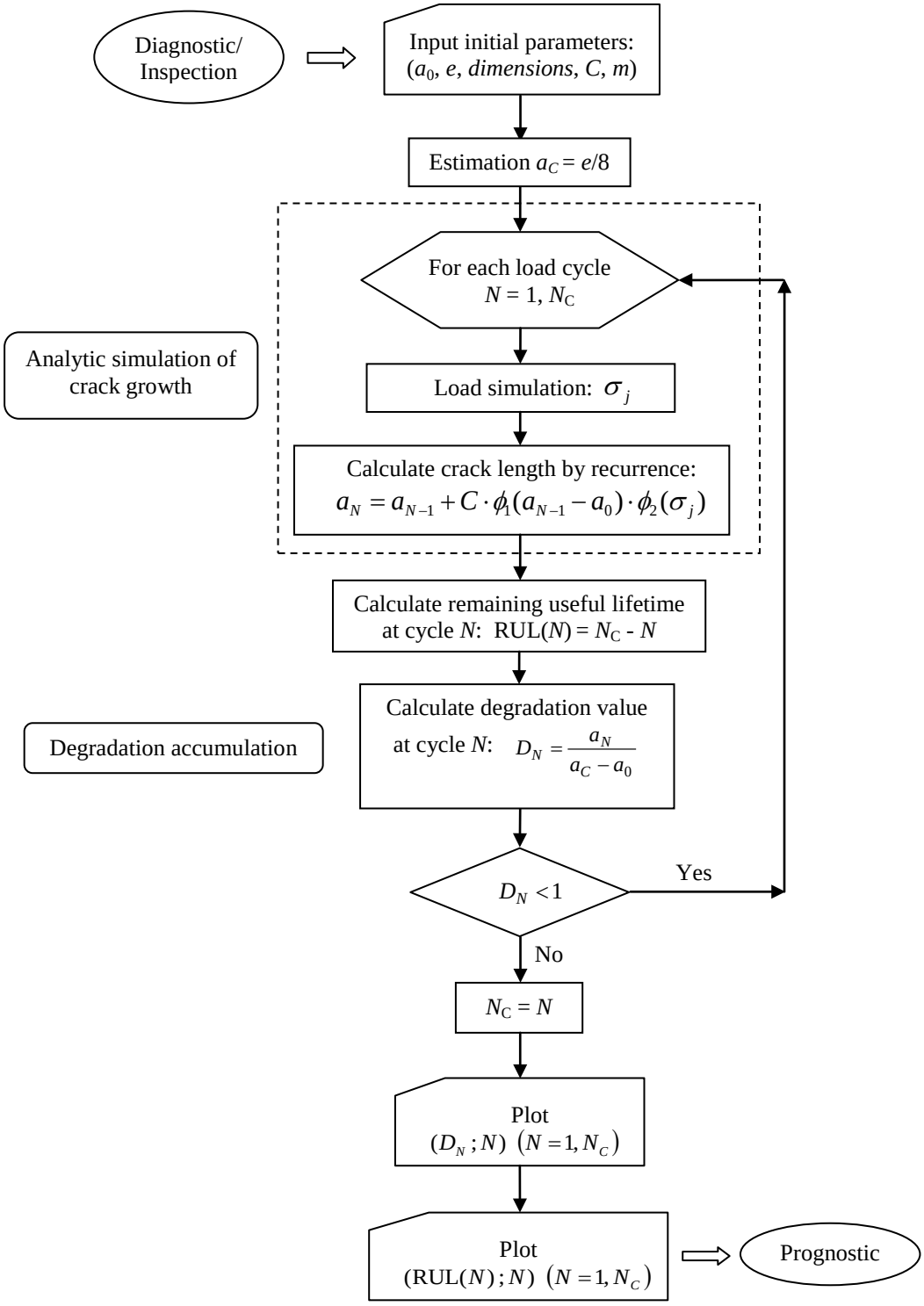

II.2.10 - Environment Effects in the Proposed Prognostic Model

The environment effects are taken into account through two parameters C and m. These parameters are related to the material in its environment.

Large values of m (m>40) correspond to the case of brittle materials (brittle failure), and small values of m ($m \rightarrow 2$) correspond to the case of ductile materials (m = 2 fully plastic). Otherwise for fatigue failure the range value of m is: $2 \leq m \leq 3$. The parameter m depends mainly on the specimen length. For lower toughness steels m is greater than or equal to 3 [15].

Coefficient C is affected by the edges and consequently its value depends on whether it is the case of a plane stress or a plane strain. However, for the case of an infinite equipment body and far from the edge effects, the coefficient C takes a constant value [16].

C and m depend on the testing conditions, such as loading ratio $\sigma_{min}/\sigma_{max}$, on the geometry and size of the specimen, and on the initial crack length.

These two parameters govern the behavior of the material during the fatigue process through the crack propagation. The environment influencing parameters on this process like temperature, humidity, geometry dimensions, material nature, water action, soil action, applied load location, body shape, are also represented by these two parameters C and m.

These two parameters are evaluated by the mean of experiments in true conditions.

Examples [15,16]: $C = 5.2.10^{-13}$ (free air)

$C = 1.3.10^{-14}$ (under soil)

$C = 2.10^{-11}$ (offshore)

and m = 3 (metal).

II.3 - Application of the Prognostic Method to Industrial Systems

To illustrate the proposed new analytic approach, it will be applied in this section to two important mechanical systems which are: the pipelines system in petrochemical industry and the suspensions in automotive industry. The prognostic studies of these two fields of industry are essential for economy reasons.

II.3.1 - Vehicle Suspension Fatigue Life

Fatigue analysis of a vehicle suspension (figure 2.11) by finite elements models was done in many works [17] beside the experimental results. It permits to define the location of potential fatigue cracks. The major feature of local strain fatigue lives to crack initiation. The original theories were developed for uniaxial stress conditions, and later, to eliminate the errors due to the simplified uniaxial conditions.

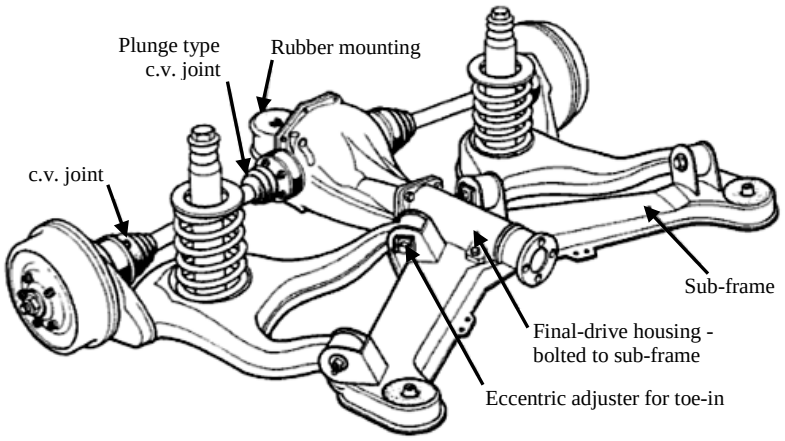

Figure 2.11 - Vehicle suspension system.

It was proposed in literature [18,19] that for high cycle fatigue successful life estimates for biaxial stress conditions could be made using combinations of axial and shear stresses.

There is much experimental evidence from fatigue testing carried out in the middle of the last century showing that stress gradients has an important effect on the total fatigue life of a component. Stress gradients have also been used in an attempt to explain the effect of notch sensitivity.

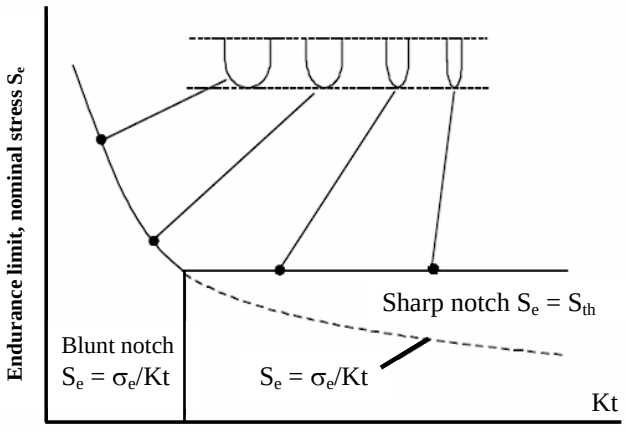

Figure 2.12 - Relationship between endurance limit stress σ_e and the stress concentration factor Kt [13].

Finite element analysis provides surface strains on the model but for real engineering components it is very difficult to determine the stress concentration factor at a notch (figure 2.12).

The stress concentration factor is the same as the stress intensity factor explained in paragraph II.2.5.

The endurance limit stress is the stress level for which the critical number of loading cycles tends to infinity (refer to paragraph II.2.4).

Where,

σ_e is the smooth specimen endurance limit stress,

S_{th} is the threshold stress for non-propagation cracks, i.e. below S_{th} fatigue is not influent and $S_e = S_{th}$

Kt is the stress concentration factor,

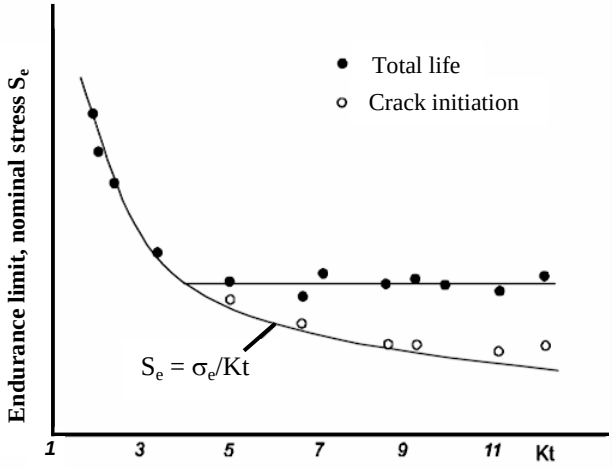

Figure 2.13 - Relationship between endurance limit stress σ_e and the stress concentration factor Kt for crack initiation and total life.

and we have: $$Kt = \frac{\text{Endurance limit of a notch free specimen}}{\text{Endurance limit of a notched specimen}}.$$

The endurance limits [19] are obtained from standard rotating beam experiments carried out under certain specific conditions. It is given by: $S_e = \sigma_e / Kt$.

As the stress concentration factor increases, and that for many ductile metals, a minimum value of fatigue limit stress occurs and is S_{th}. Further increasing the stress concentration factor by sharpening the notch produces no further reduction in fatigue strength (figure 2.13).

The parts forming the vehicle suspension are indicated in figure 2.14 where the damper's element can be seen.

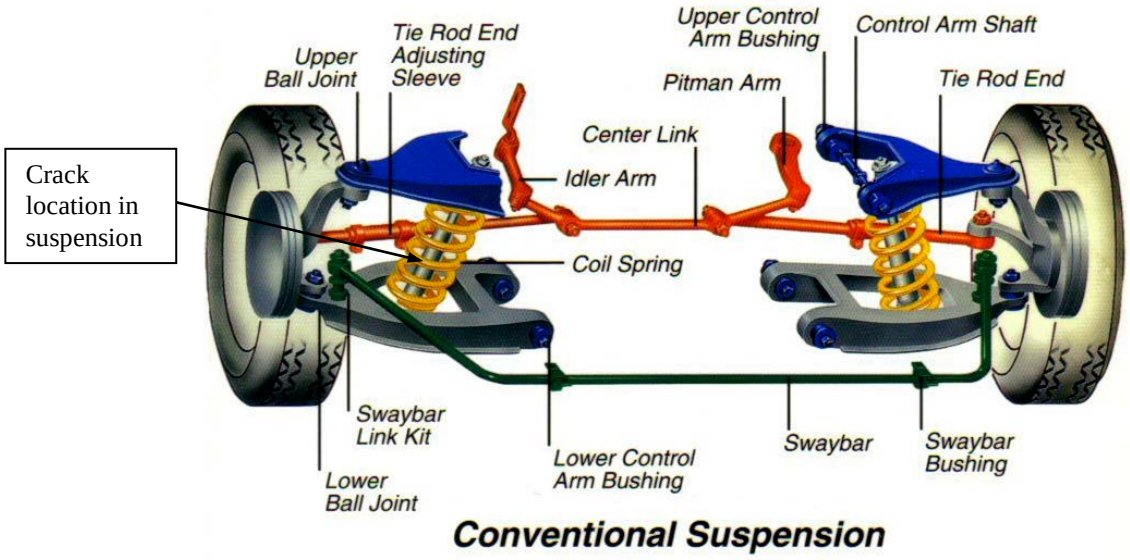

Figure 2.14 - Vehicle suspension components and crack possible location

Using test data on plate and round bar specimens in aluminum alloy and steel materials have shown that if fatigue life to first crack initiation is considered, then the fatigue strength reduces with increasing stress concentration with no limiting value (figure 2.15).

Many works [20,21,22] have shown that the constant amplitude endurance limit does not apply to the analysis of real service loading if some cycles in the loading exceed the constant amplitude endurance limit stress amplitude. For finite life design the larger cycles in the loading cause the endurance limit stress to be reduced significantly, with the result that small cycles contribute to the fatigue damage process.

Figure 2.15 below [21] shows the results of strain-controlled constant amplitude tests on an aluminum alloy at high temperature. The Finite Element calculation made by the software SAFE (FE-SAFE) from an elastic Finite Element Analysis (FEA) shows excellent correlation for high cycle fatigue. For low cycle fatigue, at 1000 cycles the calculated fatigue life is conservative by a factor of 3. This is a commonly observed phenomenon at such low fatigue lives in components where yielding occurs across the entire section. For comparison, an elastic-plastic FEA analysis of the model was used as input into the FE-SAFE analysis, and the correlation with the test result was then excellent.

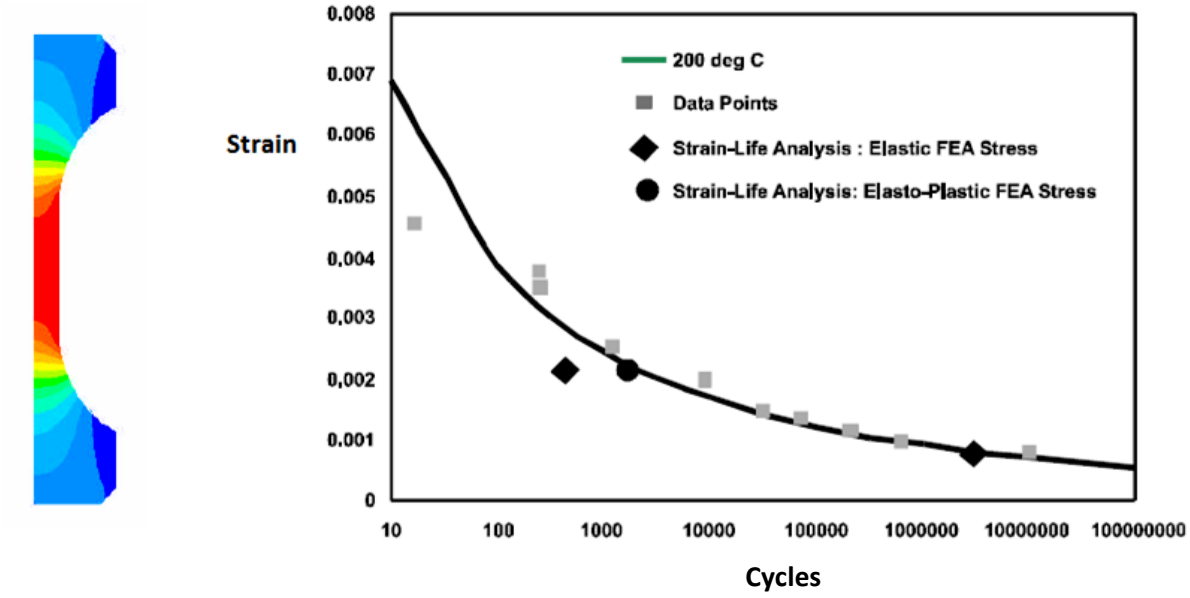

Figure 2.15 - Comparison of test data with calculated lives from elastic and elastic-plastic FE analysis.

This component was analyzed in FE-SAFE and compared with the results of fatigue testing. A scale factor was applied to the test loading to produce a failure. The correlation between the calculated life of 1631 repeats of the load history and the test life of 1650 repeats is extremely good.

The steel component was analyzed [22] with a load-time history in one direction (figure 2.16). A scale factor was applied to produce a failure. The analysis used stresses from an elastic FEA; fatigue lives were calculated for each node on the model, using averaged nodal stresses. Experience has shown that this is much more accurate than using stresses at integration points or at the element centroid.

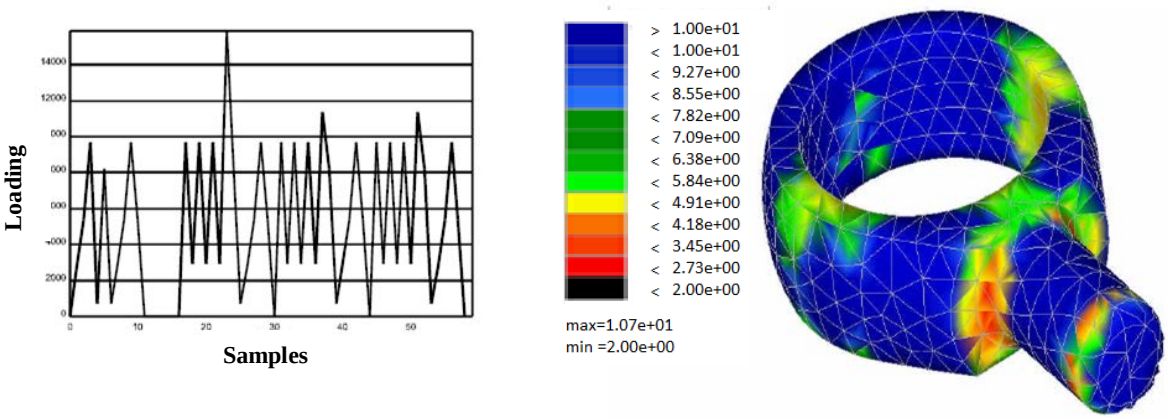

Figure 2.16 - Loading history for accelerated testing (left) and fatigue life contours (right).
Test life: 1650 repeats of loading. Calculated life: 1631 repeats of loading.

In designing engine crank shafts (figure 2.16), the finite elements analysis is used to generate stress solutions. The FEA analysis shows that the principal stresses change their orientation and magnitude during the load cycle applied to the crank shaft.

FE-SAFE uses the sequence of FEA analysis results to calculate the fatigue life at each node. FE-SAFE correctly identified the critical location in the crank shaft, using a Brown-Miller fatigue analysis, and correlated well with test results.

A common theme from these validation exercises is that a uniaxial strain-life using the maximum principal stress can fail to identify the critical location, for components where biaxial stresses (Von-Mises) and particularly non-proportional stresses are present at the critical locations.

In the computer-based fatigue analysis of the finite element model the type of loading depends very much on the customer's requirements. Some companies [22] specify a validation using simple sinusoidal loading, whereas other companies, such a Ford, require the application of measured time histories of vertical, braking and cornering forces on the tyre contact patch or wheel center (figure 2.17). At present, the test procedure uses a single actuator to apply the forces at the tyre contact patch, angled to produce a specific relationship between the three forces. FE-SAFE allows for different time histories to be applied in each direction, up to 4096 load histories of unlimited length.

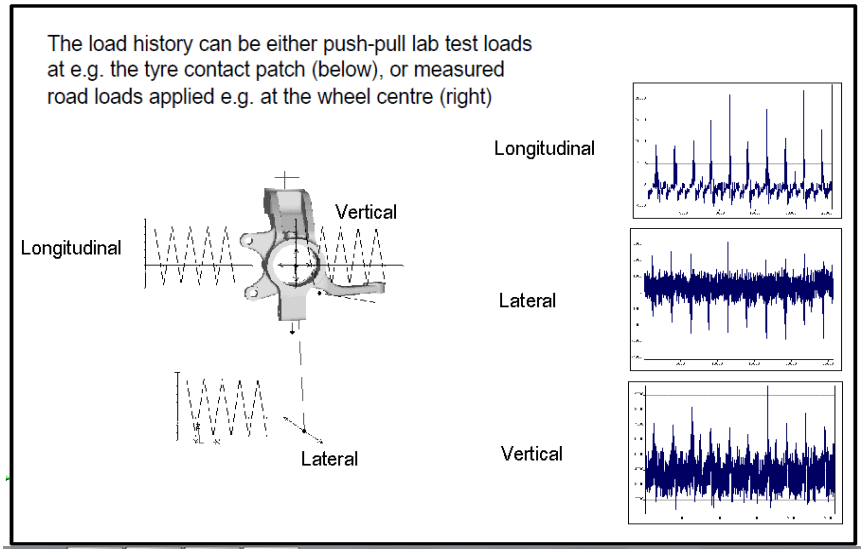

Figure 2.17 - Application of force time histories.

II.3.1.1 - Types of Mechanical Effects, Their Mechanisms, and Possible Consequences

The following flowchart describes the relationship between the sources, the mechanical effects and the consequences of various loading stresses [5].

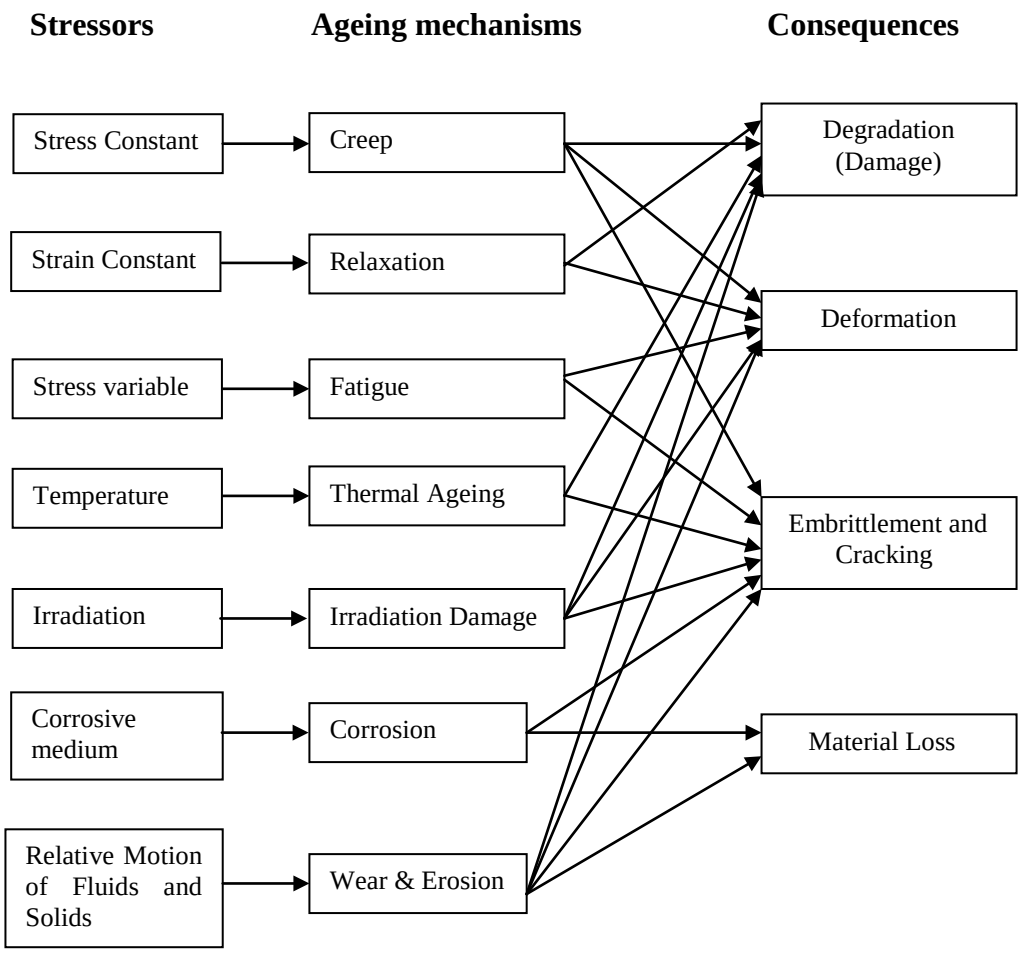

II.3.1.2 - Automatic Diagnostic of a Bad Suspension Bushing

Automobile suspension bushings come in a variety of shapes, sizes and thicknesses, according to their application. Bushings may be made from several materials, including rubber, polyurethane, urethane and graphite composites. Bushings prevent wear to expensive suspension components by absorbing vertical and lateral forces produced by the vehicle over different terrain. They cushion and absorb shock on the chassis to keep it shock from entering the passenger compartment. While absorbing these vibrations, they still allow limited movement and flex in the suspension joints, keeping the wheels firmly grounded and on track during turning manoeuvres. A vehicle's owner may check all its suspension bushings for proper shape and condition.

II.3.1.3 - Prognostic Study for Vehicle Suspension Systems

Let us consider a half-vehicle suspension system (figure 2.18) subject to non-regular road surface excitations [23]. It is composed from a front part and a rear part. To study the prognostic of this system, it is important to define the mechanical model in order to conclude the output response from the input excitation road.

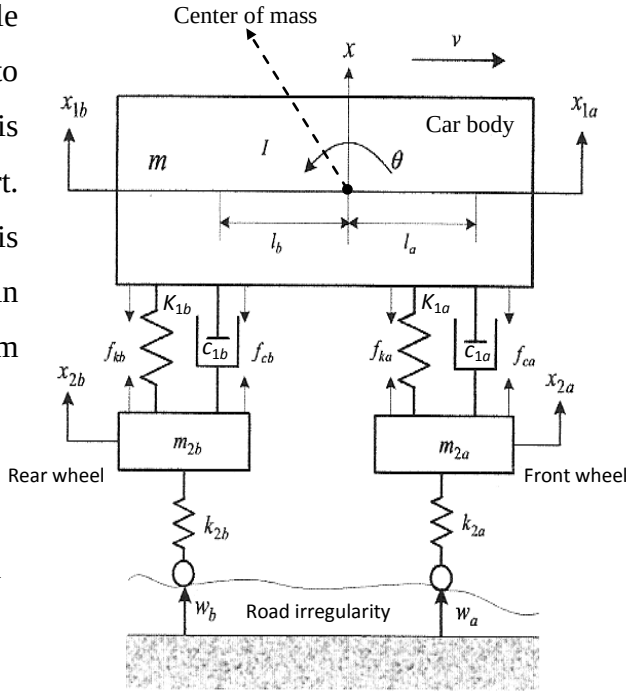

Figure 2.18 - Vehicle suspension model

The dynamic equations of the system are given by:

$$m\ddot{x} + (f_{ca} + f_{ka}) + (f_{cb} + f_{kb}) = 0$$

$$I\ddot{\theta} + l_a (f_{ca} + f_{ka}) - l_b (f_{cb} + f_{kb}) = 0$$

$$m_{2a}\ddot{x}_{2a} - (f_{ca} + f_{ka}) + k_{2a}(x_{2a} - w_a) = 0$$

$$m_{2b}\ddot{x}_{2b} - (f_{cb} + f_{kb}) + k_{2b}(x_{2b} - w_b) = 0$$

$$x = (l_b\, x_{1a} + l_a\, x_{1b})/l \ , \ \tan\theta \approx \theta = \frac{(x_{1a} - x_{1b})}{l}$$

$$l = l_a + l_b$$

$$f_{ci} = c_i(\dot{x}_{1i} - \dot{x}_{2i}), \quad i = a,b$$

$$f_{ki} = k_{1i}(x_{1i} - x_{2i}), \quad i = a,b$$

Where,

m : vehicle mass, I : moment of inertia

m_{2a} : mass of front wheel, m_{2b} : mass of rear wheel

θ : rotary angle of vehicle, x : vertical displacement

c_i : friction coefficient of dumping ($i = a,b$)

f_{ca} , f_{cb}: dumping force of the front/rear wheel

f_{ka} , f_{kb}: restoring force of the front/rear wheel

k_{1a} , k_{1b}: spring constants of the front/rear suspension

k_{2a} , k_{2b}: spring constants of the front/rear wheel

x_{2a}, x_{2b}: vertical displacement of the front/rear wheel

x_{1a}, x_{1b}: displacement of the vehicle body at front/rear wheel

l_a , l_b : distance of the front/rear suspension to center

w_a, w_b: irregular excitations from the road surface

(See figure 2.19)

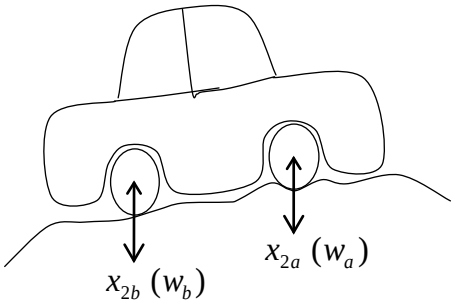

Figure 2.19 - Road profile excitation.

II.3.1.4 - System Identification

The model parameters are given by the following numerical data [23]:

m = 1200 kg, I = 2100 kg.m^2

m_{2a} = 30 kg, m_{2b} = 25 kg

c_b = 4000 N/m/s, c_a = 5000 N/m/s

k_{1a} = 56000 N/m, k_{1b} = 42000 N/m

k_{2a} = k_{2b} = 152 kN/m, l_a = 0.9 m, l_b = 1.2 m

The matrix form of the previous equations is given by (15):

$$M\ddot{z} + N\dot{z} + Kz = Eu \tag{15}$$

Where M is the mass matrix, N is the dumping coefficients matrix, and K is the stiffness matrix.

The input excitation vector is: $u = \begin{bmatrix} w_a & w_b \end{bmatrix}^T$

The output damper displacement vector is: $z = \begin{bmatrix} x_{1a} & x_{2a} & x_{1b} & x_{2b} \end{bmatrix}^T$

The vertical accelerations $\ddot{x}_{1a}, \ddot{x}_{1b}, \ddot{x}_{2a}, \ddot{x}_{2b}$ are measured variables. The matrices M, N, K, and E are given by:

$$M = \begin{bmatrix} l_b m/l & 0 & l_a m/l & 0 \\ I/l & 0 & -I/l & 0 \\ 0 & m_{2a} & 0 & 0 \\ 0 & 0 & 0 & m_{2b} \end{bmatrix} \qquad N = \begin{bmatrix} c_a & -c_a & c_b & -c_b \\ l_a c_a & -l_a c_a & -l_b c_b & l_b c_b \\ -c_a & c_a & 0 & 0 \\ 0 & 0 & -c_b & c_b \end{bmatrix}$$

$$K = \begin{bmatrix} k_{1a} & -k_{1a} & k_{1b} & -k_{1b} \\ l_a k_{1a} & -l_a k_{1a} & -l_b k_{1b} & l_b k_{1b} \\ -k_{1a} & k_{1a}+k_{2a} & 0 & 0 \\ 0 & 0 & -k_{1b} & k_{1b}+k_{2b} \end{bmatrix} \qquad E = \begin{bmatrix} 0 & 0 \\ 0 & 0 \\ k_{2a} & 0 \\ 0 & k_{2b} \end{bmatrix}$$

The state vectors (damper displacements and velocity) are:

$$x = \begin{bmatrix} z(t) \\ \dot{z}(t) \end{bmatrix} \quad , \quad \dot{x} = \begin{bmatrix} \dot{z}(t) \\ \ddot{z}(t) \end{bmatrix}$$

II.3.1.5 - Fatigue Damage Modeling of a Suspension

The modeling of the suspension damage begins by determining the stress intensity factor composed of the multiplication of two functions:

$$(K_I)^m = \left(Y(a) \cdot \sqrt{\pi a}\right)^m \cdot (\sigma_{max})^m = \phi_1(a) \cdot \phi_2(P_j) \qquad (6)$$

Where,

$\phi_1(a)$ is the crack length function determined in terms of a geometric function $Y(a)$,

$\phi_2(P_j)$ is the loading function.

Assume that the front suspension of the system has a crack length *a* perpendicular to the exterior load (figure 2.20).

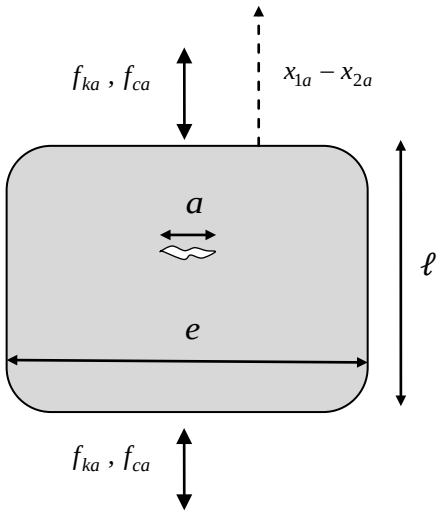

Figure 2.20 - Suspension fatigue crack modeling.

Let $m = 2$ be the material constant, then: $\phi_1(a) = \left(Y(a) \cdot \sqrt{\pi a}\right)^2$

Therefore, by empirical measurements, the first function can be considered as given by [24] (16):

$$\phi_1(a_N) = (\pi a_N)\left[1.122 - 1.4\left(\frac{a_N}{e}\right) + 7.33\left(\frac{a_N}{e}\right)^2 - 13.08\left(\frac{a_N}{e}\right)^3 + 14\left(\frac{a_N}{e}\right)^4\right]^2 \qquad (16)$$

Where,

a_N : the crack length at cycle *N*,

e : the width of the mechanical component of the suspension.

Assume that the maximum of a_N is: $a_C = \frac{e}{8}$; [5]

We define $D_N = \frac{a_N}{a_C - a_0} \approx \frac{a_N}{a_C} = \frac{8a_N}{e}$ (as $a_0 << a_C$)

We replace $\phi_1\left(a_N = \frac{eD_N}{8}\right)$ in equation (13) and we get:

$$D_N = D_{N-1} + \eta \cdot \phi_1(D_{N-1}) \cdot \phi_2(P_j) \qquad (17)$$

Knowing that P_j is the load parameter, and we have $\phi_2(P_j) = P_j^m = P_j^2$. Moreover, η is a material constant and we have $\eta = 8.10^{-6}$ [24].

II.3.1.6 - Simulation of the Degradation Model

We will simulate the degradation model by generating the load P_j of road profile $\begin{bmatrix} w_a & w_b \end{bmatrix}^T$ [3] under the Gaussian Normal law for the three modes of roads (table 2.1).

From the system of equations (15), the solution of this system of matrices gives the output vector z.

Then, the range of the suspension displacement is given, for the front wheel, by (18):

$$\Delta x_j = x_{1a}^j - x_{2a}^j \tag{18}$$

We take as mean value $\overline{x}_j$ and standard variation σ_{x_j}, we obtain a set of $\{x\}^r$ for each road mode $(r = 1,2,3)$, the load parameter is always P_j.

We have the recursive formula (19) in terms of crack length:

$$a_N = a_{N-1} + C \cdot \phi_1(a_{N-1}) \cdot \phi_2(P_j) \tag{19}$$

With [25]: $m = 2$; $C = \eta \cdot (a_C - a_0)$; $\eta = 8.10^{-6}$

$$\phi_1(a_{N-1}) = (\pi a_{N-1}) \left[1.122 - 1.4 \left(\frac{a_{N-1}}{e} \right) + 7.33 \left(\frac{a_{N-1}}{e} \right)^2 - 13.08 \left(\frac{a_{N-1}}{e} \right)^3 + 14 \left(\frac{a_{N-1}}{e} \right)^4 \right]^2 \tag{20}$$

and

$\phi_2(P_j) = P_j^m = P_j^2 = \sigma_j^2$.

The amplitude of the stresses developed in the suspension due to Δx_j is simplified by (21):

$$\Delta\sigma_j = E \times \frac{\Delta x_j}{\ell} \tag{21}$$

Where,

ℓ : the length of the suspension device ($\ell = 500$ mm)
Δx_j : the variation of this length (dilation) under road profile excitation
E : Young's modulus of the suspension material ($E = 200$ GPa)

Therefore, the recursive expression of the crack length for the suspension model is given by:

$$a_N = a_{N-1} + C \times (\pi a_{N-1}) \left[1.122 - 1.4 \left(\frac{a_{N-1}}{e} \right) + 7.33 \left(\frac{a_{N-1}}{e} \right)^2 - 13.08 \left(\frac{a_{N-1}}{e} \right)^3 + 14 \left(\frac{a_{N-1}}{e} \right)^4 \right]^2 \times \sigma_j^2 \quad (22)$$

From the equation $D_N = \frac{a_N}{a_C - a_0}$, the recursive expression of the degradation indicator for the suspension model becomes:

$$D(N) = \frac{a_{N-1}}{a_C - a_0} + \frac{C}{a_C - a_0} \times (\pi a_{N-1}) \times \left[1.122 - 1.4 \left(\frac{a_{N-1}}{e} \right) + 7.33 \left(\frac{a_{N-1}}{e} \right)^2 - 13.08 \left(\frac{a_{N-1}}{e} \right)^3 + 14 \left(\frac{a_{N-1}}{e} \right)^4 \right]^2 \times \sigma_j{}^2 \quad (23)$$

II.3.1.7 - Simulation of Three Road Profiles

To take into account various state of roads, we consider three different types of roads which are: severe, fair, and good. In the following table, we indicate the statistical characteristics of each type of roads.

Table 2.1 - Statistical characteristics of each mode of roads

Road Mode	Mean of Δx_j ($\overline{\Delta x_j}$ in mm)	Coefficient of Variation of Δx_j in %	Standard Deviation (in mm)	Law
Severe (mode 1)	100	15%	15	Normal
Fair (mode 2)	50	10%	5	Normal
Good (mode 3)	25	5%	1.25	Normal

The parabolic road profile for T = 2 seconds of a vehicle circulation time as a recurrent interval is considered. And this interval is repeated as needed until reaching the failure (D_C = 1). Figure 2.21 illustrates the road profile:

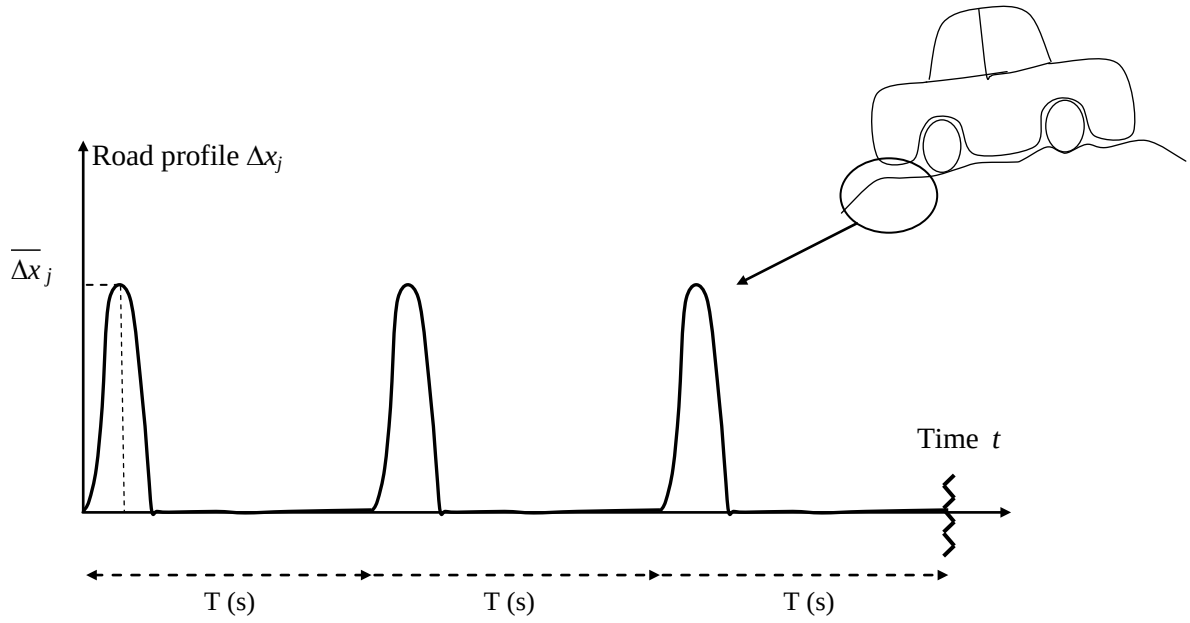

Figure 2.21 - Simulated road profile

Each interval shows that the road profile contains a symmetric curve of width T/8 = 0.25(s) with a peak value followed by a horizontal run of zero amplitude.

II.3.1.8 - Simulation Results

The prognostic study of a suspension is realized through the degradation simulation (equation 23). The methodology is composed of two parts:

- In the first part, the simulation of the road profile for the three modes (severe, fair, and good) (table 2.1) is done using the Normal law from which Δx and $\Delta\sigma$ are deduced.
- In the second part, the crack length a_N is cumulated at each cycle N (equation 22).

The resulting curves $D(N)$ are represented in the following three figures:

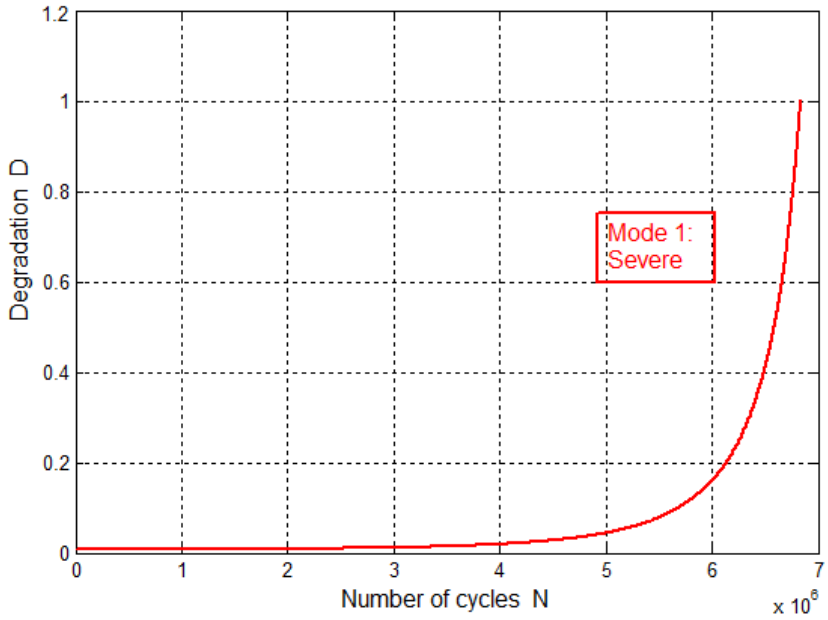

Figure 2.22 - Degradation trajectory for the road with mode 1 profile.

In mode 1 case (Severe), it is noted that (figure 2.22) for N = 6,836,000 cycles, the degradation D_N reaches the critical value D_C = 1. The deduced lifetime of the suspension is 6,836,000 cycles of road excitation in mode 1. Moreover, the first sign of damage appears at about 2,500,000 cycles. Starting from 6,000,000 cycles, the slope of the degradation curve becomes very acute; hence damage is increasing very fast.

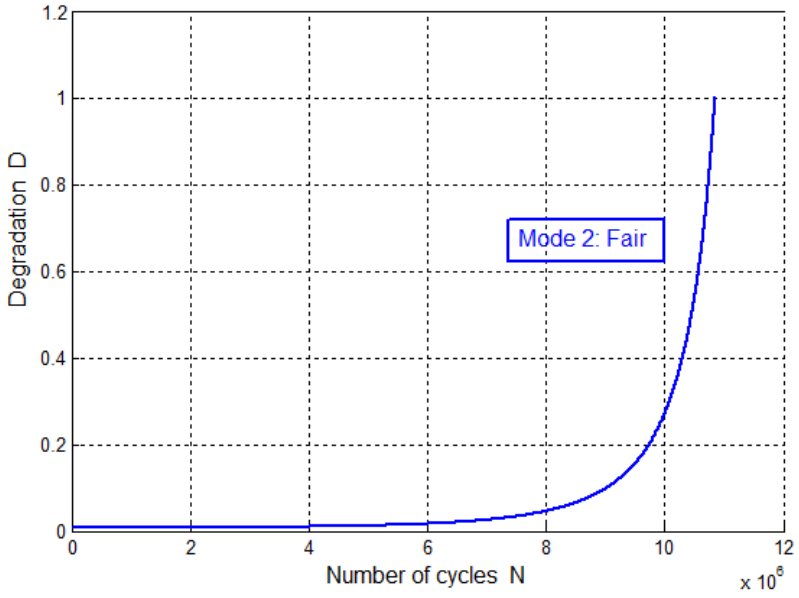

Figure 2.23 - Degradation trajectory for the road with mode 2 profile.

In mode 2 case (Fair), it is noted that (figure 2.23) for N = 10,850,000 cycles, the degradation D_N reaches the critical value D_C = 1. The deduced lifetime of the suspension is 10,850,000 cycles of road excitation in mode 2. Moreover, the first sign of damage appears at

about 4,000,000 cycles. Starting from 10,000,000 cycles, the slope of the degradation curve becomes very acute; hence damage is increasing very fast.

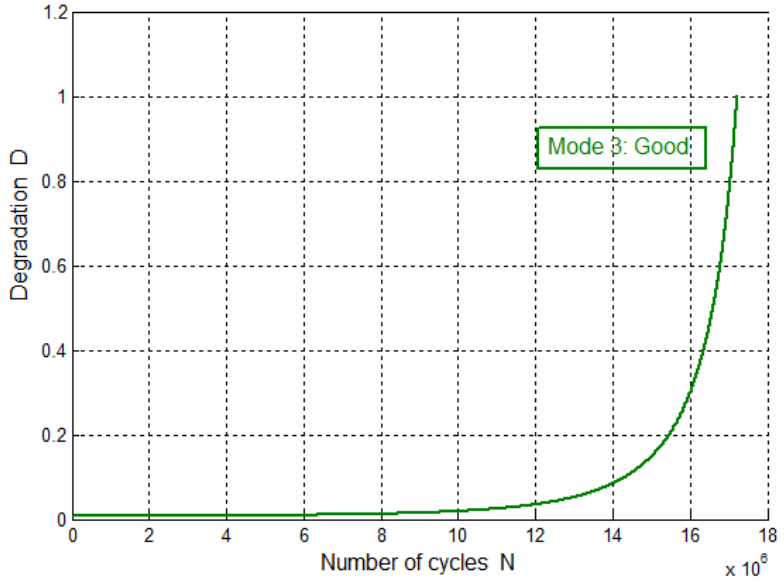

Figure 2.24 - Degradation trajectory for the road with mode 3 profile.

In mode 3 case (Good), it is noted that (figure 2.24) for N = 17,222,000 cycles, the degradation D_N reaches the critical value D_C = 1. The deduced lifetime of the suspension is 17,222,000 cycles of road excitation in mode 3. Moreover, the first sign of damage appears at about 6,200,000 cycles. Starting from 16,000,000 cycles, the slope of the degradation curve becomes very acute; hence damage is increasing very fast.

In addition, figure 2.25 recapitulates the three previous figures.

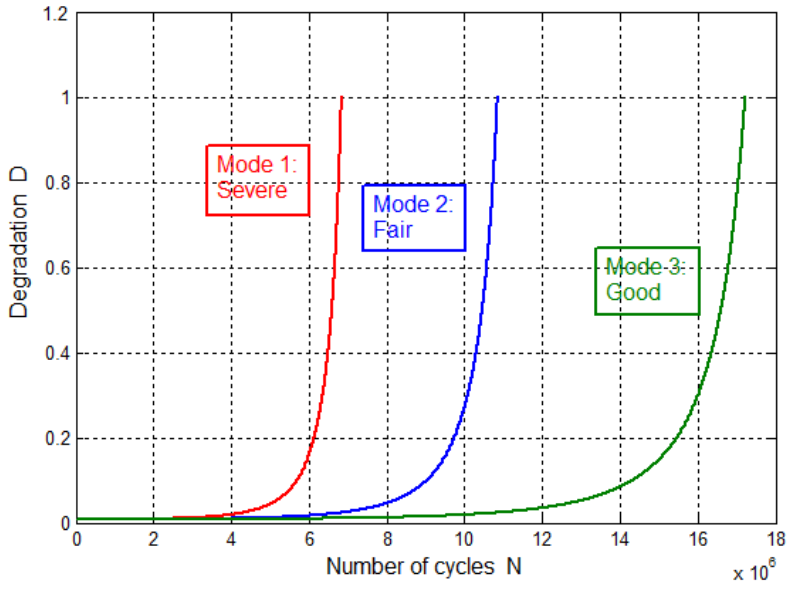

Figure 2.25 - Degradation trajectory for the three modes of roads profiles.

II.3.1.9 - Analysis of the Simulation Results

The expectation of the lifetime for mode 1 is nearly 63% of that of mode 2 and the expectation of the lifetime for mode 2 is nearly 63% of mode 3 (figure 2.25). It can be noticed from the obtained results that the increase of the suspension lifetime relative to the road of mode 3 is as follows: mode (1)/mode (3) $\approx 152\,\%$ and mode (2)/mode (3) $\approx 59\,\%$.

From the above, the three expected lifetimes are as follows: N_{C1}= 6,836,000 cycles; N_{C2}=10,850,000 cycles; N_{C3}=17,222,000 cycles. Then, our prognostic procedure yields the Remaining Useful Lifetimes (RUL) for the three modes (figure 2.26) that can now be easily deduced from these three curves at any instant or any active cycle N as follows:

For mode 1: $\mathrm{RUL}_1(N) = N_{C1} - N$;

For mode 2: $\mathrm{RUL}_2(N) = N_{C2} - N$;

For mode 3: $\mathrm{RUL}_3(N) = N_{C3} - N$;

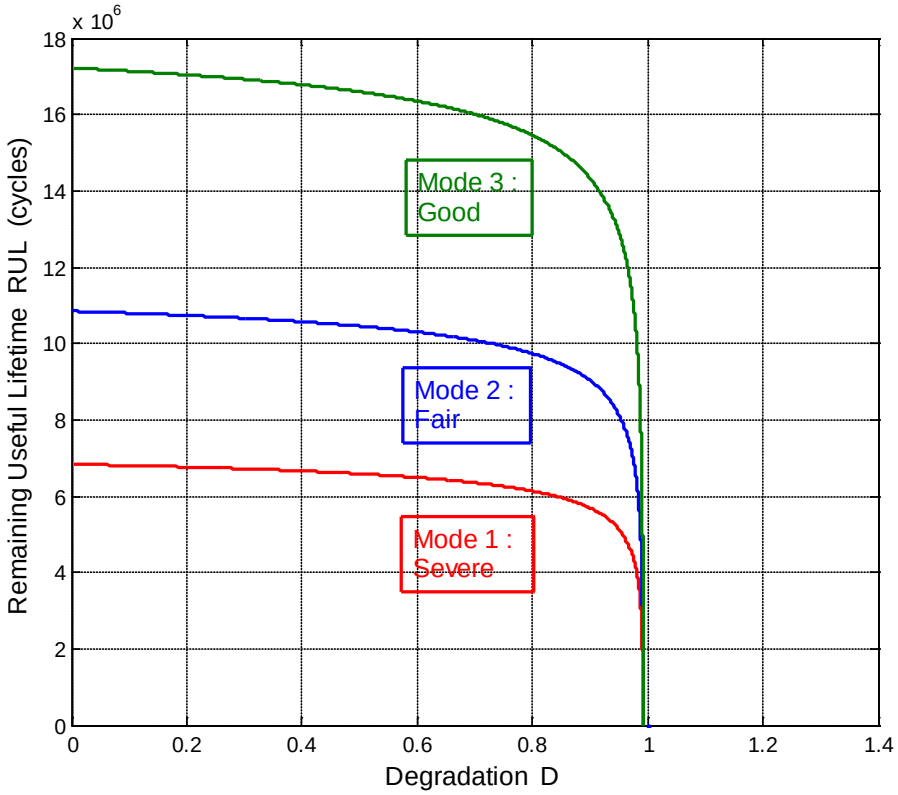

Figure 2.26 - Remaining Useful Lifetimes estimated by the prognostic model.

II.3.1.10 - Conversion of RUL into Years

To convert the suspension lifetime into years' unit, knowing that each cycle duration is 2 seconds (refer to figure 2.21), then: RUL(s) = 2 × RUL(*N*). We assume that the suspension time usage is 10% of a day, which corresponds to 2.4 hours/day.

The conversions from Cycles to Km and to Years, for a vehicle running with 50 km per hour, are given by the following literal expressions:

From Cycles to Km:

$$\text{RUL(Km)} = \frac{\text{RUL(Cycles)} \times 2\text{(s/Cycle)} \times 50\text{(Km/hour)}}{60\text{(s/min)} \times 60\text{(min/hour)}} = \frac{\text{RUL(Cycles)}}{36\ \text{(Cycles/Km)}}$$

From Km to Years:

$$\text{RUL(Years)} = \frac{\text{RUL(Km)}}{2.4\text{(hours/day)} \times 50\ \text{(km/hour)} \times 365\text{(days/Year)}} = \frac{\text{RUL(Km)}}{43{,}800\ \text{(Km/Year)}}$$

Therefore, the RUL results can be expressed by the following units: Cycles, or Km, or Years.

Thus, the expected lifetimes' durations are:

$$\text{For mode 1 :} \frac{6{,}836{,}000\text{(cycles)} \times 2\text{(s)}}{60\text{(s)} \times 60\text{(min)} \times 2.4\text{(hours)} \times 365\text{(days)}} = 4.34 \text{ years}$$

$$\text{For mode 2 :} \frac{10{,}850{,}000\text{(cycles)} \times 2\text{(s)}}{60\text{(s)} \times 60\text{(min)} \times 2.4\text{(hours)} \times 365\text{(days)}} = 6.88 \text{ years}$$

$$\text{For mode 3 :} \frac{17{,}222{,}000\text{(cycles)} \times 2\text{(s)}}{60\text{(s)} \times 60\text{(min)} \times 2.4\text{(hours)} \times 365\text{(days)}} = 10.92 \text{ years}$$

Moreover, the validation of these results can be found in the work of reference [26] on the fatigue life of suspensions. An average life of 200,000 km is deduced under severe conditions and which corresponds to 4.57 years for a vehicle running with 50 km per hour and for 2.4 hours per day.

II.3.2 - Prognostic Study for Pipelines Systems

II.3.2.1 - Introduction

Pipelines are petrochemical systems that serve to transport oil and natural gas between sites. Pipelines tubes are considered as a principal component in petrochemical industries, their life prognostic is vital in this industry since their availability has crucial consequences on the exploitation cost. The main failure cause for these systems is the fatigue due to internal pressure-depression variation along the time.

Figure 2.27 - Buried pipes.

These pipelines are usually designed for ultimate limits states (resistance). Moreover, buried pipelines are subject to corrosion due to soil aggression effects. They are manufactured as cylindrical tubes of radius R and of thickness e.

The DNV 2000 rules propose for pipelines a target probability of failure about 10^{-5}. Their main failures are due to seismic ground waves, soil settlements, buckling, deformations, internal and external corrosion, stress concentration in welding and fitting, vibration and resonance, pressure fluctuation over a long period. The fatigue failures by cracks propagation are detected by cracks detection tools.

A significant part of main pipelines are subjected to external cracking, which is a serious problem for the pipeline industry like, for example, in Russia [27], U.S., and Canada [28]. Identification of external cracks is achieved using different Nondestructive Evaluation (NDE) methods. If cracks are revealed during inspection, their influence on the remaining useful lifetime (RUL) of the pipeline should be assessed in order to choose what maintenance action should be used: do nothing/repair/replace. Pipeline integrity is assessed on the assumption that some defects after In-Line Inspection (ILI) may be: still undetected; detected, but not measured; detected and measured.

Three case studies of pipes are considered here: unburied, buried (figure 2.27) and subsea (offshore pipes). Each one of these situations requires different physical parameters like: corrosion, soil pressure and friction, water and atmospheric pressure.

II.3.2.2 - Pipes Stress Modeling

The pipes are cylindrical thin tubes since their thickness *e* to radius ratio is [29]: $e/R \leq 1/10$.

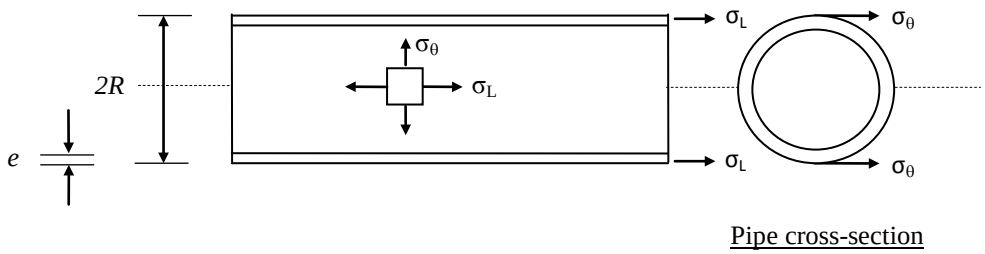

Figure 2.28 - Cylindrical pipelines.

In this case, the stresses due to internal pressure *P* are of membranes types without any bending forces. The stresses are circumferential (hoop stress) σ_θ and longitudinal (axial stress) σ_L (figure 2.28). They are given by (24):

$$\sigma_\theta = \frac{P \cdot R}{e} \quad ; \quad \sigma_L = \frac{P \cdot R}{2 \cdot e} \tag{24}$$

The critical position of cracks is longitudinal which is perpendicular to the direction of maximal stresses σ_θ. The crack has a depth (or length) *a* measured in the thickness direction (figure 2.29). Generally, the following ratio interval can be considered: $0.1 \leq a/e \leq 0.99$

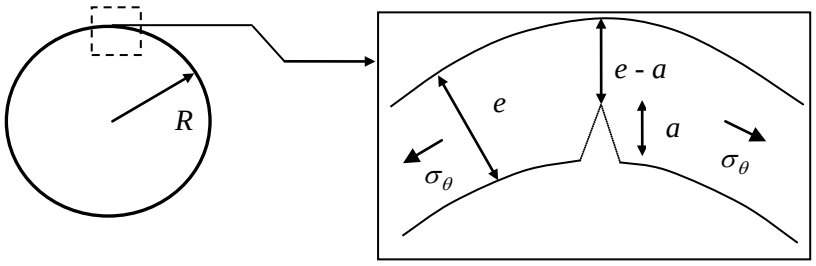

Figure 2.29 - Cracked pipe section.

We can illustrate all stresses types in a pipe body by the following figure (figure 2.30):

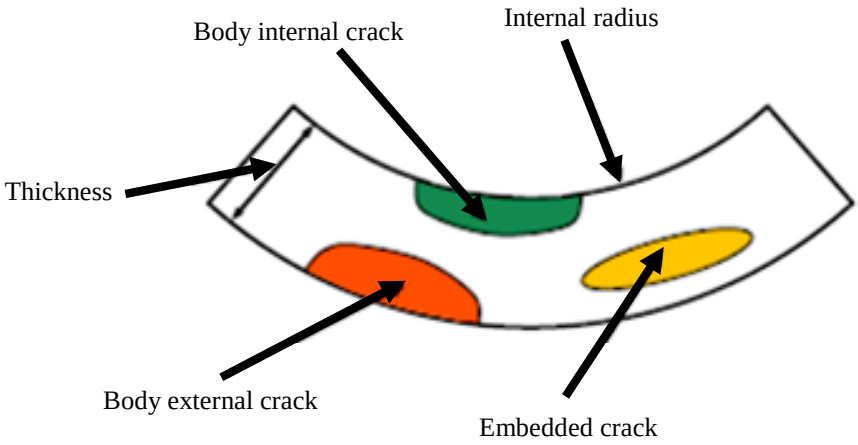

Figure 2.30 - Stresses types distribution in pipe body

It is mentioned here that only the first mode of crack ($K = K_I$) is considered, i.e. the opening mode (the other modes are sliding and tearing mode).

II.3.2.3 - State of Stresses in the Tube Body

The tubes are modeled as cylindrical shells of revolution. When thin tubes of radius *R* and of thickness *e* are under internal pressure *P*, the state of stresses is membrane-like without bending loads. The membrane stresses are circumferential (hoop stress) σ_θ and longitudinal stresses (axial stress) σ_L (figure 2.31).These stresses are given by (24).

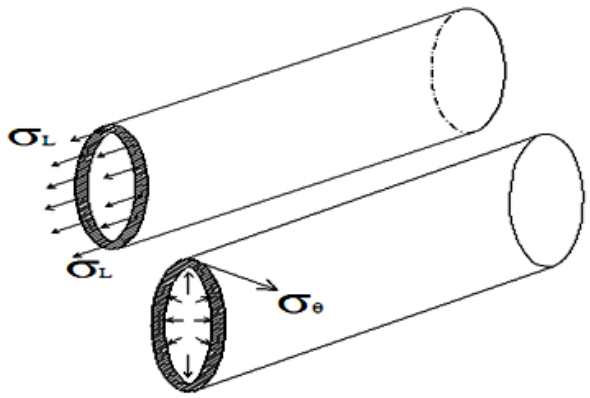

Figure 2.31 - Axial and hoop stresses in pipes.

The critical cracks are those which are perpendicular to maximal stresses σ_θ (figure 2.32), that means longitudinal cracks which are parallel to the tube axis. A crack is of depth "*a*" or of length "*a*", measured in the direction of the tube thickness "$e = R_2 - R_1$". R_2 is the external radius and R_1 is the internal radius of the pipe.

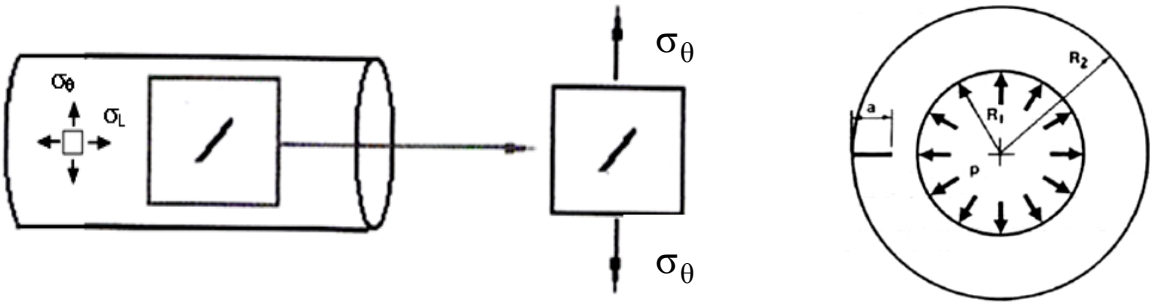

Figure 2.32 - Crack length in radial direction.

II.3.2.4 - Stress Intensity Factor

The stress intensity factor for tubes is given by [10]:

$$K_I = \sqrt[m]{\phi_1(a)\cdot\phi_2(P)} \tag{25}$$

$$\text{Where}: \phi_1(a) = \left(Y(a)\cdot\sqrt{\pi a}\right)^m \quad ; \quad \phi_2(P) = (\sigma_\theta)^m = (PR/e)^m \quad ; \quad Y(a) = 0.6\times\frac{1+2(a/e)}{(1-a/e)^{\frac{3}{2}}}$$

$$\Rightarrow K_I = 0.6\times\frac{1+2(a/e)}{(1-a/e)^{\frac{3}{2}}}\times\sqrt{\pi a}\times(PR/e) \tag{26}$$

$$K_I \le K_{IC}$$

Where,

$Y(a)$ is the geometric factor function of the pipeline geometric parameters (a, e),

K_{IC} : is the tenacity of material (or critical stress intensity factor) and is given by:

$$K_{IC} = \sqrt{\frac{J_{IC}\cdot E}{1-(\nu)^2}} \tag{27}$$

Where,

J_{IC} is the resistant crack force of the material; E is the Young's Modulus and ν is the Poisson ratio. Note that the factor K_I must not exceed the value of K_{IC} [4], and m = 3.

II.3.2.5 - Degradation Model Expression of Pipes

From the stress intensity factor defined above:

$$a_N = a_{N-1} + C\cdot\phi_1(a_{N-1})\cdot\phi_2(p_j) \ ; \text{ where } p_j \text{ is the simulated load.}$$

With,

$$\phi_1(a_{N-1}) = \left(Y(a_{N-1})\sqrt{\pi\, a_{N-1}}\right)^m = \left(0.6 \times \frac{1+2(a_{N-1}/e)}{(1-a_{N-1}/e)^{\frac{3}{2}}} \times \sqrt{\pi\, a_{N-1}}\right)^3$$

$$\phi_2(p_j) = {p_j}^m = \left(\Delta\sigma_j\right)^m = \left(P_j R/e\right)^3$$

Then the damage accumulation is given in terms of the crack length by the following recursive relation:

$$a_N = a_{N-1} + C \times \left[0.6 \times \frac{1+2(a_{N-1}/e)}{(1-a_{N-1}/e)^{\frac{3}{2}}} \times \sqrt{\pi\, a_{N-1}}\right]^3 \times \left(P_j R/e\right)^3 \qquad (28)$$

And the degradation indicator of the pipe can be written as in (29):

$$D_N = D_{N-1} + \eta \cdot \phi_1(D_{N-1}) \cdot \phi_2(p_j); \qquad \text{where} \quad \eta = C/(a_C - a_0)$$

$$D(N) = \frac{a_{N-1}}{a_C - a_0} + \frac{C}{a_C - a_0} \times (\pi a_{N-1})^{3/2} \times \left[0.6 \times \frac{1+2(a_{N-1}/e)}{(1-a_{N-1}/e)^{\frac{3}{2}}}\right]^3 \times (P_j R/e)^3 \qquad (29)$$

II.3.2.6 - Simulations of Three Levels of Internal Pressure

Consider a pipe of radius R = 240 mm and of thickness e = 8 mm transporting natural gas. In this case, the parameters are: $C = 5.2\times10^{-13}$ (free air), $C = 1.3\times10^{-14}$ (under soil), $C = 2\times10^{-11}$ (offshore), and m = 3 (metal).

Take the initial crack length a_0 = 0.2 mm. The internal pressure P_j is simulated following a triangular form to be similar to the real case of pipelines operating condition (pressure-depression) (figure 2.33). For all three pipes cases, the function $\phi_1(a)$ and the parameter m are the same [24].

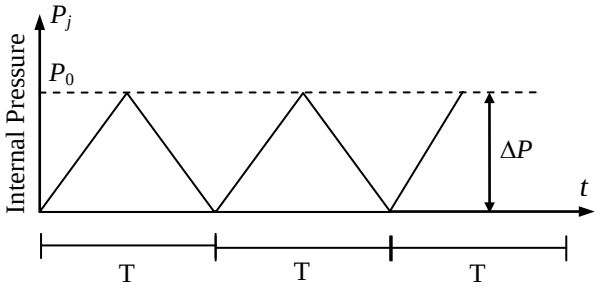

Figure 2.33 - Triangular simulation of internal pressure

Three maximal levels of P_j are considered which are P_0 = 3 MPa, 5 MPa, and 8 MPa and with a repetition period T. At each of these levels, a degradation trajectory $D(N)$ is

deduced in terms of the cycle number N. When D_N reaches the unit value, then the corresponding $N = N_C$ is the lifetime of the pipe in fatigue case.

For simulation purposes, in table 2.2, the mean values of pressure P_j are considered as the maximal values P_0. The coefficients of variation are δ_{Pj} .

Table 2.2 - Statistical characteristics of each pressure mode.

Pressure Mode	$\overline{P}_j$ (MPa)	δ_{Pj} (%)	Law
High (mode 1)	8	10%	Triangular
Middle (mode 2)	5	10%	Triangular
Low (mode 3)	3	10%	Triangular

The simulation of the analytic prognostic model (equation 29) is executed for each level of internal pressure (high, middle, and low).

The estimation of a real lifetime system necessitates a huge amount of pressure simulations of order of hundreds of millions; hence, an approximated model of lifetime simulation of order of 10,000,000 iterations has been used. Consequently, a high capacity computer (CORE i7, 3 GHZ microprocessor with an 8 GB RAM) has been considered for this purpose.

Usually, the pipelines may be placed in practice in three dispositions: onshore (unburied, buried), and offshore (under water) [30].

II.3.2.7 - Unburied Pipe Case

This situation [31] is suitable outside cities between states and countries where they do not intercept any construction or transportation facilities.

In this case, the normal service load includes only the internal pressure. The results of degradation trajectory simulation (29) are shown in figure 2.34 below. The pipe lifetimes for this case are nearly 3.31 years for mode 1 (high pressure), 4.68 years for mode 2 (middle pressure), and 6.85 years for mode 3 (low pressure). In comparison with previous lifetimes'

studies on pipelines [32], it can be concluded that in relation with pipes dimensions, internal pressure, and pressure cycle, the order of magnitudes of the present values are realistic.

It is noted that at the beginning (between 0 year and 1 year) all modes give the same degradation level of 0.25 where crack lengths are negligible when compared with the critical crack length a_C.

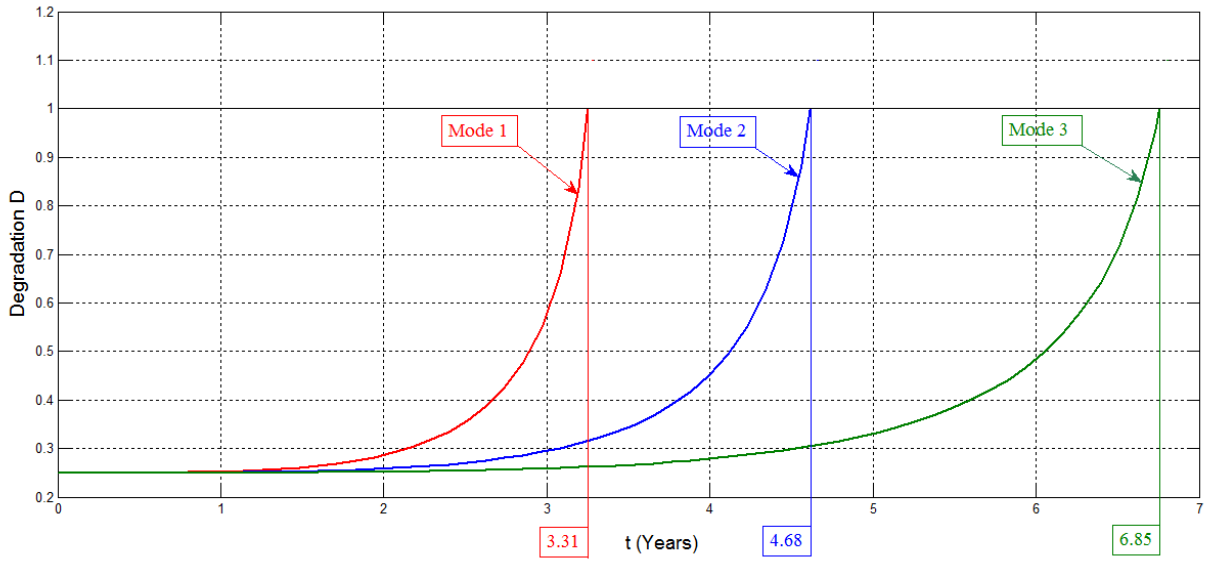

Figure 2.34 - Degradation evolution of unburied pipes under three modes of pressure.

For three modes of internal pressure, the Remaining Useful Lifetimes for the unburied tubes are evaluated in years and illustrated in the figure 2.35. It is noted that these three curves are decreasing from their corresponding global lifetime to zero value where the degradation reaches the unit value D_C.

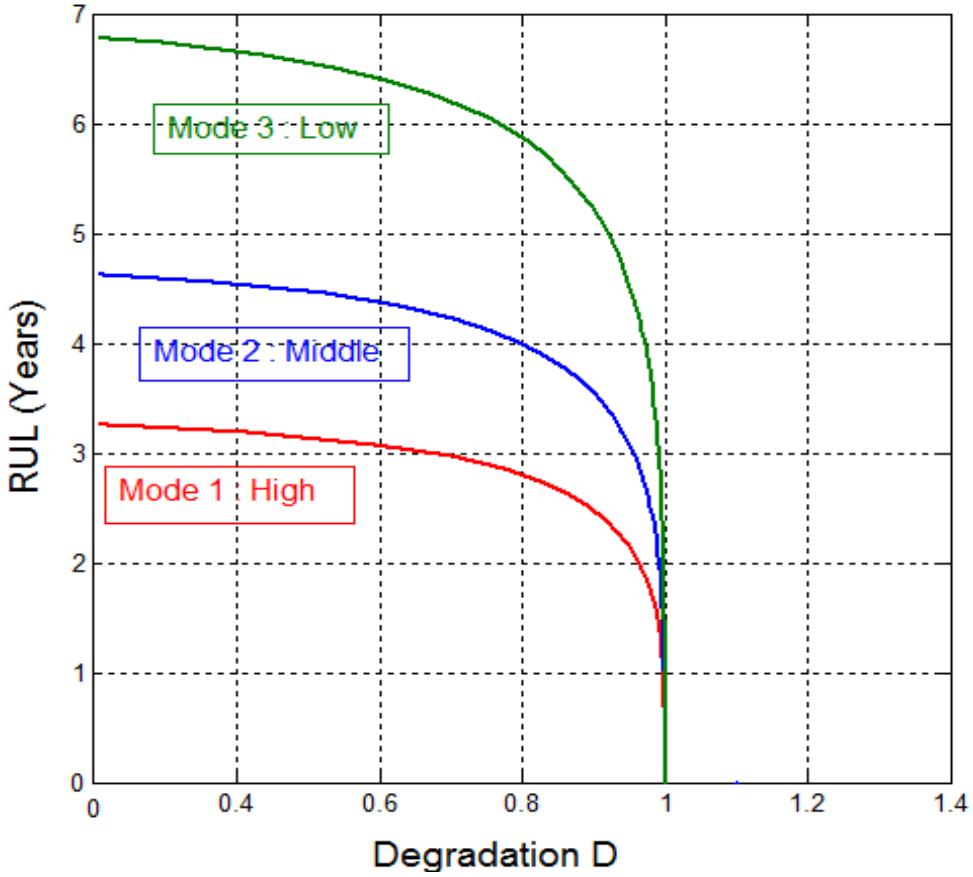

Figure 2.35 - RULs evolution of unburied pipes under three modes of pressure.

II.3.2.8 - Buried Pipe Case

This case is useful for many reasons (reduce plant congestion, fewer pipe bending, protection from ambient temperature changes, wind and other loads) [33]. This study is limited here to normal service loads that include only internal pressure P_{int} and soil action (figure 2.36).

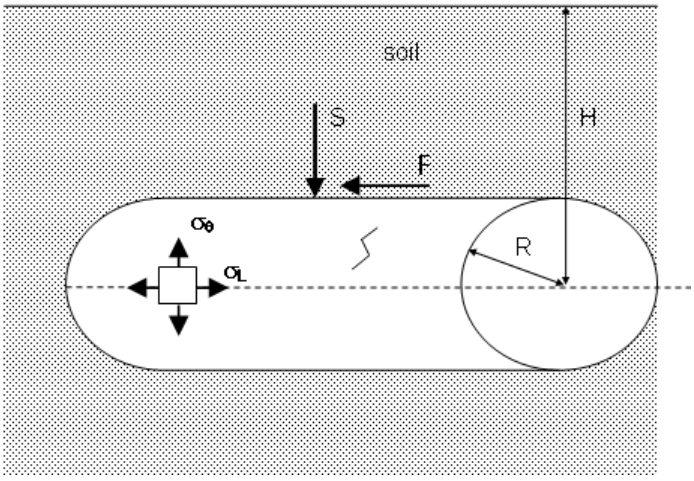

Figure 2.36 - Forces on a buried pipe under soil.

The soil effects on the pipe surface are [33]: the normal force S and the soil friction F given by:

$$S = \int_A p_S \, dA = 4\,R\,\gamma\,(H - R) + W_P \qquad (30)$$

$$\Rightarrow P_{ext} = \frac{S}{2\pi R} \qquad (31)$$

$$F = \mu \cdot S \Rightarrow \sigma_{L,F} = \frac{F}{2\pi R} \qquad (32)$$

dA: differential contact area.

$$\sigma_\theta = \frac{(P_{\text{int}} - P_{ext})R}{e};\ \sigma_L = \frac{P_{\text{int}} \cdot R}{2e} - \sigma_{L,F} \qquad (33)$$

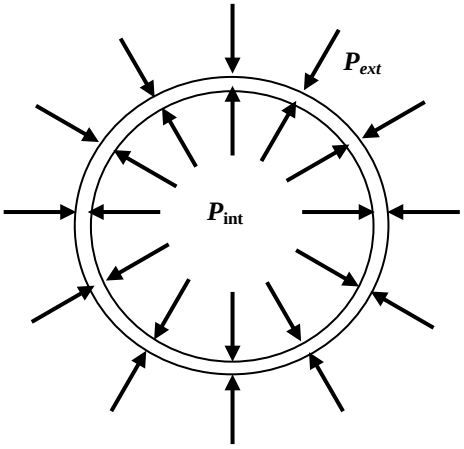

Figure 2.37 - Internal and external pressure in buried pipes.

Compute the maximal stress:

$$\left.\begin{aligned} &\Rightarrow \sigma_L = \frac{1}{2}\sigma_\theta + 14.4P_{ext} < \sigma_\theta \ \text{ for } P_{\text{int,min}} = 3\,\text{MPa} \\ &\Rightarrow \sigma_{eq} = \sqrt{\sigma_L^2 + \sigma_\theta^2 - \sigma_L \cdot \sigma_\theta} < \sigma_\theta \end{aligned}\right\} \Rightarrow \sigma_{\max} = \sigma_\theta$$

The effects of the force *S* on the pipe surface is expressed by an external pressure P_{ext} that opposes the effects of an internal pressure P_{int}.

Similarly, the effects of the friction force *F* on the pipe surface ($\sigma_{L,F}$) oppose the effects of the internal pressure P_{int} (σ_L) (figure 2.37).

The depth of the pipe is taken $H = 7R$ and the friction coefficient interval is [14]: $0.5 \le \mu \le 0.7$. The soil specific weight is γ = 9.843 kg/cm^2.

The weight per linear meter of pipe and gas content is given by equation (34):

$$W_p = 2\pi R\, e\, \gamma_{pipe} + \pi R^2 \cdot 1 \cdot \gamma_{gas} = 203.27 \text{ kg/m}. \qquad (34)$$

The specific gravity of the pipe material and of the natural gas are respectively:

$$\gamma_{pipe} = 7{,}850 \text{ kg/m}^3 \text{ and } \gamma_{gas} = 600 \text{ kg/m}^3.$$

From the simulation of the proposed analytic prognostic model (29), the pipe lifetimes are deduced from figure 2.38. They are 8.33 years for mode 1 (high pressure), 11.87 years for mode 2 (middle pressure), and 17.35 years for mode 3 (low pressure). It is noted that at the beginning (between 0 year and 3 years) all modes give the same degradation level of 0.25 where crack lengths are negligible when compared with the critical crack length a_C. Previous

pipes lifetime studies [34] show that in relation to the pipes dimensions, pressure levels and pressure cycles, the order of magnitudes of these obtained values are realistic.

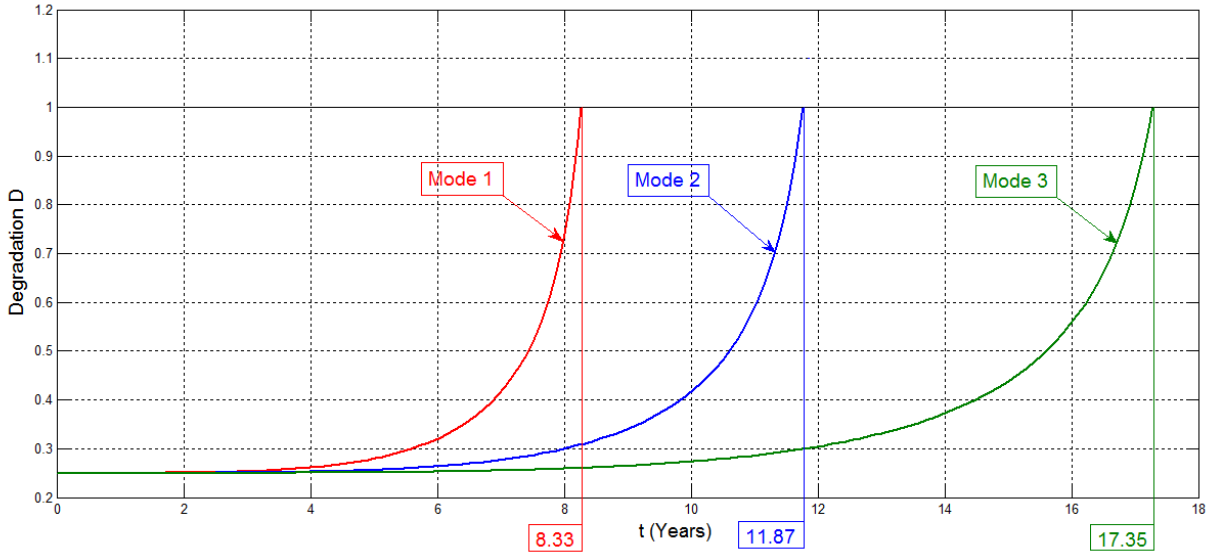

Figure 2.38 - Buried pipe degradation function of lifetime for the three modes of internal pressure.

The Remaining Useful Lifetimes in years are also evaluated for buried tubes for three modes of internal pressure and they are illustrated by the figure 2.39. We note that these three curves are decreasing from their corresponding global lifetime to zero value where the degradation reaches the unit value D_C.

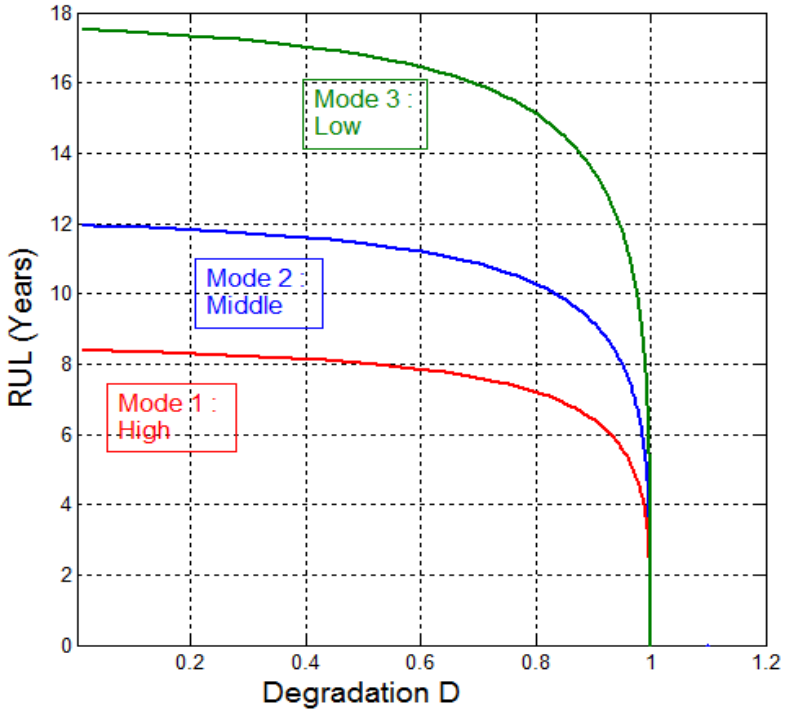

Figure 2.39 - Buried pipe RULs function of degradation for the three modes of internal pressure.

II.3.2.9 - Offshore Pipe Case

In this case, the situation where the pipes are under sea water (offshore pipeline) serving to transport oil or gas from marine offshore to refinery plant is considered [35,36,37]. They are subject, beside internal gas pressure, to external water and atmospheric pressure (figures 2.40 & 2.41).

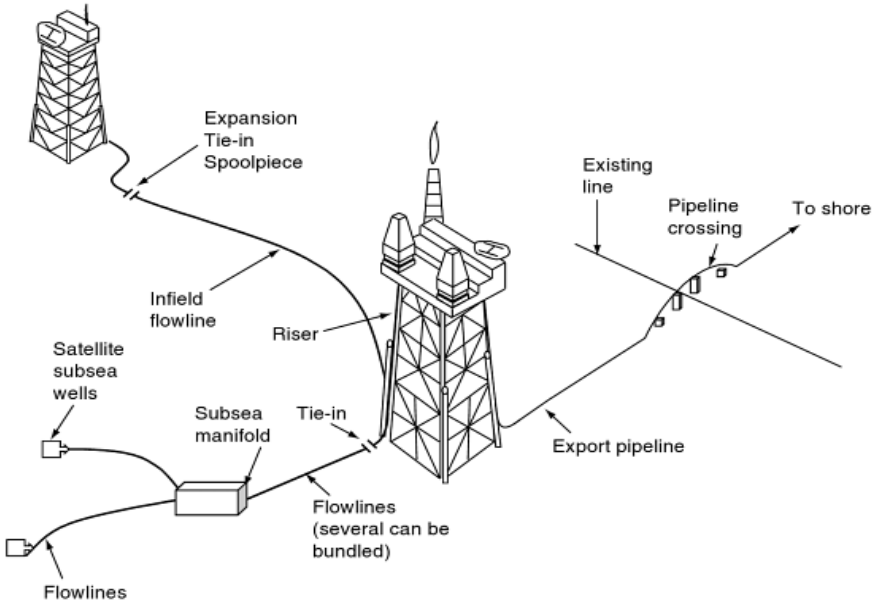

Figure 2.40 - Offshore pipelines network.

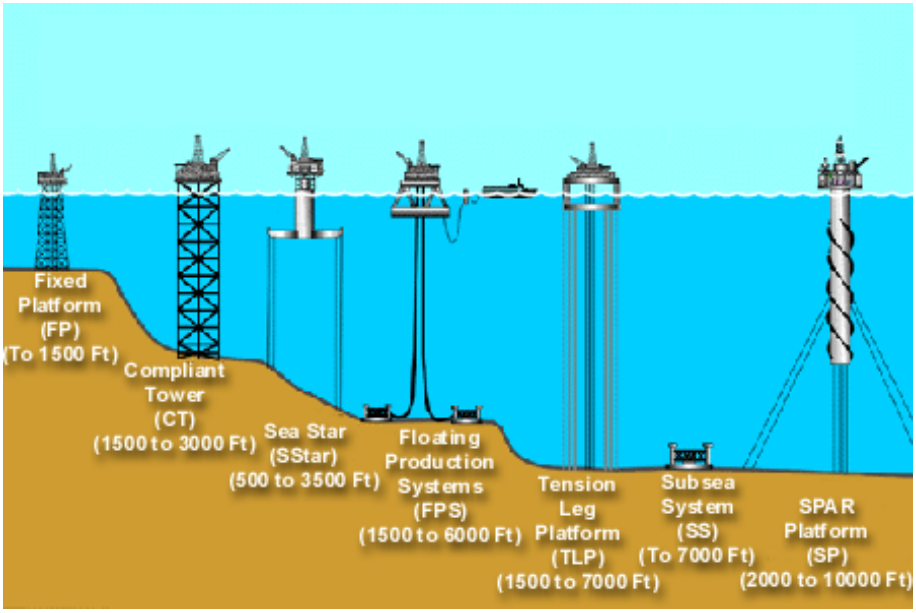

Figure 2.41 - Offshore types for various depths.

Consider a pipe (figure 2.42) of diameter ϕ = 480 mm and of thickness e = 8 mm, the external pressure around the offshore pipe is given by (35):

$$P_{ext} = P_W + P_{atm} = \rho_w \cdot g \cdot H + 1\,\text{atm} \qquad (35)$$
$$\Rightarrow P_{ext} = 6{,}163{,}905\ \text{Pa} = 6.163905\ \text{MPa}$$

Where,

The depth of offshore pipe considered here is: H = 600 m.

Atmosphere pressure at sea level = 1 atm = 0.101325 MPa.

The specific weight of seawater is: ρ_w = 1,030 kg/m^3.

The gravitational attraction is: g = 9.81 m/s^2.

Then, the net maximal stresses in the pipe body are given by (36):

$$\sigma_\theta = \frac{(P_{\text{int}} - P_{ext}) \cdot R}{e} \qquad (36)$$

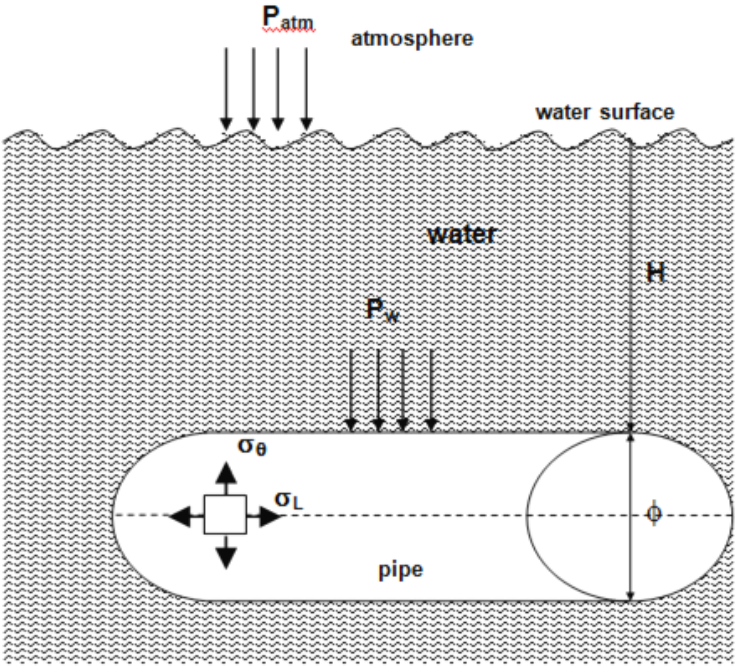

Figure 2.42 - Offshore pipe parameters.

After the simulation of the proposed prognostic model for the offshore pipeline degradation and under three levels of internal pressure P_{int} , the pipe lifetimes are illustrated by figure 2.43. They are 10.27 years for mode 1 (high pressure), 14.84 years for mode 2 (middle pressure), and 21.69 years for mode 3 (low pressure). It is noted that at the

beginning (between 0 and 5 years) all modes give the same degradation level of 0.15 where crack lengths are negligible when compared with the critical crack length a_C. Same remark, like in the previous two cases, applies for the realism of these lifetimes results [32,34].

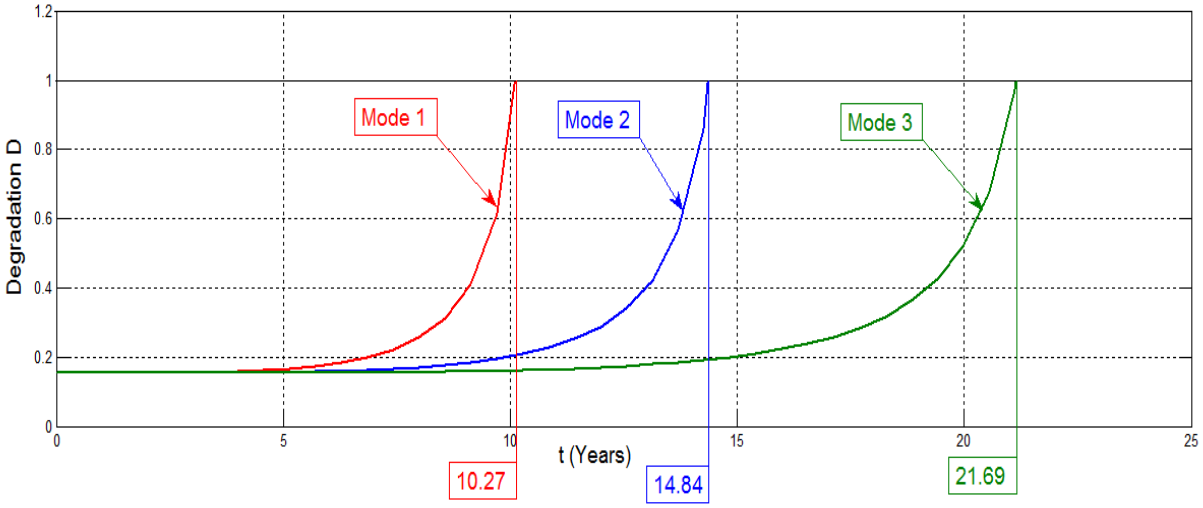

Figure 2.43 - Offshore pipe degradation function of lifetime for the three modes of internal pressure.

The Remaining Useful Lifetimes are evaluated in years for offshore tubes under three modes of internal pressure and we deduce figure 2.44. We note that the RULs curves are decreasing from their corresponding global lifetime to zero value where the degradation reaches the unit value D_C.

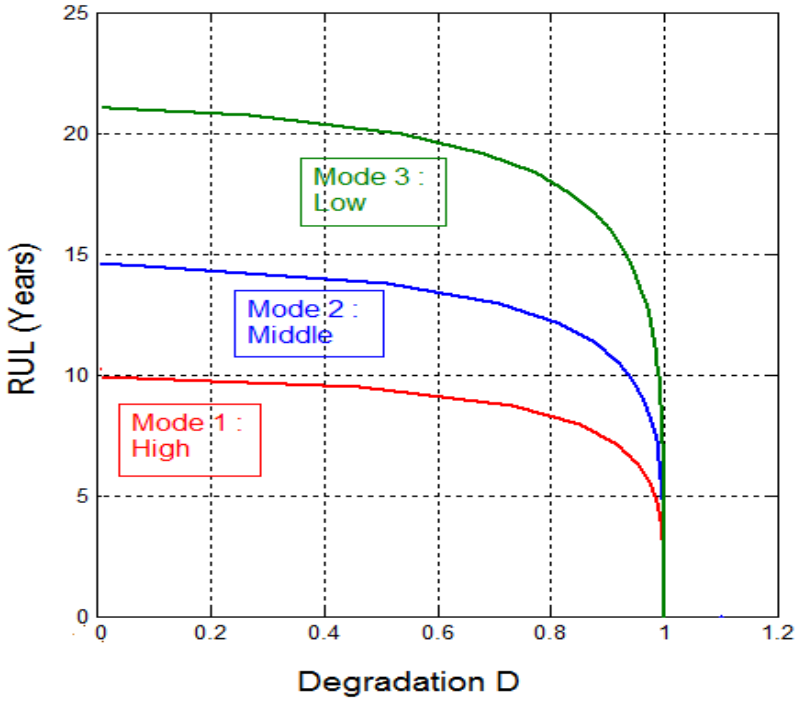

Figure 2.44 - Offshore pipe RULs function of degradation for the three modes of internal pressure.

II.4 - Conclusion

An analytic prognostic model is introduced in this chapter that permits to predict the Remaining Useful Lifetime (RUL) of dynamic systems. This model considers the fatigue as a damage parameter and hence it is based on well known laws of damage like Paris' and Miner's laws. An index of degradation was derived that varies from zero to one. Our proposed model is based on the link between this index D and the crack length a. Failure is produced when a reaches a critical length a_C. Hence, our model is given by a simple function relating the instantaneous degradation to actual crack length as a measurement of actual damage.

Our aim is to evaluate the evolution of the system lifetime at each instant. For this purpose the degradation trajectories have been used in terms of cycle numbers or the time of operation. From these degradation trajectories, the RULs variations are deduced. The prognostic of a complex system can be deduced from the prognostic of its sub-systems when their damage laws are available.

To demonstrate the effectiveness of our model, two industrial examples have been considered in simulation in this chapter. These systems are the vehicle suspension systems and the petrochemical pipelines. For the vehicle suspension, three modes of road profiles are simulated. For the pipes, three types of pipes have been considered: unburied, buried, and offshore, and three modes of internal pressure are examined.

In such industrial systems, this model proves that it is very convenient and it provides a useful tool for a prognostic analysis. Moreover, it is less expensive than other models that need a large number of data and measurements.

In the following chapters we will enlarge this study by considering the nonlinear case of cumulated damage and the probabilistic influence of the basic parameters on degradation and on RULs evolution.

References

[1] G. VACHTSEVANOS, F. LEWIS, M. ROEMER, A. HESS, and B. WU, *Intelligent Fault Diagnosis and Prognosis for Engineering Systems*, John Wiley & Sons, Inc., 2006, ch. 5,6, and 7.

[2] F. PEYSSON, M. OULADSINE, R. OUTBIB, J-B. LEGER, O. MYX, and C. ALLEMAND", A generic prognostic methodology using damage trajectory models", IEEE transactions on reliability, vol. 58 (no. 2), June 2009.

[3] D. CHELIDZE and J.P. CUSUMANO, "A dynamical systems approach to failure prognosis", J. of Vibr. and Acoustics, Vol. 126, pp. 2-8, 2004.

[4] K. EL-TAWIL, A. ABOU JAOUDE, S. KADRY, H. NOURA, and M. OULADSINE, "Prognostic based on analytic laws applied to petrochemical pipelines", International Conference on Computer-aided Manufacturing and Design (CMD 2010), China, November 2010.

[5] J. LEMAITRE and J. CHABOCHE, *Mechanics of Solid Materials.* New York: Cambridge University Press, 1990.

[6] P. PARIS and F. ERDOGAN, "A critical analysis of crack propagation laws," Journal of basic engineering, Transactions of the American society of mechanical engineers, Vol. 85, No. 4, pp. 528-534, 1963.

[7] A.J. MCEVILY and R.O. RITCHIE, *Fatigue Fract. Eng. Mater. Struct.* 21 (1988) 847-855.

[8] M. A. MINER, “Cumulative damage in fatigue”, Journal of Applied Mechanics, vol. 12, A159-A164, 1945.

[9] M. LANGON, *Introduction a la Fatigue et Mécanique de la Rupture*, Centre d’essais aéronautique de Toulouse, ENSICA April, 1999.

[10] J. LEMAITRE and R. DESMORAT, *Engineering Damage Mechanics,* New York: Springer-Verlag, ch. 6, 2005.

[11] M. TODINOV, “Necessary and sufficient condition for additivity in the sense of Palmgren-Miner rule”, Comput. Mater. Sci. , vol 21, no 1, pp 101-110, 2001.

[12] M. T. TODINOV, Reliability and risk models setting reliability requirements, Cranfield University, UK. John Wiley & Sons, Ltd, 2005.

[13] A. ABOU JAOUDE, K. EL-TAWIL, S. KADRY, H. NOURA, and M. OULADSINE, ”Analytic prognostic model for a dynamic system”, International Review of Automatic Control (IREACO), November 2010.

[14] A. ABOU JAOUDE, S. KADRY, K. EL-TAWIL, H. NOURA, and M. OULADSINE, "Analytic prognostic for petrochemical pipelines", Journal of Mechanical Engineering Research (JMER), April 2011.

[15] N. SUKUMAR, D.L. CHOPP, and B. MORAN, "Extended finite element method and fast marching method for three-dimensional fatigue crack propagation", Engrg. Fracture Mech. 70 (2003) 29-48.

[16] J.C. NEWMAN JR. and I.S. RAJU, "An empirical stress-intensity factor equation for the surface crack", Engrg. Fracture Mech. 15 (1/2) (1981) 185-192.

[17] C. COLQUHOUN, "Fatigue Analysis of an FEA Model of a Suspension Component, and Comparison with Experimental Data", Simpson International UK Ltd, Halifax, England.

[18] J. DRAPER, *Safe Technology Limited*, Sheffield, England.

[19] N.E. FROST and D.S. DUGDALE, "Fatigue Tests on Notched Mild Steel Plates with Measurements of Fatigue Cracks", Journal of the Mechanics and Physics of Solids 5:182-192, 1957.

[20] N.E. FROST, "Notch Effects And The Critical Alternating Stress Required To Propagate A Crack In An Aluminum Alloy Subject To Fatigue Loading", Journal of Mechanical Engineering Science 2, 109-119, 1960.

[21] F.A. CONLE and T.H. TOPPER, "Overstrain Effects During Variable Amplitude Service History Testing", International Journal of Fatigue, Vol 2, No.3, pp130-136, 1980.

[22] D.L. DUQUESNAY, M. A. POMPETZKI, and T. H. TOPPER, "Fatigue Life Prediction for Variable Amplitude Strain Histories", SAE Paper 930400, Society of Automotive Engineers.

[23] J. LEE, "Smart Products and Service Systems for E-business Transformation", 3e Conférence Francophone de Modélisation et Simulation « Conception, Analyse et Gestion des Systèmes Industriels » MOSIM'01, du 25 au 27 avril, Troyes (France), 2004.

[24] K. EL-TAWIL, *Mécanique Aléatoire et Fiabilité*, Cours de Master 2R Mécanique, EDST, Université Libanaise, 2004.

[25] K. EL-TAWIL, S. KADRY, *Fatigue Stochastique des Systèmes Mécaniques Basée sur la Technique de Transformation Probabiliste*, Internal report, Lebanese University, grant research program, 2010.

[26] F. VAKILI-TAHAMI, M. ZEHSAZ, and M.R. ALIDADI, "Fatigue analysis of the weldments of the suspension-system-support for an off-road vehicle under the dynamic loads due to the road profiles", Asian Journal of Applied Sciences 2(1):1-21, Malaysia, 2009.

[27] T.K. SERGEEVA, A.C. BOLOTOV, et al., "Monitoring of steel condition in main pipelines during their stress-corrosion induced failures", Chemical and oil Machinery, No. 2, pp. 72-76, 1996.

[28] C.E. JASKE, "Fitness-for-service assessment for pipelines subject to stress-corrosion cracking", The Pipeline Pigging and Integrity Conference, February 2000.

[29] A. ABOU JAOUDE, K. EL-TAWIL, S. KADRY, H. NOURA, and M. OULADSINE, "Prognostic model for buried tubes", International Conference on Advanced Research and Applications in Mechanical Engineering (ICARAME'11), Notre Dame University, Louaize, Lebanon, June 13-15, 2011.

[30] A. ABOU JAOUDE, H. NOURA, K. EL-TAWIL, S. KADRY, and M. OULADSINE, "Lifetime analytic prognostic for petrochemical pipes subject to fatigue", SAFEPROCESS, 8th IFAC Symposium on Fault Detection, Supervision and Safety of Technical Processes, Mexico City, Mexico, August 29-31, 2012.

[31] J.B. LIGON and G.R. MAYER, *Buried pipes,* Mechanical Mechanics Dept., Michigan, Technological University, Houghton.

[32] WAIMAKARIRI, District council, *Designing for Surge & Fatigue*, Standard Specification, QP-C841, Issue 1, 2008.

[33] H. S. DA COSTA MATTOS, E. M. SAMPAIO, and R. M. ALVES CORTES, 2007, "Analysis of composite sleeve reinforcement systems for metallic pipelines with localized imperfections or damage", *Mechanics of Solids in Brazil.*

[34] N. BROWN, *Intrinsic Lifetime of Polyethylene Pipelines,* University of Pennsylvania, Departmental paper, Polymer Engineering and science, vol 74, 2007.

[35] J. ANDERSON, *Design and Installation of Marine Pipeline*, Blackwell edition, 2005.

[36] Y. BAI and Q. BAI, *Subsea Pipelines and Rivers*, Elsevier, 2005.

[37] A. C. PALMER and R. A. KING, *Subsea Pipeline Engineering*, publisher Pennwell Book

CHAPTER III

ANALYTIC NONLINEAR PROGNOSTIC MODEL OF DYNAMIC SYSTEMS

III.1 - Introduction

Until now, damages have been assumed to accumulate linearly (Miner's law) even though it is unlikely to be the case of brittle material. The present chapter intends to develop a more advanced prognostic tool by exploring the nonlinear side of cumulative damage. This is in order to take into account the nature and the mode of applied constraints and influent environment that can accentuate the nonlinear aspect related to some materials behavior subject to fatigue effects.

In Chapter II we have considered the classical case of linear damage accumulation called Miner's law [1] widely used in specialized literature for most steel materials. In the present chapter we will explore the nonlinear case of damage cumulative law to take into account the real behavior of some materials subject to fatigue actions, especially when the nature of applied constraints and influent environment contribute to amplify the nonlinear aspect of damage. Its importance is clear since as we know it is not very well treated until now. In addition to this, the intended stochastic study, subject of Chapter IV, needs to consider this nonlinearity in cumulative damage.

Figures 3.1 and 3.2 represent an example of linear and nonlinear damage accumulation laws [2,3]. Where n_1 and n_2 are the number of loading cycles, N_{R1} and N_{R2} are respectively the critical number of cycles for the loading levels $\Delta\varepsilon_1$ and $\Delta\varepsilon_2$, and t is the time of loading.

These two figures show the influence of loading order between linear and nonlinear cases; in fact, when small loading $\Delta\varepsilon_1$ precedes high loading $\Delta\varepsilon_2$ (upper case) the linear rule (Palmgren-Miner) does not make the difference for this order whereas the nonlinear rule permits to give a convex curve of damage (figure 3.2) which can be modeled by a double linear damage rule (DLDR) (figure 3.1) (refer to paragraph III.3). When high loading $\Delta\varepsilon_1$ precedes small loading $\Delta\varepsilon_2$ (lower case) also the linear rule is insensible to this order contrarily to the nonlinear rule where it gives a concave curve of damage (figure 3.2) modeled in some methods by a double linear damage rule (DLDR) (figure 3.1) (refer to paragraph III.3).

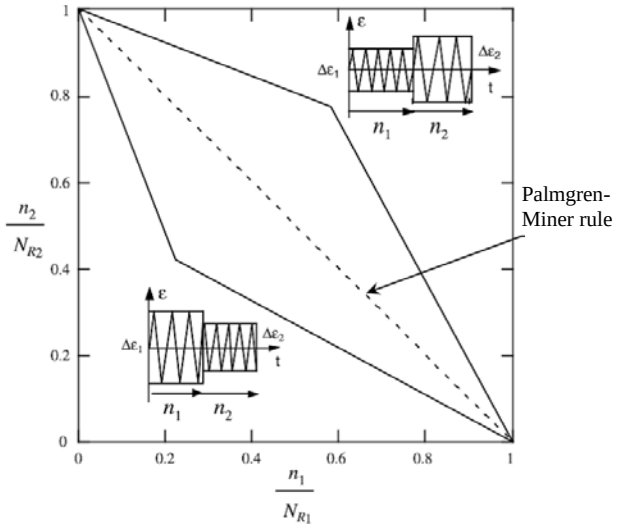

Figure 3.1 - Linear damage accumulation.

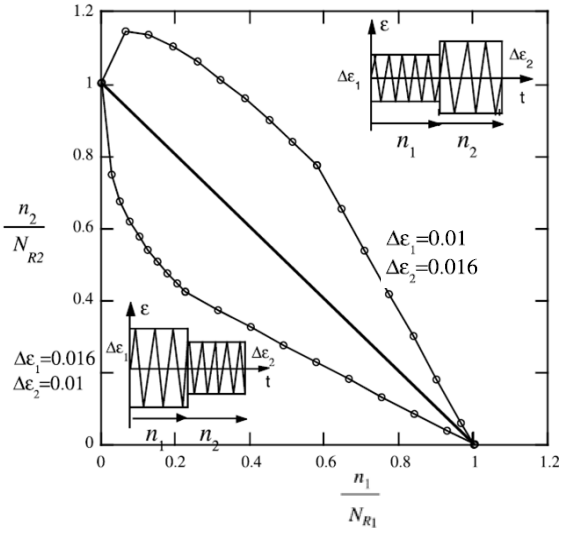

Figure 3.2 - Nonlinear damage accumulation.

III.2 - State-of-the-Art: Nonlinear Damage Accumulation

The subject of cumulative fatigue damage is extremely complex, and various theories have been proposed like in reference [4] to predict fatigue life in advance of service. The most widely known and used procedure is the linear damage rule commonly called the Miner rule**.** The linear damage rule, which indicates that a summation of cycle ratios is equal to unity, is not completely accurate; however, because of its simplicity and because of its agreement with experimental data for certain cases it is frequently used in design. If a new method is to replace the linear damage rule in practical design, much of the simplicity of the linear damage rule must be retained. For example, the double linear damage rule (DLDR) explained later, retains much of this simplicity and at the same time attempts to overcome some of the limitations inherent in the conventional linear rule.

One of the limitations of the linear damage rule is that it does not consider the effect of order of loading. For example, in a two-stress-level fatigue test in which a high load is followed by a low load, the cycle ratio summation is less than 1, whereas a low load followed by a high load produces a cycle ratio summation greater than 1.

The effect of residual stress is also not properly accounted for by the conventional linear damage rule, nor does it consider cycle ratios applied below the initial fatigue limit of the material [4]. Since prior loading can reduce the fatigue limit, cycle ratios of stresses applied below the initial fatigue limit should be accounted for [4].

In addition, coaxing effects present in some strain-aging materials [4] in which the appropriate sequence of loading may progressively raise the fatigue limit are not accounted for by the linear damage rule. Various methods have been proposed as alternatives to the linear damage rule. None overcomes all the deficiencies, and many introduce additional complexities that either preclude or make their use extremely difficult in practical design problems.

Fatigue damage increases with applied load cycles in a cumulative manner which may lead to fracture. Cumulative fatigue damage analysis plays a key role in life prediction of components and structures subjected to fields load histories. Since the introduction of damage accumulation concept by Palmgren-Miner, the treatment of cumulative fatigue damage has received increasingly more attention. As a result, many damage models have been developed. Even though early theories on cumulative fatigue damage have been reviewed by several researchers, no comprehensive report has appeared recently to review the considerable efforts made since the late 1970s.

A general cumulative damage methodology is derived from the basic relation specifying crack growth rate (increment) as a power law function of the stress intensity factor. The crack is allowed to grow up to the point at which it becomes unstable, thereby determining the lifetime of the material under the prescribed stress program.

Damage accumulation in materials is very important, but very challenging to characterize in a meaningful and reliable manner. As the possible damage accumulates, the remaining lifetime under future loads becomes more limited. The ultimate goal is to be able to predict the remaining lifetime as the past history of loading induces a growing state of damage. More succinctly, the common purpose is to be given a complete loading spectrum and then predict how far into the loading sequence the material can remain coherent before suffering catastrophic failure.

The most common approach to such problems is to recognize that cracks under fatigue conditions usually grow in a manner with the rate of growth expressed as stress level (stress intensity factor) to some exponent. This is widely known as the Paris law and has been verified for many materials over many decades of change on log scales. This power law form is then used to predict the number of load cycles until the crack reaches a pre-selected,

unacceptable size. Particular models relate the rate of crack growth to nonlinear functions of the stress intensity factor.

Another general approach is that of Linear Cumulative Damage, LCD. In this method increments of damage, expressed as fractions of lifetime at particular stress levels, are linearly added together to express total damage and thereby the lifetime (Palmgren-Miner Law). The method is completely empirical, but quite widely used because of its simplicity and utility. However, LCD is widely acknowledged to be inadequate. This is partially based upon its empirical nature and partly based upon its prediction of unsatisfactory results [5].

Miner's rule assumes that damage contribution from each cycle of the loading history is independent from the other cycles. Therefore, the damage inflicted by *n* stress cycles with defined magnitude *S* is given by:

$$D = \frac{n}{N} \tag{1}$$

Where *N* denotes the cycles to failure at *S* from the constant-amplitude S-N curve (Wöhler curve).

For all stress levels this damage rules yields [1]:

$$D = \sum_{i=1}^{m} d_i = \sum_{i=1}^{m} \frac{n_i}{N_i} \tag{2}$$

Where n_i is the number of cycles having amplitude S_i.

In the LCD, the measure of damage is simply the cycle ratio with basic assumption of constant work absorption per cycle, and characteristic amount of work absorbed at failure. The energy accumulation, therefore, leads to a linear summation of cycle ratio or damage. The main deficiencies with LCD are its load-level independance, load sequence independance and lack of load-interaction accountability. Howerver, due to the inherent deficiencies of the LCD, no matter which version is used, life prediction based on this rule is offen unsatisfactory. Experimental evidence under completely reversed loading condition often indicates that $\sum d_i > 1$ for a low-to-high (L-H) loading sequence, and $\sum d_i < 1$ for a

high-to-low (H-L) loading sequence. To remedy the deficiencies associated with the LCD, some authors like in reference [6] introduced the concept of damage curves and speculated that these curves ought to be different at different stress-levels.

Then the first nonlinear load-dependent damage theory was proposed by Marco and Starkey [6], it is represented by a power relationship $D = \sum d_i^{\alpha_i}$ where α_i is a variable quantity related to the i[th] loading level. The plots of these curves are shown in figure 3.3. In this figure, a diagonal straight line represents the Miner rule which is a special case of the above equation (2) with $\alpha_i = 1$. As illustrated by figure 3, life calculations based on Marco-Starkey theory would result in $\sum d_i > 1$ for L-H load sequence, and in $\sum d_i < 1$ for H-L load sequence.

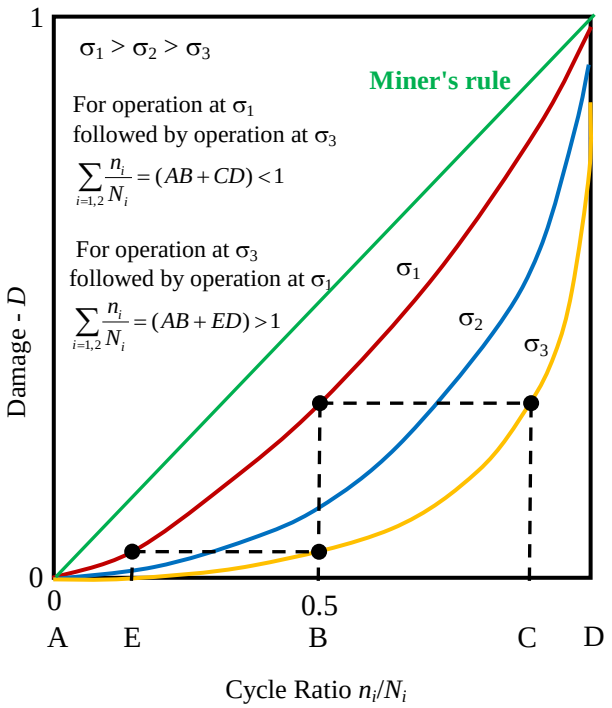

Figure 3.3 - Schematic representation of damage versus cycle ratio for the Marco-Starkey theory.

III.2.1 - Damage Theories Based on Endurance Limit Reduction

On the other hand, the concept of change in endurance limit due to pre-stress exerted an important influence on subsequent cumulative fatigue damage research. Kommers and Bennett [6] further investigated the effect of fatigue prestressing on endurance properties using a two-level step loading method. Their experimental results suggested that the reduction in endurance strength could be used as a damage measure, but they did not correlate this damage parameter to the life fraction. This type of damage models based on endurance limit reduction are non-linear and able to account for the load sequence effect. Some of these models can also be used for predicting the instantaneous endurance limit of a material, if the loading history is known. None of these models, however, take into account load interaction effects.

III.3 - Nonlinear-Damage-Based Prognostic

Various approaches to prognostics have been developed that range in fidelity from simple historical failure rate models to high-fidelity physics-based models like in reference [7]. The required information (depending on the type of prognostics approach) include: engineering model and data, failure history, past operating conditions, current conditions, identified fault patterns, transitional failure trajectories, maintenance history, environment of equipment, system degradation and failure modes.

A number of different methods have been applied to study prognosis of degraded components. In general, prognostics approaches can be classified into three primary categories:

(1) Model driven,
(2) Data driven,
(3) And probability-based prognostic techniques.

The main advantage of model based approaches is their ability to incorporate physical understanding of the monitored system. In addition, in many situations, the changes in feature vector are closely related to model parameters and a functional mapping between the drifting parameters and the selected prognostic features can be established [1]. Moreover, if the understanding of the system degradation improves, the model can be adapted to increase its accuracy and to address subtle performance problems. Consequently, they can significantly outperform data-driven approaches. But, this closed relation with a mathematical model may also be a strong weakness: it can be difficult, even impossible to catch the system's behavior. Further, some authors think that the monitoring and the prognostic tools must evolve as the system does.

An earlier proposed procedure [8] (Chapter II) belongs to the first prognostic approach. It is based on a physical model and leading to a normalized degradation indicator. It is focused on developing and implementing effective diagnostic and prognostic technologies with the ability to detect faults in the early stages of degradation. Early detection and accurate analysis may lead to better prediction and end of life estimates by tracking and modeling the degradation process.

The idea was to use these estimates to make accurate and precise prediction of the time to failure of components. The chosen failure mode was the fatigue failure formulated mathematically on the base of analytic damage laws of Paris and Miner. The last law is a linear cumulative damage model (figure 3.1). Even that these laws are very well known in mechanics of rupture but their uses in the present prognostic procedure help as a support for an example of a degradation expression.

Past research has shown there is a nonlinear interaction effect between high cycle fatigue (HCF) and low cycle fatigue (LCF) in many engineering materials. This effect has been observed within uniaxial loadings, but is often more pronounced under multiaxial loading, particularly when the loading is non-proportional. An example here is the development of fatigue damage assessment methods for turbine engine materials combining the LCF and HCF cycles.

The nonlinear interaction effect precludes the use of the most common technique for linear damage accumulation. A thorough review of nonlinear cumulative damage (figure 3.2) methodologies [9] shows that these techniques have included simple extensions of the linear damage rule to include nonlinear terms. Several nonlinear methods exist, including endurance-limit modification techniques, fracture-mechanics based approaches, continuum-damage, and life-curve approaches. Traditional methods of damage summation have been shown to provide an inaccurate life prediction when multiple load levels are simultaneously considered. This is due to the effect that one load level has on the other(s).

In the present study, the effect of HCF loading has had a more detrimental effect when coupled with the LCF loadings than predicted by a linear summation rule. Nonlinear damage accumulation theories can account for this influence and have shown an improvement in prediction. The stress levels were chosen to correspond to levels previously tested to failure, resulting in fatigue lives ranging from approximately 10^5 to 10^7 cycles. A nonlinear damage summation is required to properly define the fatigue process since the linear summation of damage is often not adequate to predict the service life of a component when subjected to variable-amplitude loadings.

III.3.1 - Disadvantages of Linear Damage Accumulation

The most common method of summing damage for a loading spectrum is the Palmgren-Miner linear damage rule [10] (figure 3.4). It is readily understood and easy to implement and is, therefore, the foundation for many of the other cumulative damage theories that have been proposed. Ideally, the summation of life ratios would equal one at failure.

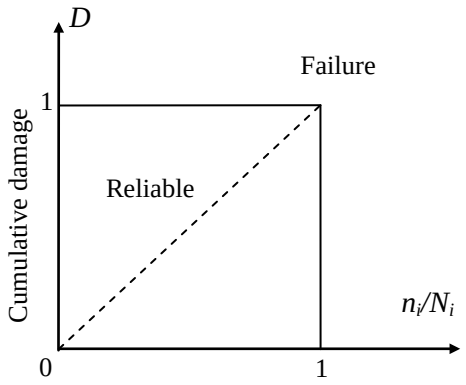

Figure 3.4 - Palmgren-Miner's linear rule of damage.

However, past experiments have yielded a range of ratios from 0.7 to 2.2 for uniaxial loadings, resulting in failure predictions erring just slightly on the side of non-conservative to more than the double for a conservative prediction [11]. For the biaxial loadings, a Miner's summation of 0.19 was found in these experiments [11], indicating thus extremely non-conservative results as it is so far from failure point (equal to 1.0). This proves the dependence of Miner' law on the load directions.

Also, the largest drawback of the linear damage rule is its inability to account for the order of loading. That is, the resulting failure prediction is independent of the load interaction effects that have been observed between high-cycle and low-cycle loadings. It is this shortcoming that has prompted the development of several nonlinear cumulative damage theories. Hence, different non-linear damage rules have been proposed in literature and presented as follows.

III.3.2 - Double Linear Damage Rule (DLDR)

The current form of the DLDR was proposed in 1966 [12]. Instead of a single straight line, a set of two straight lines that converged at a common "Kneepoint" would be used (figure 3.5). It helps differentiate between the damage caused by the LCF and HCF for multi-level loadings. Its basis is the replacement of the continuous damage curve by two straight lines. Each linear phase can be analyzed by

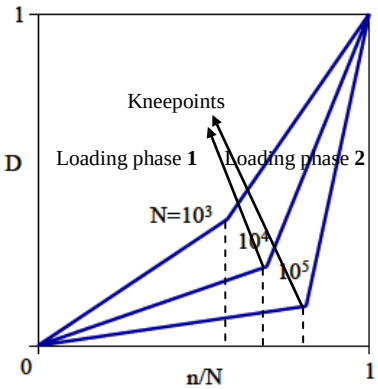

Figure 3.5 - Double Linear Damage

Palmgren-Miner linear damage rule. The difficulty encountered when utilizing the DLDR is establishing the location of the transitory point between the two loading phases (equation 3).

The DLDR is represented by the equations (3) illustrated in figure 3.5. These equations permit to calculate the damage accumulation at each loading cycle with respect to the double linear damage rule.

$$\left.\frac{n_1}{N_1}\right]_{knee} = 0.35\left[\frac{N_1}{N_2}\right]^{\alpha} \qquad \left.\frac{n_2}{N_2}\right]_{knee} = 0.65\left[\frac{N_1}{N_2}\right]^{\alpha} \tag{3}$$

Where,

n_1/N_1 and n_2/N_2 are loading phases,

α: material parameter.

III.3.3 - Damage Curve Approach (DCA)

To better describe fatigue failure using nonlinear damage, instead of a straight line, a single continuous curve reflects more accurately the influence of the loading (figure 3.6). For HCF loading a significant number of cycles had to be applied before enough damage could accumulate to cause a reduction in life. Once the appropriate number of cycles had been applied, the damage continued to accumulate at an ever-increasing rate and failure was soon to follow. For LCF loadings, this behavior was less pronounced.

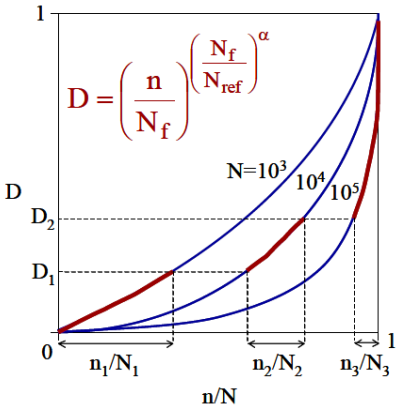

Figure 3.6 - Damage Curve Approach.

A workable equation based on early crack growth theories was provided [13]:

$$D = \left(\frac{n}{N_f}\right)^{\left(\frac{N_f}{N_{ref}}\right)^{\alpha}} \tag{4}$$

The implementation of the DCA model is illustrated in figure 3.5. The primary advantage in employing the DCA model lies in its ability to create identical damage curves

for different life references. The linear damage line becomes the reference life that is used to establish the material constant in (4), and other damage curves shift values accordingly.

Where,

D is the damage accumulated,

n_1/N_1, n_2/N_2 , and n_3/N_3 are the loading phases,

N_f is the critical number of cycles,

N_{ref} is the reference number of cycles (reference life).

III.3.4 - Double Damage Curve Approach (DDCA)

Although the DCA shows large potential in accurately predicting failure in multi-level loading, there is one serious drawback when considering high-low loading. It can be seen upon examination that with the application of just a few high-amplitude cycles, there is a rapid decrease in remaining life at the low-amplitude load level. This result is from a lack of the low-range data needed to adjust the shape of the curve during the models conception. To improve the model, Manson and Halford [14] included a linear term to shift the curves away from the x-axis.

The difficulty would be to allow this new term to have a significant influence at low life ratios but negligible effect at higher ratios. The resulting double damage curve approach (DDCA) closely approximated the DLDR in the lower-life regime and the DCA in the higher-life regime, where each model performed best. The equation for the DDCA is shown in (5):

$$D = \left(\frac{n}{N}\right) \cdot \left\{ q_1^{\gamma} + \left[1 - q_1^{\gamma}\right] \cdot \left[\frac{n}{N}\right]^{\gamma(q_2 - 1)} \right\}^{\frac{1}{\gamma}} \qquad (5)$$

Where,

D = damage accumulated,

n = number of applied cycles at a given load level,

N = number of cycles required to fail at the same load level as n.

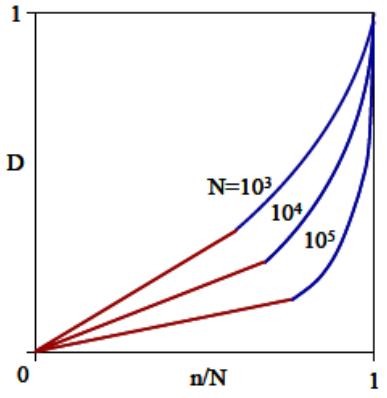

Figure 3.7 - Double Damage Curve Approach.

$$q_1 = \frac{0.35\left(\frac{N_{ref}}{N}\right)^{\alpha}}{1-0.65\left(\frac{N_{ref}}{N}\right)^{\alpha}} \quad \text{and} \quad q_2 = \left(\frac{N}{N_{ref}}\right)^{\beta} \quad \text{are parameters,}$$

$\gamma = 5$ is a constant representing two intersecting straight lines which can be replaced by a single curve,

α, β are material dependent parameters that must be experimentally determined (typically taken as 0.25 and 0.4, respectively).

The DDCA model is illustrated schematically in figure 3.7. Notice the linear damage accumulation at lower life ratios and curvilinear damage accumulation at higher life ratios. Notice that the DDCA model is a general form which can be applied to a wide range of materials and equipments.

III.4 - Nonlinear Cumulative Damage Model

The damage model proposed in this chapter, whose evolution is up to the point of macro-crack initiation, is represented in figure 3.8. The state of damage of a specimen at a particular cycle N during fatigue is represented by a scalar damage function $D(N)$. The magnitude $D_0 = 0$ corresponds to no damage, and $D_C = 1$ corresponds to the appearance of the first macro-crack (total damage).

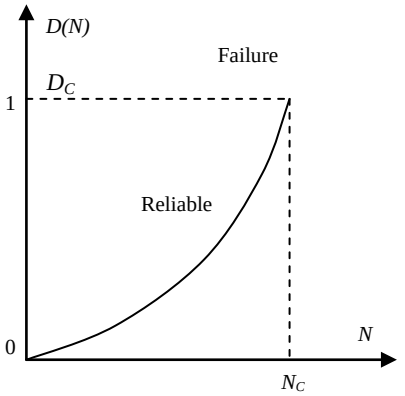

Figure 3.8 - Nonlinear law of damage.

The following model is chosen for the nonlinear prognostic study. It represents the nonlinear evolution of damage D in terms of the number of cycle N given under the following first order nonlinear ordinary differential equation [15]:

$$\frac{dD}{dN} = \begin{cases} \frac{1}{N_C}\left(1-\frac{\sigma_0}{\Delta\sigma/2}\right)^{m}\frac{1}{(1-D)^{\alpha}} & \text{if } \Delta\sigma/2 > \sigma_0 \\ 0 & \text{if } \Delta\sigma/2 < \sigma_0 \end{cases} \tag{6}$$

Where,

N_C : the number of cycles at failure as a normalizing constant,

$\Delta\sigma$: the stress range in a loading cycle,

σ_0 : the endurance limit, it is a function of the stress mean in a cycle: $\overline{\sigma}$

$$\sigma_0(\overline{\sigma}) = \sigma_0(0)\left(1-\frac{\overline{\sigma}}{\sigma_{ult}}\right) \quad ; \quad \text{where } \sigma_0 < \Delta\sigma/2$$

σ_{ult} : the ultimate tensile strength of the material,

m and α : they are constants depending on the material and the loading condition ($m \approx 2.91$ and $\alpha \approx 2.23$).

This nonlinear ordinary differential equation (6) needs to be solved in order to find an expression of *D*(*N*).

III.4.1 - Solution of the Differential Equation of Degradation

The solution of the differential equation (6) is presented as follows:

$$\frac{dD}{dN} = \begin{cases} \frac{1}{N_C}\left(1-\frac{\sigma_0}{\Delta\sigma/2}\right)^m \frac{1}{(1-D)^\alpha} & \text{if } \Delta\sigma/2 > \sigma_0 \\ 0 & \text{if } \Delta\sigma/2 < \sigma_0 \end{cases}$$

$$\Rightarrow \int_{D_0}^{D_N} (1-D)^\alpha \, dD = \int_{N_0}^{N} \frac{1}{N_C}\left(1-\frac{\sigma_0}{\Delta\sigma/2}\right)^m dN$$

$$\Rightarrow -\frac{(1-D)^{\alpha+1}}{\alpha+1}\Bigg]_{D_0}^{D_N} = \frac{N}{N_C}\left(1-\frac{\sigma_0}{\Delta\sigma/2}\right)^m\Bigg]_{N_0}^{N}$$

$$\Rightarrow \frac{-1}{\alpha+1}\left[(1-D(N))^{\alpha+1} - (1-D_0)^{\alpha+1}\right] = \frac{N-N_0}{N_C}\left(1-\frac{\sigma_0}{\Delta\sigma/2}\right)^m$$

$$\Rightarrow (1-D(N))^{\alpha+1} - (1-D_0)^{\alpha+1} = -\frac{N-N_0}{N_C}\left(1-\frac{\sigma_0}{\Delta\sigma/2}\right)^m(\alpha+1)$$

$$\Rightarrow (1-D(N))^{\alpha+1} = (1-D_0)^{\alpha+1} - \frac{N-N_0}{N_C}\left(1-\frac{\sigma_0}{\Delta\sigma/2}\right)^m(\alpha+1)$$

$$\Rightarrow (1-D(N)) = \sqrt[(\alpha+1)]{(1-D_0)^{\alpha+1} - \frac{N-N_0}{N_C}\left(1-\frac{\sigma_0}{\Delta\sigma/2}\right)^m(\alpha+1)}$$

$$\Rightarrow D(N) = 1-\left[(1-D_0)^{\alpha+1} - \frac{N-N_0}{N_C}\left(1-\frac{\sigma_0}{\Delta\sigma/2}\right)^m(\alpha+1)\right]^{\frac{1}{\alpha+1}} \qquad (7)$$

Where,

$D(N_0) = D_0$ is the damage at $N = N_0$ cycles corresponding to an initial crack length a_0.

We choose an equivalent damage parameter, to be measured by structural health monitoring. The plotting of expression (7) of $D(N)$ is presented in figure 3.9.

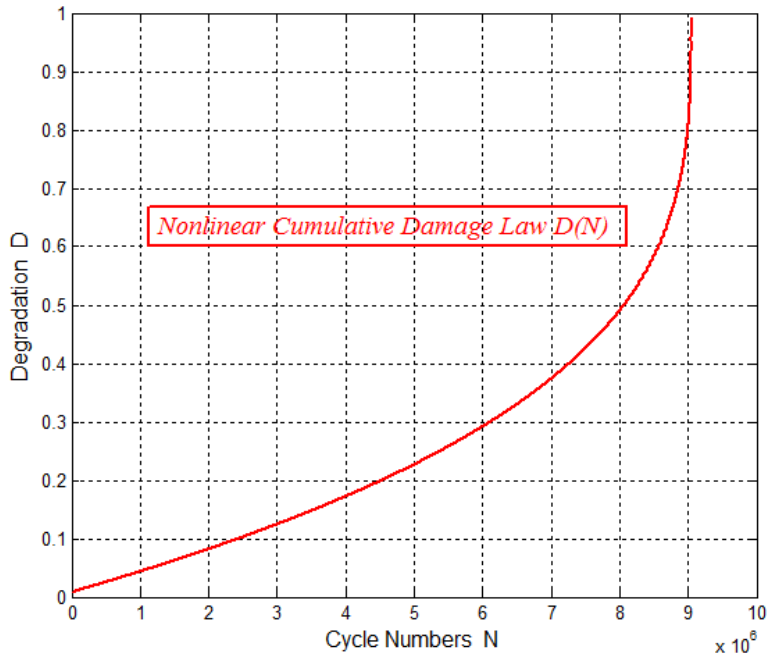

Figure 3.9 - Nonlinear $D(N)$ curve.

Particular case:

Take $D_0 = 0$ for $N = N_0$,

$$\Rightarrow D(N) = 1 - \left[1 - \left(\frac{N - N_0}{N_C}\right)\left(1 - \frac{\sigma_0}{\bar{\sigma}}\right)^m (\alpha + 1)\right]^{\frac{1}{\alpha+1}}; \quad \text{where } \bar{\sigma} = \Delta\sigma / 2. \tag{8}$$

Failure case:

At failure we have $N = N_C$ and $D(N_C) = 1$, then equation (8) gives:

$$1 = 1 - \left[1 - \left(\frac{N_C - N_0}{N_C}\right)\left(1 - \frac{\sigma_0}{\bar{\sigma}}\right)^m (\alpha + 1)\right]^{\frac{1}{\alpha+1}}$$

$$\Rightarrow 1 - \left(\frac{N_C - N_0}{N_C}\right)\left(1 - \frac{\sigma_0}{\bar{\sigma}}\right)^m (\alpha + 1) = 0 \Rightarrow \left(\frac{N_C - N_0}{N_C}\right)\left(1 - \frac{\sigma_0}{\bar{\sigma}}\right)^m (\alpha + 1) = 1$$

$$\Rightarrow \left(\frac{N_C - N_0}{N_C}\right)\left(1-\frac{\sigma_0}{\overline{\sigma}}\right)^m = \frac{1}{\alpha+1}$$

Assume that $N_0 = 0$: $$\Rightarrow \left(1-\frac{\sigma_0}{\overline{\sigma}}\right)^m = \frac{1}{\alpha+1} \Rightarrow 1-\frac{\sigma_0}{\overline{\sigma}} = \frac{1}{(\alpha+1)^{\frac{1}{m}}}$$

Therefore:

$$\sigma_0 = \overline{\sigma} \times \left(1-\frac{1}{(\alpha+1)^{\frac{1}{m}}}\right) \tag{9}$$

III.4.2 - Relation between *D* and *N* at a Specific Cycle N_1

Let us study the relation between the degradation *D* and the cycle of stress *N*. To do that easily let us integrate the relation of degradation between cycle 1 and cycle 2 assuming that failure occurs at cycle 2.

From equation (6), it can be deduced that:

$$(1-D)^{\alpha} dD = \frac{1}{N_C}\left(1-\frac{\sigma_0}{\Delta\sigma/2}\right)^m dN$$

$$\Rightarrow \int_{D_1}^{D_C=1} (1-D)^{\alpha} dD = \int_{N_1}^{N_C} \frac{1}{N_C}\left(1-\frac{\sigma_0}{\Delta\sigma/2}\right)^m dN$$

$$\Rightarrow -\frac{(1-D)^{\alpha+1}}{\alpha+1}\Bigg]_{D_1}^{1} = \frac{N}{N_C}\left(1-\frac{\sigma_0}{\Delta\sigma/2}\right)^m\Bigg]_{N_1}^{N_C}$$

$$\Rightarrow \frac{(1-D_1)^{\alpha+1}}{\alpha+1} = \frac{N_C - N_1}{N_C}\left(1-\frac{\sigma_0}{\Delta\sigma/2}\right)^m$$

$$\Rightarrow \frac{(1-D_1)^{\alpha+1}}{\alpha+1} = \left(1-\frac{N_1}{N_C}\right)\left(1-\frac{\sigma_0}{\Delta\sigma/2}\right)^m$$

$$\Rightarrow 1-\frac{N_1}{N_C} = \left(1-\frac{\sigma_0}{\Delta\sigma/2}\right)^{-m}\frac{(1-D_1)^{\alpha+1}}{\alpha+1}$$

$$\Rightarrow \frac{N_1}{N_C} = 1-\left(1-\frac{\sigma_0}{\Delta\sigma/2}\right)^{-m}\frac{(1-D_1)^{\alpha+1}}{\alpha+1}$$

It can be inferred also:

$$\Rightarrow 1-D_1 = \left[(\alpha+1)\left(1-\frac{N_1}{N_C}\right)\left(1-\frac{\sigma_0}{\Delta\sigma/2}\right)^m\right]^{\frac{1}{\alpha+1}}$$

Then:

$$D_1(N_1) = 1 - \left[(\alpha+1)\left(1 - \frac{N_1}{N_C}\right)\left(1 - \frac{\sigma_0}{\Delta\sigma/2}\right)^m \right]^{\frac{1}{\alpha+1}} \tag{10}$$

III.4.3 - Recursive Relation of Nonlinear Damage *D*

To construct a recursive relation for the sequence of *D*, the procedure is as follows:

$$(1-D)^\alpha \, dD = \frac{1}{N_C}\left(1 - \frac{\sigma_0}{\Delta\sigma/2}\right)^m dN$$

$$\Rightarrow \int_{D_N}^{D_{N+1}} (1-D)^\alpha \, dD = \int_N^{N+1} \frac{1}{N_C}\left(1 - \frac{\sigma_0}{\bar{\sigma}}\right)^m dN \quad ; \quad \text{where } \bar{\sigma} = \Delta\sigma/2$$

$$\Rightarrow -\frac{(1-D)^{\alpha+1}}{\alpha+1}\Bigg]_{D_N}^{D_{N+1}} = \frac{N}{N_C}\left(1 - \frac{\sigma_0}{\bar{\sigma}}\right)^m \Bigg]_N^{N+1}$$

$$\Rightarrow \left(\frac{1}{\alpha+1}\right)\left[(1-D_N)^{\alpha+1} - (1-D_{N+1})^{\alpha+1}\right] = \frac{1}{N_C}\left(1 - \frac{\sigma_0}{\bar{\sigma}}\right)^m$$

$$\Rightarrow (1-D_{N+1})^{\alpha+1} = (1-D_N)^{\alpha+1} - \frac{(\alpha+1)}{N_C}\left(1 - \frac{\sigma_0}{\bar{\sigma}}\right)^m$$

$$\Rightarrow D_{N+1} = 1 - \left[(1-D_N)^{\alpha+1} - \frac{(\alpha+1)}{N_C}\left(1 - \frac{\sigma_0}{\bar{\sigma}}\right)^m \right]^{\frac{1}{\alpha+1}}$$

The previous recursive relation leads to a sequence of values D_N whose limit is D_C=1:

$$D_0,\ D_1,\ D_2,\ \cdots,\ D_N,\ D_{N+1},\ \cdots,\ D_C = 1 \tag{11}$$

And as the stress-load is expressed in terms of time (*t*), then we can plot the curve of degradation *D* in terms of time (*t*).

Therefore, our prognostic model in the nonlinear case is given by:

$$D_{N+1} = 1 - \left[(1-D_N)^{\alpha+1} - \frac{(\alpha+1)}{N_C}\left(1 - \frac{\sigma_0}{\bar{\sigma}}\right)^m \right]^{\frac{1}{\alpha+1}} \tag{12}$$

III.5 - Application to a Suspension System

Reconsider the example of Chapter II concerning the vehicle suspension system and apply the nonlinear model of damage developed in paragraph III.4.3 (equation 12) in order to calculate the prognostic of this system. The following parameters are considered in the simulation [16]:

N_C is a normalizing constant taken to be equal to the number of cycles at failure ($N_C = 10^7$)

α = estimated to be 2.23,

m = 2.91,

$\overline{\sigma} = \Delta\sigma / 2$ is the stress load amplitude in one cycle, this parameter is generated as an input load resulting from the road profile and whose mean is taken to be equal to 280 MPa,

σ_0 is the fatigue limit (endurance limit of the material) taken to be equal to 180 MPa.

Table 3.1 - Statistical characteristics of each mode of roads.

Road Mode	Mean of Δx_j ($\overline{\Delta x_j}$ in mm)	Coefficient of Variation of Δx_j in %	Standard Deviation (in mm)	Law
Severe (mode 1)	100	15%	15	Normal
Fair (mode 2)	50	10%	5	Normal
Good (mode 3)	25	5%	1.25	Normal

For more details about the data of this application, refer to Chapter II.

III.5.1 - Results of the Simulation

The simulations of the degradation of a vehicle suspension subject to the severe, fair, and good modes of road profiles are represented respectively in figures 3.10, 3.11, and 3.12.

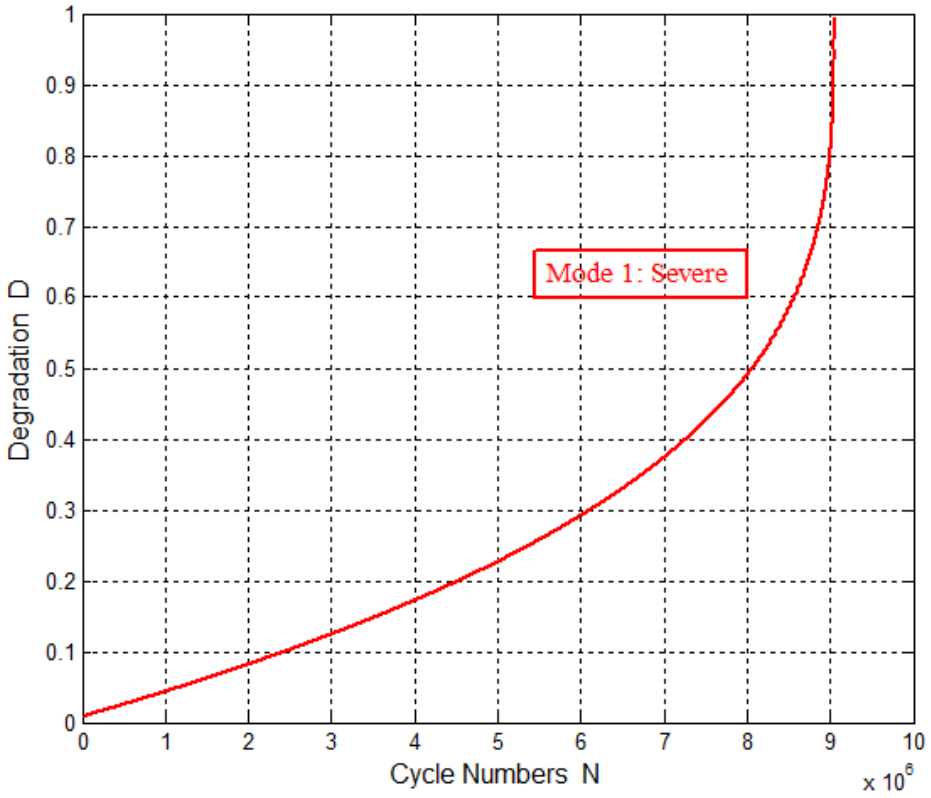

Figure 3.10 - Suspension degradation under nonlinear law for severe mode of road excitation.

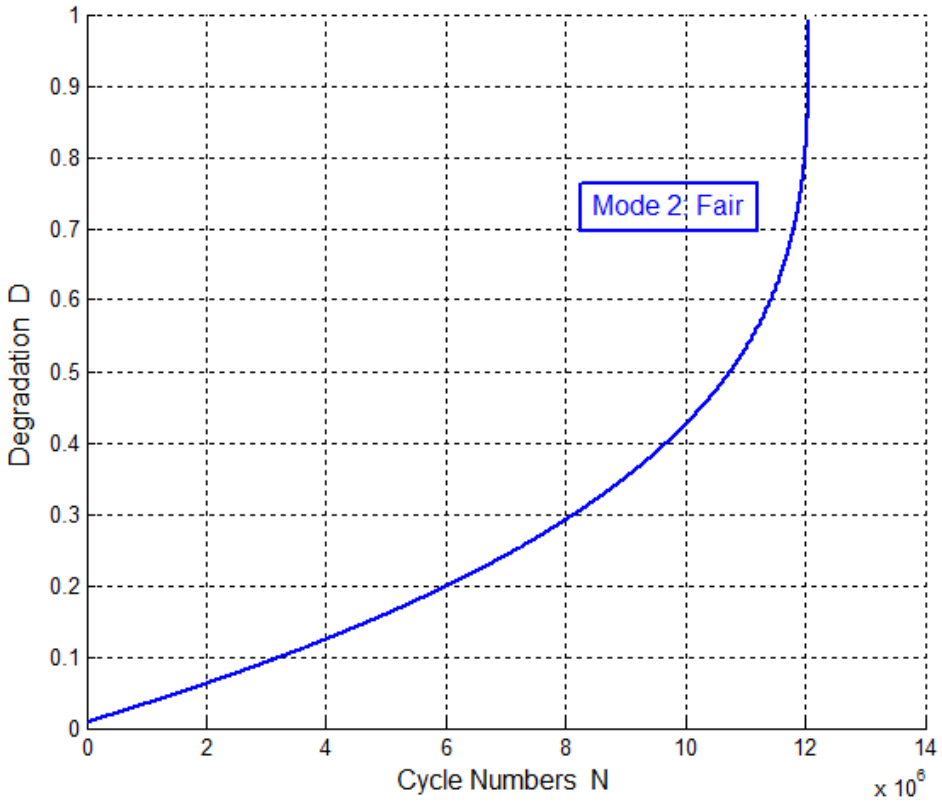

Figure 3.11 - Suspension degradation under nonlinear law for fair mode of road excitation.

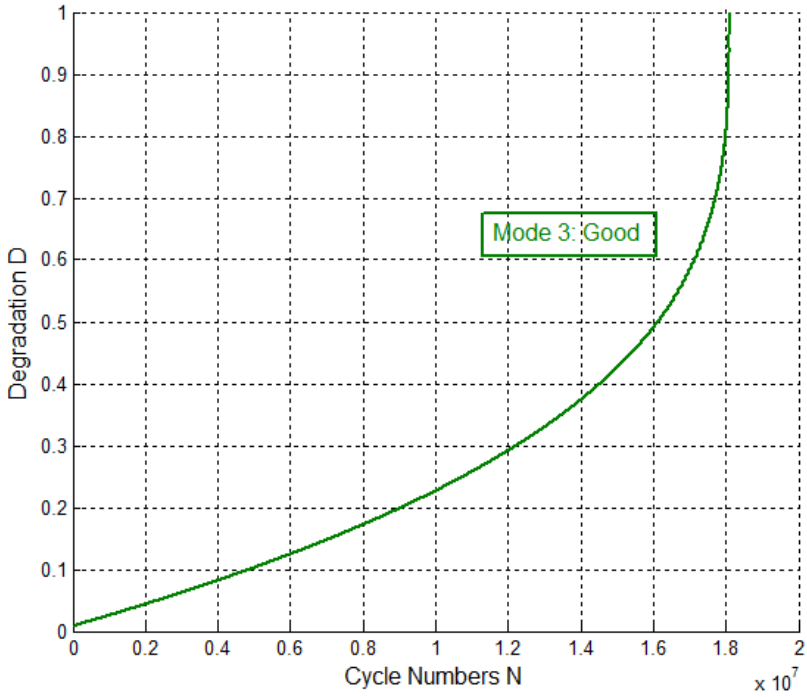

Figure 3.12 - Suspension degradation under nonlinear law for good mode of road excitation.

Figures 3.13 and 3.14 represent respectively the evolution of degradation *D* and of the RULs for the suspension for three modes of roads with profile properties indicated in table 3.1.

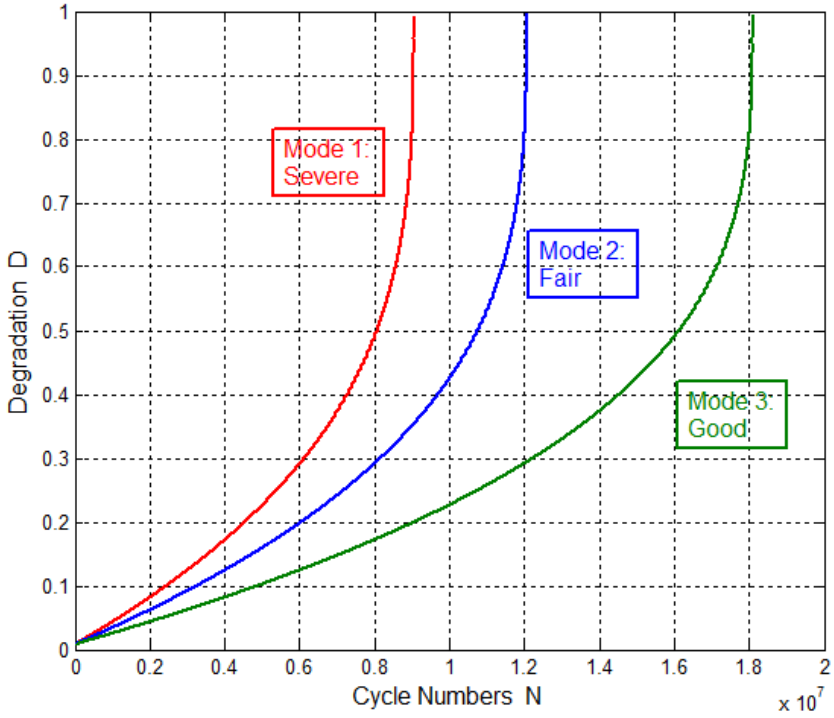

Figure 3.13 - Suspension degradation under nonlinear law for three modes of road excitations.

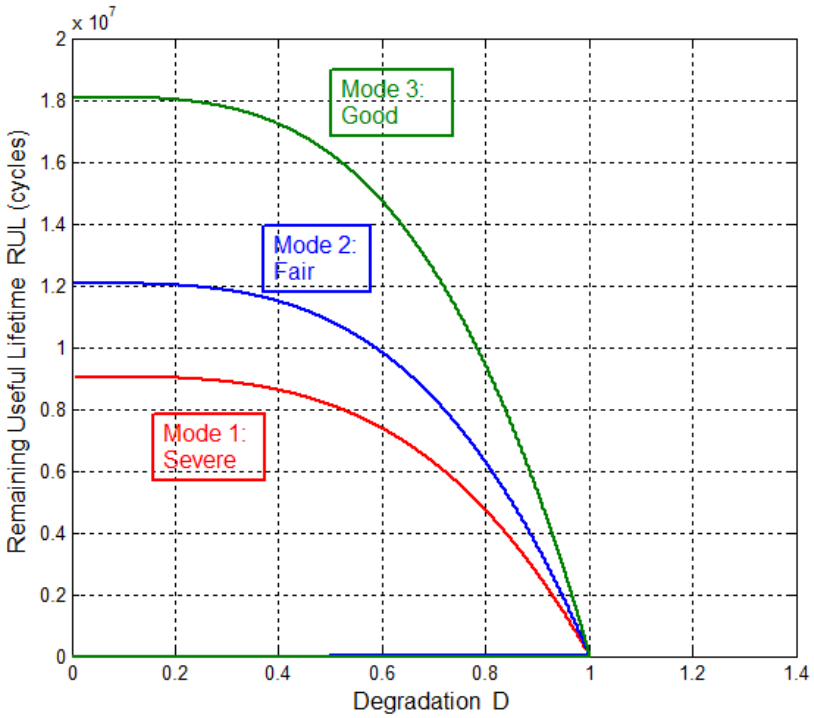

Figure 3.14 - Suspension RULs under nonlinear law for three modes of road excitation.

The RULs evaluations in figure 3.14 are deduced from the expression N_C - N. In fact N_C is the necessary cycle number to reach failure (appearance of the first macro-cracks) and N is the cycle number corresponding to a crack length a_N . Note that N_0 is the initial cycle number at the beginning taken generally equal to 0. These curves decrease from entire lifetime of the device to zero where D_C = 1. From these curves we can deduce at each cycle N RUL(N) of the device and hence the prognostic result can be inferred. The expected lifetimes are as follows:

Mode 1: N_{C1} = 9,047,700 cycles

Mode 2: N_{C2} = 12,063,800 cycles

Mode 3: N_{C3} = 18,095,400 cycles

III.5.2 - Conversion of RUL into Years

To convert the suspension lifetime into years' unit, knowing that each cycle's duration is 2 seconds, then:

$$\text{RUL(s)} = 2 \times \text{RUL}(N).$$

If we assume that the suspension time usage is 10% of a day (2.4 hours/day), then the expected lifetimes' durations are (refer to Chapter II, Paragraph 3.1.10):

For mode 1: $$\frac{9{,}047{,}700(\text{cycles})\times 2(\text{s})}{60(\text{s})\times 60(\text{min})\times 2.4(\text{hours})\times 365(\text{days})} = 5.738 \text{ years}$$

For mode 2: $$\frac{12{,}063{,}800(\text{cycles})\times 2(\text{s})}{60(\text{s})\times 60(\text{min})\times 2.4(\text{hours})\times 365(\text{days})} = 7.651 \text{ years}$$

For mode 3: $$\frac{18{,}095{,}400(\text{cycles})\times 2(\text{s})}{60(\text{s})\times 60(\text{min})\times 2.4(\text{hours})\times 365(\text{days})} = 11.476 \text{ years}$$

III.5.3 - Comparison with the Linear Case

We can deduce from the two figures 3.15 and 3.16 that, first of all, the nonlinear case of damage is more optimistic and accurate than the linear case concerning the lifetime because the values are larger. Secondly, the decreasing of RULs in the nonlinear case is less steep at the end than the linear case because the nonlinear curves reach the zero value progressively.

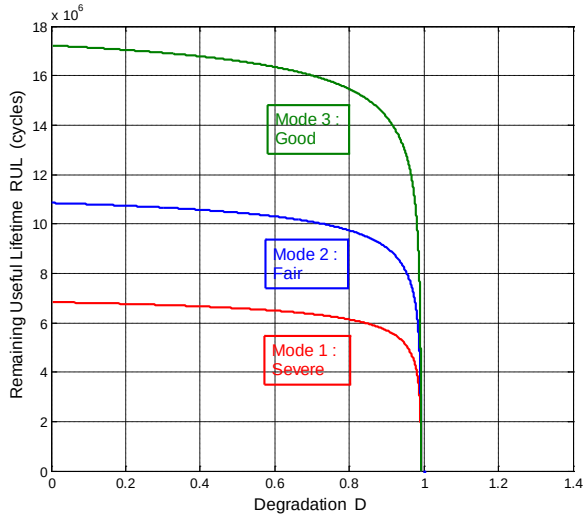

Figure 3.15 - Linear case.

N_{C1} = 6,836,000 cycles; N_{C2} = 10,850,000 cycles; N_{C3} = 17,222,000 cycles.

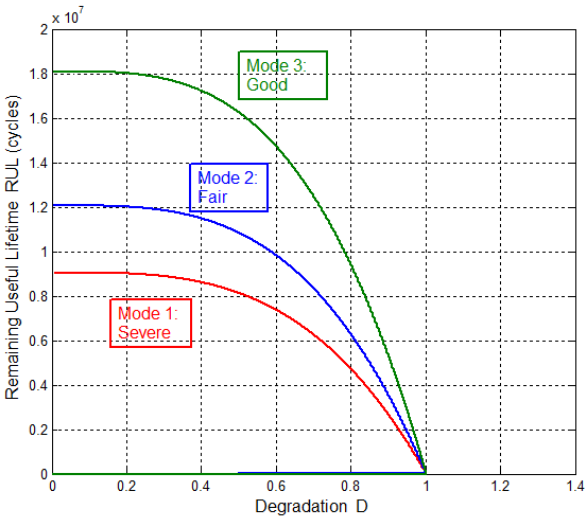

Figure 3.16 - Nonlinear case.

N_{C1} = 9,047,700 cycles; N_{C2} = 12,063,800 cycles; N_{C3} = 18,095,400 cycles.

Finally, we can remark that near the failure zone where $D = D_C = 1$ the nonlinear study seems to give here a more logical and realistic damage behavior for the different road profiles than the linear case where the damage curves become identical. In fact, between good

and severe profiles, the nonlinear case makes the difference when approaching failure limit whereas the linear case does not. The optimistic results obtained from the nonlinear case can be explained by the fact that when the real nonlinear trends of degradation are of concave form then the damage accumulation is overestimated when using a linear form (figure 3.17).

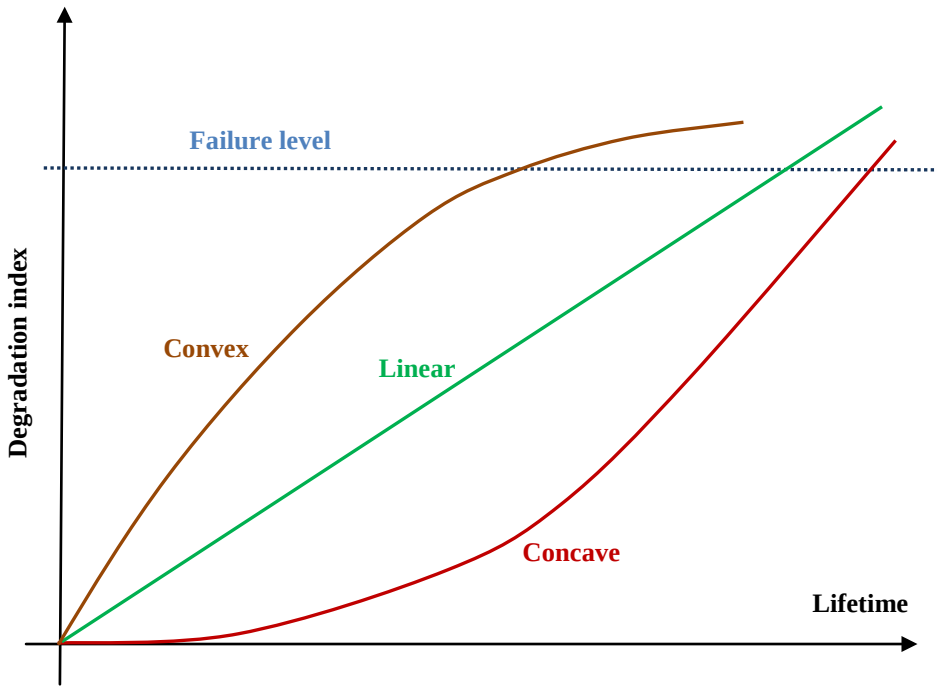

Figure 3.17 - Different degradation trends.

Referring to the references [17,18,19,8], the validation of the present results cannot be explained without taking into consideration the nonlinear basis of the current study contrary to the linear damage model adopted in the previous references. Therefore, the results got here are realistic when compared to those obtained by the works of these authors.

III.5.4 - Advantages of the Proposed Model

In comparison with predictive RUL models available in literature [20], the advantages of the present model are:

a) It is simple and practical in application to various industrial systems for fatigue life prediction.

b) The fact of using a nonlinear law, if it exists, for damage accumulation, makes it more efficient and realistic in predicting the remaining useful lifetime.

c) When multiple load levels are simultaneously considered, the linear law of damages accumulation like Miner's law leads to inaccuracy [10] in life prediction whereas the nonlinear law of damage permits to consider the effect mentioned above.

d) It takes into account the load interaction effects between high-cycle and low-cycle loadings contrary to predictive models based on linear damage law.

e) Its efficiency relatively to other models has been often more pronounced under multi-axial loading, particularly when the loading is non-proportional.

f) It considers the influent environment that can accentuate the nonlinear aspect related to some materials behavior subject to fatigue effects (brittle materials for example).

g) The Paris' law of fatigue for crack growth adopted in the present model is simple to use and requires two parameters easily obtained. It is the simplest to perform because no load history has to be considered. In fact, it allows an excellent prediction model results for crack lives below 10^5 cycles.

III.6 - Application to a Pipeline System

Reconsider the example of Chapter II concerning the pipeline system and apply the nonlinear model developed in paragraph III.4.3 (equation 12).

The deterministic triangular simulation of the three modes of internal pressure is made using the parameters given in table 3.2.

Table 3.2 - Statistical characteristics of each pressure mode.

Pressure Mode	$\overline{P}_j$ (MPa)	δ_{Pj} (%)	Law
High (mode 1)	8	10%	Triangular
Middle (mode 2)	5	10%	Triangular
Low (mode 3)	3	10%	Triangular

The study covers three types of pipes: unburied, buried and offshore.

III.6.1 - Unburied Pipe Case

The case studied here is that of unburied pipes (in free air). The simulations of the pipe degradation for high, middle and low modes of internal pressure are represented respectively in figures 3.18, 3.19, and 3.20.

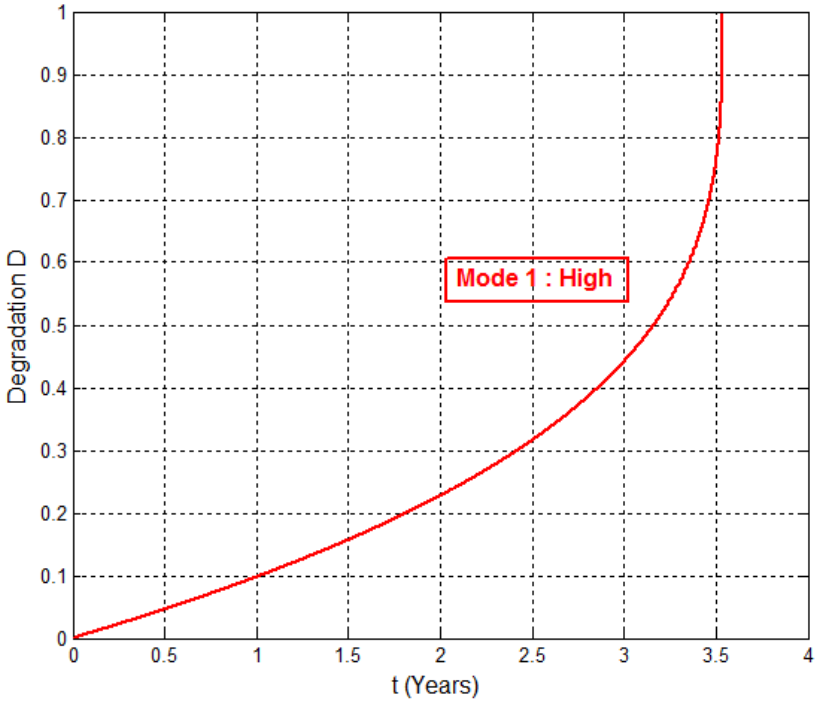

Figure 3.18 - Pipelines degradation under high mode pressure for nonlinear law case (unburied pipes).

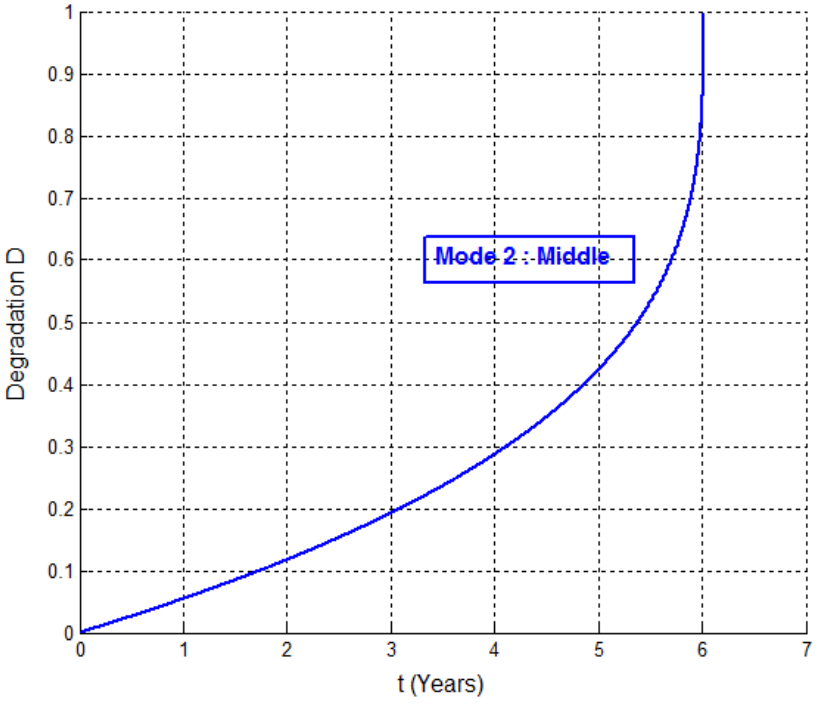

Figure 3.19 - Pipelines degradation under middle mode pressure for nonlinear law case (unburied pipes).

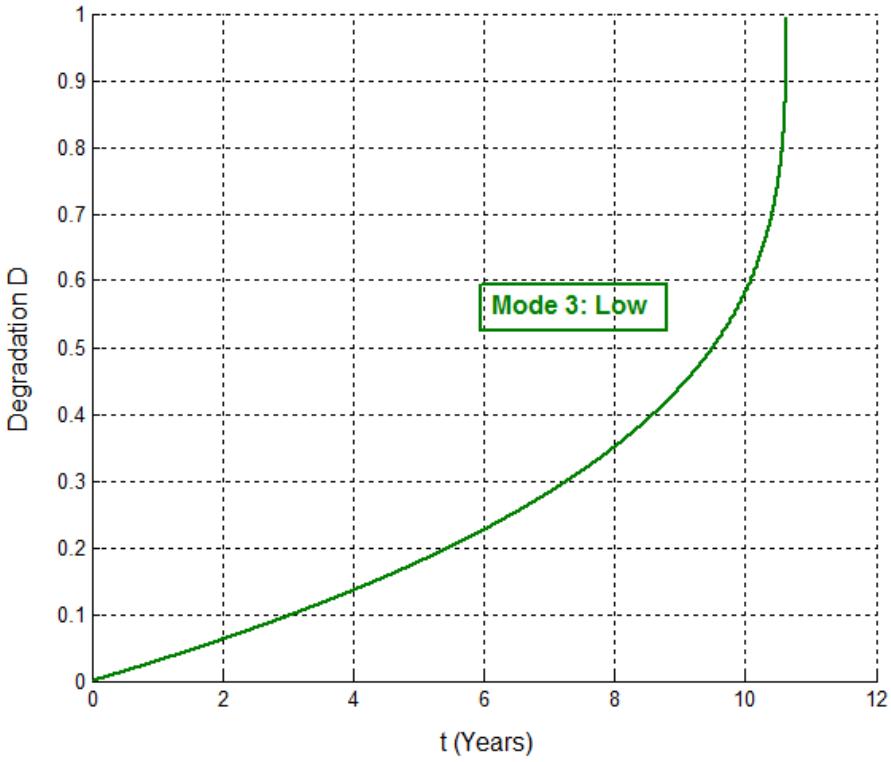

Figure 3.20 - Pipelines degradation under low mode pressure for nonlinear law case (unburied pipes).

The degradation evolution (figure 3.21) and the RULs evolution (figure 3.22) are obtained for each mode of internal pressure in terms of exploitation time and degradation state *D*.

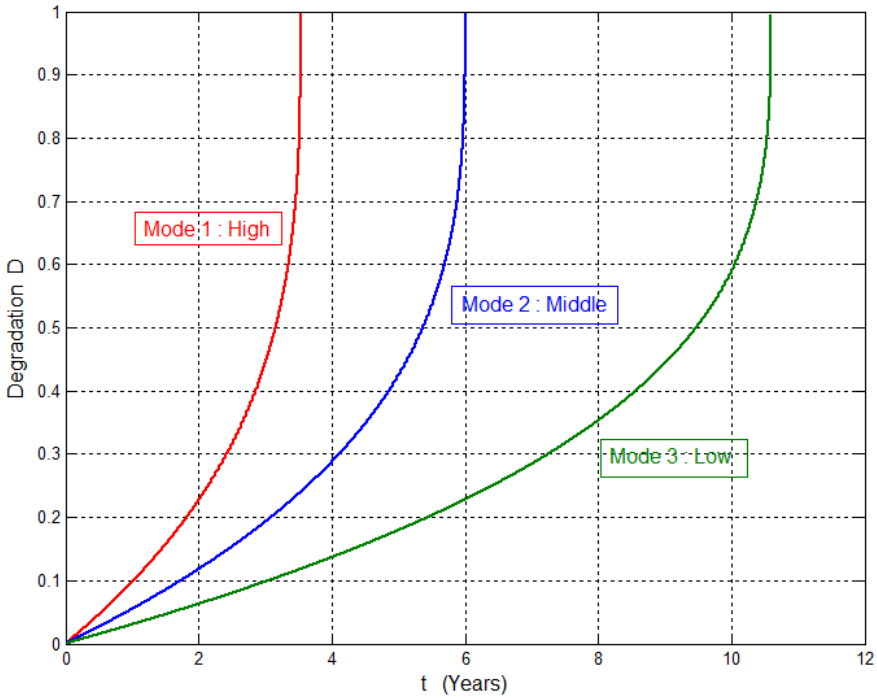

Figure 3.21 - Pipelines degradation under three modes of pressure for nonlinear law case (unburied pipes).

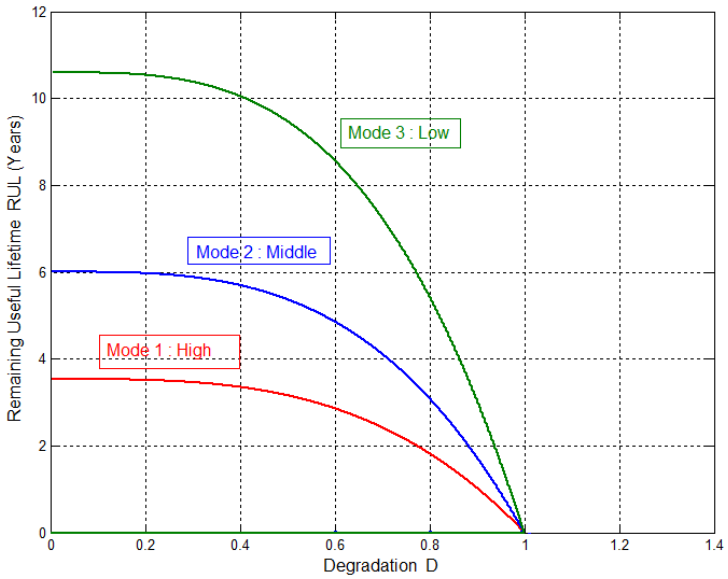

Figure 3.22 - RULs evolution for pipelines under three modes of pressure for nonlinear law case (unburied pipes).

The expected lifetimes deduced are as follows:

Mode 1: N_{C1}= 3.53 years

Mode 2: N_{C2}= 6.00 years

Mode 3: N_{C3}=10.59 years.

III.6.1.1 - Comparison with the Linear Case

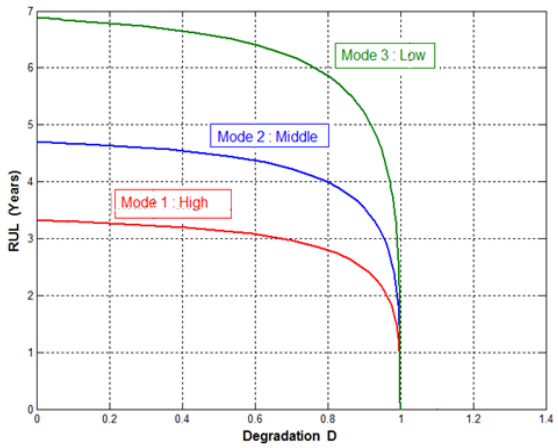

Figure 3.23 - Linear case.

N_{C1}= 3.31 years; N_{C2}= 4.68 years; N_{C3}= 6.85 years.

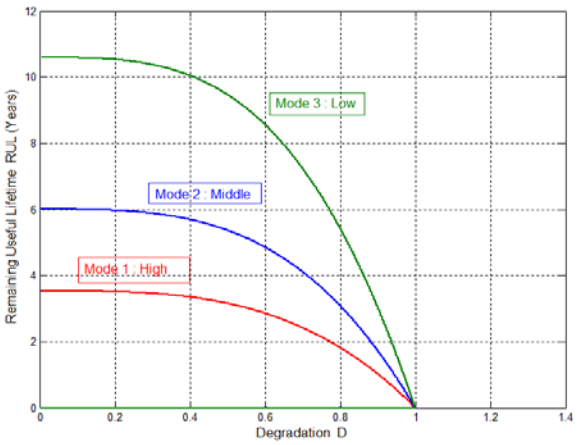

Figure 3.24 - Nonlinear case.

N_{C1}= 3.53 years; N_{C2}= 6.00 years; N_{C3}= 10.59 years.

It can be deduced from these two figures 3.23 and 3.24 that first of all the nonlinear case of damage is slightly less conservative than the linear case concerning the lifetime. Secondly, the decreasing of RULs in the nonlinear case is less acute at the end than the linear case because the nonlinear curves reach progressively the zero value.

Finally, we can remark that near the failure zone where $D = D_C = 1$ the nonlinear study seems to give here a more logical and realistic damage behavior for the different pressure values than the linear case where the curves coincide. In fact, we note in the nonlinear case a clear difference between low and high pressures when approaching failure limit whereas the linear case does not.

III.6.2 - Buried Pipe Case

In the case of buried pipes (underground), the simulations of degradation under high, middle, and low modes of internal pressure are represented respectively in figures 3.25, 3.26, and 3.27.

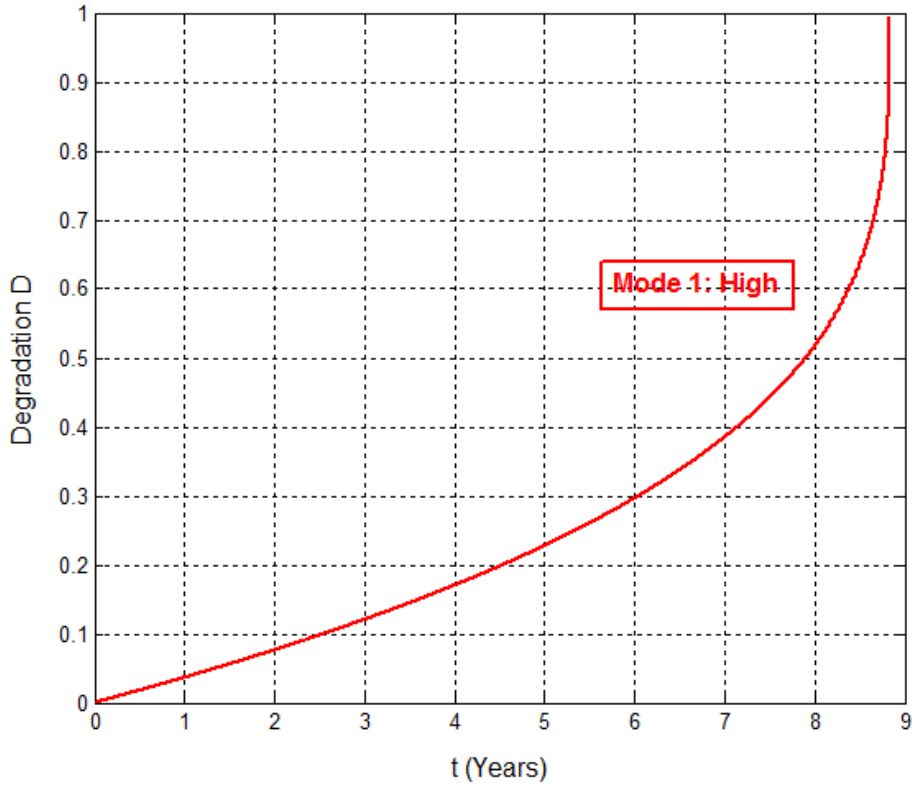

Figure 3.25 - Pipelines degradation under high mode of pressure for nonlinear law (buried pipes).

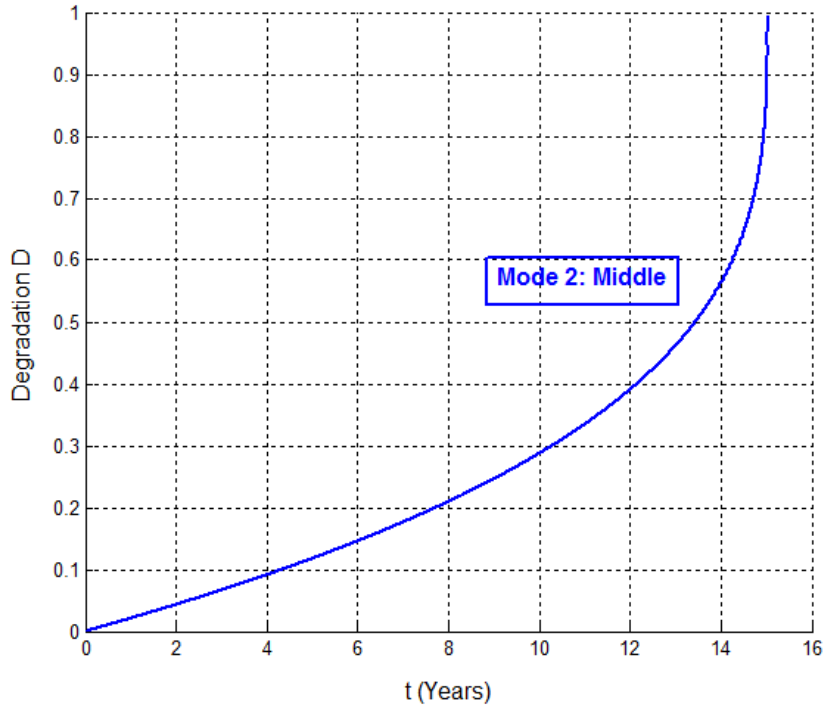

Figure 3.26 - Pipelines degradation under middle mode of pressure for nonlinear law (buried pipes).

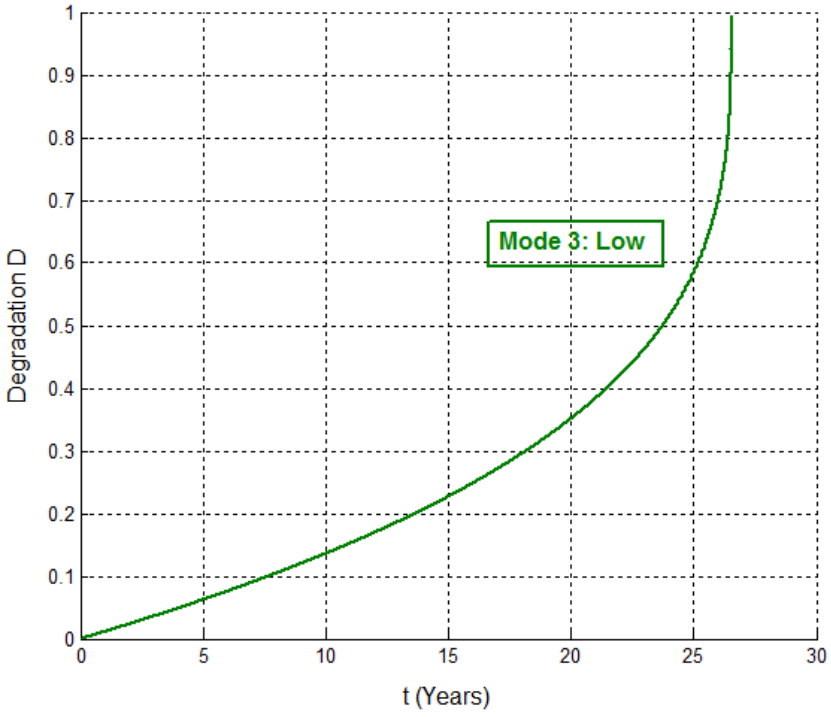

Figure 3.27 - Pipelines degradation under low mode of pressure for nonlinear law (buried pipes).

We therefore obtain the degradation evolution (figure 3.28) and the RULs evolution (figure 3.29) for each mode of internal pressure in terms of exploitation time and degradation state *D*.

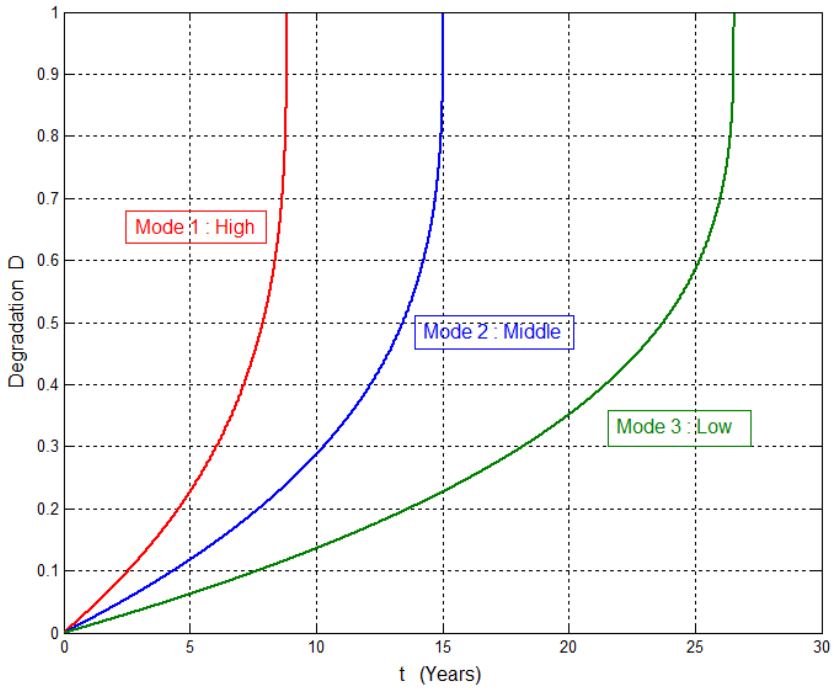

Figure 3.28 - Pipelines degradation under three modes of pressure for nonlinear law (buried pipes)

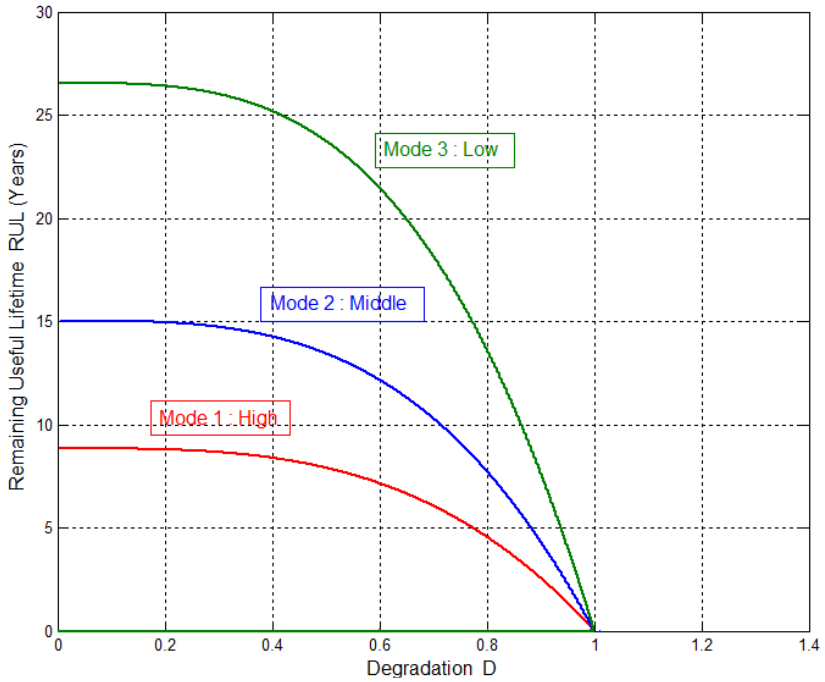

Figure 3.29 - RUL evolution for pipelines under three modes of pressure for nonlinear law (buried pipes).

The expected lifetimes deduced are as follows:

Mode 1: N_{C1} = 8.84 years

Mode 2: N_{C2} =15.03 years

Mode 3: N_{C3} =26.54 years.

III.6.2.1 - Comparison with the Linear Case

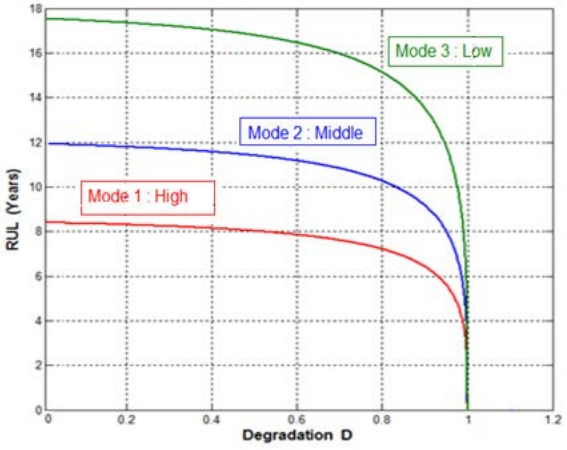

Figure 3.30 - Linear case.

N_{C1}= 8.33 years; N_{C2}= 11.87 years;
N_{C3}= 17.35 years.

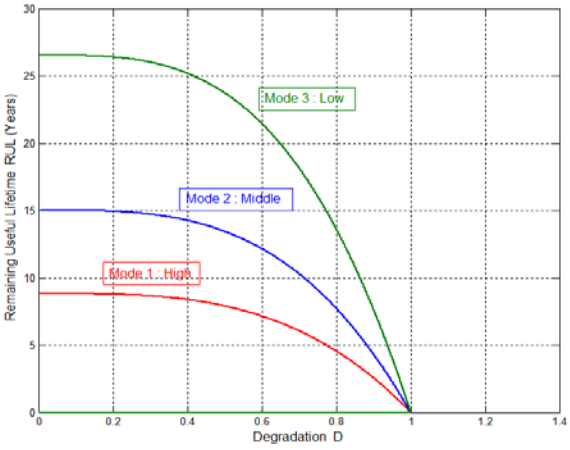

Figure 3.31 - Nonlinear case.

N_{C1}= 8.84 years; N_{C2}= 15.03 years;
N_{C3}= 26.54 years.

We can deduce from the two figures 3.30 and 3.31 that first of all the nonlinear case of damage is obviously less conservative than the linear case concerning the lifetimes. Secondly, the decreasing of RULs in the nonlinear case is less acute at the end than the linear case because the nonlinear curves reach progressively the zero value.

Finally, we can notice that near the failure zone where $D = D_C = 1$ the nonlinear study seems to give here a more logical and realistic damage behavior for the different pressure values than the linear case where the curves coincide. In fact, we note in the nonlinear case a clear difference between the different pressures when approaching failure limit whereas the linear case does not.

III.6.3 - Offshore Pipe Case

For offshore pipes (under sea water), the simulations of degradation under high, middle, and low modes of internal pressure are represented respectively in figures 3.32, 3.33, and 3.34.

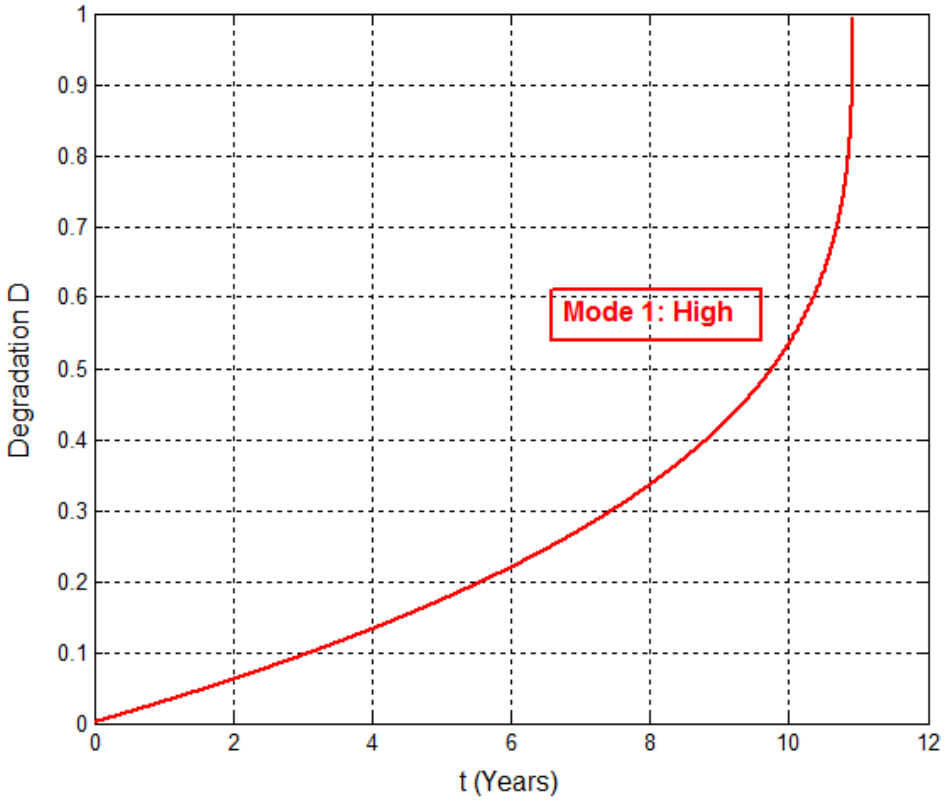

Figure 3.32 - Pipelines degradation under high mode of pressure for nonlinear law (offshore pipes).

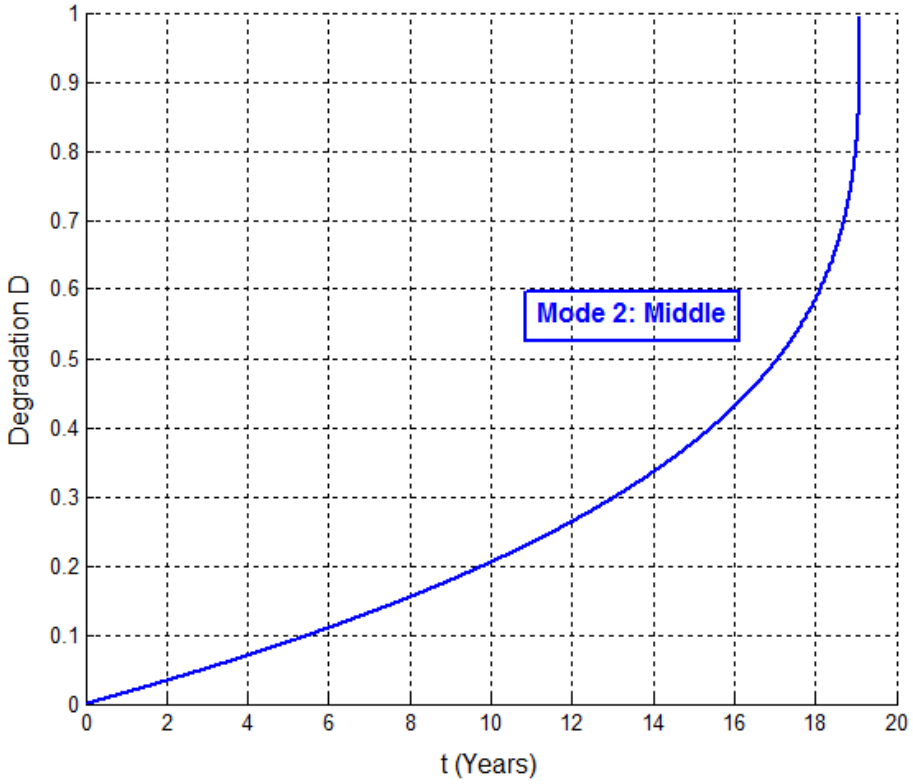

Figure 3.33 - Pipelines degradation under middle mode of pressure for nonlinear law (offshore pipes).

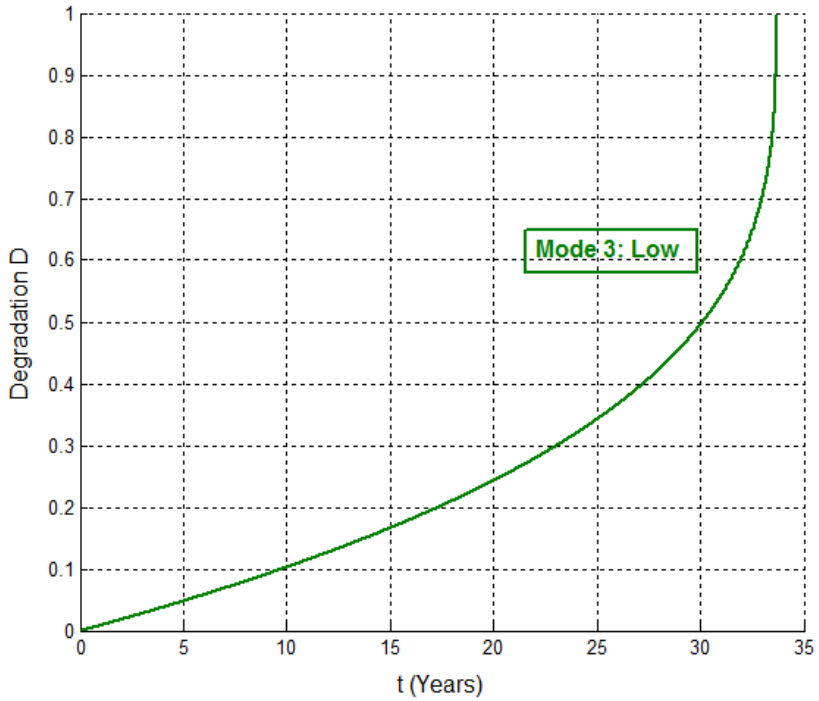

Figure 3.34 - Pipelines degradation under low mode of pressure for nonlinear law (offshore pipes).

We therefore obtain the degradation evolution (figure 3.35) and the RULs evolution (figure 3.36) for each mode of internal pressure in terms of exploitation time and degradation state *D*.

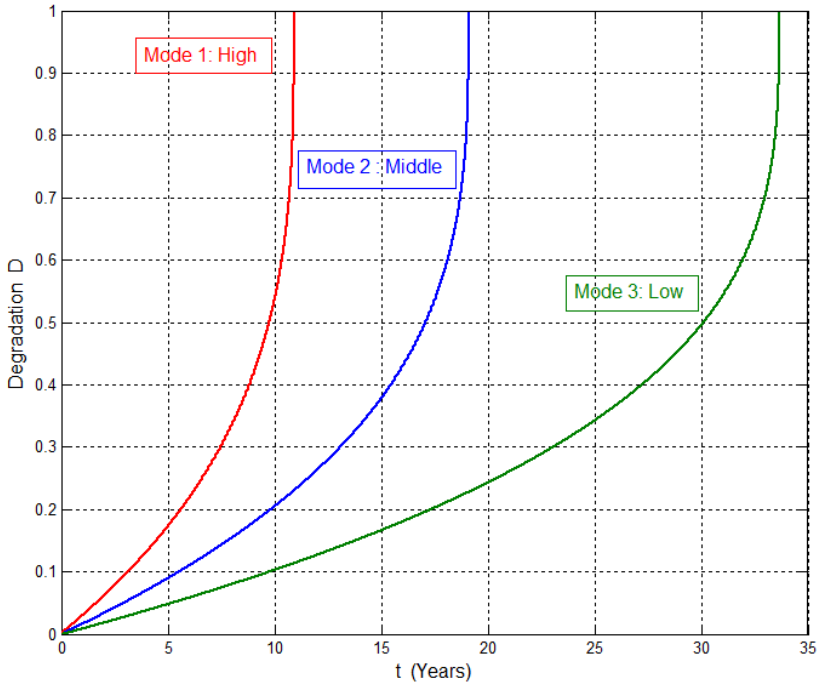

Figure 3.35 - Pipelines degradation under three modes of pressure for nonlinear law (offshore pipes).

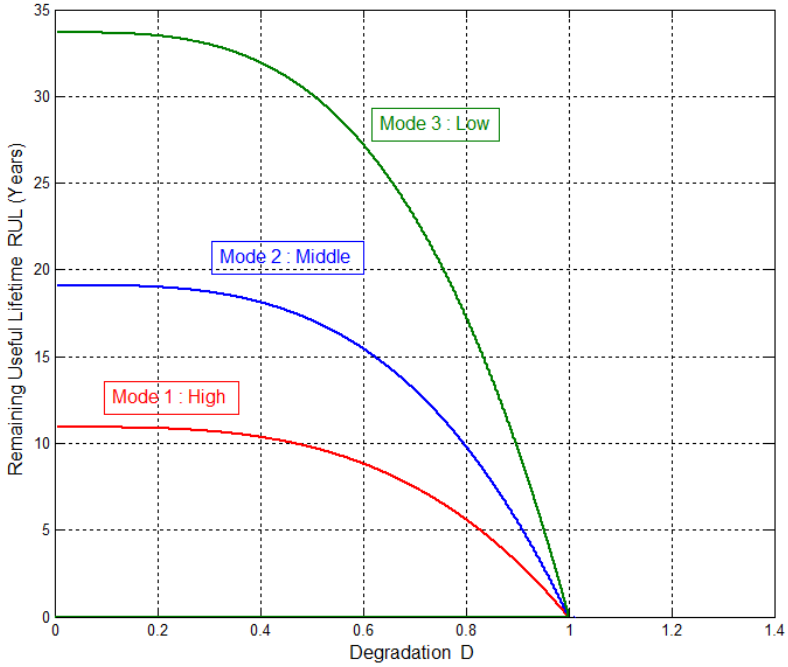

Figure 3.36 - Pipelines RUL evolution under three modes of pressure for nonlinear law (offshore pipes).

The expected lifetimes deduced are as follows:

Mode 1: N_{C1} =10.92 years

Mode 2: N_{C2} =19.11 years

Mode 3: N_{C3} =33.67 years.

III.6.3.1 - Comparison with the Linear Case

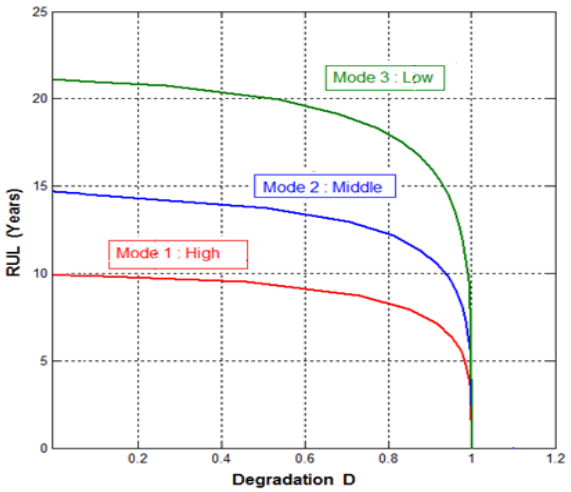

Figure 3.37 - Linear case

N_{C1}= 10.27 years; N_{C2}= 14.84 years;
N_{C3}= 21.69 years.

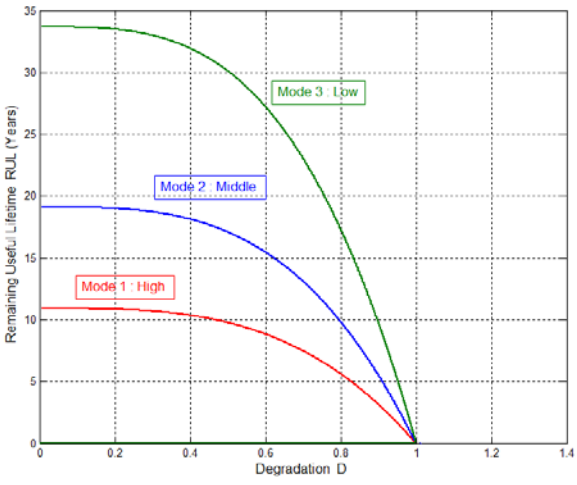

Figure 3.38 - Nonlinear case

N_{C1}= 10.92 years; N_{C2}= 19.11 years;
N_{C3}= 33.67 years.

We can deduce from these two figures 3.37 and 3.38 that, first of all, the nonlinear case of damage is undoubtedly less conservative than the linear case concerning the lifetime. Secondly, the decreasing of RULs in the nonlinear case is less steep at the end than the linear case because the nonlinear curves reach progressively the zero value.

Finally, we can notice that near the failure zone where $D = D_C = 1$ the nonlinear study seems to give here a more logical and realistic damage behavior for the different pressure values than the linear case where the curves coincide. In fact, we can see in the nonlinear case a clear difference between the different pressures when approaching failure limit whereas the linear case does not.

III.6.4 - Validation of the Pipelines Lifetimes

Referring to the references [21,22,23], the present results of pipelines nonlinear damage model are realistic when compared to those obtained by the works of these authors. In comparison with the linear model, the lifetimes in the nonlinear case are more accurate and more economic since they lead to larger maintenance intervals.

In fact, the typical lifetime of offshore pipes is 25 years on average [23] which is very close to the lifetimes' average for the offshore pipes obtained by the nonlinear simulation model:

$$\frac{10.92 \text{ years (for mode 1)} + 19.11 \text{ years (for mode 2)} + 33.67 \text{ years (for mode 3)}}{3} \approx 21.23 \text{ years}$$

.

Moreover, the design procedures for offshore pipelines are still under development which has lead to a substantial field of research that deals with a proper physical determination of the many aspects of a pipeline life cycle. In general, many different aspects before and during the life cycle of a pipeline must be considered. In fact, planning demands a great deal of considerations. During the life cycle from fabrication to abandoning the installed pipeline after years of operation, the pipeline must provide safe transportation. Therefore, in case of failure, severe environmental pollution and great economic loss may occur.

III.7 - Conclusion

In this chapter, the nonlinear aspect of damage accumulation is introduced in the developed model at the place of the linear accumulation of Miner. It allows taking into account the multiaxial loading, particularly when the loading is non-proportional, and a nonlinear interaction effect exists between LCF and HCF loading cycles.

From the resolution of a first order nonlinear ordinary differential equation relating the degradation to the number of cycles, we deduce a recursive relation between two consecutive degradation measures beside the environmental and material parameters. The deduced relation constitutes the nonlinear prognostic model.

This advanced prognostic model is applied to study the lifetime of two systems in simulation: the suspension components and the petrochemical pipelines in their three modes. The results of prognostic studies show that the nonlinear study gives a more logical and realistic damage behavior for the different loading values than the linear case. In fact, we note in the nonlinear case a clear difference between two extreme loadings when approaching failure limit whereas the linear case does not.

The nonlinear case study of suspensions shows optimistic results explained by the fact that when the real trends of degradation have a concave shape then the damage accumulation is overestimated when using a linear shape.

References

[1] M.A. MINER, “Cumulative Damage in Fatigue”, Journal of Applied Mechanics, vol. 12, A159-A164, 1945.

[2] J. LEMAITRE and R. DESMORAT, *Engineering Damage Mechanics*, Springer, 2005.

[3] Z. HASHIN and A. ROTEM, “A Cumulative Damage Theory of Fatigue Failure", Mats. Sci and Eng., 34, pp. 147-160, 1978.

[4] C. BYINGTON, M. ROEMER, G. KACPRZYNSKI, and T. GALIE, "Prognostic Enhancements to Diagnostic Systems for Improved Condition-Based Maintenance", in: Proc. of IEEE Aerospace Conference, 2002.

[5] S.S. MANSON, J.C. FRECHE, and C.R. ENSIGN, "Application of a double linear damage rule to cumulative fatigue, Lewis research center", Presented at Symposium on Crack Propagation sponsored by the American Society for Testing Materials, Atlantic City, New Jersey, June 26 to July 1, 1966.

[6] R.M. CHRISTENSEN, "A Physically Based Cumulative Damage Formalism", Lawrence Livermore National Laboratory and Stanford University, 2007.

[7] A. FATEMI and L. TANGT, Department of Mechanical, industrial and Manufacturing Engineering, The University of Toledo, Toledo, OH 43606, USA, June 1997.

[8] J. LUO, M. NAMBURU, K. PATTIPATI, L. QIAO, M. KAWAMOTO, and S. CHIGUSA, "Model-Based Prognostic Techniques", in: Proc. of IEEE Autotestcon, pp. 330-340, 2003.

[9] A. ABOU JAOUDE, K. EL-TAWIL, S. KADRY, H. NOURA, and M. OULADSINE, ”Analytic Prognostic Model for a Dynamic System”, International Review of Automatic Control (IREACO), November 2010.

[10] E. GOODIN, A. KALLMEYER, and P. KURATH, "Evaluation of Nonlinear Cumulative Damage Models for Assessing HCF/LCF Interactions in Multiaxial Loadings", Research report, University of Dayton Research Institute, 2007.

[11] J. SHIGLEY and C. MISCHKE, *Mechanical Engineering Design*, 5th ed. p. 310. McGraw-Hill, Inc., 1989.

[12] S.S. MANSON, J.C. FRECHE, and C.R. ENSIGN, "Application of a Double Linear Damage Rule to Cumulative Fatigue", ASTM STP 415, pp. 384-412, 1967.

[13] S.S. MANSON and G.R. HALFORD, "Practical Implementation of the Double Linear Damage Rule and Damage Curve Approach for Treating Cumulative Fatigue Damage", International Journal of Fatigue. vol. 17, pp. 169-192, 1981.

[14] G.R. HALFORD and S.S. MANSON, "Reexamination of Cumulative Fatigue Damage Laws", Structure Integrity and Durability of Reusable Space Propulsion Systems, NASA CP-2381, pp. 139-145, 1985.

[15] S.S. KULKARNI, L. SUN, B. MORAN, S. KRISHNASWAMY, and J.D. ACHENBACH, "A Probabilistic Method to Predict Fatigue Crack Initiation", International Journal of Fracture (2006) 137:9-17, Springer, 2006.

[16] A. ABOU JAOUDE, H. NOURA, K. EL-TAWIL, S. KADRY, and M. OULADSINE, "Analytic and Nonlinear Prognostic for Vehicle Suspension Systems", 2012 IEEE International Conference on Prognostic and Health Management (PHM 2012), Denver, Colorado, USA, June 18-21, 2012.

[17] C. SANKAVARAM *et al.*, "Model-based and data-driven prognosis of automotive and electronic systems", 5th Annual IEEE Conference on Automation Science and Engineering, Bangalore, India, August 22-25, 2009.

[18] J. WREN, "Fatigue and durability testing", Prosig Noise and Vibration Measurement Blog, May 2006.

[19] Z. HUSIN, M.M. RAHMAN, K. KADIRGAMA, M.M. NOOR, and R.A. BAKAR, "Prediction of fatigue life on lower suspension arm subjected to variable amplitude loading", National Conference in Mechanical Engineering Research and Postgraduate Studies, 2nd NCMER 2010, pp. 100-116, Malaysia, December 2010.

[20] S.M. BEDEN, S. ABDULLAH, and A.K. ARIFFIN, "Review of fatigue crack propagation models for metallic components", European Journal of Scientific Research, vol. 28, No.3, pp. 364-397, EuroJournals Publishing, Inc., 2009.

[21] C. HUANG, *Structural Health Monitoring System for Deepwater Risers with Vortex-induced Vibration: Nonlinear Modeling, Blind Identification Fatigue/Damage Estimation and Local Monitoring using Magnetic Flux Leakage,* A Thesis Submitted in Partial Fulfillment of the Requirements for the Degree Doctor of Philosophy, Mechanical Engineering and Material Science, Houston, Texas, June 2012.

[22] DNV2010, Recommended Practice Det Norske Veritas Dnv-Rp-F107, *Risk Assessment of Pipeline Protection*, October 2010.

[23] K. RUBY and P.A. HARTVIG, *Free-span Analyses of an Offshore Pipeline, Theme: Design and Analysis of Advanced/Unusual Structures*, Department of Civil Engineering, Aalborg University, 2008.

CHAPTER IV

STOCHASTIC LINEAR AND NONLINEAR ANALYTIC PROGNOSTIC MODEL

IV.1 - Introduction

In our analytical model of Chapter II, damages have been assumed to accumulate linearly (using Miner's law) even though it is unlikely to be the case of brittle material. Afterward a nonlinear cumulative damage is explored in Chapter III [1] to take into account the level and the mode of the applied constraints and influent environment that can accentuate the nonlinear aspect related to some materials behavior subject to fatigue effects.

Other reasons can disturb the prediction capacity of the model which is the fluctuations of some basic parameters; these factors can be taken into account by adopting a stochastic modeling.

In the present chapter, a stochastic analysis is introduced in addition to the previous nonlinear model in order to make it more accurate in the RUL prediction. It is done by considering some parameters as random variables [2]. Our aim is to make the model a general prognostic tool that can be capable of well predicting the RUL of a system based on an analytical linear and nonlinear damage accumulation in either deterministic or stochastic context. Knowing that the RUL can be expressed in fatigue by means of various forms like: critical crack length a_C or critical number of loading cycles N_C or material tenacity K_{IC} from which we can write various limit states or performance criteria.

IV.2 - State-of-the-Art: Stochastic Fatigue Modeling

There is a significant interest in improving our understanding of fatigue related damage and prediction of the useful residual life of components experiencing fatigue damage. One of the principal tools for modeling fatigue damage is linear elastic fracture mechanics, and the resulting models have facilitated the design of fatigue resistant mechanical and aerospace structural components [3]. Decision tools for failure prognostics must have the capability to incorporate material damage under both normal and peak operating conditions [3,4].

The science and technology of prognosis and structural health management offer the potential for significant enhancements in the safety, reliability and availability of high-value resources [5,6]. This concept is based on a closed-loop process whose successful

implementation depends on the integration of several multi-disciplinary elements including [7]:

1) Onboard sensing of operational parameters and material damage states;
2) Diagnosing trends, fault conditions, and underlying damage;
3) Predicting remaining useful life in terms of probability of failure and limits on reliable performance;
4) And deciding upon appropriate courses of action: whenever or not the resource is capable of performing a given mission, or alternatively, is in need of inspection, maintenance, or replacement.

Considerable uncertainty exists in the usage and sensor inputs, as well as the required modeling and associated material property inputs. Consequently, there is an inherent need for the reasoning element of the prognosis system to be probabilistically-based.

Complementing the variety of onboard sensors are traditional health monitoring software tools for pattern recognition, neural networks, Bayesian updating, expert systems, and fuzzy logic. The advantage of these tools is that, when properly applied, they are highly efficient and thus amenable to onboard monitoring and real-time data fusion and interpolation. However, the disadvantage of these tools is that they rarely involve consideration of the underlying physical processes. Consequently, they require considerable empirical calibration or "training" for each specific application of interest.

In contrast, probabilistic life prediction is typically based on material property data, finite element thermal and stress analysis, pre-service inspection and in-service monitoring for defects, and damage accumulation algorithms. The advantage of this approach is that it is more amenable to linkage with the underlying physical mechanisms of damage (i.e., crack nucleation and growth). Thus, the process is inherently suitable for extension into materials prognosis, a novel concept that seeks to combine information on the material damage state with mechanistically-based predictive models.

The fundamental goal of all of these approaches is to facilitate better-informed decisions — whether for mission planning in the field (over the short term), or sustainment at the depot (over the longer term). In fact, the optimum prognosis system is likely to be some

combination of traditional data-driven methods and probabilistic mechanics methods. Thus, in many respects the above tools can be viewed as being complementary.

Probabilistic analyses of prognostic uncertainty were performed using a probabilistic life prediction code DARWIN [8,9] as a demonstration platform. DARWIN integrates finite-element stress analysis results, fracture-mechanics-based life assessment for low-cycle fatigue, material anomaly data, probability of anomaly detection, and inspection/monitoring schedules to determine the probability-of-fracture of rotor disks as a function of operating cycles.

In the study on lives of turbine engines [7], enhancements were added to the DARWIN code to enable the type of analyses required for prognosis:

1) Establishment of interface with engine sensor data;
2) Adding of the fatigue crack initiation analysis to existing fatigue crack propagation analysis;
3) Incorporates the integration of crack initiation and propagation algorithms; including correlation effects between the two damage processes;
4) Adding a damage-based load filtering method to reduce computational time;
5) Capability to analyze a large number of inspections (or interrogation — up to once per flight cycle) to simulate continuous monitoring with an on-board sensor.

Although DARWIN contains several probabilistic solutions methods, the analyses in reference to [7] were performed using Monte Carlo simulation.

Other models have been proposed to describe the random behavior of fatigue crack growth in metals. In Yang and Manning's stochastic model [10,11], a simple second order approximation of a deterministic crack growth model is used with a random component. An experimental study was conducted by Wu and Ni [12,13] using this concept, which confirmed the practical applications of Yang and Manning's model. Other applicable models based on discrete continuous random processes were proposed by Sobczyk and Spencer [14]. Bogdanoff and Kozin [15,16] explored the Markov chain theory and utilized it to create discrete and continuous fatigue crack growth models. In earlier studies, Lin proposed a Fokker-Planck equation that relates the continuous Markov process [17].

The Yang and Manning model is used in reference [18] to analyze the variable type loading because of its versatile functionality. This model utilizes only the crack growth rate and crack length data; the information about loading and material is not employed into the model and is accounted for in the random component and model parameters.

For instance, with transitional loading the model parameters will vary as the fatigue damage propagates. The model parameter variability was taken into account in the data driven part of the analytical crack exceedance probability, which is the probability that the crack length will exceed a number of cycles, with the respective load period. To directly account for the variance in the crack growth rate, the random component is assumed to follow a lognormal distribution [19,20,21].

A significant part of main pipelines are subjected to external cracking, which is a serious problem for the pipeline industry like, for example, in Russia [22], in U.S., and in Canada [23]. Identification of external cracks is achieved using different Nondestructive Evaluation (NDE) methods. If cracks are revealed during inspection, their influence on the remaining life (RUL) of the pipeline should be assessed in order to choose what maintenance action should be used: do nothing/repair/replace.

Pipeline integrity is assessed on the assumption that some defects after In-Line Inspection (ILI) may be: still undetected; detected, but not measured; detected and measured. It is possible to update the stochastic remnant life of pipelines using the data available due to ILI.

A robust pipeline failure model is needed that could be used in practice. Usually pipelines demonstrate non-linear behavior of the material. Because of this, the toughness fracture criteria is used in reference [24], described by the J-integral of non-linear fracture mechanics. The J-integral is a good descriptor of crack growth. The works of Timashev [24] describe a new practical method of updating the stochastic remaining life of pipelines with defects using the latest ILI data. It describes a comprehensive algorithm for assessing pipeline remnant life taking into account the results of holistic statistical analysis of In-Line Inspection (ILI) data.

It is assumed that the pipeline segment wall has a longitudinal external crack of semi-elliptical form and is described by the J-integral. The Limit State Function (LSF) is described as the difference of the critical and current value of the J-integral. The critical crack depth is defined using the notion of fracture toughness and the J-integral approach.

IV.2.1 - Definition of the J-Integral

Consider a nonlinear elastic body containing a crack (figure 4.1).

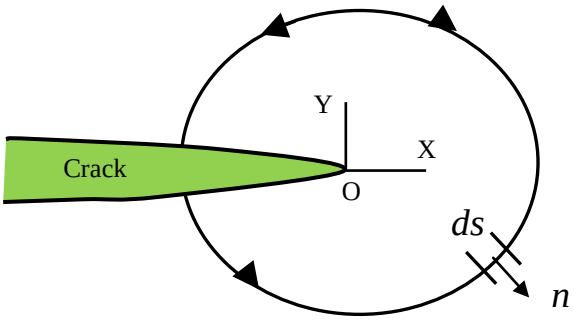

Figure 4.1 - Nonlinear elastic body with a crack.

The J-integral is defined as:

$$J = \int_{\Gamma} w dy - T_i \frac{\partial u_i}{\partial x} dS \tag{1}$$

Where $w = \int_0^{\varepsilon_{ij}} \sigma_{ij} d\varepsilon_{ij}$ is the strain energy density, $T_i = \sigma_{ij} n_j$ is the traction vector, Γ is an arbitrary contour around the tip of the crack, n is the unit vector normal to Γ ; σ, ε, and u are the stress, strain, and displacement field, respectively.

The defined J-integral is a *path-independent* line integral and it represents the *strain energy release rate of nonlinear elastic materials*:

$$J \equiv -\frac{d\Pi}{dA} \tag{2}$$

Where $\Pi = U - W$ is the potential energy, the strain energy U stored in the body minus the work W done by external forces and A is the crack area.

The probability of failure assessment algorithm is based on the Adaptive Important Sampling (AIS) procedure. Finally, the results of the latest ILI are fused into the algorithm, providing best possible assessment of pipeline remnant life as a random variable.

The remaining life update for pipeline segment with crack-like defects using ILI data takes into account three possible outcomes: defect not discovered: defect is discovered but not measured; defect is discovered and measured. This result permits solving most important problems of pipeline maintenance: prioritization of pipeline segments for repair/rehabilitation; optimization of the time between ILI; minimization of pipe operational risk.

Model-based prognostic techniques rely on a dynamic model of the predicted process. This approach uses a mathematical model of the process in order to implement the physical understanding of the system into the diagnostic problem. Such models should describe both nominal and faulty behavior of the system. As a result, it is possible to explain the fault progress in time, and to make End of Life (EOL) and RUL predictions.

These methods involve the estimation of residuals as a deviation between the real system measurements and proposed model outputs. In the ideal case, the residuals are zero but in reality there are permanent noise and modeling errors. It is, therefore, expected that the residuals are small in the nominal working mode and larger in the presence of a failure. Once the residuals are obtained, it is possible to use some statistic representation to estimate the distribution of RUL as a function of present uncertainties and to calculate possible damage.

The system modeling considered by the physics-based prognosis is derived by using physics laws and principles. Crack initiation models must include all the available information about component and its environment. The crack propagation models can be divided into two main groups: deterministic and stochastic. Deterministic crack propagation models, which usually describe the growth of the crack, are based on Paris' law [25]. Stochastic crack propagation involves models with random parameters which can be estimated using Monte Carlo simulations.

In reality, all previously mentioned parameters are affected by some probability of realization that influences the resulting RUL deduced from $D(a)$. The sampling of the basic

parameters for a large number N leads to N curves of $D(a)$ from which we can compute the mean curve $\overline{D}(a)$ and the standard deviation $\sigma(D(a))$.

Two industrial applications are considered in order to prove the efficiency of the proposed model. The evaluation of the lifetime of suspension damping systems is considered as the main part of the vehicles prognostic purpose. The main source of suspension failure is the fatigue occurrence due to the road profile fluctuations. The life prognostic of petrochemical pipelines is vital in their domain since their availability has crucial consequences. Fatigue failure is their main failure cause due to internal pressure-depression variation along time. Usually, three situations for these pipes exist: unburied, buried and under sea water (offshore pipes). Each one of these situations requires different physical parameters like: corrosion, soil pressure and friction, water and atmosphere pressure.

Hence, in the present chapter, the two main applications are treated as follows:

First of all, the prognostic study is applied to predict the lifetime of a suspension system for the cases of linear and nonlinear damage accumulation in stochastic condition where one and two random variables are considered and which are the initial crack length and the road profile.

Secondly, the prognostic study is applied to buried, unburied, and offshore pipes taking into account the linear and nonlinear damage cases and considering one and two random variables which are the initial crack length a_0 with a lognormal simulation and the internal pressure P with a triangular simulation based on three models: uniformly sampling of the instant T, one-triangular period, and multi-triangular period.

IV.3 - Stochastic Linear Damage Accumulation

To estimate the residual lifetime in fatigue failure risk, an analytical prognostic model presented in Chapter II [26,27] aims giving a RUL prediction tool, whenever analytical physical laws exist. Such physical laws are: Paris-Erdogan [25] and the linear damage accumulation of Palmgren-Miner [28] laws.

The analytical prognostic model consists of the evaluation of a normalized degradation indicator D ($0 \leq D \leq 1$) in terms of a load cycle number N. The fatigue failure is

reached when the crack size a grows to a critical size a_C with respect to Paris' law where the necessary number of cycles is the critical number N_C. Using Miner cumulative damage, after each one load cycle, the damage indicator D increases by a relative crack length increment da as indicated by the following equation:

$$D_N = \frac{1}{a_C - a_0} \sum_{j=1}^{N} da_j = \frac{a_N}{a_C - a_0} \tag{3}$$

In Chapter III, an enhancement was made on the analytical model in order to introduce the nonlinear aspect of the damage accumulation [1]. This enhancement using a nonlinear damage function $D(N)$ allows to perform a more accurate prognostic evaluation.

The deterministic Paris' law is given by the following formula: $\frac{da}{dN} = C \cdot [\Delta K(a)]^m$ and $\Delta K(a) = Y(a) \cdot \Delta\sigma \cdot \sqrt{\pi a}$;

Where,

a is the crack length,

N is the load cycle,

C and m are the material and environment parameters ($0 < C << 1$) ; ($2 \leq m \leq 4$) [29],

$\Delta K(a)$ is the stress intensity factor range,

$Y(a)$ is the geometric factor function of the body dimensions,

$\Delta\sigma$ is the applied stress range.

IV.4 - Stochastic Modeling

The stochastic modeling [30,2] aims considering some influent parameters as random variables and hence, the Paris' law becomes a stochastic crack propagation law. The diagnostic data permit to consider the initial crack length a_0 as the main random variable where the second variable is the stress loading. Many other parameters can be also considered as random and the stochastic prognostic model can be expressed by the following general function:

$$\tilde{D}(a) = P_{rog}(a) = fct(\tilde{a}_0, \text{loading } \tilde{\sigma}, \text{thickness } \tilde{e}, \text{dimensions}, \tilde{C}, \tilde{m}, ...)$$

The degradation indicator D variant from 0 to 1 gives us instantaneously the remaining useful lifetime (RUL) in terms of time, or cycle, or distance, depending on the type of the concerned device.

A probabilization of the basic parameters leads to a probabilistic trajectory $\tilde{D}(a)$. Therefore, a bundle of curves $D(a)$ is obtained for which a mean value and a standard deviation can be deduced. Hence, a characteristic curve $D_K(a)$ can be computed in terms of a fractal $\alpha\%$ that depends on the level of the acceptable risk. The characteristic RUL is then deduced from $D_K(a)$.

All previously mentioned basic parameters are affected by a some probability of realization that influences the resulting RUL deduced from $\tilde{D}(a)$. Contrary to the deterministic-based prognosis, the RULs concluded in stochastic-based prognosis are related to the probabilistic aspect.

These relevant basic parameters must be modeled stochastically using a convenient well known probability distribution laws. For example, the initial crack length a_0 can be modeled by either a normal or a lognormal distributions, the loading σ is modeled by a normal distribution.

IV.5 - Stochastic RUL

The last parameters must be modeled stochastically using convenient probability distribution laws. When this is not taken into consideration, the prognostic results may not reflect really the evaluated lifetime of a device.

The estimated RUL is then no longer deterministic, but affected by some risk percentage in order to be realized. Hence a bundle of RULs trajectories can be plotted.

Knowing that the RUL can be expressed by various forms like for example in fatigue by: crack length $a_{C\,,}$ or critical number of cycles N_C , or material tenacity K_{IC} depending on the chosen limit states: service limit state ($a \le a_C$), or lifetime limit state ($N \le N_C$), or strength limit state ($K \le K_{IC}$).The RUL adopted in this work is the lifetime limit state: N_C - N which is expressed in terms of the number of loading cycles.

IV.6 - Reliability Evaluation of Damage State

Each of the limit states cited above is a function of random variables that makes them also random functions in their turn. For this reason, they occur with a certain probability.

The evaluation of these probabilities is the main goal of this section. This can be done by many reliability methods.

The term reliability is the probabilistic evaluation of a limit state performance on a domain of basic variables. In other words, it is obtained by the computation of the failure probability toward a criterion or a limit state.

The methodology is as follows:

1) Identify the limit states that govern the lifetime of the structure.
2) Identify the basic parameters intervening in these limit states.
3) Deduce their probability density functions.
4) Compute the failure probability that quantifies the risk of non-satisfaction of these limit states.

Many types of methods exist: the Monte Carlo simulation, the approximate method FORM (First Order Reliability Method), and SORM (Second Order Reliability Method).

The Monte Carlo simulation method is based on a large number of simulations, it is a time consuming tool and we must use N simulations when we want to evaluate a probability of order of $10^{-(N+4)}$ (i.e. for a very small probability of failure, a huge simulation number is needed).

The approximate method FORM is an iterative procedure that allows calculating an index of reliability (denoted β). The index β is the distance between the origin and the limit state equation $G(t) = 0$ in a standard space. Once we have calculated β we can deduce the failure probability:

$$P_{rob} = \Phi(-\beta)$$

In FORM approximation the real limit state (usually nonlinear) is replaced by its tangent plane at a specific point called the most probable failure point (MPFP). This point is the closest point on the curve: $G(t) = 0$ from the origin.

The limit state $G(t)$ divides the space into two regions:

- First region where $G(t) > 0$ called safe region.
- And the second region where $G(t) \leq 0$ called failure region.

Other methods aim to evaluate the probability of success of performance by means of the reconstruction of the system response PDF (probability density function) under an analytic form.

In SORM approximation the real limit state (usually nonlinear) is replaced by its tangent parabola at the point MPFP which is the closest point on $G(t) = 0$ to the origin.

The limit states are the functions of performance or of satisfaction of some criteria. In our model we are interested in the criteria of a lifetime; in fatigue case the serviceability limit state is usually used.

The serviceability limit state governs the crack length $a(N)$ at cycle N, in order to be under the allowable limit a_C. This function is given by:

$$G = a_C - a(N) = a_C - a_N \tag{4}$$

The probability of failure is:

$$P_{rob}(G \leq 0) = P_{rob}(a_N \geq a_C) = \int_{a_C}^{\infty} f_N(a_N)\, da_N \tag{5}$$

The probability of success is:

$$P_{rob}(G > 0) = P_{rob}(a_N < a_C) = \int_{-\infty}^{a_C} f_N(a_N)\, da_N \tag{6}$$

With:

$$a_C = \frac{\Delta K_I^2}{Y^2(a) \cdot \pi \cdot \sigma_{\max}^2}$$

IV.7 - Stochastic Basic Parameters

IV.7.1 - Initial Crack Width a_0

The measurements of the initial crack length a_0 derived from sensors output are treated as realizations of a random variable $\tilde{a}_0$. Here we consider a Probability Density Function (PDF) for a_0 that follows a lognormal distribution (figure 4.2), then:

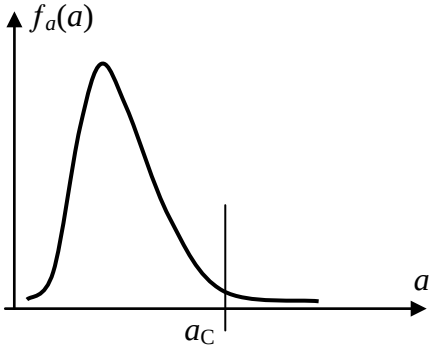

Figure 4.2 - PDF of the crack length.

$$f_0(a_0) = \frac{1}{a_0 \cdot \xi \cdot \sqrt{2\pi}} \exp\left[-\frac{1}{2 \cdot \xi^2} \left(Ln(a_0) - \lambda \right)^2 \right] \tag{7}$$

With:

ξ is the standard deviation of the variable $Ln(a_0)$ which is the equivalent normal distribution,

λ is the mean of the variable $Ln(a_0)$,

Expectation of a_0: $E(a_0) = \exp[\lambda + \xi^2 / 2]$,

Variance of a_0: $V(a_0) = \exp[2\lambda + \xi^2] \times \left(\exp[\xi^2] - 1 \right)$

Inversely, we have also:

$$\lambda = Ln\left[E(a_0)\right] - \frac{1}{2} Ln\left(1 + \frac{V(a_0)}{E(a_0)^2} \right) \tag{8}$$

$$\xi^2 = Ln\left(1 + \frac{V(a_0)}{E(a_0)^2} \right) \Rightarrow \xi = \sqrt{Ln\left(1 + \frac{V(a_0)}{E(a_0)^2} \right)} \tag{9}$$

The allowable value of the crack length (a_C) is fixed when the number of cycles reaches the critical value (N_C) (figure 4.3).

The probability of fatigue failure is given by:

$$P_{rob}(a_N > a_C) = \int_{a_C}^{\infty} f_N(a_N)\, da_N$$

Where $f_N(a_N)$ is the PDF of the crack width a_N at cycle N.

It can be assumed that $a_C = e/8$ [29], where e is the device dimension in the crack direction (figure 4.4).

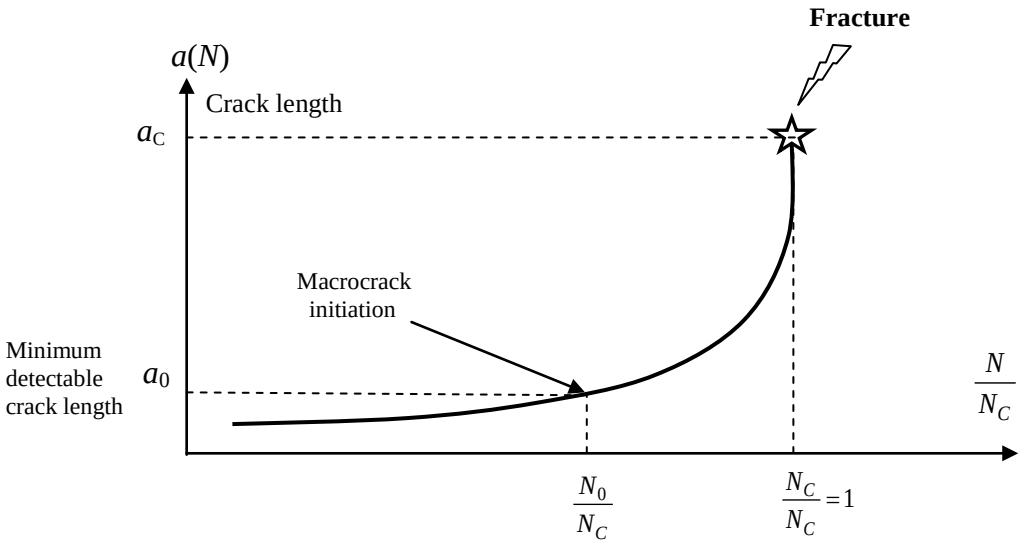

Figure 4.3 - Pre-crack fatigue damage.

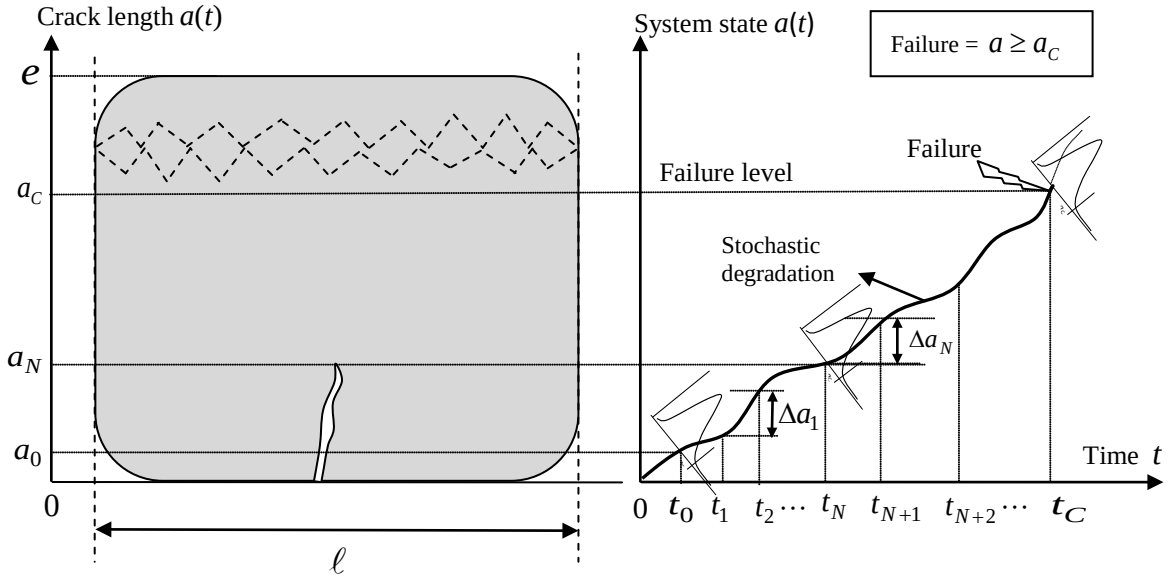

Figure 4.4 - Probabilistic crack growth.

IV.7.2 - PDF of Crack Length a_N at Loading Cycle N

Since the initial crack length a_0 is a random variable, it is expected that the crack length at cycle N is also random and is denoted by $\tilde{a}_N$.

To calculate the PDF of $\tilde{a}_N$, we proceed as follows: From Paris' law we can deduce:

$$\frac{da}{dN} = C \cdot \left[\Delta K(a)\right]^m \Rightarrow \frac{da}{\left[\Delta K(a)\right]^m} = C \cdot dN \tag{10}$$

Where, $\Delta K(a) = Y(a) \cdot \Delta\sigma \cdot \sqrt{\pi\, a}$

If we integrate the two sides between the initial state N_0 and an arbitrary state N, we get:

$$\int_{a_0}^{a_N} \frac{da}{\left[\Delta K(a)\right]^m} = \int_{N_0}^{N} C \cdot dN$$

$$\Rightarrow \int_{a_0}^{a_N} \frac{da}{\left[\Delta K(a)\right]^m} = \int_{a_0}^{a_N} \frac{da}{\left[Y(a) \cdot \Delta\sigma \cdot \sqrt{\pi\, a}\right]^m}$$

$$= \int_{a_0}^{a_N} \frac{da}{\left[Y^m \cdot (\Delta\sigma)^m \cdot \pi^{m/2} \cdot a^{m/2}\right]} = \frac{1}{Y^m \cdot (\Delta\sigma)^m \cdot \pi^{m/2}} \int_{a_0}^{a_N} \frac{da}{a^{m/2}}$$

$$= \frac{1}{Y^m \cdot (\Delta\sigma)^m \cdot \pi^{m/2}} \int_{a_0}^{a_N} a^{-m/2}.da = \frac{1}{Y^m \cdot (\Delta\sigma)^m \cdot \pi^{m/2}} \left[\frac{a^{1-m/2}}{1-m/2}\right]_{a_0}^{a_N}$$

$$= \frac{1}{Y^m \cdot (\Delta\sigma)^m \cdot \pi^{m/2}} \left[\frac{a_N^{1-m/2} - a_0^{1-m/2}}{1-m/2}\right] = C \cdot \left[N\right]_{N_0}^{N} = C \cdot \left(N - N_0\right) = C \cdot N \quad ; \quad \text{where } (N_0 = 0)$$

$$\Rightarrow \left[\frac{a_N^{1-m/2} - a_0^{1-m/2}}{1-m/2}\right] = N \cdot C \cdot Y^m \cdot (\Delta\sigma)^m \cdot \pi^{m/2}$$

$$\Rightarrow a_N^{1-m/2} - a_0^{1-m/2} = N \cdot C \cdot \left(1 - \frac{m}{2}\right) \cdot Y^m \cdot (\Delta\sigma)^m \cdot \pi^{m/2}$$

$$\Rightarrow a_N^{1-m/2} = a_0^{1-m/2} + N \cdot C \cdot \left(1 - \frac{m}{2}\right) \cdot \left(Y \cdot \Delta\sigma \cdot \sqrt{\pi}\right)^m$$

$$\Rightarrow a_N = \left[a_0^{1-m/2} + N \cdot C \cdot \left(1 - \frac{m}{2}\right) \cdot \left(Y \cdot \Delta\sigma \cdot \sqrt{\pi}\right)^m\right]^{1/(1-m/2)}$$

$$\Rightarrow a_N = \left[a_0^{1-m/2} + N \cdot C \cdot \left(1 - \frac{m}{2}\right) \cdot \left(Y \cdot \Delta\sigma \cdot \sqrt{\pi}\right)^m\right]^{\frac{2}{2-m}}$$

$$\text{and } a_0 = \left[a_N^{1-m/2} - N \cdot C \cdot \left(1 - \frac{m}{2}\right) \cdot \left(Y \cdot \Delta\sigma \cdot \sqrt{\pi}\right)^m\right]^{\frac{2}{2-m}}$$

Where Y is the geometric factor function of the body dimensions.

Then, we have the crack length a_N given by the following expression:

$$a_N = \left[a_0^{1-m/2} + N \cdot C \cdot \left(1 - \frac{m}{2}\right) \cdot \left(Y \cdot \Delta\sigma \cdot \sqrt{\pi}\right)^m \right]^{\frac{2}{2-m}} \tag{11}$$

And the initial crack length a_0 is given by the following expression:

$$a_0 = \left[a_N^{1-m/2} - N \cdot C \cdot \left(1 - \frac{m}{2}\right) \cdot \left(Y \cdot \Delta\sigma \cdot \sqrt{\pi}\right)^m \right]^{\frac{2}{2-m}} \tag{12}$$

As: $a_0 \le a_N \le a_C$,

Therefore, if we have the PDF of a_0: $f_0(a_0)$, then we can deduce the PDF of a_N: $f_N(a_N)$, and of a_C: $f_C(a_C)$, as follows:

$$f_0(a_0) \xrightarrow[Jacobian]{} f_N(a_N) \xrightarrow[Jacobian]{} f_C(a_C)$$

Initial state (N_0=0) Arbitrary state (N) Critical (final) state (N_C)

We can write the following probabilistic transformation:

$f_N(a_N) = f_0(a_0) \times |J| = f_0(a_0) \times \left| \frac{da_0}{da_N} \right|$, with the Jacobian $J = \frac{da_0}{da_N}$

and $f_0(a_0) = f_0\left(\left[a_N^{1-m/2} - N \cdot C \cdot \left(1 - \frac{m}{2}\right) \cdot \left(Y \cdot \Delta\sigma \cdot \sqrt{\pi}\right)^m \right]^{\frac{2}{2-m}} \right)$

Let $\beta = 1 - \frac{m}{2} \Rightarrow m = 2(1-\beta)$ and $\frac{m}{2-m} = \frac{1-\beta}{\beta}$ and $\frac{2}{2-m} = \frac{1}{\beta}$

$$\Rightarrow f_0(a_0) = f_0\left(\left[a_N^{\beta} - N \cdot C \cdot \beta \cdot \left(Y \cdot \Delta\sigma \cdot \sqrt{\pi}\right)^{2(1-\beta)} \right]^{\frac{1}{\beta}} \right)$$

$$\Rightarrow f_0(a_0) = f_0\left(\left[a_N^{\beta} - N \cdot A \right]^{\frac{1}{\beta}} \right)$$

Where $A = C \cdot \beta \cdot \left(Y \cdot \Delta\sigma \cdot \sqrt{\pi}\right)^{2(1-\beta)}$

Then the Jacobian J is calculated as follows:

$$\frac{da_0}{da_N} = \frac{d\left[f(a_N)\right]}{da_N} = \frac{d}{da_N}\left[\left[a_N^{\beta} - N \cdot C \cdot \beta \cdot \left(Y \cdot \Delta\sigma \cdot \sqrt{\pi}\right)^{2(1-\beta)} \right]^{\frac{1}{\beta}} \right]$$

$$= \frac{1}{\beta}\left[a_N^{\beta} - N \cdot C \cdot \beta \cdot \left(Y \cdot \Delta\sigma \cdot \sqrt{\pi}\right)^{2(1-\beta)} \right]^{\frac{1}{\beta}-1} \times \frac{d}{da_N}\left[a_N^{\beta} - N \cdot C \cdot \beta \cdot \left(Y \cdot \Delta\sigma \cdot \sqrt{\pi}\right)^{2(1-\beta)} \right]$$

$$= \frac{1}{\beta}\left[a_N^{\beta} - N \cdot C \cdot \beta \cdot \left(Y \cdot \Delta\sigma \cdot \sqrt{\pi}\right)^{2(1-\beta)} \right]^{\frac{1-\beta}{\beta}} \times \left[\beta \cdot a_N^{\beta-1} - 0 \right] = a_N^{\beta-1} \times \left[a_N^{\beta} - N \cdot C \cdot \beta \cdot \left(Y \cdot \Delta\sigma \cdot \sqrt{\pi}\right)^{2(1-\beta)} \right]^{\frac{1-\beta}{\beta}}$$

$$\Rightarrow \frac{da_0}{da_N} = a_N^{\beta-1} \times \left[a_N^{\beta} - N \cdot A\right]^{\frac{1-\beta}{\beta}}$$

Since $f_N(a_N) = f_0(a_0) \times \left|\frac{da_0}{da_N}\right|$

Then the PDF of a_N is given as follows:

$$f_N(a_N) = f_0\left(\left[a_N^{\beta} - N \cdot A\right]^{\frac{1}{\beta}}\right) \times \left|a_N^{(\beta-1)} \cdot \left[a_N^{\beta} - N \cdot A\right]^{\frac{1-\beta}{\beta}}\right| \quad (13)$$

IV.7.3 - PDF of the Initial Damage D_0

We have the relation between the initial crack length a_0 and the initial damage D_0 as follows:

$$D_0 = \frac{a_0}{a_C - a_0} \Rightarrow a_0 = \frac{a_C D_0}{1 + D_0}$$

The probabilistic transformation theory gives:

$$f(D_0) = f(a_0) \times \left|\frac{da_0}{dD_0}\right| \quad , \quad \text{As:} \quad \frac{da_0}{dD_0} = \frac{a_C}{(1+D_0)^2} \geq 0 \quad \Rightarrow f(D_0) = f(a_0) \times \frac{a_C}{(1+D_0)^2}$$

If the proposed law for a_0 is lognormal, then the law of D_0 is also lognormal with the following PDF function:

$$f(D_0) = \frac{1}{a_0 \cdot \xi \cdot \sqrt{2\pi}} \exp\left[-\frac{1}{2 \cdot \xi^2}\left(Ln(a_0) - \lambda\right)^2\right] \times \frac{a_C}{(1+D_0)^2}$$

As $a_0 = \frac{a_C D_0}{1+D_0}$ and $a_C = \frac{e}{8}$;

Then we can write the PDF as follows:

$$f(D_0) = \frac{1}{\xi\sqrt{2\pi}} \exp\left[-\frac{1}{2 \cdot \xi^2}\left(Ln\left[\frac{e \cdot D_0}{8(1+D_0)}\right] - \lambda\right)^2\right] \times \frac{1}{D_0(1+D_0)} \quad (14)$$

After that we have determined the PDF of a_N which is $f_N(a_N)$ (equation 13), we can calculate the probability of failure by the following serviceability criterion: $a_C < a_N$.

IV.8 - Equation of the Stochastic-Based Prognostic

The stress range in fatigue is governed by the Wöhler's curve (figure 4.5). The transversal crack is critical when it is normal to the stress loading range Δσ (figure 4.6).

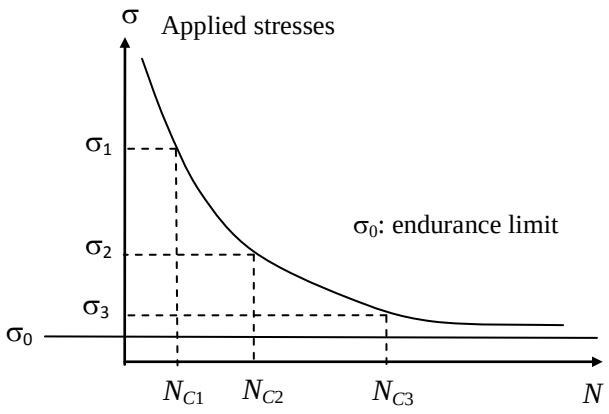

Figure 4.5 - Wöhler's curve of fatigue.

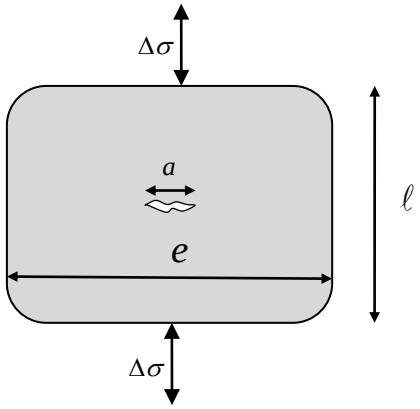

Figure 4.6 - Critical crack length *a* perpendicular to stress loading.

The degradation evolution in terms of the basic variables is the following stochastic recursive relation [30]:

$$\tilde{D}_N(\tilde{a}_N) = \tilde{D}_{N-1}(\tilde{a}_{N-1}) + d\tilde{D}_N(\tilde{a}_N) \qquad (15)$$

Where $d\tilde{D}_N$ is the probabilized damage increment at the end of each loading cycle *N*.

IV.8.1 - Development of $d\tilde{D}_N$

We have from Paris' law:

$$\frac{da_N}{dN} = C \cdot [\Delta K(a_N)]^m \Rightarrow \frac{da_N}{[\Delta K(a_N)]^m} = C \cdot dN \quad ; \quad \text{as } \Delta K(a_N) = Y(a_N) \cdot \Delta\sigma_j \cdot \sqrt{\pi\, a_N}$$

$$\Rightarrow \frac{da_N}{\left[Y(a_N) \cdot \Delta\sigma_j \cdot \sqrt{\pi\, a_N}\right]^m} = C \cdot dN$$

As: $da_N = dD_N \times (a_C - a_0)$ and for $dN = 1$ (at the end of each one cycle)

$$\Rightarrow \frac{dD_N(a_C - a_0)}{\left[Y(a_N) \cdot \Delta\sigma_j \cdot \sqrt{\pi\, a_N}\right]^m} = C \times 1 \quad \Rightarrow dD_N = \frac{C}{a_C - a_0}\left(Y(a_N) \cdot \sqrt{\pi\, a_N} \cdot \Delta\sigma_j\right)^m$$

For a stochastic initial crack length $\tilde{a}_0$, the probabilized damage increment is given under the following stochastic form:

$$d\tilde{D}_N(\tilde{a}_N) = \frac{C}{a_C - \tilde{a}_0}\left(Y(\tilde{a}_N)\cdot\sqrt{\pi\,\tilde{a}_N}\cdot\Delta\tilde{\sigma}_j\right)^m \tag{16}$$

Where it is assumed that: $a_C = e/8$ and $1.01 \le e/a \le 10$.

From equations (15) and (16), the prognostic model under the linear stochastic condition can be written as follows:

$$\tilde{D}_N(\tilde{a}_N) = \tilde{D}_{N-1}(\tilde{a}_{N-1}) + d\tilde{D}_N(\tilde{a}_N) = \tilde{D}_{N-1}(\tilde{a}_{N-1}) + \frac{C}{a_C - \tilde{a}_0}\left(Y(\tilde{a}_N)\cdot\sqrt{\pi\,\tilde{a}_N}\cdot\Delta\tilde{\sigma}_j\right)^m \tag{17}$$

The previous relation describes the degradation evolution in terms of the following random variables: initial crack size $\tilde{a}_0$, loading $\Delta\tilde{\sigma}_j$, and the current crack size $\tilde{a}_N$. This relation represents the stochastic recursive prognostic model as it permits to relate the degradation indicator $\tilde{D}_N$ to the basic random variables.

At each loading cycle ($0 \le N \le N_C$), the degradation indicator D_N increments of a quantity dD_N starting from $D_0 = 0$ till reaching the unit value ($D_C = 1$) which is the failure state. Equation (17) gives the realization of the stochastic degradation at cycle N.

The parameters C and m are the variables with the environment and the material properties, these parameters can also be taken as random variables.

IV.8.2 - Development of $d\tilde{a}_N$

Inversely, in terms of crack width, the degradation can be expressed by the crack length increment at the end of each one loading cycle ($dN = 1$) by the following recursive relation:

$$\begin{aligned} d\tilde{a}_N &= C\cdot\left(Y(\tilde{a}_N)\cdot\sqrt{\pi\,\tilde{a}_N}\cdot\Delta\tilde{\sigma}_j\right)^m \\ \tilde{a}_N &= \tilde{a}_{N-1} + d\tilde{a}_N = \tilde{a}_{N-1} + C\cdot\left(Y(\tilde{a}_N)\cdot\sqrt{\pi\,\tilde{a}_N}\cdot\Delta\tilde{\sigma}_j\right)^m \end{aligned} \tag{18}$$

In the following sections, we will apply the proposed prognostic model (equations 17 and 18) to industrial systems like vehicle suspensions and petrochemical pipelines.

IV.9 - Flowchart of the Stochastic-Based Linear Prognostic

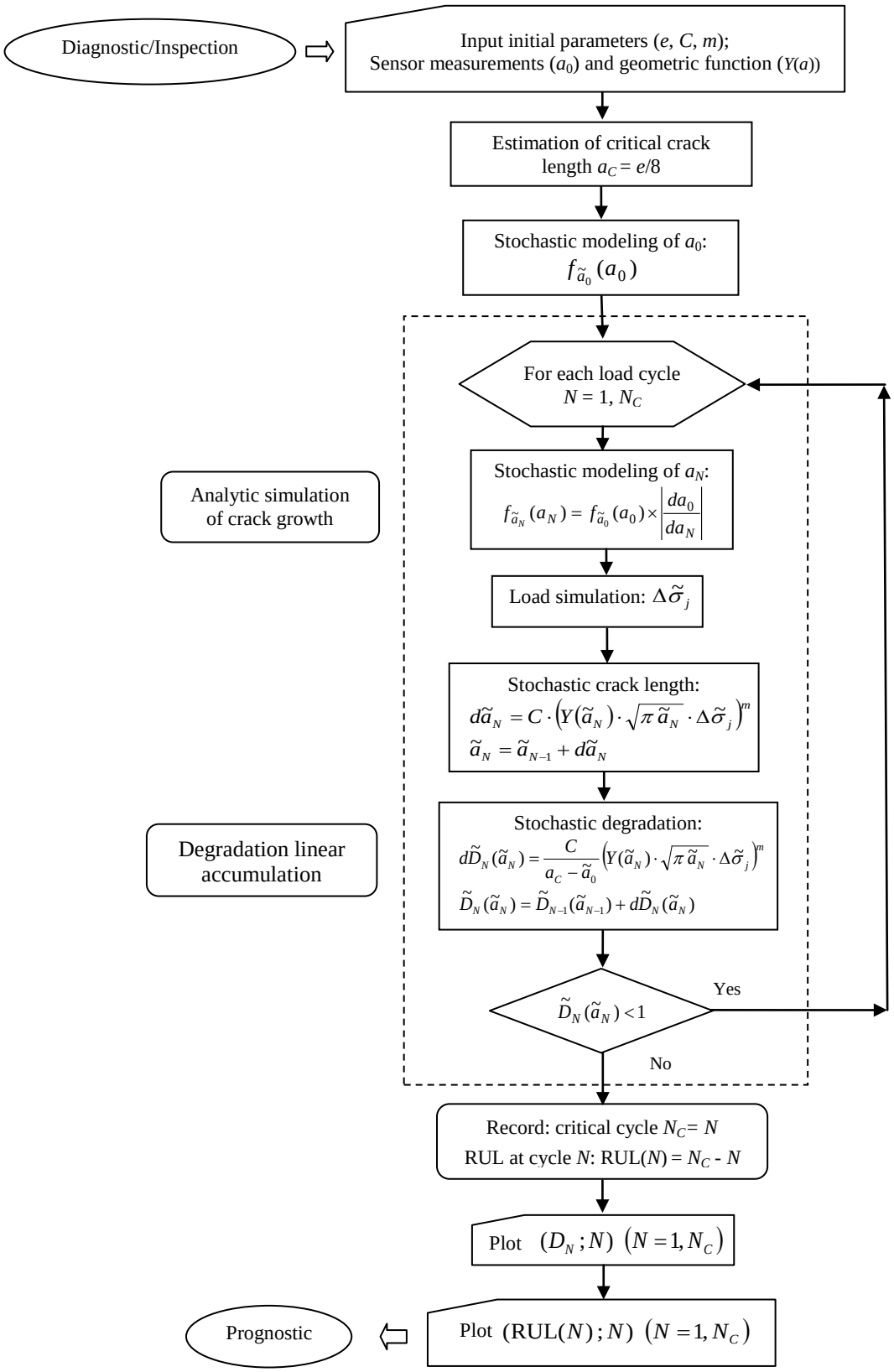

IV.10 - Application to the Suspension System

Referring to Chapter II, the same automotive suspension system is taken in this section as an industrial application. Two kinds of parameters are present in this application, deterministic parameters and random parameters.

The two random variables in this application are the initial crack length a_0 and the road profile variation Δx that creates a range of stresses $\Delta\sigma$.

Consider the statistical lognormal parameters of the initial crack length a_0 which are presented as follows:

Mean value (or expectation): $E(a_0) = 0.2 \text{ mm}$

Standard Deviation and Variance:

$$\sigma(a_0) = 0.002945 \text{ mm} \Rightarrow V(a_0) = \sigma^2(a_0) = (0.002945)^2 = 8.673\times10^{-6} \text{ mm}^2$$

And the statistical parameters of the initial damage D_0 can be deduced as follows:

Mean value (or expectation): $E(D_0) = E\left(\frac{a_0}{a_c - a_0}\right) \approx \frac{E(a_0)}{a_c - E(a_0)} = \frac{0.2}{200/8 - 0.2} = 0.008$

Variance:

$$V(D_0) = V\left(\frac{a_0}{a_c - a_0}\right) = \left(\frac{E(a_0)}{E(a_c - a_0)}\right)^2 \left[\frac{V(a_0)}{E(a_0)^2} + \frac{V(a_c - a_0)}{E(a_c - a_0)^2} - 2.\frac{COV(a_0,(a_c - a_0))}{E(a_0).E(a_c - a_0)}\right]$$

$$= \left(\frac{0.2}{200/8 - 0.2}\right)^2 \left[\frac{8.673\times10^{-6}}{0.2^2} + \frac{8.673\times10^{-6}}{(200/8 - 0.2)^2} - 2.\frac{COV(a_0,(a_c - a_0))}{E(a_0).E(a_c - a_0)}\right]$$

$$\text{Note}: COV(X,Y) = E(X.Y) - E(X).E(Y)$$

$$E(a_0^2) = COV(a_0, a_0) + [E(a_0)]^2 = V(a_0) + [E(a_0)]^2$$

$$\Rightarrow COV(a_0,(a_c - a_0)) = -V(a_0) = -8.673\times10^{-6}$$

$$\Rightarrow V(D_0) = \left(\frac{0.2}{200/8 - 0.2}\right)^2 \left[\frac{8.673\times10^{-6}}{0.2^2} + \frac{8.673\times10^{-6}}{(200/8 - 0.2)^2} + 2.\frac{8.673\times10^{-6}}{0.2.(200/8 - 0.2)}\right]$$

$$= 0.00065 \times \left[2.16825\times10^{-4} + 1.41\times10^{-8} + 3.497\times10^{-6}\right] = 1.432\times10^{-7}$$

$$\Rightarrow \sigma(D_0) = \sqrt{V(D_0)} = \sqrt{1.432\times10^{-7}} = 3.784\times10^{-4}$$

Moreover, the equivalent normal parameters of a_0 are deduced as follows:

$$\lambda = Ln[E(a_0)] - \frac{1}{2}Ln\left(1+\frac{V(a_0)}{E(a_0)^2}\right) = Ln(0.2) - 0.5Ln\left(1+\frac{8.673\times10^{-6}}{0.04}\right)$$

$$= -1.6094 - 0.5\times 2.168\times10^{-4} = -1.6095\,\text{mm}$$

$$\xi^2 = Ln\left(1+\frac{V(a_0)}{E(a_0)^2}\right) \Rightarrow \xi = \sqrt{Ln\left(1+\frac{V(a_0)}{E(a_0)^2}\right)} = \sqrt{Ln\left(1+\frac{8.673\times10^{-6}}{0.04}\right)}$$

$$= \sqrt{2.168\times10^{-4}} = 0.014724\,\text{mm}$$

The stress range in the suspension in terms of the road profile range is simplified by the following expression:

$$\Delta\sigma_j = E\times\frac{\Delta x_j}{\ell} \tag{19}$$

Where,

ℓ : is the length of the suspension device (ℓ = 500 mm)

Δx_j : is the variation of this length (dilation) under profile excitation (see table 4.1).

E: is the Young's modulus of the suspension material (*E* = 200 GPa).

We study two cases: the case of one random variable $\left(\Delta\tilde{x}_j\right)$ and the case of two random variables which are the $\left(\Delta\tilde{x}_j\right)$ and the initial damage $\left(\tilde{a}_0\right)$.

IV.10.1 - Linear Stochastic Case

This case is treated for one random variable and two random variables.

IV.10.1.1 - One Random Variable

We consider here the case of a linear damage (Miner's law) with one stochastic parameter $\left(\Delta\tilde{x}_j\right)$ normally distributed from which we deduce the parameters of the applied stress range $\left(\Delta\tilde{\sigma}_j\right)$ as follows:

$$\Delta\tilde{\sigma}: \text{Normal Law}\begin{cases} E(\Delta\tilde{\sigma}_j) = \dfrac{E}{\ell}\times\Delta\bar{x}_j & \text{(for each mode of road profile)} \\ V(\Delta\tilde{\sigma}_j) = \left(\dfrac{E}{\ell}\right)^2\times V\left(\Delta\tilde{x}_j\right) \end{cases}$$

The statistical parameters for each mode of road profile are summarized in table 4.1 below.

Table 4.1 - Statistical characteristics of each mode of roads profile.

Road Mode	Mean of $\Delta\tilde{x}_j$ ($\Delta\bar{x}_j$ in mm)	Coefficient of Variation of $\Delta\tilde{x}_j$ (in %)	Standard Deviation $\sigma(\Delta\tilde{x}_j)$ (in mm)	Law
Severe (mode 1)	100	15%	15	Normal
Fair (mode 2)	50	10%	5	Normal
Good (mode 3)	25	5%	1.25	Normal

From the simulation of the stochastic prognostic model proposed under equation (17), the degradations evolution of the suspension is obtained and presented in figure 4.7 below.

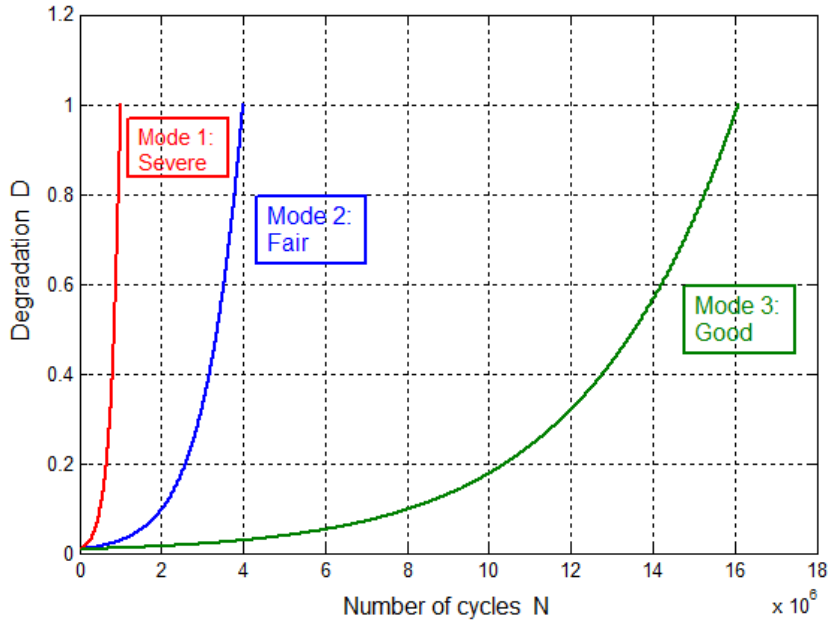

Figure 4.7 - Suspension degradation under linear damage law and stochastic road excitations.

The lifetimes noted from figure 4.7 are as follows:

Mode 1: 1,010,000 cycles.

Mode 2: 3,995,000 cycles.

Mode 3: 16,092,500 cycles.

IV.10.1.1.1 - Conversion of Lifetimes into Years

To convert the suspension lifetime into years' unit, assume that a new road profile realization occurs each 2 seconds. If we assume also that the suspension time usage is 10% of

a day (2.4 hours/day) then the expected lifetimes' durations are (refer to Chapter II, Paragraph 3.1.10):

$$\text{For mode 1 : } \frac{1{,}010{,}000(\text{cycles})\times 2(\text{s})}{60(\text{s})\times 60(\text{min})\times 2.4(\text{hours})\times 365(\text{days})} = 0.64 \text{ years}$$

$$\text{For mode 2 : } \frac{3{,}995{,}000(\text{cycles})\times 2(\text{s})}{60(\text{s})\times 60(\text{min})\times 2.4(\text{hours})\times 365(\text{days})} = 2.53 \text{ years}$$

$$\text{For mode 3 : } \frac{16{,}092{,}000(\text{cycles})\times 2(\text{s})}{60(\text{s})\times 60(\text{min})\times 2.4(\text{hours})\times 365(\text{days})} = 10.21 \text{ years}$$

IV.10.1.2 - Two Random Variables

In this section, two stochastic parameters are considered for the linear case of damage accumulation and which are the following:

1) The road excitation effect :

$$\Delta\tilde{\sigma} : \text{Normal Law} \begin{cases} E(\Delta\tilde{\sigma}_j) = \dfrac{E}{\ell}\times\Delta\bar{x}_j \qquad \text{(for each mode of road profile)} \\ V(\Delta\tilde{\sigma}_j) = \left(\dfrac{E}{\ell}\right)^2 \times V\left(\Delta\tilde{x}_j\right) \end{cases}$$

2) The initial crack length :

$$\tilde{a}_0 : \text{Lognormal Law} \begin{cases} E(\tilde{a}_0) = 0.2 \text{ mm} \\ V(\tilde{a}_0) = 8.673\times 10^{-6} \text{ mm}^2 \quad \Rightarrow \sigma(\tilde{a}_0) = \sqrt{V(\tilde{a}_0)} = 0.002945 \text{ mm} \end{cases}$$

The parameters of the road profiles $\left(\Delta\tilde{x}_j\right)$ are given in table 4.1.

The results of degradations evolution of the suspension are presented in figures 4.8 and 4.9 below.

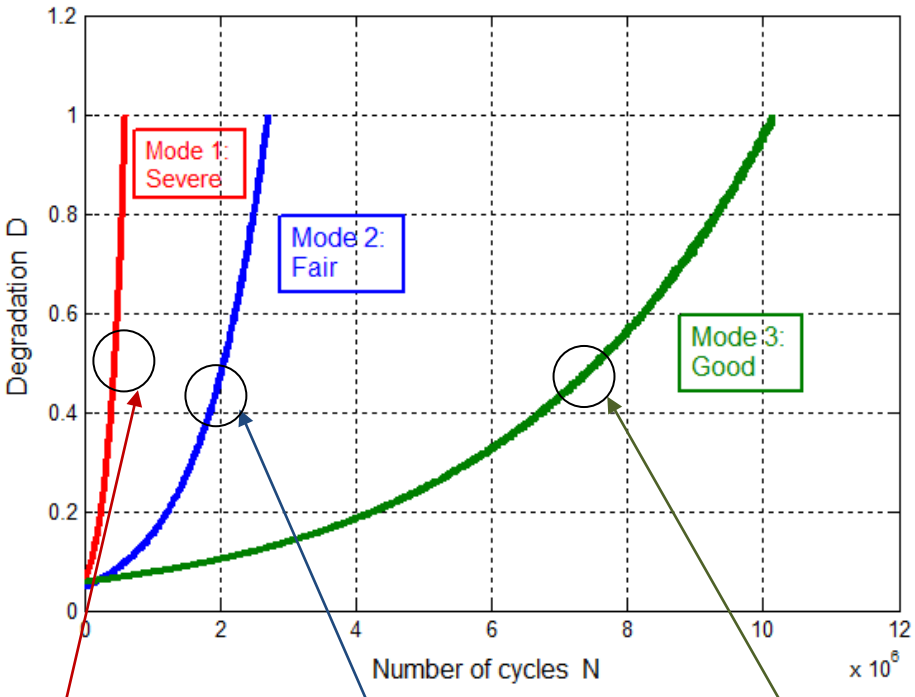

Figure 4.8 - Suspension degradation under linear law of damage and stochastic road excitations and initial crack width.

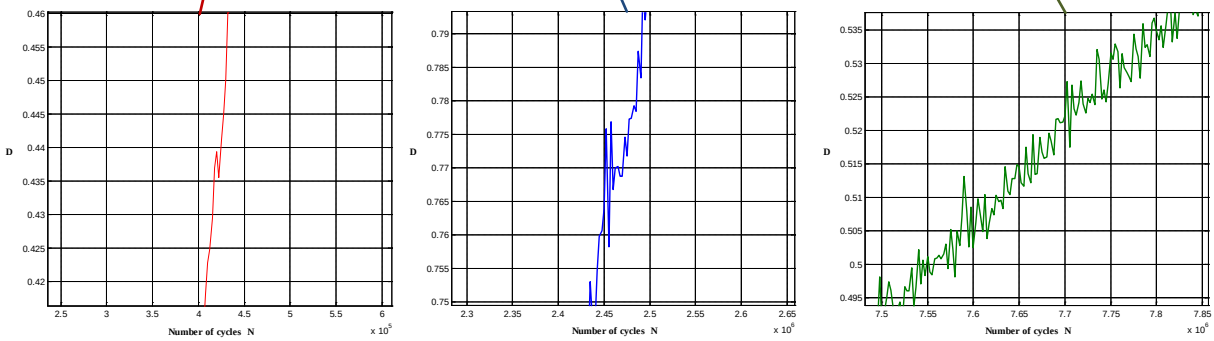

Figure 4.9 - Zoom-in for the three cases.

From the zooming-in shown in figure 4.9, we note that the fluctuations of the curve due to stochastic effects increase as the road condition gets better. This phenomenon can be explained by the fact that the stochastic dispersion parameters are more influent in good road condition (mode 3) case than in severe condition (mode 1) where the mean road profile is much higher (table 4.1).

By comparison to the case of one random variable it is clear that the lifetimes decrease for the three modes as follows:

	One random variable	Two random variables	Decrease (%)
Mode 1	1,010,000 cycles	610,000 cycles	39.6%
Mode 2	3,995,000 cycles	2,712,500 cycles	32.1%
Mode 3	16,092,500 cycles	10,150,000 cycles	36.9%

The conclusion drawn here is it is important to consider all parameters as random when these parameters show some sensibility on the lifetime value.

IV.10.1.2.1 - Conversion of Lifetimes into Years

To convert the suspension lifetime into years' unit, assume that a new road profile realization occurs each 2 seconds. If we assume also that the suspension time usage is 10% of a day (2.4 hours/day), then the expected lifetimes' durations are (refer to Chapter II, Paragraph 3.1.10):

$$\text{For mode 1 : } \frac{610{,}000(\text{cycles})\times 2(\text{s})}{60(\text{s})\times 60(\text{min})\times 2.4(\text{hours})\times 365(\text{days})} = 0.39 \text{ years}$$

$$\text{For mode 2 : } \frac{2{,}712{,}500(\text{cycles})\times 2(\text{s})}{60(\text{s})\times 60(\text{min})\times 2.4(\text{hours})\times 365(\text{days})} = 1.72 \text{ years}$$

$$\text{For mode 3 : } \frac{10{,}150{,}000(\text{cycles})\times 2(\text{s})}{60(\text{s})\times 60(\text{min})\times 2.4(\text{hours})\times 365(\text{days})} = 6.44 \text{ years}$$

IV.10.1.2.2 - Comparison: Deterministic - Stochastic Results (for Linear Damage Law)

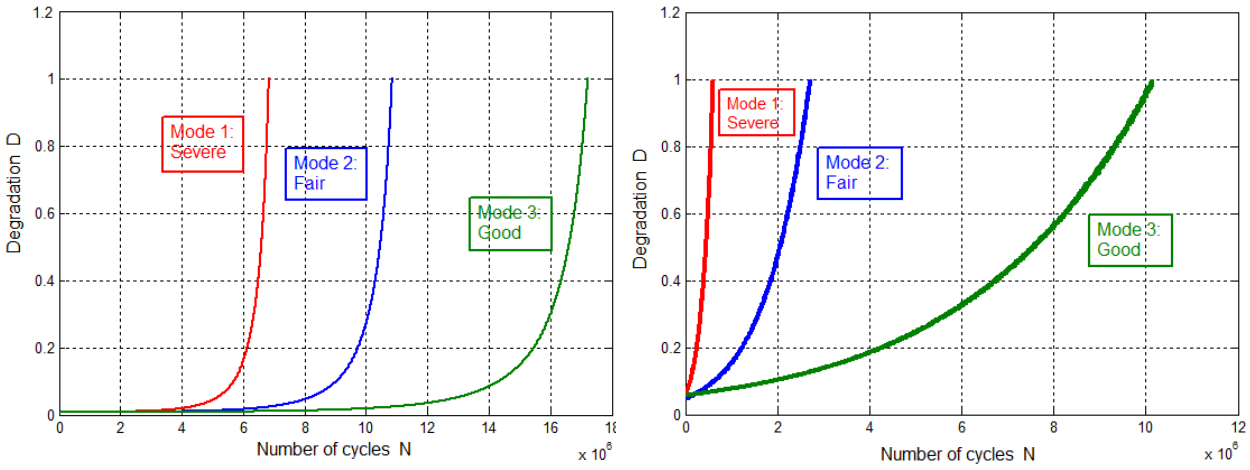

Deterministic case *Stochastic case* (2 RV)

Figure 4.10 - Deterministic and stochastic study of suspension degradation under linear damage law.

From figure 4.10, it can be noted that in the stochastic case the lifetimes are reduced significantly relatively to the deterministic case like as follows:

Mode 1 (severe condition) : from 6,836,000 cycles to 610,000 cycles (nearly 91.1%)

Mode 2 (fair condition) : from 10,850,000 cycles to 2,712,500 cycles (nearly 75.0%)

Mode 3 (good condition) : from 17,222,000 cycles to 10,150,000 cycles (nearly 41.1%)

It is a logical conclusion since the stochastic effects are generally negative on the suspension lifetimes. In fact, it is known that the dispersions (standard deviations) introduced by these random variables (load stresses induced by road profile and initial crack length of suspension) propagate through all the degradation equations and resulting in reduced lifetime values. Moreover, the better the road conditions the smaller the lifetime reductions.

IV.10.1.2.3 - RUL Evaluation of a Suspension in Stochastic Case

The global RUL evaluations are deduced from the expression N_C - N_0. In fact N_C is the necessary cycle number to reach failure (appearance of the first macro-cracks) and N_0 is the initial cycle number at the beginning of service taken generally equal to 0. These curves decrease from total lifetime of the device to zero where $D = D_C = 1$.

From these curves we can deduce at each instant N the remaining useful lifetime of the device (RUL = N_C - N) and hence, the prognostic result can be inferred (figure 4.11).

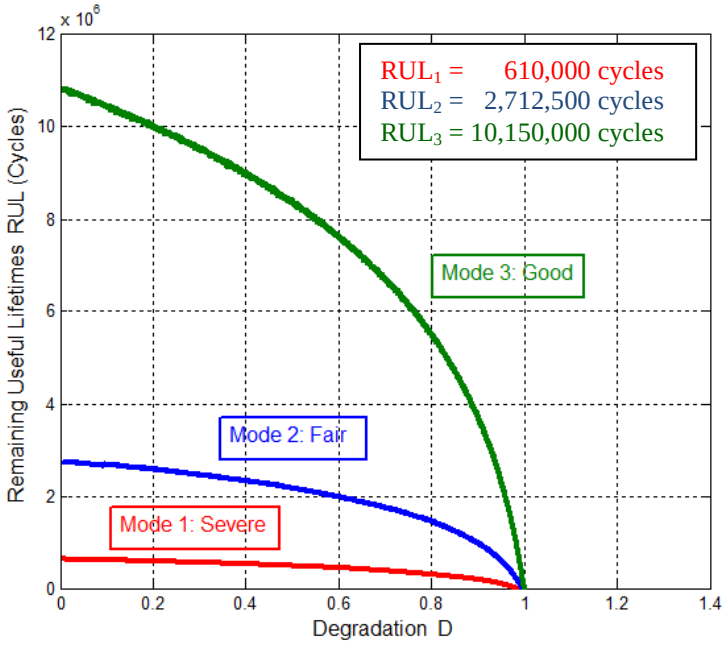

Figure 4.11 - RUL evolution of the suspension stochastic degradation under linear damage law.

IV.10.1.3 - Validation of the Suspension Life under Linear Damage Rule

The validation of these results can be found in the work of reference [31] on the fatigue life of suspensions. An average life of 100,375 km is deduced under normal conditions and which corresponds to 2.30 years for a vehicle running with 50 km per hour and for 2.4 hours per day.

IV.10.2 - Nonlinear Stochastic Case

IV.10.2.1 - Stochastic Nonlinear Cumulative Damage

The case of fatigue degradation taken in the precedent section is mathematically formulated and based on the analytic laws of Paris and Miner. The last law is a linear cumulative damage model. Its largest drawback is its inability to account for the order of loading. That is, the resulting failure prediction is independent of the load interaction effects that have been observed between high-cycle and low-cycle loadings.

Past research has shown there is a nonlinear interaction effect between high cycle fatigue (HCF) and low cycle fatigue (LCF) in many engineering materials. This effect has been observed within uniaxial loadings, but is often more pronounced under multiaxial loading, particularly when the loading is non-proportional.

The nonlinear interaction effect precludes the use of the linear damage rule for damage accumulation. In the present study, the effect of HCF loading has had a more detrimental effect when coupled with the LCF loadings than predicted by a linear summation rule. Nonlinear damage accumulation theories can account for this influence and have shown an improvement in prediction. The stress levels were chosen to correspond to levels previously tested to failure, resulting in fatigue lives ranging from approximately 10^5 to 10^7 cycles. A nonlinear damage summation is required to properly define the fatigue process since the linear summation of damage given by Miner's sum is often not adequate to predict the service life of a component when subjected to variable-amplitude loadings.

The nonlinear cumulative damage is demonstrated in Chapter III and given at each cycle N by:

$$D(N) = 1 - \left[\left(1 - D_0\right)^{\alpha+1} - \frac{N - N_0}{N_C} \left(1 - \frac{\sigma_0}{\Delta\sigma / 2}\right)^m (\alpha + 1) \right]^{\frac{1}{\alpha+1}} \tag{20}$$

The growth of $D(N)$ at the end of each cycle N in terms of the crack width $a(N)$ is given by the following relation:

$$D(N) = \frac{a(N)}{a_C - a_0} \tag{21}$$

Where,

$\overline{\sigma} = \Delta\sigma / 2$: is the stress amplitude in one cycle, this parameter is generated as an input load whose mean is taken to be equal to 280 MPa,

σ_0 = the fatigue limit (is the endurance limit stress of material) taken to be equal to 180 MPa.

Here two cases are considered: one random variable (loading $\Delta\tilde{\sigma}$) and two random variables (loading $\Delta\tilde{\sigma}$ and initial crack width $\tilde{a}_0$).

The stochastic nonlinear prognostic model can be written as follows:

$$\tilde{D}(N) = 1 - \left[\left(1 - \tilde{D}_0\right)^{\alpha+1} - \frac{N - N_0}{N_C} \left(1 - \frac{\sigma_0}{\Delta\tilde{\sigma}_j / 2}\right)^m (\alpha + 1) \right]^{\frac{1}{\alpha+1}}$$

$$\tilde{D}_0 = \frac{\tilde{a}_0}{a_C - \tilde{a}_0} \tag{22}$$

IV.10.2.2 - Flowchart of the Stochastic-Based Nonlinear Prognostic

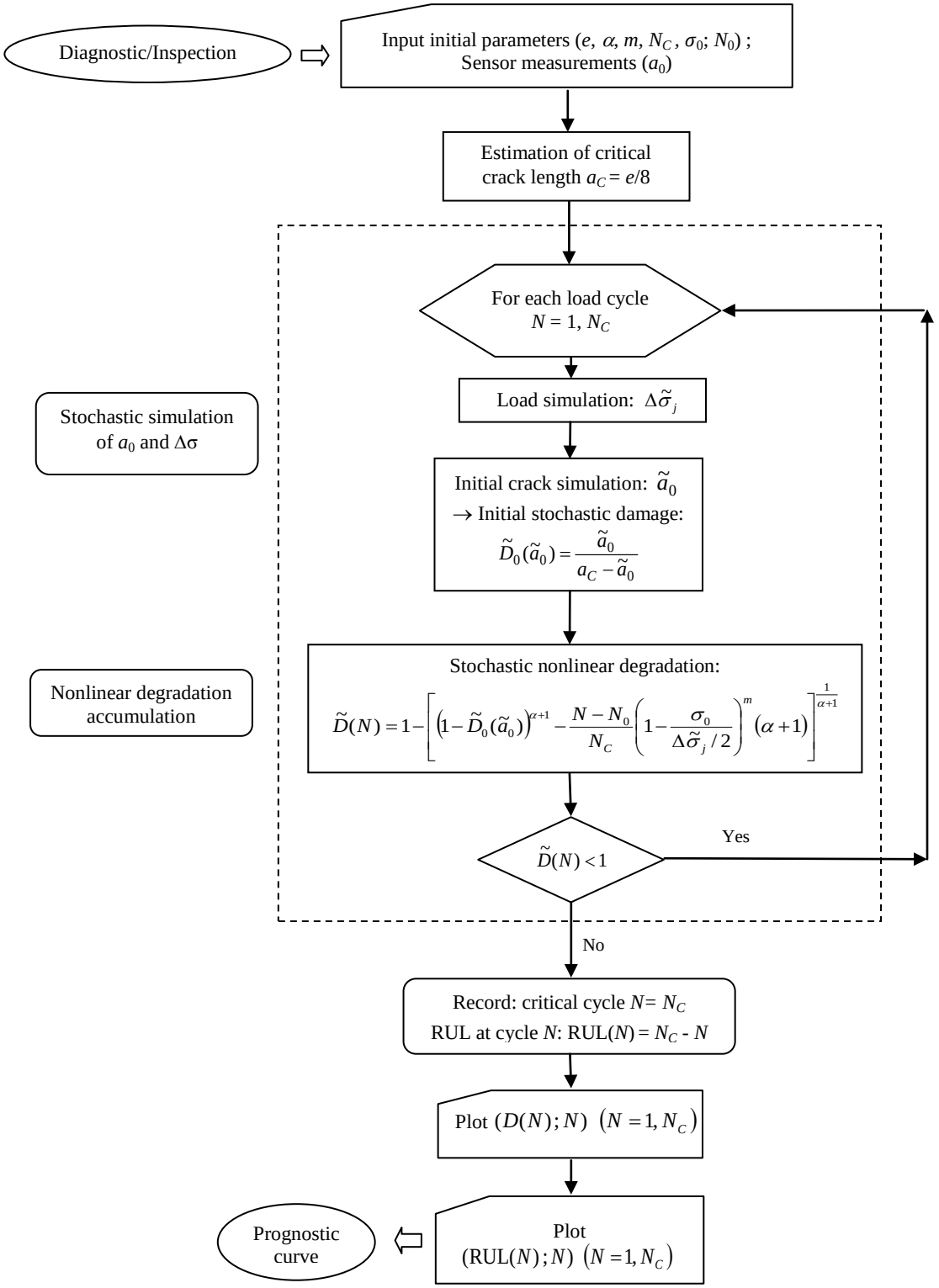

IV.10.2.3 - One Random Variable

We consider here the case of a nonlinear damage with one stochastic parameter $\Delta\tilde{\sigma}$ following the normal law (table 4.1).

From the simulation of the stochastic prognostic model proposed under equation (22), the degradations evolution of the suspension is obtained and presented in figure 4.12.

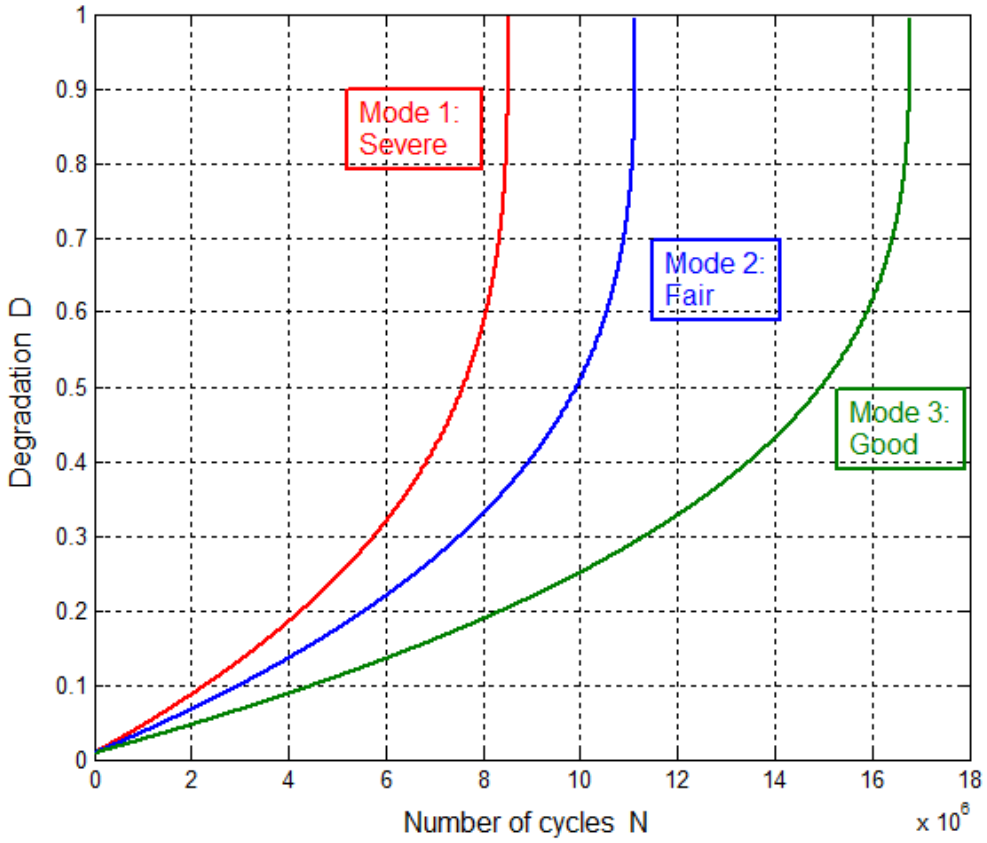

Figure 4.12 - Suspension degradation under nonlinear damage law and stochastic road excitations.

The lifetimes noted from the figure 4.12 are for each mode as follows:

Mode 1: 8,520,325 cycles.

Mode 2: 11,134,900 cycles.

Mode 3: 16,781,000 cycles.

IV.10.2.3.1 - Conversion of Lifetimes into Years

To convert the suspension lifetime into years' unit, assume that a new road profile realization occurs each 2 seconds. If we assume also that the suspension time usage is 10% of

a day (2.4 hours/day), then the expected lifetimes' durations are (refer to Chapter II, Paragraph 3.1.10):

$$\text{For mode 1 : } \frac{8{,}520{,}325(\text{cycles})\times 2(\text{s})}{60(\text{s})\times 60(\text{min})\times 2.4(\text{hours})\times 365(\text{days})} = 5.4 \text{ years}$$

$$\text{For mode 2 : } \frac{11{,}134{,}900(\text{cycles})\times 2(\text{s})}{60(\text{s})\times 60(\text{min})\times 2.4(\text{hours})\times 365(\text{days})} = 7.06 \text{ years}$$

$$\text{For mode 3 : } \frac{16{,}781{,}000(\text{cycles})\times 2(\text{s})}{60(\text{s})\times 60(\text{min})\times 2.4(\text{hours})\times 365(\text{days})} = 10.64 \text{ years}$$

IV.10.2.4 - Two Random Variables

We consider here the case of a nonlinear damage with two stochastic parameters: the loading from the road excitation $\Delta\tilde{\sigma}$ and the initial crack length $\tilde{a}_0$

1) The road excitation effect :

$$\Delta\tilde{\sigma} : \text{Normal Law} \begin{cases} E(\Delta\tilde{\sigma}_j) = \dfrac{E}{\ell}\times\Delta\bar{x}_j \qquad \text{(for each mode of road profile)} \\ V(\Delta\tilde{\sigma}_j) = \left(\dfrac{E}{\ell}\right)^2 \times V\left(\Delta\tilde{x}_j\right) \end{cases}$$

2) The initial crack length :

$$\tilde{a}_0 : \text{Lognormal Law} \begin{cases} E(\tilde{a}_0) = 0.2 \text{ mm} \\ V(\tilde{a}_0) = 8.673\times 10^{-6} \text{ mm}^2 \quad \Rightarrow \sigma(\tilde{a}_0) = \sqrt{V(\tilde{a}_0)} = 0.002945 \text{ mm} \end{cases}$$

The results of degradations evolution of the suspension are presented in figures 4.13 and 4.14 below.

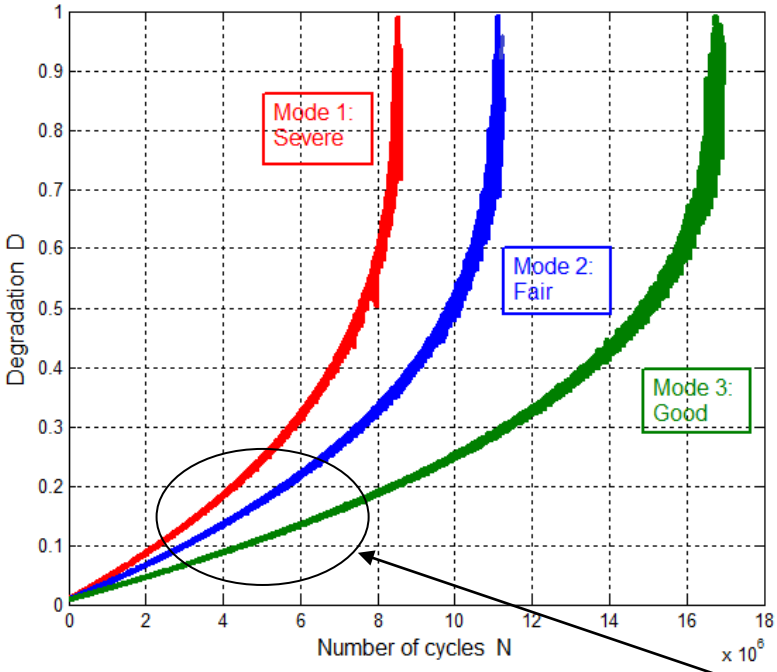

Figure 4.13 - Suspension degradation under nonlinear law and two random variables: stochastic road excitations and initial damage.

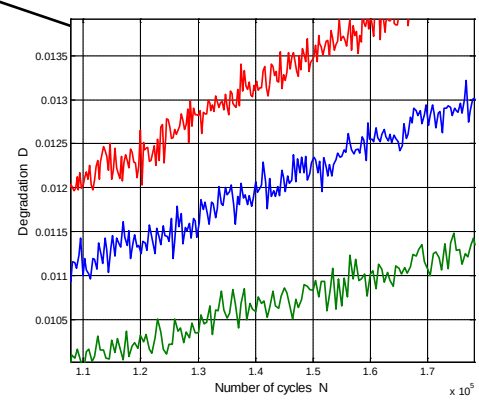

Figure 4.14 - Zoom in for the three cases.

The lifetimes noted from the figure 4.13 are for each mode as follows:

Mode 1: 8,613,825 cycles.

Mode 2: 11,269,650 cycles.

Mode 3: 16,881,000 cycles.

From the zooming-in shown in figure 4.14, we note that the fluctuations of the curves due to stochastic effects are similar for all road conditions. This can be explained by the fact that in nonlinear damage, the stochastic dispersion effects dominate for all road conditions.

By comparison to the case of one random variable, the following lifetimes are indicated:

	One random variable	Two random variables	Increase (%)
Mode 1	8,520,325 cycles	8,613,825 cycles	1.1%
Mode 2	11,134,900 cycles	11,269,650 cycles	1.2%
Mode 3	16,781,000 cycles	16,881,000 cycles	0.6%

Contrarily to the linear case, the lifetimes increase from one random variable to two random variables for all modes; this conclusion is explained by the fact that the nonlinearity dominates the stochastic effect.

IV.10.2.4.1 - Conversion of Lifetimes into Years

To convert the suspension lifetime into years' unit, assume that a new road profile realization occurs each 2 seconds. If we assume also that the suspension time usage is 10% of a day (2.4 hours/day), then the expected lifetimes' durations are (refer to Chapter II, Paragraph 3.1.10):

$$\text{For mode 1 : } \frac{8{,}613{,}825(\text{cycles}) \times 2(\text{s})}{60(\text{s}) \times 60(\text{min}) \times 2.4(\text{hours}) \times 365(\text{days})} = 5.46 \text{ years}$$

$$\text{For mode 2 : } \frac{11{,}269{,}650(\text{cycles}) \times 2(\text{s})}{60(\text{s}) \times 60(\text{min}) \times 2.4(\text{hours}) \times 365(\text{days})} = 7.15 \text{ years}$$

$$\text{For mode 3 : } \frac{16{,}881{,}000(\text{cycles}) \times 2(\text{s})}{60(\text{s}) \times 60(\text{min}) \times 2.4(\text{hours}) \times 365(\text{days})} = 10.71 \text{ years}$$

IV.10.2.4.2 - Comparison: Deterministic - Stochastic Results (Nonlinear Damage Law)

To show the stochastic effects, a comparison is done between the deterministic results and the stochastic results (two random variables case).

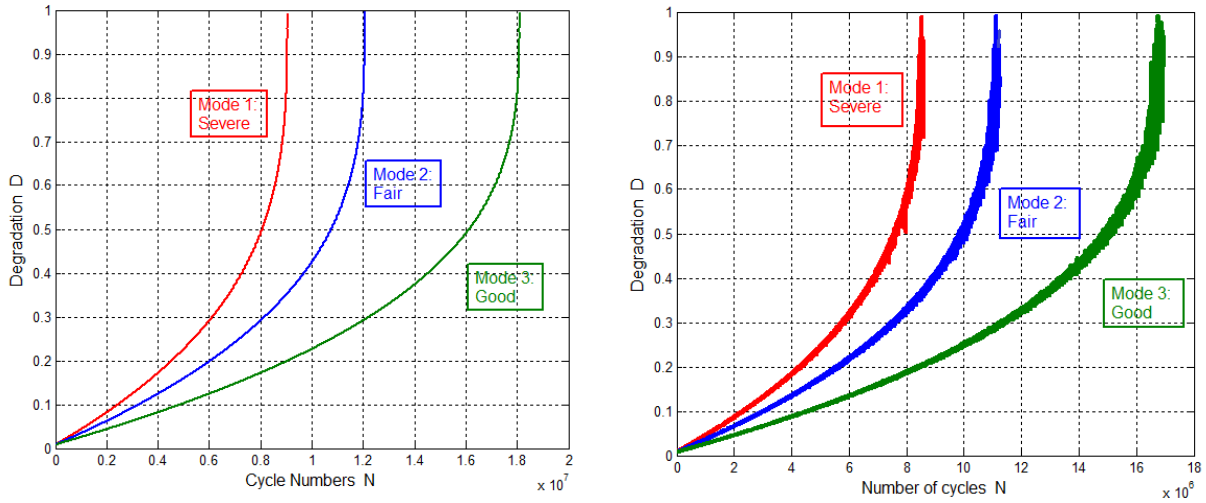

Deterministic case *Stochastic case* (2 RV)

Figure 4.15 - Deterministic and stochastic study of the suspension degradation under nonlinear damage law.

From figure 4.15, it can be noted that the lifetimes are reduced from the deterministic case to the stochastic case as follows:

Mode 1 (severe condition): from 9,047,700 cycles to 8,613,825 cycles (nearly 4.8%)
Mode 2 (fair condition) : from 12,063,800 cycles to 11,269,650 cycles (nearly 6.6%)
Mode 3 (good condition) : from 18,095,400 cycles to 16,881,000 cycles (nearly 6.7%)

It is noted that more the road conditions become better more the lifetime reductions become greater. Moreover, the fluctuations in stochastic curves are due to the stochastic dispersions (standard deviations). In fact, the stochastic effects are generally considerable on the suspension lifetimes due to the dispersions introduced by these random variables that propagate through all the degradation equations and resulting in reduced lifetime values.

The final remark is that the stochastic effects dominate here over the nonlinear effects in lifetimes estimations. Hence, it is important to include the stochastic effects for a more realistic prognosis under the condition that we consider reliable statistical data for the initial crack widths and the road profile excitations.

IV.10.2.5 - Validation of the Suspension Life under Nonlinear Damage Rule

The validation of these results can be found in the work of reference [32] on the fatigue life of suspensions. An average life of 322,000 km is deduced under normal conditions and which corresponds to 7.35 years for a vehicle running with 50 km per hour and for 2.4 hours per day.

IV.11 - Application to the Pipeline Systems to Three Cases

We restudy the prognostic of the pipeline system already treated in Chapter II; this, by taking into account the linear and the nonlinear damage law but this time for the stochastic case of variables [33]. The study is done for one and two random variables (internal pressure P_0 and initial crack length a_0). The geometric properties of pipes are presented in Chapter II.

Three maximal levels of internal pressure P_0 are considered (table 4.2) with a repetition period T_P. At each of these levels, a degradation trajectory $D(N)$ is deduced in terms of cycle number N. When $D(N)$ reaches the unit value, then the corresponding N is the lifetime of the pipe that failed by fatigue.

We simulate three modes of P_j with the statistical parameters given in table 4.2.

Table 4.2 - The three pressure modes.

Pressure Mode	P_0 (MPa)
High (mode 1)	8
Middle (mode 2)	5
Low (mode 3)	3

IV.11.1 - Equation of the Stochastic-Based Prognostic

In the case of pipes of thickness e, the stress ranges are created by the applied internal pressure; hence, the following relation gives the critical hoop stress range $\Delta\sigma_\theta$ in terms of the pressure range ΔP (figure 4.16):

$$\Delta\sigma_\theta = 2 \cdot \Delta\sigma_L = \frac{\Delta P \cdot R}{e} \tag{23}$$

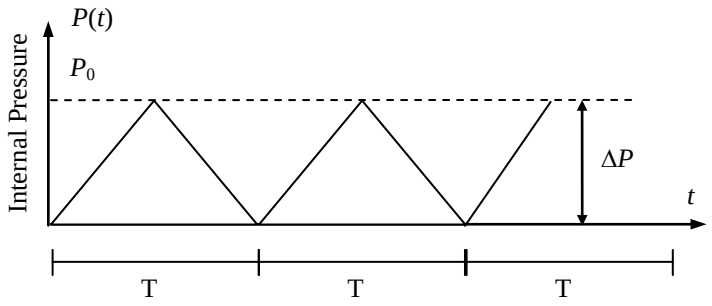

Figure 4.16 - Triangular pressure law.

The simulation of the internal pressure following a triangular law $\Delta\tilde{P}$ (figure 4.16) generates a sample of stress ranges $\Delta\tilde{\sigma}$ following the same triangular law from the equation below:

$$\Delta\sigma_j = \frac{P_j \cdot R}{e} \qquad \text{knowing that : } \Delta P_j = P_j - 0 = P_j$$

From the following equation:

$$d\tilde{D}_N = \frac{C}{a_C - \tilde{a}_0}\left(Y(\tilde{a}_N)\cdot\sqrt{\pi\,\tilde{a}_N}\cdot\Delta\tilde{\sigma}_j\right)^m \tag{24}$$

It can be deduced that:

$$d\tilde{D}_N = \frac{C}{(e/8 - \tilde{a}_0)}\times\left(0.6\times\frac{1+2(\tilde{a}_N/e)}{(1-\tilde{a}_N/e)^{\frac{3}{2}}}\times\sqrt{\pi\,\tilde{a}_N}\times\frac{\tilde{P}_j.R}{e}\right)^m \tag{25}$$

Where,

$Y(a) = 0.6\times\dfrac{1+2(a/e)}{(1-a/e)^{\frac{3}{2}}}$ is the geometric function of the pipes.

IV.11.2 - Generation of Internal Pressure P_i

The Monte-Carlo simulation of the random P_i is completed using three models:

Model A) : Triangular with uniform sampling of time *t*;

Model B) : Over one initial triangular period T_P;

Model C) : Over multi triangular periods T_P.

IV.11.2.1 - Monte-Carlo Simulation Principle

The Monte-Carlo simulation (figure 4.17) consists of a random sampling of a large number of u in [0,1] interval with the same probabilities (using the uniform distribution). As $u^i = F_U(u^i)$ (the second bisector) and hence $u^i = F_U(u^i) = F_X(x^i)$, $x^i = F_X^{-1}(u^i)$. The generation of x^i leads to the reconstruction of the random variable sample following the law $F_X(x)$.

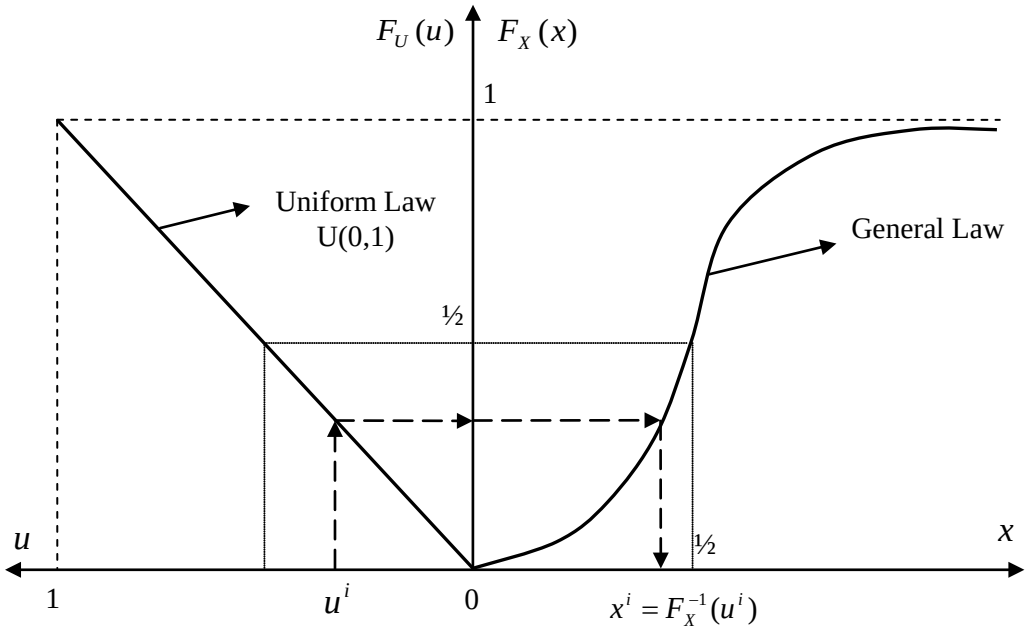

Figure 4.17 - Monte-Carlo simulation principle.

Where u is the uniform-based generated value.

IV.11.2.2 - Model A: Uniform Generation of Time *t*

Here, the triangular pressure P_j is simulated at each instant t considering a uniform distribution for the time $t \in [0,1]$.

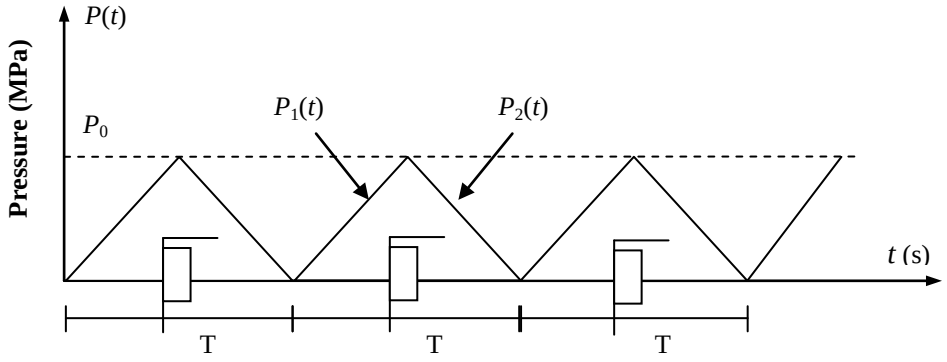

Figure 4.18 - Triangular simulation of the pressure in terms of uniform time sampling.

The simulated pressure diagram is given in terms of time *t* by the following function:

$$P(t)=\begin{cases} P_1(t)=\dfrac{2P_0}{T}\times\tilde{t} \quad ; \quad if\ t\le\dfrac{T}{2} \\ P_2(t)=\dfrac{-2P_0}{T}\times\tilde{t}+2P_0 \quad ; \quad if\ t>\dfrac{T}{2} \end{cases} \tag{26}$$

Where the variable *t* is simulated randomly under uniform law (figure 4.18).

IV.11.2.3 - Model B: One Initial Triangular Period T_P

In this case, the internal pressure *P* is simulated by Monte-Carlo method using a triangular distribution over one initial period of pressure T_P.

The triangular law of the internal pressure is given by the following functions (figure 4.19):

The PDF function of *P*:

$$f_P(p)=\begin{cases} \dfrac{2(P-a)}{(b-a)(c-a)} & a\le P\le c \\ \dfrac{2(b-P)}{(b-a)(b-c)} & c\le P\le b \\ 0 & P<a \text{ and } P>b \end{cases} \tag{27}$$

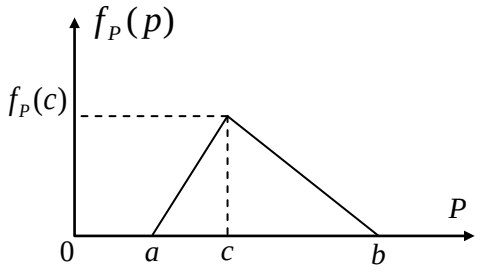

Figure 4.19 - Triangular PDF function of *P*.

The Cumulative Density Function (CDF) of *P*:

$$F_P(p)=\begin{cases} 0 & P<a \\ \dfrac{(P-a)^2}{(b-a)(c-a)} & a\le P\le c \\ 1-\dfrac{(b-P)^2}{(b-a)(b-c)} & c<P<b \\ 1 & P\ge b \end{cases} \tag{28}$$

The inverse of the CDF function gives a realization P_j for P as follows:

$$P_j = F^{-1}(u_j) = \begin{cases} a + \sqrt{u_j (b-a)(c-a)} & 0 \le u_j \le \theta \\ b - \sqrt{(1-u_j)(b-a)(b-c)} & \theta \le u_j \le 1 \end{cases} \tag{29}$$

Where,

u_j: the uniform-based generated value in the interval [0,1],

$\theta = \dfrac{c-a}{b-a}$,

The mean value: $\overline{P} = \dfrac{(1-\theta^3)}{6(1-\theta)} \approx \dfrac{a+c+b}{3}$,

The variance:

$$V(P) = \frac{1-\theta \times (1-\theta)}{18} = \left(\frac{b-a}{18}\right)^2 \times \left\{1 - \frac{(c-a)(b-c)}{(b-a)^2}\right\}.$$

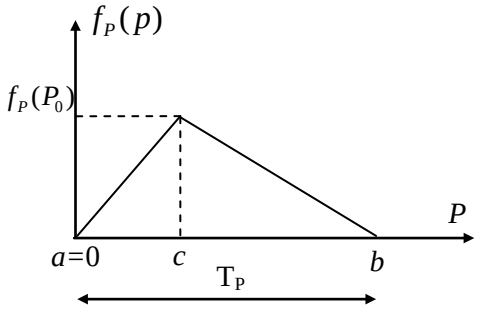

Figure 4.20 - Triangular PDF of *P*.

Here, the simulation of the internal pressure is completed along one period T_P under a triangular law distribution of mean value $\overline{P}$:

$$\overline{P} = \frac{(1-\theta^3)}{6(1-\theta)} \approx \frac{a+c+b}{3} = \frac{0+P_0+T_P}{3}$$

For the same initial period T_P, each simulation gives a different realization of the PDF; thus, a new value for $c = P_0$ is given, keeping always $a = 0$ and $b = T_P$.

We consider the following values for the simulation (figure 4.20):

$a = 0$; $b = T_P$ (pressure interval); and $c = P_0$ (pressure value).

Where the period T_P is a pressure interval that can be taken as a percentage of the maximal pressure P_0.

IV.11.2.4 - Model C: Multi-Triangular Period

In this case, we do the Monte-Carlo simulation of the symmetric triangular distribution repeated stochastically along time with respect to a pressure period T_P. In each period, a new simulation gives a different realization of the density function; thus, new values for *a*, *b*, *c* are given each time (figure 4.21).

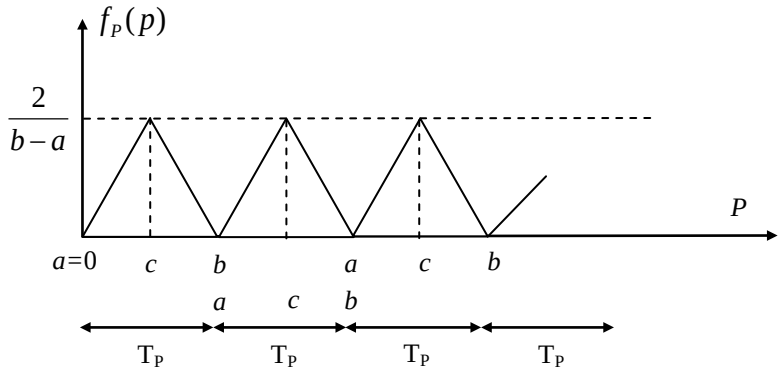

Figure 4.21 - Multi-Triangular PDF function.

We take the following values for each simulation:

$a = i \times T_P$ (i = instants: 0,1,2,...) ; $b = a + T_P$; $c = (b+a)/2$

IV.11.3 - Linear Case of Damage

In this part, the linear Miner's law of damage is used. One and two random variables are considered and which are the pressure P_0 and the initial crack length a_0. The simulation model adopted here for pressure P is the triangular law in terms of a uniform simulation of time t (model A).

IV.11.3.1 - One Random Variable (Pressure)

As for the deterministic study executed in Chapter II, the study encompasses three models for pressure generation (table 4.3) and three types of pipes: unburied, buried and offshore.

Table 4.3 - Statistical characteristics of each pressure mode.

Pressure Mode	$\overline{P_j}$ (MPa)	δ_{Pj} (%)	Law
High (mode 1)	8	10%	Triangular
Middle (mode 2)	5	10%	Triangular
Low (mode 3)	3	10%	Triangular

IV.11.3.1.1 - Model A for Pressure Generation

For the case of model A pressure generation, the degradation evolutions for the unburied pipes are given in figure 4.22. We note here the following lifetimes: 4.80 years

(High pressure), 6.75 (Middle pressure), and 9.1 years (Low pressure). The results show a steep increase of degradation from the 4th year onward for the High mode while it is from 6.5 years for the Middle mode and from 9 years for the Low mode.

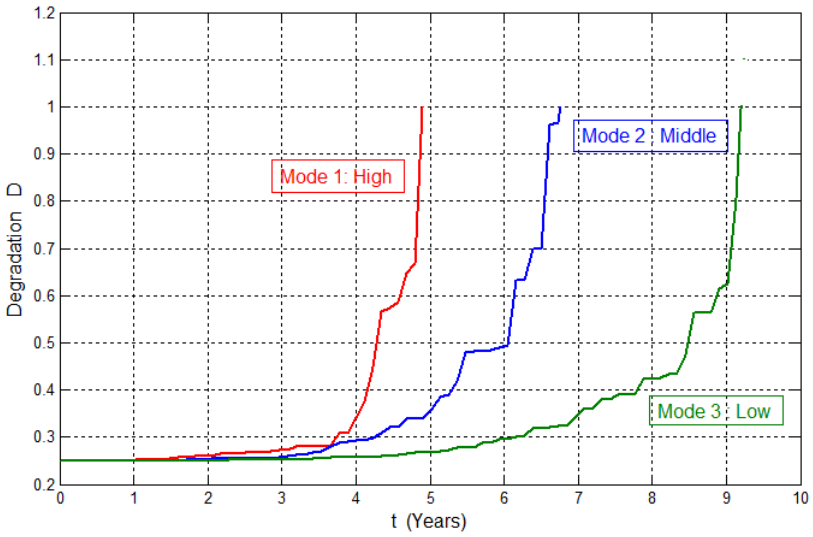

Figure 4.22 - Unburied pipelines under linear damage law and stochastic *P*.

In buried pipes case, the degradation evolutions for the case of model A of pressure generation are given in figure 4.23. The following lifetimes are noted: 4.50 years (High pressure), 6.30 (Middle pressure), and 10.5 years (Low pressure). The results show also a sharp increase of degradation from the 4th year onward for the High mode while it is from the 6th year for the Middle mode and the Low mode shows more progressive increase in degradation with time.

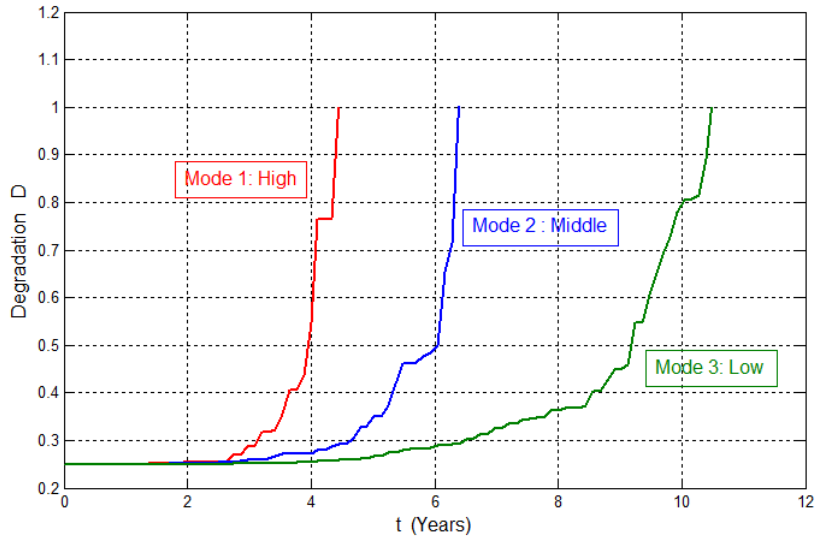

Figure 4.23 - Buried pipelines under linear damage law and stochastic *P*.

The degradation evolutions for the offshore pipes for the case of model A of pressure generation are given in figure 4.24. We note here the following lifetimes: 18.5 years (High pressure), 22 years (Middle pressure), and 33 years (Low pressure). The results show a progressive increase of degradation along time for all pressure modes except for the Low mode where a steep increase is noted from 32 years after a clear progressive degradation.

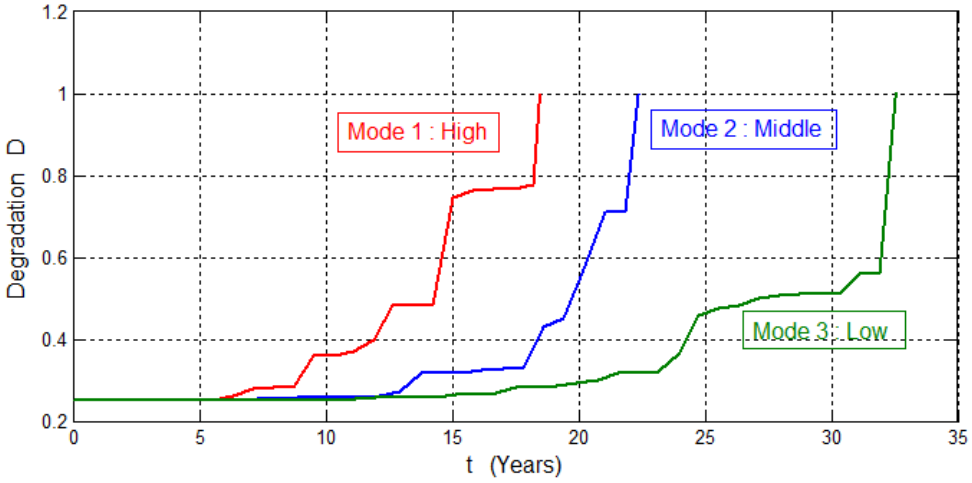

Figure 4.24 - Offshore pipelines under linear damage law and stochastic *P*.

IV.11.3.1.2 - Model B for Pressure Generation

For the case of model B pressure generation, the degradation evolutions show different results from the model A. In fact, for the unburied pipes, the results are represented in figure 4.25. We note here the following lifetimes: 2.9 years (High pressure), 4.2 years (Middle pressure), and 6.5 years (Low pressure). The results show a progressive increase of degradation for all modes except for the High and Middle modes where steep increases occur at the final stage.

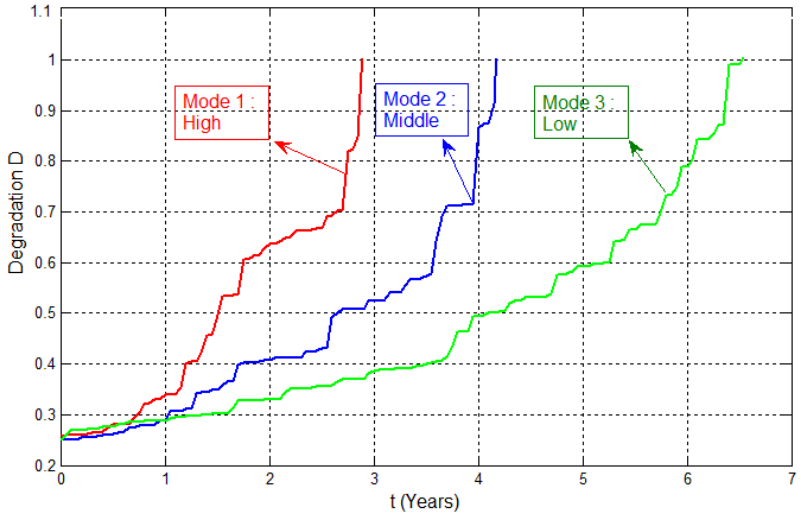

Figure 4.25 - Degradation evolution for unburied pipe under stochastic *P*.

The degradation evolutions for the buried pipes for model B of pressure generation are given in figure 4.26. The following lifetimes are noted: 8.2 years (High pressure), 11.3 years (Middle pressure), and 15.9 years (Low pressure). The results show a progressive increase of degradation for all modes especially for the last mode.

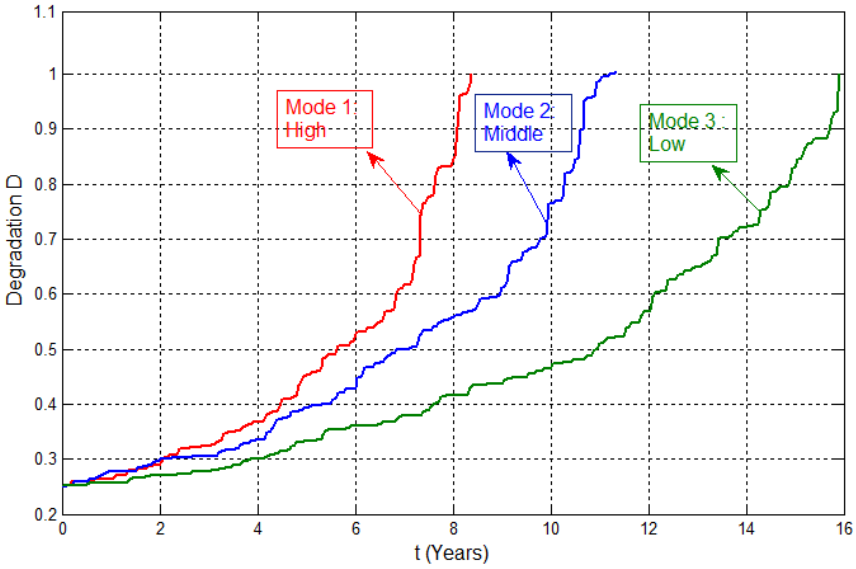

Figure 4.26 - Degradation evolution for buried pipe with stochastic *P*.

Finally, for model B of pressure generation, the degradation evolutions for the offshore pipes are given in figure 4.27. We note here the following lifetimes: 8 years (High pressure), 16 years (Middle pressure), and 20.5 years (Low pressure). The results show a progressive increase of degradation for all modes especially for the last mode.

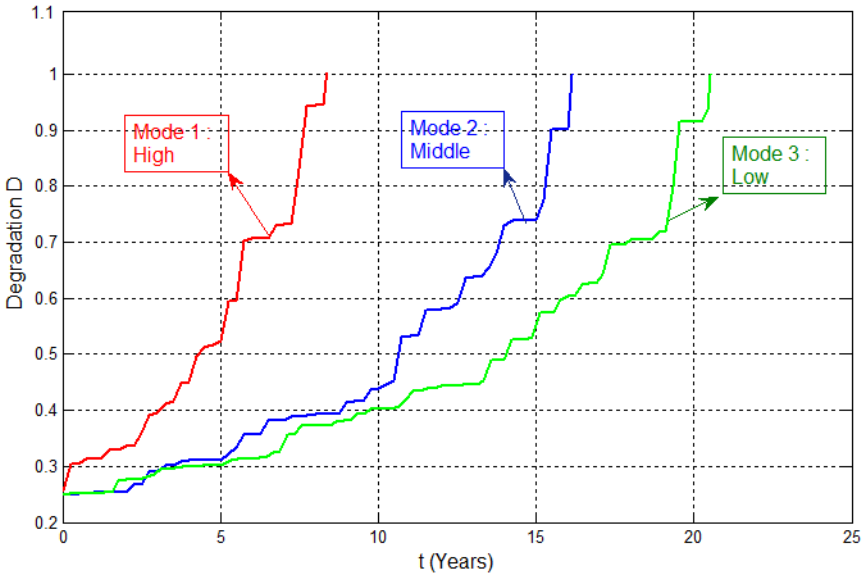

Figure 4.27 - Degradation evolution for offshore pipe under stochastic *P*.

IV.11.3.1.3 - Model C for Pressure Generation

For the case of model C pressure generation, the degradation evolutions for the unburied pipes are given in figure 4.28. We note here the following lifetimes: 2.9 years (High pressure), 4.2 years (Middle pressure), and 6.5 years (Low pressure). The results show a steep increase of degradation for the modes High, Middle, and Low from the years: 2.5, 3.5, and 6 respectively.

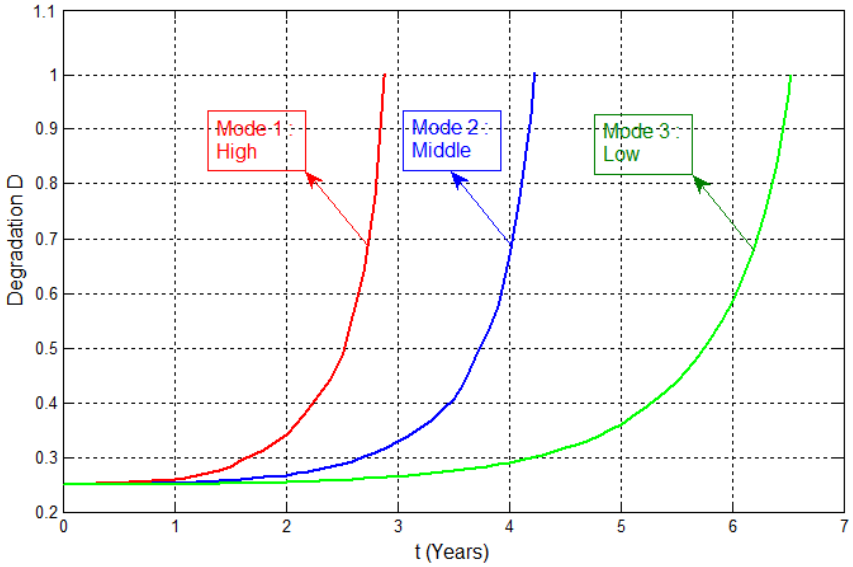

Figure 4.28 - Degradation evolution for unburied pipe with stochastic *P*.

The degradation evolutions for the buried pipes in the case of model C of pressure generation are given in figure 4.29. We note here the following lifetimes: 8 years (High pressure), 11.2 years (Middle pressure), and 17.2 years (Low pressure). The results show a steep increase of degradation for the modes High, Middle, and Low from the years: 6.5, 11.5, and 16.8 respectively.

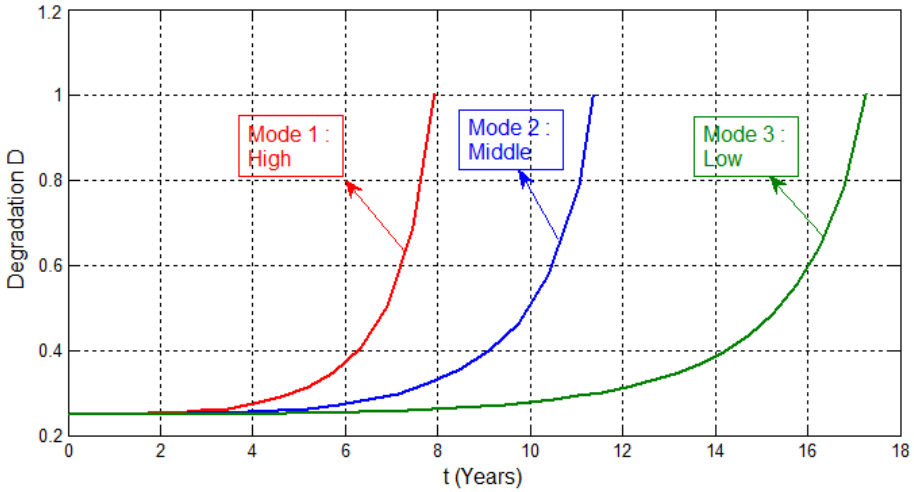

Figure 4.29 - Degradation evolution for buried pipe with stochastic *P*.

For the offshore pipes in the case of model C of pressure generation, the degradation evolutions are given in figure 4.30. We note here the following lifetimes: 9 years (High pressure), 13.5 years (Middle pressure), and 22 years (Low pressure). The results show a progressive increase of degradation for all modes especially for the last mode.

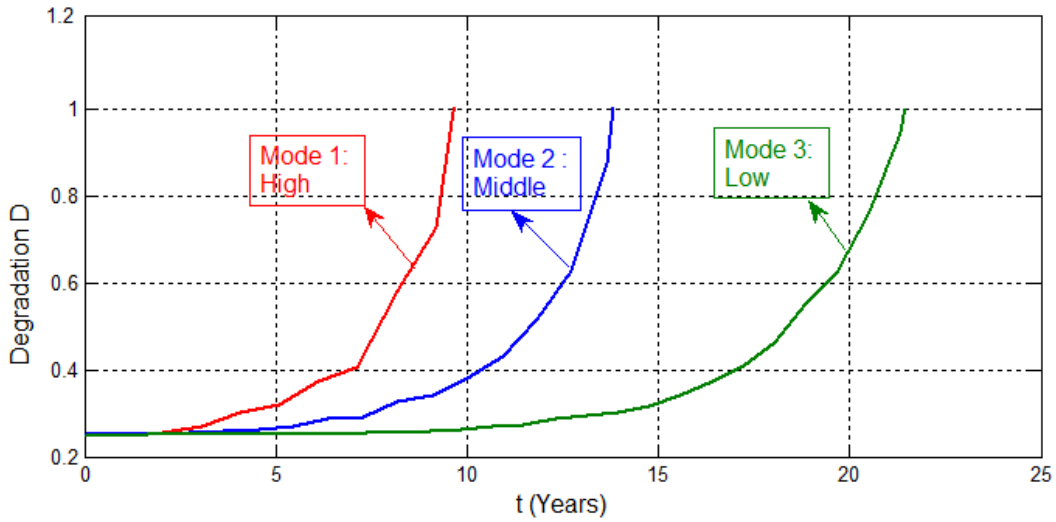

Figure 4.30 - Degradation evolution for offshore pipe with stochastic *P*.

IV.11.3.2 - Two Random Variables: Pressure (One Triangular Period) - a_0 (Lognormal Law)

Here, for each instant, the simulation of the internal pressure is done along one initial period T_P (model B) under a triangular distribution law of mean value $\overline{P}$:

$$\overline{P} \approx \frac{a+c+b}{3} = \frac{0+P_0+T_P}{3}$$

For the same initial period, each simulation gives a different realization of the density function; thus, a new value for $c = P_0$ is given, keeping always $a = 0$ and $b = T_P$.

We consider the following values for the simulation: $a = 0$; $b = T_P$ (pressure interval); and $c = P_0$ (pressure value).

The Triangular simulation of the internal pressure, with respect to model B and for the three modes, leads to the applied stress blocks shown in figure 4.31. This figure shows that, for the three blocks of applied stresses, the randomness is clearly illustrated by the fluctuation values of these stresses with the cycle numbers. The mean values of the three blocks are respectively 240 MPa, 150 MPa, and 90 MPa.

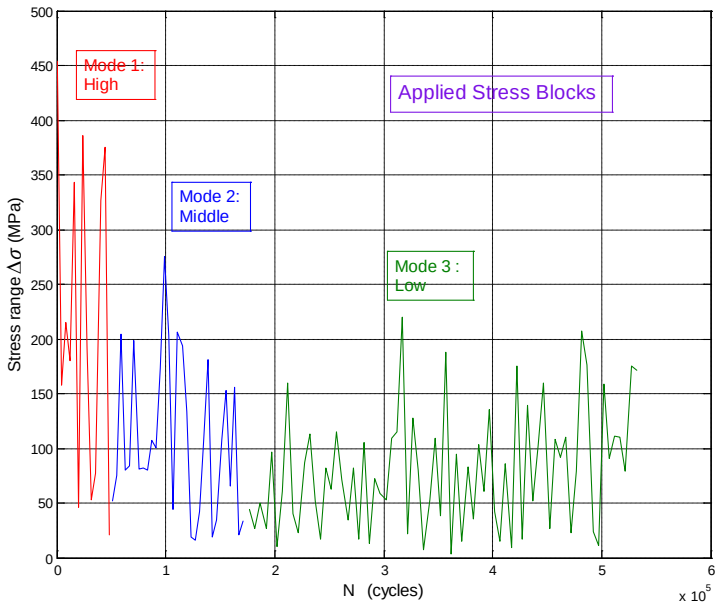

Figure 4.31 - Applied stress blocks on pipes for three modes of pressure.

The initial crack length is simulated along a lognormal law with the following parameters: $\tilde{a}_0$: Lognormal Law $\begin{cases} E(\tilde{a}_0) = 0.2 \text{ mm} \\ \sigma(\tilde{a}_0) = \sqrt{V(\tilde{a}_0)} = 0.002945 \text{ mm} \end{cases}$

The crack length $a(t)$ growth versus time is given in figure 4.32 that shows for the three modes the length evolution from an initial value a_0 to the critical value $a_C = e/8$. They grow from an initial value $a_0 = 0.2$ mm to the end of life where all curves $a(t)$ reach the critical width $a_C = e/8 = 1$. The High pressure mode reveals the fastest width increase. The critical crack lengths reached for each pressure mode at the instants are: 3.15 years, 5.3 years, and 6.8 years respectively.

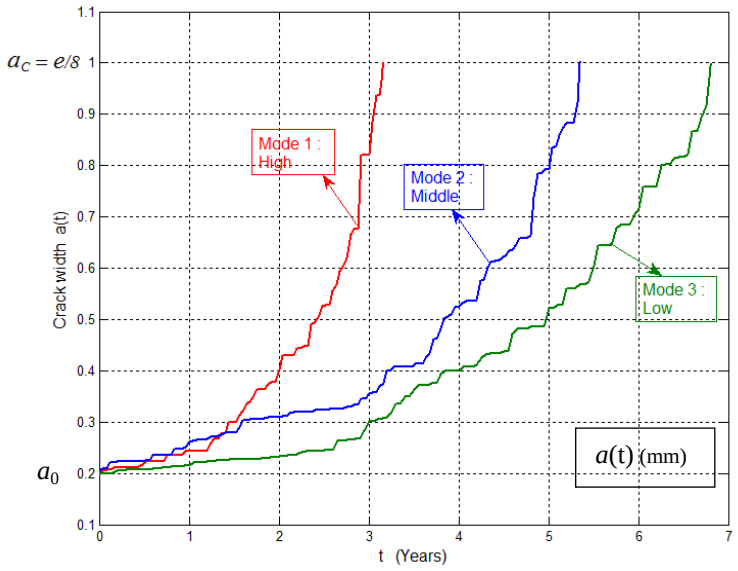

Figure 4.32 - Crack length evolution with time for unburied pipe with random P_0 and a_0.

The simulation of the prognostic equation (17) previously developed permits to draw, for each level of pressure (High, Middle, and Low), the degradation trajectory D in terms of time t. The results of degradation trajectory simulations are shown in figure 4.33 below.

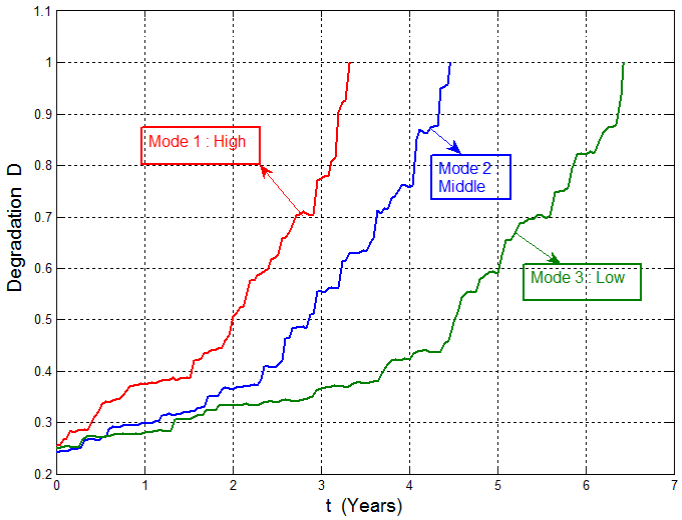

Figure 4.33 - Degradation evolution for unburied pipe with triangular P_0 and lognormal a_0.

Conversely, at each instant t, the Remaining Useful Lifetime RUL(t) = t_C - t (figure 4.34) can be deduced starting from the raw state of the pipe RUL(t_0) = t_C - t_0 which gives the entire age of the pipe, till reaching the failure state (D = D_C = 1) where RUL(t_C) = t_C - t_C = 0 (See example on figure 4.34 for Mode 1: High). The RULs for unburied pipes is nearly 3.6 years for mode 1 (High pressure), 5.1 years for mode 2 (Middle pressure), and 6.35 years for mode 3 (Low pressure).

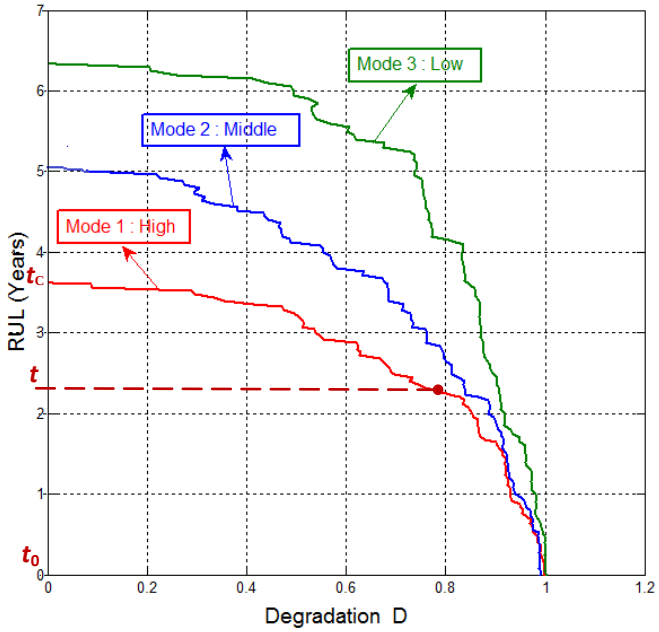

Figure 4.34 - RUL evolution for unburied pipe with triangular P_0 and lognormal a_0.

For buried pipes (figure 4.35), it is nearly 8.75 years for mode 1 (High pressure), 12.08 years for mode 2 (Middle pressure), and 16.33 years for mode 3 (Low pressure).

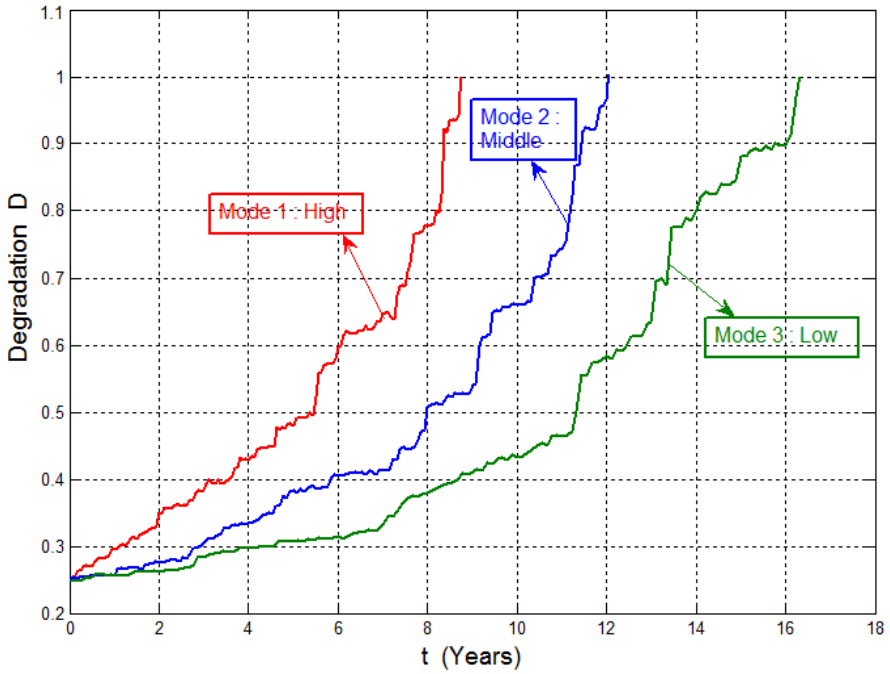

Figure 4.35 - Degradation evolution for buried pipe with triangular P_0 and lognormal a_0.

For offshore pipes (figure 4.36), it is nearly 10.00 years for mode 1 (High pressure), 13.71 years for mode 2 (Middle pressure), and 21.43 years for mode 3 (Low pressure).

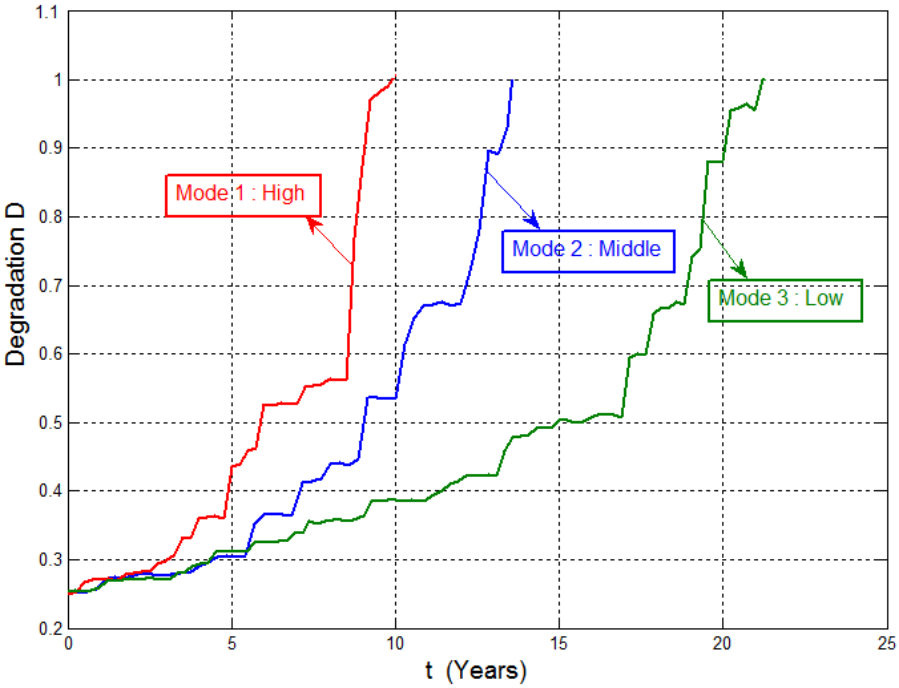

Figure 4.36 - Degradation evolution for offshore pipe with triangular P_0 and lognormal a_0.

The degradation indicator D evolves from D_0 to $D_C = 1$ where the pipe is at the end of its life and this for each pressure mode. The obtained lifetime values are verified to be in the range of real lifetimes according to the references [33,34]. As we can notice, these curves are stochastic and the lifetimes deduced from them are also stochastic. Therefore, we do not have a unique value for the corresponding RUL(t), but a new realization is derived from each simulation of $D(t)$ and the mean values $\overline{D}(t)$ and $\overline{\mathrm{RUL}}(t)$ can be inferred.

IV.11.4 - Nonlinear Case

In this case, we adopt the nonlinear law for damage accumulation developed in Chapter III. As in the previous linear case, we make the stochastic study for one and two random variables.

IV.11.4.1 - One Random Variable (Pressure)

Here, the internal pressure is the result of a triangular simulation using the model B. Three pressure modes are considered: High (in red), Middle (in blue), and Low (in green) where the values are given in table 4.3. The results are represented by the following figures.

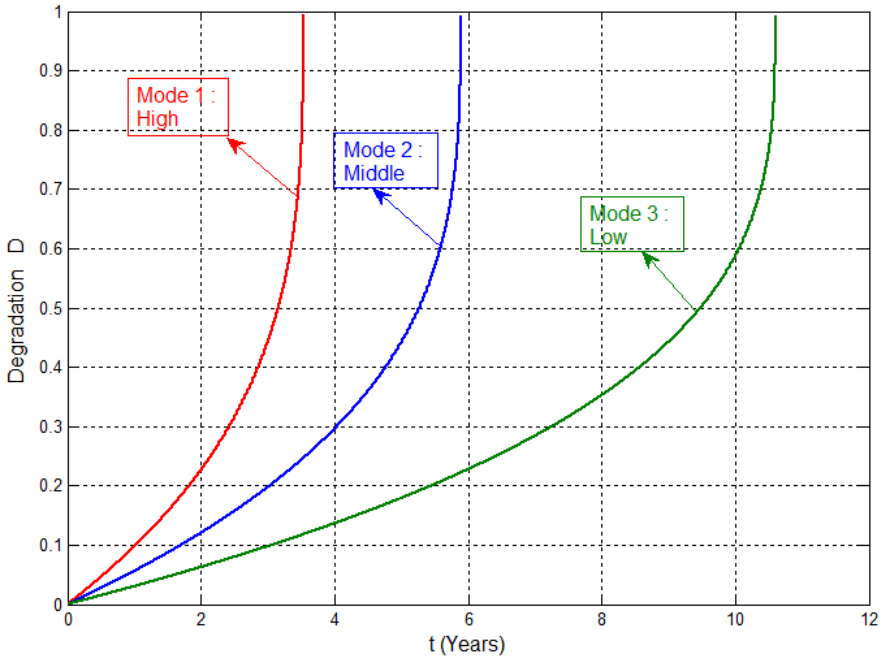

Figure 4.37 - Degradation evolution of unburied pipes under stochastic P and nonlinear damage.

We note from the previous figure 4.37 that the RULs are respectively: 3.53 years for mode 1, 5.89 years for mode 2, and 10.6 years for mode 3. It can be seen clearly that the

smoothness of all the curves can be explained by the dominance of the nonlinear effect on the stochastic one. The degradations increase largely at the final stage of their lives.

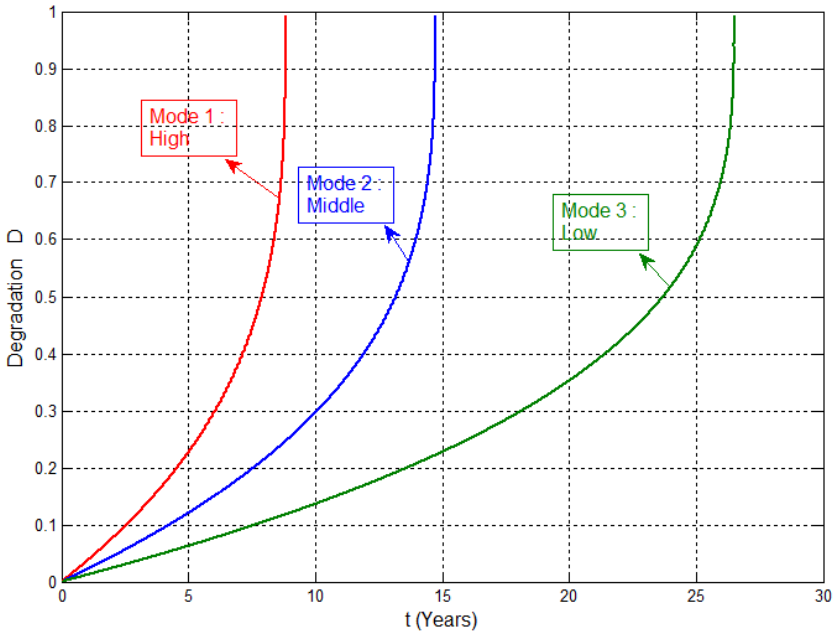

Figure 4.38 - Degradation evolution of buried pipe under stochastic *P* and nonlinear damage.

From the previous figure 4.38, it is noted that the RULs are respectively: 8.8 years for mode 1, 14.7 years for mode 2, and 26.5 for mode 3. It can be seen clearly that the smoothness of all the curves can be explained by the dominance of the nonlinear effect on the stochastic one. The degradations increase considerably at the final stage of their lives.

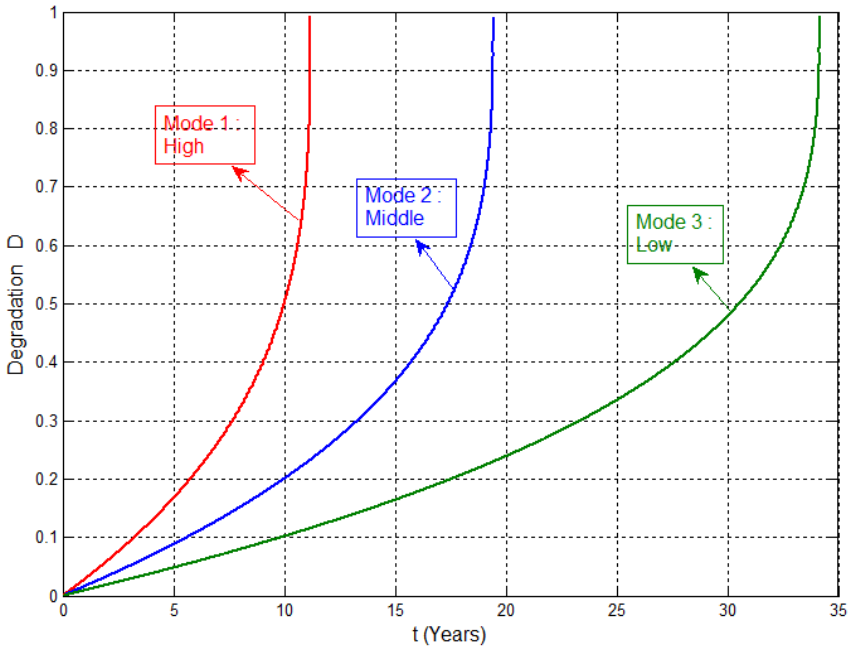

Figure 4.39 - Degradation evolution of offshore pipe under stochastic *P* and nonlinear damage.

Figure 4.39 shows that the RULs are respectively: 11.2 years for mode 1, 19.4 years for mode 2, and 34.2 for mode 3.

As in the three precedent simulations, it can be seen clearly that the smoothness of all the curves can be explained by the fact that the dispersion introduced from the stochastic condition is not very influent. Actuality, the nonlinear effect here dominates the stochastic one related to the random variable *P*. Moreover, degradations increase significantly at the final stage of their lives.

The value obtained for pipes lifetimes are logical knowing that the end of life does not mean necessarily the total replacement of the pipe but that means that the pipe maintenance should be done now.

IV.11.4.2 - Two Random Variables (Pressure and Initial Crack Length)

In this section, two random variables are considered: the pressure and the initial crack length. We execute a triangular simulation of internal pressure *P* using model B for the three modes: High, Middle, and Low (table 4.3). The initial crack length is simulated as a lognormal distribution using the following parameters:

$$\tilde{a}_0 : \text{Lognormal Law} \begin{cases} E(\tilde{a}_0) = 0.2 \text{ mm} \\ \sigma(\tilde{a}_0) = \sqrt{V(\tilde{a}_0)} = 0.002945 \text{ mm} \end{cases}$$

The equivalent normal parameters for a_0 are inferred as follows:

$$\lambda = Ln\left[E(a_0)\right] - \frac{1}{2}Ln\left(1 + \frac{V(a_0)}{E(a_0)^2}\right) = Ln(0.2) - 0.5Ln\left(1 + \frac{8.673\times10^{-6}}{0.04}\right) = -1.6094 - 0.5\times2.168\times10^{-4}$$

$$= -1.6095 \text{ mm}$$

$$\xi^2 = Ln\left(1 + \frac{V(a_0)}{E(a_0)^2}\right) \Rightarrow \xi = \sqrt{Ln\left(1 + \frac{V(a_0)}{E(a_0)^2}\right)} = \sqrt{Ln\left(1 + \frac{8.673\times10^{-6}}{0.04}\right)} = \sqrt{2.168\times10^{-4}} = 0.014724 \text{ mm}$$

The initial damage D_0 is deduced from a_0 as follows:

$$D_0 = \frac{a_0}{a_C - a_0} \Rightarrow \tilde{D}_0 = \frac{\tilde{a}_0}{a_C - \tilde{a}_0}$$

$$\Rightarrow \tilde{D}_0 : \text{Lognormal Law} \begin{cases} E(\tilde{D}_0) = 0.008 \\ \sigma(\tilde{D}_0) = \sqrt{V(\tilde{D}_0)} = 3.784\times10^{-4} \end{cases}$$

The nonlinear cumulative damage, previously demonstrated, is given at each cycle N by:

$$\tilde{D}(N) = 1 - \left[\left(1 - \tilde{D}_0\right)^{\alpha+1} - \frac{N - N_0}{N_C} \left(1 - \frac{\sigma_0}{\Delta\tilde{\sigma}_j / 2}\right)^m (\alpha + 1) \right]^{\frac{1}{\alpha+1}}$$

$$\tilde{D}_0 = \frac{\tilde{a}_0}{a_C - \tilde{a}_0}$$

Figure 4.40 below reveals the crack width growth as a function of time t. It is noted that the low pressure mode reveals the lowest increase rate (slope) in crack width in comparison with the two other pressure modes. Consequently, these two previous modes reach earlier the critical width a_C.

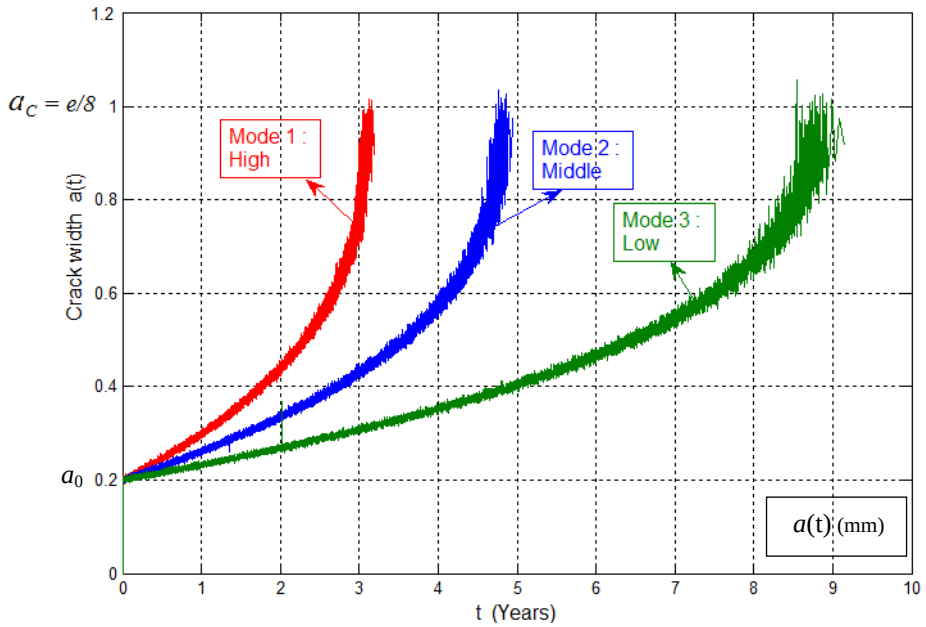

Figure 4.40 - Crack width evolution with time of unburied pipe under stochastic pressure and initial crack length for nonlinear damage.

The simulation of the prognostic equation (22) permits to draw the degradation trajectory for each level of pressure: High (red), Middle (blue), and Low (green), by considering the three cases of pipelines.

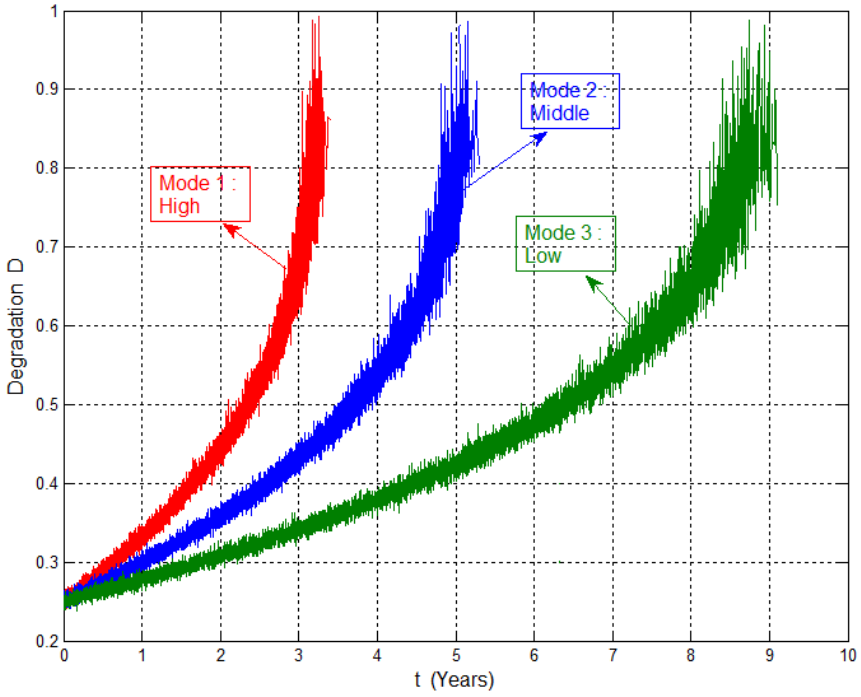

Figure 4.41 - Degradation evolution of unburied pipe under stochastic P and a_0 for nonlinear damage.

The results for unburied pipes (figures 4.41 & 4.42) show that the pipe lifetime for this case is nearly 3.20 years for mode 1 (High pressure), 5 years for mode 2 (Middle pressure), and 9 years for mode 3 (Low pressure). The degradation curves show more steep evolution for the two first modes than the third mode.

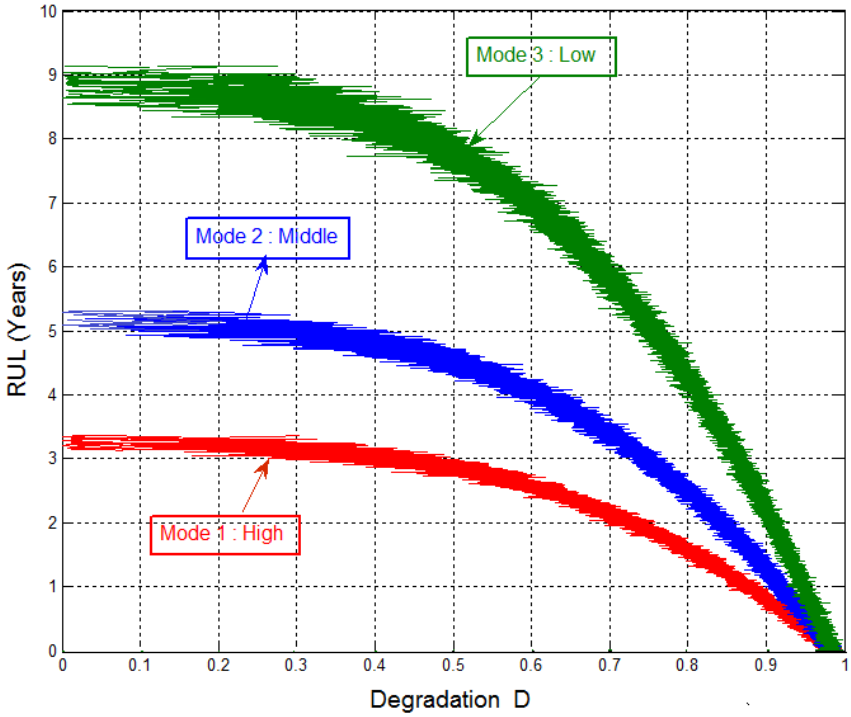

Figure 4.42 - RUL evolution of unburied pipe under stochastic P and a_0 for nonlinear damage.

For buried pipes (figure 4.43) the lifetime is nearly 7.49 years for mode 1 (High pressure), 12.91 years for mode 2 (Middle pressure), and 22.64 years for mode 3 (Low pressure). The degradation curves show also more steep evolution for the two first modes than the third mode.

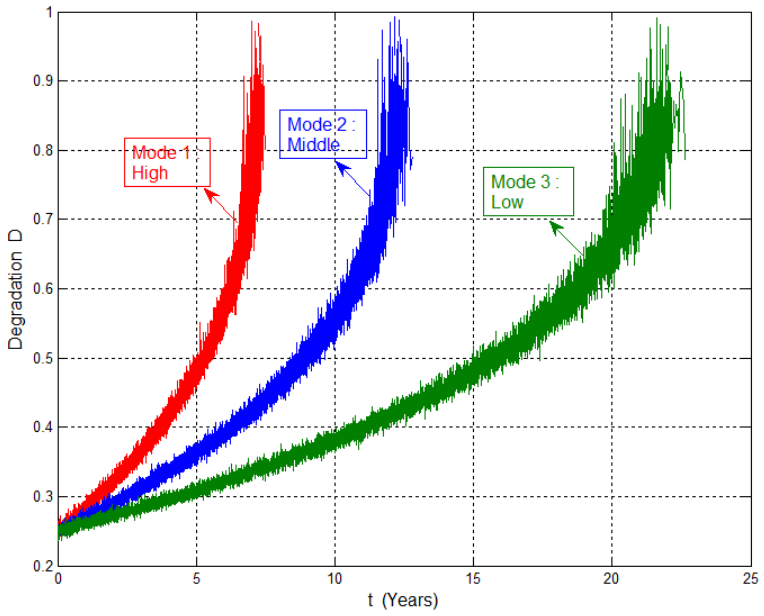

Figure 4.43 - Degradation evolution of buried pipe under stochastic P and a_0 for nonlinear damage.

The lifetimes for offshore pipes (figure 4.44) show that is nearly 9.25 years for mode 1 (High pressure), 16.41 years for mode 2 (Middle pressure), and 28.72 years for mode 3 (Low pressure). The degradation evolutions are steeper for the two first modes than the third mode.

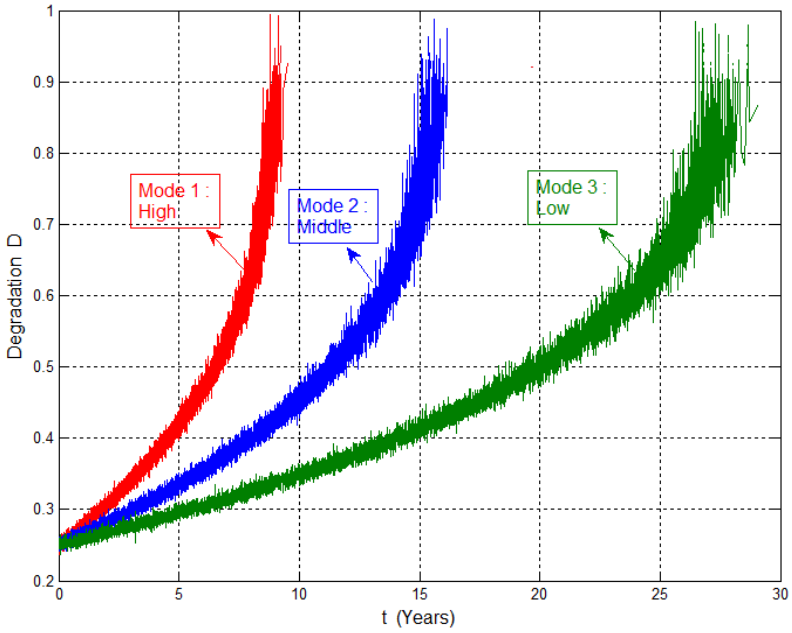

Figure 4.44 - Degradation evolution of offshore pipe under stochastic P and a_0 for nonlinear damage.

The stochastic influence can be seen through the variability over the curve realizations of $D(t)$ obtained by many simulations and not from just one realization. Contrarily to the case of one random variable, the curves are not smooth and the stochastic effects are clearer here.

To more exploit these results, a mean curve $\overline{D}(t)$ can be plotted from the mean value of these realizations. The conservative curves are those that give the maximum values. For each mode, a characteristic curve of lifetime can be computed from the mean values, the standard deviation values, and a certain fractal percentage depending on the risk adopted by decision makers.

IV.11.4.2.1 - Comparison: Deterministic - Stochastic Results (Nonlinear Damage Law)

To show the stochastic effects, a comparison is done between the deterministic results and the stochastic results (figure 4.45).

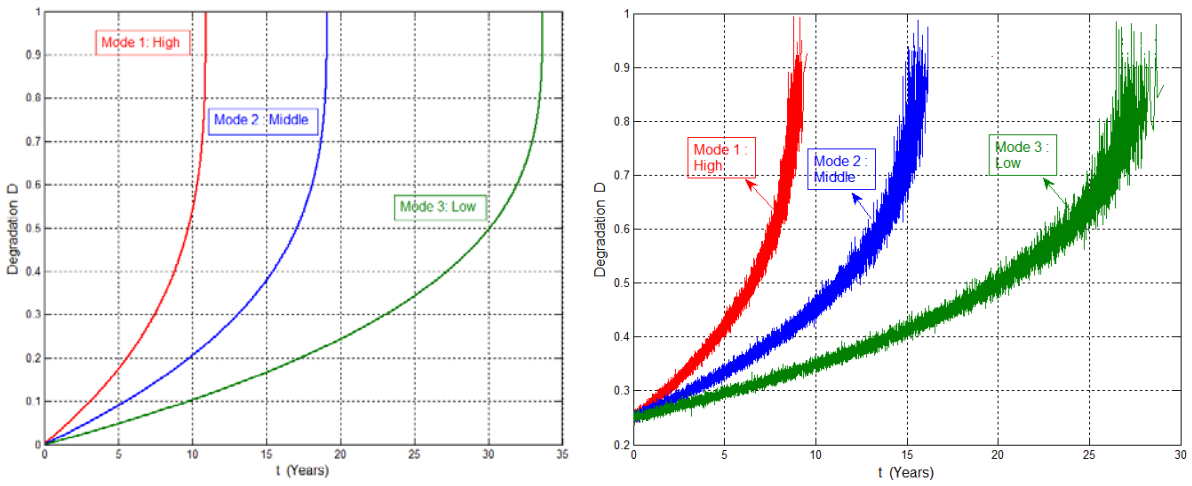

Figure 4.45 - Deterministic and stochastic (P, a_0) study of offshore pipes degradation under nonlinear damage law.

	Deterministic nonlinear	Stochastic nonlinear	Decrease (%)
Mode 1	10.92 years	9.25 years	15.3%
Mode 2	19.11 years	16.41 years	14.1%
Mode 3	33.67 years	28.72 years	14.7%

For all modes of internal pressure, the lifetimes of pipes decrease about 15% from the deterministic case to the stochastic case. These reductions are explained by the fact that the dispersions introduced by the random variables have a negative effect on the lifetimes' predictions. The stochastic effect is more pronounced and effective for two random variables than for one random variable. The curves for each mode fluctuate and they constitute a bundle of trajectories which are the realizations of many simulations.

IV.11.5 - Validation of the Pipelines Lifetimes in Stochastic Conditions

The obtained lifetimes values for linear and nonlinear damage rules in stochastic conditions can be verified to be in the range of real lifetimes according to the references [34,35,36]. In fact, a fatigue life of pipes under good exploitation conditions was found to be 26 years in average which is very close to the results obtained for pipes in mode 3 in stochastic nonlinear case.

IV.12 - Conclusion

In this chapter the prognostic model is developed to consider the prognostic computation in stochastic conditions. Hence, the model is a general one as it is based on the linear and nonlinear accumulation of damage due to fatigue crack propagation in stochastic conditions. These last conditions are taken into account by considering two random variables which are the applied loading and the initial crack length. Two cases are explored separately: one random variable and two random variables.

The fatigue failure is considered and the damage state of the device is measured by a degradation indicator in terms of the number of loading cycles starting from an initial damage. The lifetimes are concluded from the time reading at each instant on the degradation curve. The Remaining Useful Lifetimes at each instant are deduced from the degradation curve by subtracting the current instant from the last predicted instant.

To show the efficiency of this stochastic prognostic model, it is applied to predict the fatigue life of vehicle suspension systems and of petrochemical pipelines under three modes of internal pressure. Lifetimes results are obtained for linear and nonlinear stochastic cases.

The stochastic results for one random variable show that the nonlinear case is always dominant where the curves are not fluctuant. Contrarily, for two random variables case the stochastic effects become more influent and the curves of degradation are fluctuant and constituted of bundles of trajectories. In this case the lifetimes are reduced due to the dispersion effects.

References

[1] A.K.S. JARDINE. D.L. and D. BANJEVIC: A review on machinery diagnostics and prognostics implementing condition-based maintenance. *Mechanical Systems and Signal Processing*, 20 (7): 1483-1510, 2006.

[2] A. ABOU JAOUDE, H. NOURA, K. EL-TAWIL, S. KADRY, and M. OULADSINE, "Analytic and Nonlinear Prognostic for Vehicle Suspension Systems," 2012 IEEE International Conference on Prognostic and Health Management (PHM 2012), Denver, Colorado, USA, June 18-21, 2012.

[3] A. ABOU JAOUDE, H. NOURA, K. EL-TAWIL, S. KADRY, and M. OULADSINE, "Stochastic Prognostic Paradigm for Petrochemical Pipelines Subject to Fatigue," International Journal of Systems Science (IJSS), Taylor & Francis publishers, London, 2012, submitted.

[4] A. HESS, G. CALVELLO, P. FRITH, S. ENGEL, and D. HOITSMA, "Challenges, Issues, and Lessons Learned Chasing the 'Big P': Real Predictive Prognostics Part 2," Proc. IEEE 1489 (2), 2005.

[5] S. MOHANTY, S. DAS, A. CHATTOPADHYAY, P. PERALTA, and C. WILLHAUCK, "Time Series Prediction of Fatigue Crack Growth Using Multi-Variate Gaussian Processes," International Journal of Fatigue, 2008.

[6] J.M. LARSEN and L. CHRISTODOULOU, "Integrated Damage State Awareness and Mechanism-Based Prediction," Journal of Metals, TMS, p.14, March 2004.

[7] L. CHRISTODOULOU and J.M. LARSEN, "Using Materials Prognosis to Maximize the Utilization Potential of Complex Mechanical Systems," Journal of Metals, TMS, pp. 15-19, March 2004.

[8] S.J. HUDAK, JR., M.P. ENRIGHT, R.C. MCCLUNG, H.R. MILLWATER, A. SARLASHKAR, and M.J. ROEMER, "Potential Benefits of Adding Probabilistic Damage Accumulation to Prognosis of Turbine Engine Reliability," SwRI Final Report to AFRL/DARPA, Contract No. F33615-97-D-5271, June 30, 2002.

[9] G.R. LEVERANT, D.L. LITTLEFIELD, R.C. MCCLUNG, H.R. MILLWATER, and J.Y. WU, "A Probabilistic Approach to Aircraft Turbine Material Design," Paper 97-GT-22, ASME International Gas Turbine & Aeroengine Congress, 1977.

[10] M.P. ENRIGHT, Y.D. LEE, R.C. MCCLUG, L. HUYSE, G.R. LEVERANT, H.R. MILLWATER, and S.K. FITCH, "Probabilistic Surface Damage Tolerance Assessment of Aircraft Turbine Rotors," Paper GT-2003-38731, Proceedings, 48th ASME International Gas Turbine & Aeroengine Technical Congress, Atlanta, GA, June 2003.

[11] J.N. YANG and S.D. MANNING, "Stochastic Crack Growth Analysis Methodologies for Metallic Structures," Engineering Fracture Mechanics, 37 (5),1105-1124, 1990.

[12] J.N. YANG and S.D. MANNING, "A Simple Second Order Approximation for Stochastic Crack Growth Analysis," Probabilistic Engineering Mechanics, 18, 107-118, 2003.

[13] W.F. WU and C.C. NI, "A Study of Stochastic Fatigue Crack Growth Modeling through Experimental Data," Probabilistic Engineering Mechanics, 18,107-118, 2003.

[14] W.F. WU and C.C. NI, "Probabilistic Models of Fatigue Crack Propagation and Their Experimental Verification," Probabilistic Engineering Mechanics 19,247-257, 2004.

[15] K. SOBCZYK, and B.F. SPENCER, "Random Fatigue: from Data to Theory," Academic press, Boston, MA, 1992.

[16] J.L. BOGDANOFF and F. KOZIN, "Probabilistic Models of Cumulative Damage," Wiley, New York, 1985.

[17] F. KOZIN and J.L. BOGDANOFF, "Probabilistic Models of Fatigue Crack Growth: Results and Speculations," Nuclear Engineering and Design 115, 143-171, 1989.

[18] W.Q. ZHU, Y.K. LIN, and Y. LEI, "On Fatigue Crack Growth under Random Loading," Engineering Fracture Mechanics 43 (1), 1-12, 1992.

[19] C. WILLHAUCK, S. MOHANTY, A. CHATTOPADHYAY, and P. PERALTA, "Stochastic Crack Growth under Variable Loading for Health Monitoring and Prognosis," Proceeding of SPIE 6926 69260L, San Diego, California, USA, 2008.

[20] J.N. YANG, S.D. MANNING, J.L. RUDD, and M.E. ARTLEY, "Probabilistic Durability Analysis Methods for Metallic Airframes," Probabilistic Engineering Mechanics 2 (1), 9-15, 1987.

[21] Y.J., HONG, J. XING, and J.B. WANG, "Statistical Analysis of Fatigue Crack Growth for 16MnR Steel under Constant Amplitude Loads," International Journal of Pressure Vessels and Piping 76, 379-385, 1999.

[22] B. MORENO, J. ZAPATERO, and J., DOMINGUEZ, "An Experimental Analysis of Fatigue Crack Growth under Random Loading," International Journal of Fatigue 25, 597-608, 2003.

[23] T.K. SERGEEVA, A.C. BOLOTOV, et al., "Monitoring of Steel Condition in Main Pipelines during Their Stress-Corrosion Induced Failures," Chemical and oil Machinery, No. 2, pp. 72-76, 1996.

[24] C.E. JASKE, "Fitness-for-service Assessment for Pipelines Subject to Stress-corrosion cracking," The pipeline pigging and integrity conference, February 2000.

[25] S.A. TIMASHEV, M.G. MALYUKOVA, and, LL. MALTSEV, "Updating the Assessment of Remaining Life of Pipelines using Latest ILI Data and the Importance Sampling Method," Science and Engineering center, *Reliability and resource of large machine systems*, Ural Branch, Russian academy of sciences, Rotterdam, ICOSSAR 2005.

[26] P. PARIS, F. ERDOGAN, "A Critical Analysis of Crack Propagation Laws," Journal of Basic Engineering, Transactions of the American Society of Mechanical Engineers, Vol. 85, No. 4, pp. 528-534, 1963.

[27] A. ABOU JAOUDE, S. KADRY, K. EL-TAWIL, H. NOURA, and M. OULADSINE, "Analytic Prognostic for Petrochemical Pipelines," Journal of Mechanical Engineering Research (JMER), Vol. 3(3), pp. 64-74, March 2011.

[28] A. ABOU JAOUDE, K. EL-TAWIL, S. KADRY, H. NOURA, and M. OULADSINE, "Prognostic Model for Buried Tubes," International Conference on Advanced Research and Applications in Mechanical Engineering (ICARAME'11), Notre Dame University, Louaize, Lebanon, June 13-15, 2011.

[29] M.A. MINER, "Cumulative Damage in Fatigue," Journal of Applied Mechanics, vol. 12, A159-A164, 1945.

[30] J. LEMAITRE and J. CHABOCHE, *Mechanics of Solid Materials.* New York: Cambridge University Press, 1990.

[31] G. PETRUCCI and B ZUCCARELLO, "Fatigue life prediction under wide band random loading," Dipartimento di Meccanica, Universita degli Studi di Palermo, Viale delle Scienze, Italy, April 2004.

[32] J. MADSEN, D. GHIOCEL, D. GORSICH, D. LAMB, and D. NEGRUT,"A Stochastic Approach to Integrated Reliability Prediction," University of Wisconsin-Madison, June 4, 2009

[33] A. ABOU JAOUDE, H. NOURA, K. EL-TAWIL, S. KADRY, and M. OULADSINE, "Analytic Prognostic Model for Stochastic Fatigue of Petrochemical Pipelines," Australian Control Conference (AUCC 2012), Sydney, Australia, November 15-16, 2012.

[34] X. GUAN, R. JHA, and Y. LIU, "Trans-dimensional MCMC for Fatigue Prognosis Model Determination, Updating, and Averaging," Annual Conference of the Prognostic and Health Management society, 2010.

[35] Y. XIANG and Y. LIU, "Efficient Probabilistic Methods for Real-time Fatigue Damage Prognosis," Annual Conference of the Prognostic and Health Management Society, 2010.

[36] R. PALMER-JONES and T. E. TURNER, "Pipeline Buckling, Corrosion and Low Cycle Fatigue," Offshore Mechanics and Arctic Engineering, OMAE '98 Lisbon, United Kingdom July 5-9, 1998.

CONCLUSION and FUTURE WORKS

A prognostic model is introduced in this thesis that permits to predict the degradation trajectory of a dynamic system; it is based firstly on analytical laws of damage such as the crack propagation law and linear damage accumulation law. Secondly, it is based on nonlinear damage accumulation and finally, the stochastic influences are considered.

In the approaches based on physical or mathematical models, the knowledge of the fundamental equations of the dynamic behavior of degradation appears to be very useful. In fact, in case we change the system properties or of degradation, the parameters can be readjusted and then the approach is adaptable to a new case. The approaches guided by data assume a reliable estimation of the current state of degradation in order to predict the future evolution of the system. They lack reactivity when facing a change in usage conditions and the efficiency is strongly linked to the sample of data that serves to compute the model parameters. The third approach which is the Experience-based approach requires little expert knowledge of the degradation mechanisms. It remains simple to implement but it is also insensitive to a change in the system operating mode. In addition, the models derived have only two states: a state of functioning, and a state of failure, and do not comprise a state of degraded functioning.

The proposed model belongs to the first prognostic approach which is the model-based approach. Whenever the analytic damage laws are available, this model can be adaptable to new situations or cases. In industrial systems, this model shows that it is convenient and practical as a flexible tool for prognostic analysis.

The failure mode treated in this thesis is the fatigue of the device material. The considered damage is the crack propagation due to fatigue. The damage state of the device is measured by a degradation indicator D in terms of the number of loading cycles N. The proposed model is based on the link between a conventional index of degradation D that varies from zero to one and the crack length a. A failure is produced when a reaches a critical length a_C. The model is then expressed by a recursive function relating the degradation in two consecutive cycles to the critical number of cycles and the endurance stress limit of the

material. From a detected initial crack, the degradation trajectories have been drawn in terms of cycle loading.

The analytic prognostic model introduced in this thesis permits to predict, at each cycle or instant, the remaining useful lifetime of the system by a simple and practical way. The lifetimes are concluded from the time reading at each instant on the degradation curves or trajectories. To show the efficiency of this prognostic model, it is applied in simulation to predict the fatigue life of the petrochemical pipeline systems and of the vehicle suspension systems. In fact, the degradation trajectories deduced allow us to determine their remaining useful lifetimes.

There are many causes and contributors to pipelines failures, including construction errors, material defects, pressure fluctuations, gas blows, internal and external corrosion, operational errors, malfunction of control systems and outside force damage (e.g., by third parties during excavation). Pipeline incidents can result in a loss of life, serious injury, property damage, and environmental damage, although major incidents are infrequent. In many cases, pipelines placed underground, under runways or roadways are required to resist the influence of the overlying soil and many surface traffic loads accidents as well as the effect of corrosion and material failure like fatigue. For these reasons, the fatigue life prediction is done for unburied, buried and offshore pipelines under three modes of internal pressure.

Additionally, a nonlinear interaction effect exists between high cycle fatigue (HCF) and low cycle fatigue (LCF) in many engineering materials. It has been observed within uniaxial loadings, and more pronounced under multiaxial loading, particularly when the loading is non-proportional. This nonlinear modeling is especially important to take into account the nature of the applied constraints and influent environment that can accentuate the nonlinear aspect related to some materials behavior subject to fatigue effects.

In the proposed nonlinear accumulation of damage, the damage state of the device is measured by a recursive nonlinear degradation function in terms of the number of cycles or usage time. This nonlinear prognostic model is applied to estimate the fatigue life of a pipeline system and a vehicle suspension system in order to reveal the effectiveness of this model. The RUL results obtained are compared to previous results of a linear model and the

differences are justified by the multiple trends of degradation (linear, convex, and concave). The present nonlinear prognostic model will allow us to include the stochastic aspect which will improve the intended prediction capacity of the model.

In the extended stochastic model, based on the accumulation of damage due to fatigue crack propagation in stochastic conditions, the initial crack length and the loading are taken as random. The prognostic model becomes more precise in RUL prediction. Lifetime results are obtained for linear and nonlinear damage cases and the differences are justified by the multiple trends of degradation also. Stochastic crack propagation involves models with random parameters which can be estimated using Monte Carlo simulations. The stochastic parameters are affected by some probability of realization that influences the resulting RUL deduced from the degradation trajectory.

As prospective and future works, it is planned to more develop the proposed prognostic methodology and apply it to a wide set of dynamic systems. This is by taking into consideration other analytic laws besides Paris-Erdogan's law for crack propagation and other damage accumulation laws. Additionally, more probabilistic basic parameters like the material and the environmental parameters can be considered. Furthermore, additional probabilistic laws for the parameters other than the Normal and the Log-normal laws can be explored. Also, it is planned to more explore the variability of the stochastic lifetimes and to deduce a bundle of degradation curves from which a mean curve and a characteristic lifetime curve can be inferred. The characteristic curve is the one attached to some predefined acceptable risk.

As well, in the pipeline application, other internal pressure model fluctuation can be taken into account as for example the model of the Fourier series. In the automotive suspension system, the output variables (vertical displacements of dampers) can be derived from the input variables (road profile). This is done by a resolution of a convenient dynamic model by considering the inertial forces which are due to the vehicle oscillatory movement on a road with an irregular surface.

LIST OF PUBLICATIONS

International Journals

[1] A. ABOU JAOUDE, K. EL-TAWIL, S. KADRY, "Prediction in Complex Dimension Using Kolmogorov's Set of Axioms", Journal of Mathematics and Statistics, vol. 6(2), pp. 116-124, 2010.

[2] A. ABOU JAOUDE, K. EL-TAWIL, S. KADRY, H. NOURA, and M. OULADSINE, "Analytic Prognostic Model for a Dynamic System", International Review of Automatic Control (IREACO), November 2010.

[3] A. ABOU JAOUDE, S. KADRY, K. EL-TAWIL, H. NOURA, and M. OULADSINE, "Analytic Prognostic for Petrochemical Pipelines", Journal of Mechanical Engineering Research (JMER), April 2011.

[4] A. ABOU JAOUDE, H. NOURA, K. EL-TAWIL, S. KADRY, and M. OULADSINE, "Stochastic Prognostic Paradigm for Petrochemical Pipelines Subject to Fatigue", International Journal of Systems Science (IJSS), Taylor & Francis publishers, London, 2012, submitted.

International Conferences

[1] K. EL-TAWIL, A. ABOU JAOUDE, S. KADRY, H. NOURA, and M. OULADSINE, "Prognostic Based on Analytic Laws Applied to Petrochemical Pipelines", International Conference on Computer-aided Manufacturing and Design (CMD 2010), China, November 2010.

[2] A. ABOU JAOUDE, K. EL-TAWIL, S. KADRY, H. NOURA, and M. OULADSINE, "Prognostic Model for Buried Tubes", International Conference on Advanced Research and Applications in Mechanical Engineering (ICARAME'11), Notre Dame University, Louaize, Lebanon, June 13-15, 2011.

[3] A. ABOU JAOUDE, H. NOURA, K. EL-TAWIL, S. KADRY, AND M. OULADSINE, "Lifetime Analytic Prognostic for Petrochemical Pipes Subject to Fatigue", SAFEPROCESS, 8th IFAC Symposium on Fault Detection, Supervision and Safety of Technical Processes, Mexico City, Mexico, August 29-31, 2012.

[4] A. ABOU JAOUDE, H. NOURA, K. EL-TAWIL, S. KADRY, and M. OULADSINE, "Analytic and Nonlinear Prognostic for Vehicle Suspension Systems", 2012 IEEE International Conference on Prognostic and Health Management (PHM 2012), Denver, Colorado, USA, June 18-21, 2012.

[5] A. ABOU JAOUDE, H. NOURA, K. EL-TAWIL, S. KADRY, and M. OULADSINE, "Analytic Prognostic Model for Stochastic Fatigue of Petrochemical Pipelines", Australian Control Conference (AUCC 2012), Sydney, Australia, November 15-16, 2012.

THESIS ABSTRACTS

Advanced Analytical Model for the Prognostic of Industrial Systems Subject to Fatigue

The high availability of technological systems like aerospace, defense, petro-chemistry and automobile, is an important goal of earlier recent developments in system design technology knowing that the expensive failure can generally occur suddenly.

To make the classical strategies of maintenance more efficient and to take into account the evolving product state and environment, a new analytic prognostic model is developed as a complement of existent maintenance strategies. This new model is applied to mechanical systems that are subject to fatigue failure under repetitive cyclic loading. Knowing that, the fatigue effects will initiate micro-cracks that can propagate suddenly and lead to failure.

This model is based on existing damage laws in fracture mechanics, such as the crack propagation law of Paris-Erdogan beside the damage accumulation law of Palmgren-Miner. From a predefined threshold of degradation D_C, the Remaining Useful Lifetime (RUL) is estimated by this prognostic model. Damages can be assumed to be accumulated linearly (Palmgren-Miner's law) and also nonlinearly to take into consideration the more complex behavior of loading and materials.

The degradation model developed in this work is based on the accumulation of a damage measurement D after each loading cycle. When this measure reaches the predefined threshold D_C, the system is considered in wear out state. Furthermore, the stochastic influence is included to make the model more accurate and realistic.

In this work, two main applications are considered: in automobile industry, a prognostic assessment of the suspension component permits to enhance its maintenance strategies; and in petrochemical industries, pipelines are studied to prevent the sudden and harmful leakage or blows.

Keywords: Prognostic, Remaining Useful Lifetime, Fatigue, Degradation, Analytic model, Linear accumulation, Nonlinear accumulation, Damage, Stochastic.

Modèle Analytique Avancé pour le Pronostic des Systèmes Industriels Soumis à la Fatigue

La disponibilité élevée des systèmes technologiques comme l'aérospatial, la défense, la pétrochimie et l'automobile, est un but important des nouveaux développements de la technologie de conception des systèmes sachant que la défaillance onéreuse survient, en général, soudainement.

Afin de rendre les stratégies classiques de maintenance plus efficaces et pour prendre en considération l'état et l'environnement évolutifs du produit, un nouveau modèle de pronostic analytique est développé en tant que complément des stratégies de maintenance existantes. Ce nouveau modèle est appliqué aux systèmes mécaniques soumis à la défaillance par fatigue sous charge cyclique répétitive. Sachant que l'effet de fatigue va initier des microfissures qui peuvent se propager soudainement et conduire à la défaillance.

Ce modèle est basé sur des lois d'endommagement existantes dans la mécanique de la rupture comme la loi de propagation de fissures de Paris-Erdogan à côté de la loi de cumul de dommage de Palmgren-Miner. A partir d'un seuil prédéfini de dégradation D_C, la durée de vie résiduelle (RUL) est estimée à l'aide de ce modèle de pronostic. Les dommages peuvent être cumulés linéairement (Loi de Palmgren-Miner) et aussi non linéairement afin de prendre en compte un comportement plus complexe des chargements et des matériaux.

Le modèle de dégradation développé dans ce travail est basé sur une sommation d'une mesure de dommage D à la suite de chaque cycle de chargement. Quand cette mesure devient égale à un seuil prédéfini D_C, le système est considéré dans l'état de panne. En plus, l'influence stochastique est incluse dans notre modèle pour le rendre plus précis et réaliste.

Dans ce travail, deux applications principales sont considérées: dans l'industrie automobile, l'évaluation de pronostic des éléments de suspension permet d'améliorer ses stratégies de maintenance; et dans l'industrie pétrochimique, les pipelines sont étudiés afin de prévenir des fuites et des explosions soudaines et nocives.

Mots-clefs: Pronostic, Durée de vie résiduelle, Fatigue, Dégradation, Modèle analytique, Cumul linéaire, Cumul non-linéaire, Dommage, Stochastique.

RÉSUMÉ DE LA THÈSE

Modèle Analytique Avancé pour le Pronostic des Systèmes Industriels Soumis à la Fatigue

La disponibilité élevée des systèmes technologiques comme l'aérospatial, la défense, la pétrochimie et l'automobile, est un but crucial des nouveaux développements de la technologie de conception des systèmes. En général, la défaillance est onéreuse et elle survient soudainement.

Le pronostic consiste en la capacité de "prévoir et prévenir" des défauts possibles ou de la dégradation du système avant l'occurrence des pannes. S'il était possible de prédire efficacement l'état des machines et des systèmes, les actions de maintenance peuvent être exécutées au bon moment. Le pronostic est défini comme "prédire la défaillance quand elle survient", autrement, parvenir à un moyen de calcul de la durée de vie résiduelle d'un composant. Afin d'obtenir un pronostic efficace et fiable, il est nécessaire d'avoir un diagnostic efficace et fiable.

Au sens Automatique du terme, le pronostic est généralement associé à la notion de dégradation qui représente le cumul de l'usure d'un système. Il consiste à prévoir la future évolution de la dégradation en prenant en considération les facteurs qui modifient les dynamiques de la dégradation. Ces facteurs peuvent être divisés en deux catégories: les facteurs liés à la sollicitation du système et ceux liés à l'environnement dans lequel le système évolue. Normalement, l'influence de ces deux catégories sur la dégradation n'est pas bien connue.

Comme les stratégies classiques de maintenance peuvent être améliorées puisqu'elles négligent l'état et l'environnement évolutifs du produit, alors les approches de pronostic ont prouvé leurs intérêts dans ce domaine.

Différentes méthodes ont été appliquées au pronostic des composants dégradés. En général, les approches de pronostic peuvent être classifiées en trois catégories fondamentales:

(1) Approches "à base de modèles",
(2) Approches "guidées par les données", et
(3) Approches basées sur les techniques probabilistes.

L'avantage principal des approches "à base de modèles" est leur capacité à inclure les informations physiques du système surveillé. De même, si les informations recueillies de la dégradation du système deviennent plus disponibles, alors le modèle de pronostic peut être réadapté pour prendre en compte ces nouvelles informations afin d'augmenter sa précision de prédiction et de traiter des problèmes de performance plus délicats.

Cependant, les approches "guidées par les données" s'appliquent lorsque le modèle n'existe pas mais elles nécessitent un nombre suffisant de mesures de bonnes qualités afin de bien refléter l'image de dégradation du système.

Les approches basées sur les techniques probabilistes nécessitent un excellent retour d'expérience (historique, données expertes, etc.) permettant une modélisation stochastique ou probabiliste de la dégradation. Ces approches sont bien adaptées aux systèmes complexes pour lesquels il est difficile d'avoir un modèle physique.

Une nouvelle procédure analytique de pronostic "à base de modèles" est développée dans cette thèse et appliquée aux systèmes mécaniques soumis à la fatigue sous charge cyclique répétitive; sachant que les effets de la fatigue initieront des microfissures qui peuvent se propager soudainement et conduire à la défaillance.

Ce modèle est basé sur des lois d'endommagement existantes dans la mécanique de la rupture comme la loi de propagation de fissures de Paris-Erdogan à côté de la loi de cumul de dommage de Palmgren-Miner. A partir d'un seuil prédéfini de dégradation D_C, la durée de vie résiduelle (RUL) est estimée à l'aide de ce modèle de pronostic. Les dommages peuvent être cumulés linéairement (Loi de Miner) et aussi non linéairement afin de prendre en compte un comportement plus complexe.

Cette thèse est dédiée au pronostic des systèmes dynamiques. Les travaux de cette thèse ont pour but le développement d'un outil avancé permettant de traiter l'évaluation du pronostic dans un contexte déterministe linéaire et non-linéaire dans un premier temps, et

dans un contexte stochastique dans un second temps. Notre objectif est de préparer un moyen général de pronostic capable de bien prédire la durée de vie résiduelle (RUL) d'un système. Cette prédiction est basée sur un cumul analytique de dommage et ceci dans les deux contextes déterministe et stochastique.

Notre modèle de dégradation est fondé sur un cumul d'une mesure de dommage D à la suite de chaque cycle de chargement. Quand cette somme devient égale à D_C, le système est considéré dans un état de panne. En plus, l'effet stochastique est inclus dans notre modèle pour le rendre plus précis.

Dans ce travail, deux applications principales sont considérées: dans l'industrie automobile où l'évaluation de pronostic des éléments de suspension permet d'améliorer ses stratégies de maintenance; et dans l'industrie pétrochimique dans laquelle les pipelines sont étudiés afin de prévoir des éventuelles fuites et des explosions soudaines et nocives.

Le premier chapitre est consacré à la littérature et à l'état de l'art général de la science de pronostic. Il décrit amplement les différentes approches proposées dans ce domaine par les spécialistes de pronostic.

En effet, dans ce premier chapitre, un tour d'horizon complet des approches de pronostic est présenté, aussi bien que les avantages et les inconvénients de chacune des trois familles de pronostic sont abordés. Il montre la grande importance de ces genres d'étude pour les systèmes technologiques et industriels. La méthodologie basée sur les abaques de dégradation est discutée. Elle a montré l'importance de cette nouvelle approche qui permet de surmonter les inconvénients des modèles de pronostic existants à conditions d'avoir un grand nombre de données disponibles et fiables.

Le problème principal de l'approche basée sur l'expérience est qu'elle ne peut pas être appliquée dans le cas des nouveaux systèmes pour lesquels les données collectées par retour d'expérience n'existent pas ou s'avèrent insuffisantes.

Les approches guidées par les données s'appuient sur une estimation fiable de l'image de l'état courant de dégradation afin de prédire la future évolution du système. L'efficacité des méthodes d'apprentissage est liée fortement à l'échantillon des données qui sert à calculer les

paramètres du modèle. Si une situation non apprise surviendra, le pronostic peut être aléatoire. De même, les approches guidées par les données manquent de réactivité face à des changements dans les conditions d'utilisation. Quand les approches sont dépourvues des formes analytiques, elles montrent souvent une inflexibilité durant l'application à des comportements variés des systèmes.

L'approche de pronostic basée sur l'expérience nécessite peu de connaissance experte des mécanismes de dégradation. Elle reste facile à mettre en œuvre mais elle n'est pas réactive face à l'éventuel changement dans le mode de fonctionnement du système. En plus, les modèles construits dans cette approche, ont seulement deux états: un état de fonctionnement et un état de défaillance, ils ne comprennent pas un état de fonctionnement dégradé.

Dans les approches basées sur les modèles mathématiques ou physiques, la connaissance des équations du comportement dynamique de la dégradation s'avère très utile. En cas de changement des propriétés du système ou de la dégradation, les paramètres peuvent être réajustés et le modèle peut être réadapté à un nouveau cas. Cependant, il est nécessaire d'avoir une haute qualification afin de bien maitriser les mécanismes de dégradation en question, d'où le coût élevé de l'utilisation ce type de modèle. Néanmoins, la précision et l'exactitude recherchées méritent le surcoût payé. Donc le choix d'une nouvelle approche à base physique, fondée sur un nouveau modèle mathématique de dégradation, devient logique et justifié. Par suite, des lois mathématiques précises, utiles et élégantes nous aideront dans les chapitres qui suivent afin d'achever le but de cette thèse. Notre modèle propose l'utilisation des lois analytiques de dommage.

Le deuxième chapitre définit le critère adopté, à savoir la rupture par fatigue, et développe un modèle basé sur l'aspect linéaire de cumul de dommage. Le modèle de pronostic proposé dans cette thèse permet de prédire la trajectoire de dégradation d'un système dynamique; il est basé, premièrement, sur des lois analytiques de dommage à cumul linéaire déjà évoquées, deuxièmement, il est basé sur une loi de cumul non-linéaire de dommage (troisième chapitre) et troisièmement, il fait inclure les influences stochastiques (quatrième chapitre).

La loi de Paris nous a permis de modéliser l'évolution de la longueur de fissure avec le nombre de cycles de chargement dans la phase stable de propagation. A chaque cycle, la longueur de fissure subit un incrément; et quand cette longueur atteint une certaine valeur critique, au-delà de laquelle la rupture devient imminente, la pièce est déclarée en état défectueux. La mesure de dégradation adoptée est un scalaire *D* normalisé variant entre 0 et 1 et relié au nombre de cycles à travers la loi de Miner en profitant de la propriété d'additivité linéaire de cette loi.

Le mode de défaillance traité dans ce travail est la fatigue des matériaux du dispositif. Le dommage considéré est dû à la propagation de fissure par fatigue. L'état d'endommagement du dispositif est mesuré par un indice de dégradation *D* en fonction du nombre de cycles de chargement *N*. Le modèle proposé est basé sur une relation entre un indice conventionnel de dégradation *D* et une longueur de fissure *a*. La défaillance sera déclarée quand *a* atteint la longueur critique a_C. Le modèle est donc exprimé par une fonction linéaire récursive reliant la dégradation dans deux cycles consécutifs au nombre critique de cycles et à la contrainte limite d'endurance du matériau du système. A partir d'une fissure initiale détectée, les trajectoires de dégradation peuvent être tracées en fonction de cycles de chargement.

Le modèle analytique de pronostic développé dans cette thèse permet de prédire, à chaque cycle ou instant, la durée de vie résiduelle (RUL) du système. Les durées de vie sont déduites à partir d'une lecture de temps, en chaque point, sur les courbes et les trajectoires de dégradation obtenues.

Ce modèle appartient à la première famille des approches de pronostic. Dans le cas où les lois analytiques de dommage sont disponibles, ce modèle est qualifié d'adaptable aux nouvelles situations. A notre avis, ce modèle permettra d'assure un moyen utile pour l'analyse de pronostic des systèmes industriels.

Afin d'illustrer la méthodologie présentée et de montrer son efficacité, l'approche proposée est appliquée à la prédiction de l'âge des deux systèmes en fatigue. L'étude considère premièrement l'application industrielle à un système de suspension d'automobile, et deuxièmement, l'application à un système pétrochimique comme les pipelines. Dans ces deux

applications, des courbes de dégradations sont déduites permettant ainsi de déterminer les durées de vie des éléments industriels étudiés.

On considère dans notre application un système formé de la moitié d'une suspension à cause de la symétrie. Les suspensions sont soumises à un chargement répété dû à la surface d'une route non régulière. Cette surface est modélisée par une fonction polynomiale périodique. Trois modes d'excitation de route sont examinés en fonction de l'amplitude de la surface modélisée afin de tenir compte des cas extrêmes d'état de route et du fonctionnement de la suspension.

En ce qui concerne la deuxième application, l'importance de l'étude du pronostic des pipelines réside dans le fait qu'il existe plusieurs origines de la défaillance de ces tuyaux, y compris: erreurs de construction, défauts de matériaux, fluctuation de pression, explosion de gaz, corrosion interne et externe, erreurs opérationnelles, dysfonctionnement des systèmes de contrôle et force d'endommagement extérieure (issue d'un tiers durant l'excavation).

Les accidents des pipelines peuvent conduire à des pertes de vie, à des blessures graves, à l'endommagement des propriétés et à la nuisance à l'environnement bien que les accidents majeurs sont rares. Dans plusieurs cas, les tuyaux placés sous terre, sous routes et sous autoroutes sont supposés résistants à l'influence des couches supérieures du sol et de plusieurs chargements routiers de trafic, aussi bien à l'effet de la corrosion et de la rupture de matériau par fatigue.

Pour toutes ces raisons, la prédiction de vie en fatigue est effectuée pour des tuyaux avec leurs trois modes de placement: à surface, enterrés, et offshore (sous-marins). En plus, trois modes de pressions internes sont pris en compte afin d'explorer les cas extrêmes de fonctionnement.

Dans le chapitre trois, nous introduisons une loi non linéaire pour le cumul de dommage à la place de la loi linéaire de Miner. L'importance de cette amélioration réside dans le fait qu'un effet non linéaire d'interaction existe entre la fatigue à haut cycle (HCF) et la fatigue à bas cycle (LCF) dans plusieurs matériaux utilisés surtout en génie mécanique. Cette non-linéarité est observée dans le chargement uni-axial et, encore plus prononcée, dans le chargement multiaxial. Ceci existe particulièrement quand le chargement est non

proportionnel. En plus, cette modélisation non-linéaire est encore importante puisqu'elle prend en compte la nature des contraintes appliquées et l'environnement influant. Ce dernier peut accentuer encore plus l'aspect non-linéaire relatif aux certains comportements de matériaux sous l'effet de la fatigue. En plus, des méthodes traditionnelles de cumul de dommage ont montré une prédiction de vie imprécise quand des niveaux de charge multiples sont simultanément considérés.

Dans le modèle proposé ici, basé sur un cumul non-linéaire de dommage, l'état d'endommagement du dispositif est mesuré à chaque cycle par une fonction récursive non-linéaire de dégradation en fonction des marges des contraintes appliquées et du nombre de cycles de chargement ou du temps écoulé de fonctionnement.

Cette fonction récursive est déduite d'une résolution d'une équation différentielle ordinaire du premier ordre incluant la dérivée de la dégradation par rapport au nombre de cycles en fonction de contraintes de chargement, des paramètres des matériaux et de l'environnement, du nombre critique de cycles, de l'endurance et de la dégradation instantanée.

Afin de montrer l'efficacité de ce modèle non-linéaire, il est appliqué pour prédire la vie en fatigue du système de suspension d'automobile et du système des tuyaux. Les résultats du calcul de la durée de vie résiduelle (RUL) sont comparés aux résultats issus du modèle linéaire et l'écart est justifié par les différentes tendances de dégradation (linéaire, convexe et concave).

Dans les applications effectuées, les résultats optimistes du cas non-linéaire peuvent être expliqués par le fait que quand les tendances réelles de dégradation (non-linéaires) sont de formes concaves, alors le cumul de dommage est surestimé quand une forme linéaire est utilisée à la place d'une forme non-linéaire.

Dans l'application aux pipelines, l'étude non-linéaire semble fournir un comportement de dommage plus réaliste pour les différentes valeurs de pression relativement au cas linéaire. En effet, contrairement au cas linéaire, le cas non-linéaire présente une nette différence entre les trois modes de pression quand on s'approche de l'état de défaillance. Ce modèle de

pronostic non-linéaire facilite l'introduction de l'aspect stochastique qui améliorera la capacité prédictive du modèle proposé.

Le quatrième chapitre étend le paradigme déterministe développé dans cette thèse au domaine stochastique. Les outils de pronostic de défaillance doivent avoir la capacité d'inclure le dommage des matériaux sous des conditions de fonctionnement normales et extrêmes. Le modèle s'appuie sur un cumul de dommage dû à la propagation des fissures de fatigue dans des conditions probabilistes. La longueur initiale de fissure et le chargement appliqué sont considérés alors aléatoires.

En plus, la durée de vie résiduelle (RUL) peut être exprimée en fatigue sous plusieurs formes: soit la longueur critique de la fissure a_C soit le nombre critique de cycles de chargement N_C soit la ténacité des matériaux K_{IC}. Nous pouvons écrire alors différents états limites ou différents critères de performance qui ne sont que les marges entre une mesure instantanée de dommage intrinsèque et une valeur limite (critique) à ne pas dépasser. Plusieurs états limites peuvent être alors considérés et rendus aléatoires si leurs variables de base sont probabilistes.

Des incertitudes considérables existent dans l'utilisation et dans les entrées des capteurs aussi bien que dans la modélisation et dans les entrées des propriétés des matériaux associés. Par conséquence, il existe un besoin inhérent pour que les éléments du système de pronostic soient à base aléatoire.

Étant donné que la modélisation stochastique considère quelques paramètres du système comme aléatoires, alors la loi de propagation de Paris devient stochastique. Les données de diagnostic permettent de prendre la longueur initiale de fissure a_0 en tant qu'une première variable aléatoire et la contrainte de chargement en tant qu'une seconde variable aléatoire.

Notre modèle de dégradation stochastique est donné sous la forme d'une relation récursive reliant deux réalisations consécutives de dégradation $\tilde{D}_{N-1}(\tilde{a}_{N-1})$ et $\tilde{D}_N(\tilde{a}_N)$ en deux cycles voisins avec un incrément de dommage $d\tilde{D}_N$ à la fin de chaque cycle de chargement. Notons que chaque réalisation de dégradation est fonction d'une réalisation de

longueur de fissure $\tilde{a}$ donnée à son tour en fonction d'une longueur initiale de fissure $\tilde{a}_0$ rendue aléatoire.

Donc, la relation récursive du modèle décrit l'évolution de la dégradation $\tilde{D}_N$ en fonction des variables aléatoires suivantes: longueur initiale de fissure $\tilde{a}_0$, chargement $\Delta\tilde{\sigma}$ et la longueur courante de fissure $\tilde{a}_N$. A chaque cycle de chargement N ($0 \leq N \leq N_C$), l'indice de dégradation D_N augmente d'une quantité dD_N partant de $D_0 = 0$ jusqu'à une valeur unitaire ($D_C = 1$) qui n'est autre que l'état de défaillance du système.

Ainsi, le modèle de pronostic devient plus précis dans la prédiction des RUL. Les résultats des durées de vie résiduelles sont obtenus pour le dommage dans les cas linéaires et non-linéaires et les différences sont justifiées aussi par les tendances multiples de dégradation. La propagation stochastique de fissures implique des modèles avec des paramètres aléatoires qui peuvent être estimés en utilisant les simulations de Monte-Carlo. Ces paramètres stochastiques sont affectés par certaines probabilités de réalisation influant les RUL résultantes déduites des trajectoires de dégradation. Encore une fois, les deux mêmes applications déjà traitées concernant les suspensions et les pipelines sont considérées de nouveau dans ce quatrième chapitre.

Comme perspectives, il est planifié de mieux développer la méthodologie de pronostic proposée et l'appliquer sur un large ensemble des systèmes dynamiques. Ceci est réalisé en prenant en considération d'autres lois analytiques de la propagation de fissures et d'autres lois de cumul de dommage.

Ajoutons sur ceci qu'un plus grand nombre de paramètres de base peuvent être assimilées comme variables aléatoires, à noter, les paramètres des matériaux et de l'environnement et d'autres paramètres géométriques et mécaniques. De même, des nouvelles lois probabilistes autres que la loi Normale et la loi Log-Normale peuvent être explorées.

Aussi, il est planifié de mieux aborder la variabilité des durées de vie stochastiques et d'en déduire un faisceau des courbes de dégradation. En effet, des paramètres de base rendus aléatoires aboutissent à une trajectoire de dégradation probabilisée $\tilde{D}(a)$. Ainsi, un faisceau

de courbes $D(a)$ est obtenu pour lequel une courbe moyenne et une courbe d'écart-type sont déduites. Par conséquence, une courbe caractéristique $D_K(a)$ peut être calculée en termes d'un fractile α% qui dépend du niveau acceptable du risque. La valeur caractéristique de RUL est donc déduite à partir de la courbe $D_K(a)$.